

**Organocatalytic synthesis of chiral non-racemic aziridines,
labelled with ^2H , ^{15}N , ^{13}C stable isotopes**

Victor Zdorichenko

Thesis submitted in part fulfilment of the requirements for the degree of Doctor of
Philosophy

Supervisor: Dr. Sean Patrick Bew



School of Chemistry
University of East Anglia
Norwich Research Park

May 2015

This copy of the thesis has been supplied on condition that anyone who consults it is understood to recognise that its copyright rests with the author and that use of any information derived therefrom must be in accordance with current UK Copyright Law. In addition, any quotation or extract must include full attribution

Declaration

The research presented in this thesis is, to the best of my knowledge, original, except where due reference is made.

Victor Zdorichenko

Acknowledgements

I would like to express my genuine appreciation to everyone who in one way or another has helped me, supported me and shared with me the past four years. I am very grateful for the opportunity to work at UEA, for which special thank you goes to my primary academic supervisor Dr. Sean Bew, without him it would be impossible to achieve all this. I want to say thank you to my industrial supervisor Prof. Brian Cox and Novartis for funding my research. Additionally, I want to thank my secondary supervisor Prof. Andrew Cammidge for his help and support. Big thank you goes to Dr. Colin Macdonald for his help with NMR data and specialised NMR experiments. Special appreciation goes to everyone in Dr. Bew's group for their dedication, collaboration and hard-work. Thank you Glyn, Polly, Will, Dominika, Luis, Deeptee and many, many others! Big thanks goes to my friends for their good advice, support and encouragement. Cheers Dani, Sonia, César, Teresa, Hanae, Flavia, Desi, Franco, Łukasz, Davide, Simon, Lisa, Alex, Claudia, Francesca, Giulia, Marco, Melania, Ryan, Julien, Yohan, Tony, Emma, Ed, Dave, Brian, Fran, Ian, Jay, Johanna, Ketan, Mark, Michael, Oli, Ross, James, Doyle, Becky, Amanda, James, Jamie and others! I am incredibly lucky to have amazing teachers who taught me very well: Dawn, Malle, Joan, Caroline, Dan, Matthew. My teachers from Russia made my dream come true, they educated me to pursue my education and career abroad: Лилия Ивановна, Ольга Александровна, Ольга Семёновна, Анна Николаевна, Надежда Александровна, Лидия Николаевна, Людмила Юрьевна. I would also like to say thank you to Aiste Petraityte for her encouragement and being extremely helpful in keeping me on track and focused on my work. Her family is amazing! Thank you Vaida, Christopher, Jonas, Daiva, Valentinas, Anne, Richard. My deep gratitude goes to my parents and family: Ирина, Евгений, Галина, Борис, Надя, Александр, Сергей, Оксана, Надежда, Зинаида, Владислав. Without all of you I would have never achieved this, words will never be enough.

Abstract

Aziridines are ‘keystone’ synthetic building blocks - relatively reactive, three-membered heterocycles with the potential for generating ‘secondary’ high value entities such as α - or β -amino acids *via* ring-opening reactions. Within this thesis, a one-pot asymmetric organocatalytic methodology is utilised for the synthesis of enantiomerically enriched *cis*-*N*-aryl-3-aryl-aziridine-2-carboxylates, labelled with stable isotopes: ^2H , ^{13}C and ^{15}N . The reactions were catalysed by (*S*)-BINOL derived *N*-triflylphosphoramidate Brønsted acid and stable isotopes were selectively introduced within an aziridine ring with > 95% isotopic enrichment. The desired compounds were generated in yields of up to 81% and up to 87% e.e. Furthermore optically active β -bromo- α -amino acid derivatives were generated *via* aziridine ring-opening methodology without loss of the isotopic label or e.e.

α -Arylglycinols are α -amino- β -alcohols, that can be found as structural motifs in synthetic and natural compounds or used as building blocks to access other functional groups. When oxidised, α -arylglycinols are converted to the α -arylglycines - a class of α -amino acids found in a wide range of bioactive compounds such as vancomycin and teicoplanin glycopeptide antibiotics. Successful incorporation of ^2H or ^{13}C stable isotopes at α - or β -positions of enantiomerically enriched *N*-Cbz protected α -arylglycinols is reported with > 95% isotopic enrichment, yields of up to 73% and up to 98% e.e.

Teicoplanin is a glycopeptide antibiotic, used against methicillin-resistant *Staphylococcus aureus* (MRSA), but the emerging bacterial resistance has escalated the search for new antibiotics. The synthesis of a non-labelled model fragment of the glycopeptide antibiotic teicoplanin is reported. The fragment is synthesised *via* an aziridination reaction and can be used as a template to generate teicoplanin analogues, both non-labelled and labelled with stable isotopes.

It is anticipated that the stable isotope incorporating methodologies described within this thesis will be applicable not only to the synthesis of novel glycopeptide antibiotics, but also to other biologically active compounds. The installation of stable isotopes affords compounds with highly valuable properties that can be used to study drug metabolism, toxicology, pharmacokinetics and reaction mechanisms.

List of Abbreviations

AA	asymmetric aminohydroxylation
Ac	acetyl
ADME	absorption, distribution, metabolism and excretion
AMU	atomic mass unit
Ar	aryl
BINOL	1,1'-bi-2-naphthol
Bn	benzyl
Boc	<i>tert</i> -butoxycarbonyl
Bu	butyl
CAN	cerium(IV) ammonium nitrate
Cbz	carboxybenzyl
CNS	central nervous system
Cp	cyclopentadienyl
D	deuterium
DBU	1,8-Diazabicyclo[5.4.0]undec-7-ene
DCC	<i>N,N'</i> -dicyclohexylcarbodiimide
DCM	dichloromethane
d.e.	diastereomeric excess
DEAD	diethyl azodicarboxylate
DIBAL-H	diisobutylaluminium hydride
DMF	<i>N,N</i> -dimethylformamide
e.e.	enantiomeric excess
GABA	gamma (γ) amino butyric acid
FT-IR	Fourier transform infrared spectroscopy
h	hour(s)
HPLC	high performance liquid chromatography
i.v.	intravenously
kDa	kilo Dalton
KIE	kinetic isotope effect
LD	lethal dose
MIC	minimum inhibitory concentration
MRSA	methicillin-resistant <i>Staphylococcus aureus</i>
MS	molecular sieves
NMR	nuclear magnetic resonance
Ph	phenyl
ppm	parts per million
<i>p</i> TSA	<i>para</i> -toluenesulfonic acid
PyTf	pyridinium triflate
rt	room temperature
SNAr	nucleophilic aromatic substitution
<i>t</i> Bu	<i>tert</i> -butyl
THF	tetrahydrofuran
TLC	thin layer chromatography
TMG	1,1,3,3-tetramethylguanidine
Ts	tosyl
VANOL	3,3'-diphenyl-2,2'-bi-1-naphthol
VAPOL	2,2'-diphenyl-(4-biphenanthrol)
VRE	vancomycin-resistant <i>enterococci</i>
VRSA	vancomycin-resistant <i>Staphylococcus aureus</i>

Contents

Section 1. Introduction	1
<i>Chapter 1. Proteins and amino acids</i>	2
1.1. Natural and unnatural amino acids.....	2
1.2. Synthesis of α -amino acids: creating the building blocks.....	3
1.3. Applications of stable isotopes in protein studies.....	5
<i>Chapter 2. Aziridines and aziridination</i>	6
2.1. Definition of aziridines.....	6
2.2. Synthesis of aziridines.....	7
2.2.1. Nitrene addition to olefins.....	7
2.2.2. Carbene or ylid addition to imines.....	9
2.2.3. Cyclisation reactions.....	13
2.3. Natural products with an aziridine motif.....	15
2.3.1. Mitomycins.....	15
2.3.2. (2 <i>S</i> ,3 <i>S</i>)-(+)-Aziridine-2,3-dicarboxylic acid (2.50).....	17
2.4. Ring opening of aziridines.....	18
2.4.1. Ring opening of activated aziridines.....	18
2.4.2. Ring opening of non-activated aziridines <i>via</i> protonation.....	19
2.4.3. Ring opening of non-activated aziridines <i>via</i> quaternisation.....	20
2.4.4. Ring opening of non-activated aziridines <i>via</i> an adduct formation.....	21
2.4.5. Regioselective control of an aziridine ring-opening with halogen nucleophiles.....	22
2.4.6. Regioselective control of an aziridine ring-opening with carbon nucleophiles.....	22
2.4.7. Reductive ring opening.....	23
2.5. Chapter conclusion.....	24
<i>Chapter 3. Glycopeptide antibiotics</i>	25
3.1. Definition of antibiotics.....	25
3.2. Classes.....	25
3.3. Vancomycin and teicoplanin glycopeptide antibiotics.....	26

3.4. α -Arylglycines	27
3.5. α -Arylglycine structural motif in glycopeptide antibiotics	27
3.6. Aminohydroxylation reaction to afford arylglycines <i>via</i> aminoalcohols.....	28
3.7. Bacterial resistance and overcoming the problem	28
3.8. Chapter conclusion.....	30
<i>Chapter 4. Properties and applications of compounds labelled with stable isotopes</i>	<i>32</i>
4.1. Discovery of isotopes.....	32
4.2. Deuterium, kinetic isotope effect	33
4.3. Application of isotopes	35
4.4. Magnetic properties of atomic nuclei.....	36
4.5. Synthesis of isotopically labelled compounds	37
4.5.1. H/D exchange without the addition of acid or base	38
4.5.2. Acid-catalysed H/D exchange.....	39
4.5.4. Homogeneous metal catalysts.....	41
4.5.5. Heterogeneous catalysts.....	42
4.6. Chapter conclusion.....	44
Section 2. Results and Discussion	45
<i>Chapter 5. Synthesis and applications of chiral non-racemic aziridines labelled with stable isotopes</i>	<i>46</i>
5.1. Chapter introduction	46
5.2. Studies towards a racemic aziridination protocol	46
5.3. Studies towards an asymmetric aziridination protocol	52
5.4. Synthesis of α - ² H-aldehydes	56
5.5. Asymmetric synthesis of 1- ¹⁵ N-3- ² H- <i>tert</i> -butyl 3-(4-nitrophenyl)-1-phenyl aziridine-2-carboxylate <i>cis</i> -(5.18)	59
5.6. Synthesis of α - ² H- <i>tert</i> -butyl diazoacetate (5.24).....	63
5.7. Asymmetric synthesis of 1- ¹⁵ N-2,3- ² H- <i>tert</i> -butyl 3-(4-nitrophenyl)-1-phenyl aziridine-2-carboxylate <i>cis</i> -(5.16)	65
5.8. Synthesis of α - ¹³ C-3-nitrobenzaldehyde (5.29).....	66

5.9. Asymmetric synthesis of 1- ¹⁵ N-3- ¹³ C- <i>tert</i> -butyl 3-(3-nitrophenyl)-1-phenyl aziridine-2-carboxylate <i>cis</i> -(5.31) and 1- ¹⁵ N-2- ² H-3- ¹³ C- <i>tert</i> -butyl 3-(3-nitrophenyl)-1-phenylaziridine-2-carboxylate <i>cis</i> -(5.32)	68
5.10. Synthesis of ¹⁵ N-2,4-dimethoxyaniline (5.35)	70
5.11. Asymmetric synthesis of 1- ¹⁵ N-3- ² H- <i>tert</i> -butyl 1-(2,4-dimethoxy phenyl)-3-(4-fluorophenyl)aziridine-2-carboxylate <i>cis</i> -(5.37) with cleavable <i>N</i> -2,4-dimethoxy phenylprotecting group	71
5.12. Synthesis of α - ¹³ C-3-azidobenzaldehyde (5.40)	74
5.13. Synthesis of α - ¹³ C, ² H-3-nitrobenzaldehyde (5.44)	75
5.14. Synthesis of 1- ¹⁵ N-3- ¹³ C, ² H- <i>tert</i> -butyl 1-(2,4-dimethoxyphenyl)-3-(3-nitrophenyl)aziridine-2-carboxylate <i>cis</i> -(5.46)	77
5.15. Summary table of enantiomerically enriched <i>N</i> -aryl aziridine-2-carboxylates labelled with stable isotopes	78
5.16. Oxidative cleavage of <i>N</i> -2,4-dimethoxyphenyl protecting group from 1- ¹⁵ N-2,3- ² H- <i>tert</i> -butyl 3-(4-bromophenyl)-1-(2,4-dimethoxyphenyl)aziridine-2-carboxylate <i>cis</i> -(5.46).....	79
5.17. Ring opening of <i>N</i> -aryl aziridines with magnesium bromide diethyl etherate	80
5.18. Triple-Resonance Isotope-Edited (TRIED) NMR	85
5.19. Chapter conclusion.....	88
<i>Chapter 6. Synthetic efforts towards a model fragment of teicoplanin glycopeptide antibiotic</i> .	89
6.1. Introduction.....	89
6.2. Synthesis of 3-(4,4,5,5-tetramethyl-1,3-dioxolan-2-yl)phenol (6.19).....	92
6.3. Synthesis of 3-(3-(4,4,5,5-tetramethyl-1,3-dioxolan-2-yl)phenoxy)benzaldehyde (6.24)	93
6.4. Synthesis of 4,4,5,5-tetramethyl-2-(3-(3-vinylphenoxy)phenyl)-1,3-dioxolane (6.27) ...	94
6.5. Synthesis of chiral non-racemic benzyl (<i>R</i>)-(2-hydroxy-1-(3-(3-(4,4,5,5-tetramethyl-1,3-dioxolan-2-yl)phenoxy)phenyl)ethyl)carbamate (R)-(6.32)	96
6.6. Synthesis of (<i>R</i>)-2-(((benzyloxy)carbonyl)amino)-2-(3-(3-(4,4,5,5-tetramethyl-1,3-dioxolan-2-yl)phenoxy)phenyl)acetic acid (R)-(6.39) and methyl (<i>R</i>)-2-(((benzyloxy)carbonyl)amino)-2-(3-(3-(4,4,5,5-tetramethyl-1,3-dioxolan-2-yl)phenoxy) phenyl)acetate (R)-(6.40)	100
6.7. Synthesis of methyl (<i>R</i>)-2-(2-bromoacetamido)-2-(3-(3-(4,4,5,5-tetramethyl-1,3-dioxolan-2-yl)phenoxy)phenyl)acetate (R)-(6.47)	102
6.8. Synthesis of (<i>R</i>)-methyl 2-(2-diazoacetamido)-2-(3-(3-(4,4,5,5-tetramethyl-1,3-dioxolan-2-yl)phenoxy)phenyl)acetate (R)-(6.49)	103

6.9. Synthesis of a key E-F-O-G fragment derivative <i>cis</i> -(6.55) via aziridination reaction .	105
6.10. Chapter conclusion.....	111
<i>Chapter 7. Synthesis and applications of chiral non-racemic α-aryl glycinols labelled with stable isotopes</i>	112
7.1. Introduction.....	112
7.2. Synthesis of benzyl α - ² H-(<i>R</i>)-(1-(4-bromophenyl)-2-hydroxyethyl)carbamate (R)-(7.3)	112
7.3. Synthesis of benzyl α - ¹³ C-(<i>R</i>)-(2-hydroxy-1-(3-nitrophenyl)ethyl)carbamate (R)-(7.7)	115
7.4. Synthesis of benzyl β - ¹³ C-(<i>R</i>)-(2-hydroxy-1-(4-nitrophenyl)ethyl)carbamate (R)-(7.10)	116
7.5. Synthesis of benzyl β - ² H, ² H-(<i>R</i>)-(2-hydroxy-1-(4-nitrophenyl)ethyl)carbamate (R)-(7.13)	118
7.6. Chapter conclusion.....	119
Section 3. Experimental	121
8.1. General directions	122
8.2. Characterisation	122
8.3. Preparation of the cooling bath for asymmetric aziridination reactions	123
8.4. Synthesis of stable isotope labelled optically active aziridines.....	124
8.5. Synthesis of racemic non-labelled aziridines.....	138
8.6. Synthesis of ring-opened aziridines	146
8.7. Synthesis of deprotected NH-aziridines	154
8.8. Synthesis of teicoplanin fragment analogue	156
8.9. Synthesis of α -arylglycinols.....	167
8.10. Synthesis of styrenes	176
8.11. Synthesis of isotopically labelled aldehydes.....	181
8.12. Synthesis of diazoacetates.....	190
8.13. Synthesis of the aziridination catalyst (<i>S</i>)-3,3'-bis(anthracen-9-yl)-[1,1']-binaphthalen-2,2'-yl <i>N</i> -triflyl phosphoramidate (S)-(5.9)	192
8.14. Asymmetric synthesis of model aziridines using catalyst (S)-(5.9).....	197
<i>References</i>	198
<i>Appendix: crystal structure data for compounds (\pm)-cis-(5.8) and (5.63)</i>	206

Section 1.

Introduction

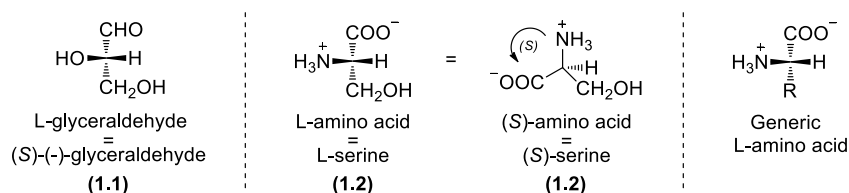
Chapter 1. Proteins and amino acids

1.1. Natural and unnatural amino acids

Proteins have vital physiological functions: they act as building blocks (tissue construction), enzymes (catalysis of chemical reactions) and antibodies (defence against pathogens).¹ Each protein consists of a precise sequence of amino acids that allows it to fold up into a particular three-dimensional shape, or conformation. Amino acids that constitute proteins are known as proteinogenic amino acids.

The surface of each protein molecule has a unique chemical reactivity that depends not only on which amino acid side chains are exposed, but also on their exact orientation relative to one another. For this reason, even two slightly different conformations of the same protein molecule may differ greatly in their chemistry.

Depending on the R-group substituent, amino acids can be divided into three subgroups: acidic, basic, neutral.² Except for glycine, which is not a chiral molecule, natural α -amino acids, that are found in proteins, are all L-amino acids. In other words, their absolute configurations are related to L-glyceraldehyde (1.1) (Scheme 1.1).



Following Cahn-Ingold-Prelog's rule, most (except cysteine) L- α -amino acids have the (S) configuration, because the carbonyl groups in natural α -amino acids take priority over the substituent R-groups (Scheme 1.1. L-serine (1.2) example).

Apart from L-amino acids, naturally occurring D- α -amino acids have been discovered as well. Crow *et al* and Rosenberg *et al* reported D-serine to be abundant in forebrains of mammals and to be very biologically active.^{3,4} D-aspartic acid was found in nerve endings in a mammal (*Rattus norvegicus*) and a mollusk (*Loligo vulgaris*).⁵ D-alanine was found in frog skin peptide dermorphin.⁶ While screening the plasma samples of patients with renal diseases, D-serine, D-alanine and D-proline were identified by Nagata *et al*.⁷

Additionally a multiple types of non-proteinogenic α -, β -, γ -amino acids have been found in nature and they have multiple functions in living organisms. β -alanine

and γ -amino butyric acid (GABA) are widely distributed in plants, involved in metabolism and neurotransmission respectively.^{8,9}

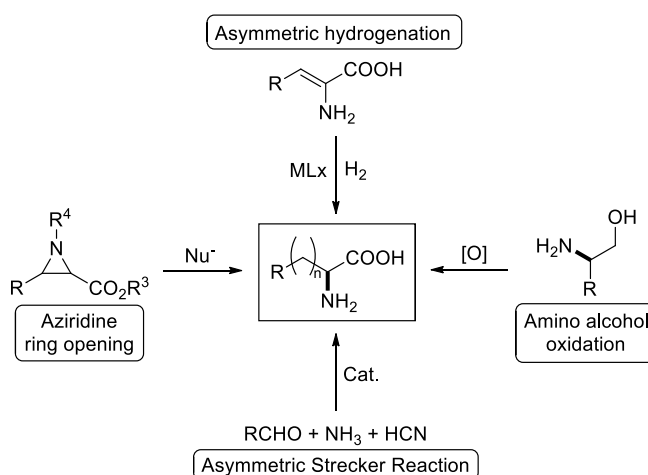
There are many unnatural (synthetic) amino acids which are widely used in place of natural amino acids during the synthesis of peptides. The peptides (sequence of at least two amino acids) bearing uncommon synthetic amino acids may have some additional physiological properties, which may be of medical significance and have clinical applications.

1.2. Synthesis of α -amino acids: creating the building blocks

An efficient synthesis of enantiomerically pure α -amino acids has drawn a considerable research interest.¹⁰ A diversity of methods has been developed for the stereoselective construction of naturally occurring amino acids as well as optically active non-proteinogenic amino acids.¹¹

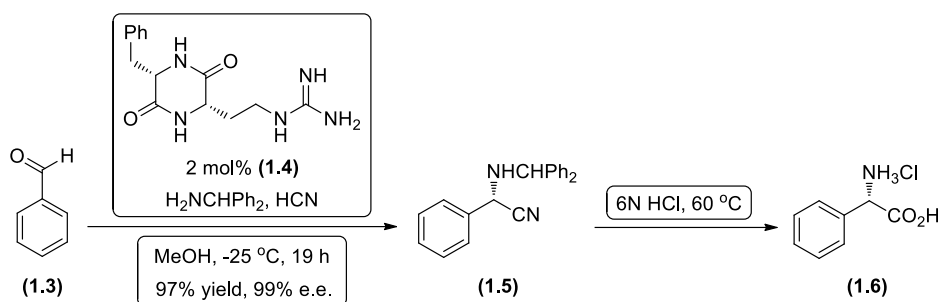
Unnatural α -amino acids are very valuable tools for modern drug discovery research. Due to their unlimited structural diversity and functional versatility, they are widely used as chiral building blocks and molecular scaffolds in constructing combinatorial libraries. They represent a powerful tool in drug discovery when incorporated into peptide analogues. Used as molecular probes they provide a better understanding of the function of biological systems. Structural modifications allow the design of drug candidates with a perfect match to their biological target, which may ultimately lead to improved *in vivo* stability, enhanced potency, better oral absorption, improved tissue distribution, and increased selectivity of biological response.¹²

The biological importance of α -amino acids has led to the development of a large variety of methods for their synthesis.¹³ Below there are selected methods of asymmetric synthesis of α -amino acids.



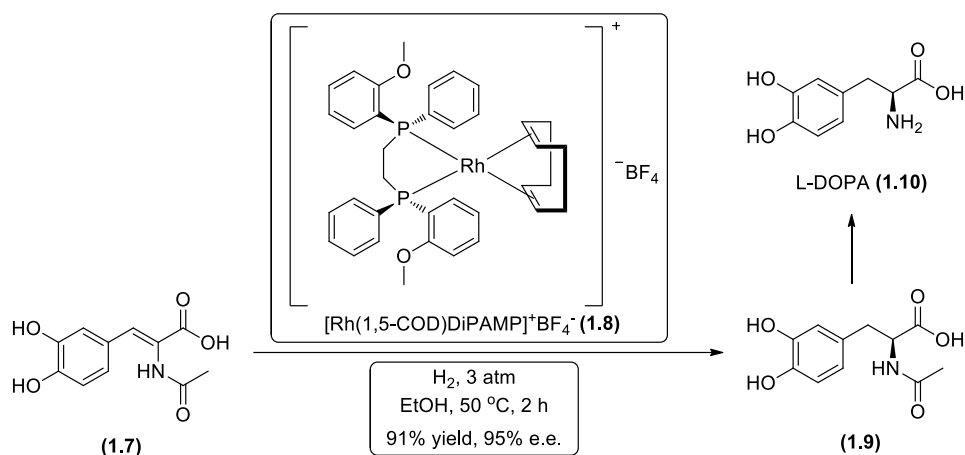
Scheme 1.2. Asymmetric synthesis of α -amino acids

The Strecker reaction was developed by Adolph Strecker in 1850.¹⁴ It is a three-component reaction between an aldehyde, an amine and hydrogen cyanide to form an α -amino nitrile. The nitrile can then be hydrolysed resulting in a racemic α -amino acid.¹⁵ The first non-metal catalysed asymmetric Strecker synthesis, reported by Lipton and co-workers, used a cyclic dipeptide catalyst (Cyclo[(*S*)-norarginyl-(*S*)-phenylalanyl]) (*S,S*)-(1.4) to achieve high yields and enantiomeric excess (**Scheme 1.3**). In particular, (*S*)-phenylglycine salt (*S*)-(1.6) was synthesised in > 99% e.e. and 92% overall yield in 3 steps from benzaldehyde (1.3) *via* the α -amino nitrile intermediate (*S*)-(1.5).¹⁶



Scheme 1.3. (*S*)-phenylglycine hydrochloride (*S*)-(1.6) asymmetric Strecker synthesis by Lipton *et al*

Knowles *et al* developed asymmetric hydrogenation of dehydroamino acids, catalysed by rhodium chiral bisphosphine catalyst.¹⁷ To demonstrate the activity and selectivity of the catalyst, Knowles synthesised (*S*)-3,4-dihydroxyphenylalanine (L-DOPA) (*S*)-(1.10), a drug used for treating Parkinson's disease (**Scheme 1.4**).¹⁸ The synthesis of L-DOPA (*S*)-(1.10) employed the asymmetric hydrogenation of (*Z*)-2-acetamido-3-(3,4-dihydroxyphenyl)acrylic acid (1.7) using the [Rh(1,5-COD)DiPAMP]⁺BF₄⁻ catalyst (1.8) followed by deprotection of the amine (*S*)-(1.9).



Scheme 1.4. L-DOPA (*S*)-(1.10) synthesis *via* asymmetric hydrogenation by Knowles *et al*

Optically active α - and β -amino acids can be synthesised *via* ring opening of enantiomerically enriched aziridine-2-carboxylic esters with a variety of nucleophiles.^{19,20} Another method employs chiral α -amino- β -alcohols, oxidation of which affords desired α -amino acids. Aziridines and α -amino- β -alcohols are discussed in more detail in **Chapter 2 and Chapter 3**.

1.3. Applications of stable isotopes in protein studies

In order to fine-tune the protein structure and properties, it is important to study the amino acid configuration and interactions. One of the main areas of interest is high-throughput protein structure determination by nuclear magnetic resonance (NMR) or X-ray crystallography.²¹ NMR spectroscopy provides information about the structure and dynamic properties of proteins in solution, and offers an approach for determining the three-dimensional protein structures of systems that fail to crystallize. However, it is difficult to determine the NMR structures of proteins larger than 30 kDa because their spectra are complicated by many complex overlapping signals and significant line broadening. A common approach for addressing these problems is to label proteins with deuterium to simplify the proton spectra. Additionally, the incorporation of ¹³C, ¹⁵N and other stable isotopes into proteins, combined with heteronuclear NMR experiments, facilitates the assignments of the complex NMR resonances of proteins and thus enables the elucidation of their three-dimensional structures. In addition, amino acids labelled with stable isotopes are valuable for metabolic studies.²²

Buděšínský *et al* constructed the Pro-Leu-Gly-NH₂ moiety, with ¹³C and ¹⁵N fully labelled backbone, which was used as a terminal fragment of neurohypophyseal hormone oxytocin.²³ The labeled oxytocin exhibited biological activity identical to natural oxytocin. Detailed ¹H-, ¹³C- and ¹⁵N-NMR studies confirmed the assigned oxytocin conformation containing a β -turn in the cyclic part of the molecule, stabilised by hydrogen bonding.

Apart from naturally occurring amino acids, unnatural acids can provide valuable information about binding site distances and interactions of protein analogues. Additionally, ligand-protein complexes can be characterised.²⁴

Chapter 2. Aziridines and aziridination

2.1. Definition of aziridines

Aziridines are classified as three membered heterocycles containing one nitrogen atom (**Figure 2.1**).²⁵ Structurally aziridines are similar to epoxides, possessing nearly identical ring strain energy of 27 kcal mol^{-1} .²⁶

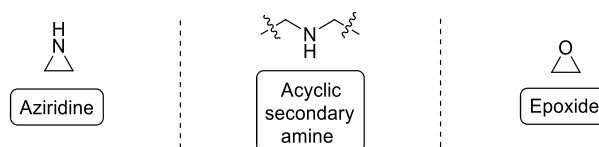


Figure 2.1. Generic aziridine, acyclic secondary amine and epoxide

The ring strain of aziridine arises from the bond angles of $\sim 60^\circ$, which is considerably smaller than the ideal tetrahedral angle of 109.5° .²⁷ Bonding within this type of compound can be explained by a "banana" bond model (**Figure 2.2**).²⁸ As a result of bending, the orbitals gain more "s" character, which translates into the decreased basicity of the nitrogen lone pair in aziridines.²⁹ Thus, the conjugate acid of aziridine has a pK_a value of ~ 8 , whereas the conjugate acid of an acyclic secondary amine has a value of ~ 11 .³⁰

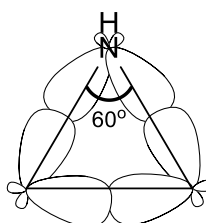


Figure 2.2. Aziridine "banana" bond model

Due to the ring strain, aziridines readily undergo ring-opening reactions, which makes them very useful synthetic precursors to compounds like alkaloids, diamines and β -lactam antibiotics.³¹ Chiral non-racemic *trans*- and *cis*-aziridine-2-carboxylates are very important compounds, because they serve as useful intermediates to many organic molecules, including enantiomerically enriched α - and β -amino acids (**Figure 2.3**).

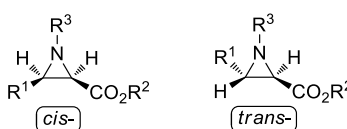


Figure 2.3. Generic *cis*- and *trans*-aziridine-2-carboxylates

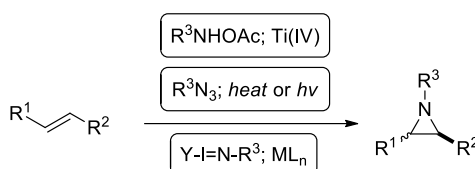
2.2. Synthesis of aziridines

Synthetic methodologies for the preparation of aziridines can be divided into the following categories:³²

- 1) Nitrene addition to olefins
- 2) Carbene or ylide addition to imines
- 3) Cyclisation reactions

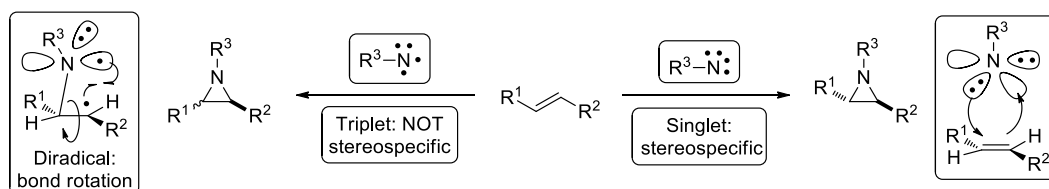
2.2.1. Nitrene addition to olefins

Nitrene is a reactive intermediate in which nitrogen atom bears only one substituent, one lone pair and two other electrons. The nitrene method of aziridination involves addition of nitrenes to the unsaturated partner (**Scheme 2.1.**).



Scheme 2.1. Aziridination of a generic alkene *via* the nitrene method

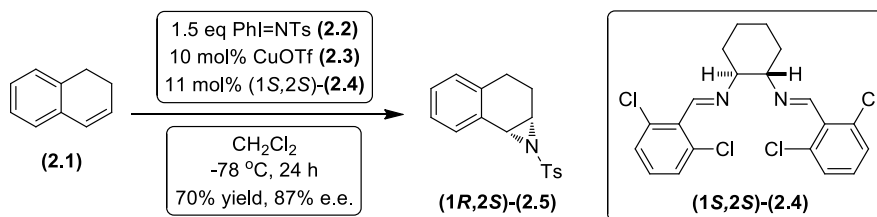
The biggest limitation of this method is the lack of stereoselectivity.³³ Nitrenes are typically generated by thermal or photochemical decomposition of the corresponding azides and therefore exist as mixtures of singlet (more reactive) and triplet (more stable) nitrenes (**Scheme 2.2.**). Only singlet nitrenes react stereospecifically with alkenes, because both new C–N bonds are formed in a concerted process. Triplet nitrenes react in a two-step process with alkenes, in which a C–N bond is formed in each consecutive step. Due to unrestricted C–C bond rotation, the stereoselectivity is generally quite low.



Scheme 2.2. Reactions of triplet and singlet nitrenes with a generic alkene

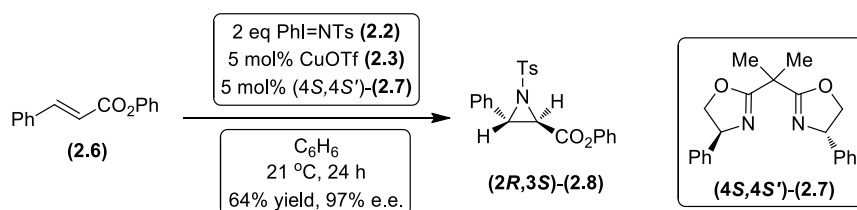
Jacobsen *et al* demonstrated that chiral non-racemic (1*S*,2*S*)-*bis*((2,6-dichlorobenzylidene)diamino)cyclohexane (**1*S*,2*S*)-(2.4)**) stabilised a singlet nitrene and generated *cis*-(1*R*,2*S*)-*N*-tosylaziridine (**1*R*,2*S*)-(2.5)**) in 70% yield and 87% e.e., which

was determined by chiral HPLC analysis (**Scheme 2.3**).³⁴ This enantioselective aziridination of *cis*-alkene (**2.1**) was achieved by using copper(I) triflate (**2.3**) and (*N*-(*p*-toluenesulfonyl)imino)phenyliodinane (**2.2**) as a nitrene source, that generated a nitrene *in situ*.



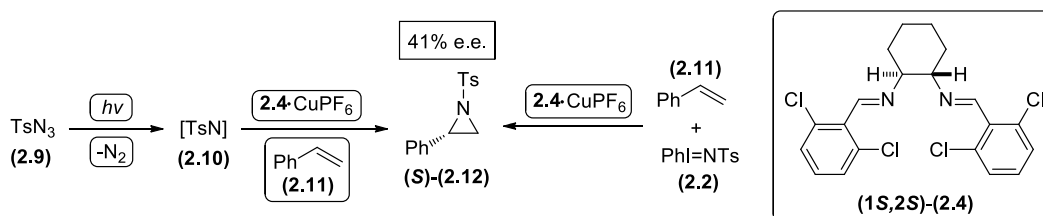
Scheme 2.3. Asymmetric synthesis of *cis*-*N*-tosylaziridine (**1R,2S**)-(2.5) by Jacobsen *et al*

Evans *et al* published the enantioselective aziridination of *trans*-alkene (**2.1**) using copper(I) triflate (**2.3**) and (*N*-(*p*-toluenesulfonyl)imino)phenyliodinane (**2.2**) as a nitrene source. Chiral non-racemic 4,4'-disubstituted (*4S,4S'*)-*bis*(oxazoline) (**4S,4S'**)-(2.7) was used to stabilise a singlet nitrene, affording phenyl *trans*-(*2R,3S*)-*N*-tosylaziridine-2-carboxylate (**2R,3S**)-(2.8) in 64% yield and 97% e.e., which was determined by chiral HPLC analysis (**Scheme 2.4**).³⁵



Scheme 2.4. Asymmetric synthesis of phenyl *trans*-*N*-tosylaziridine-2-carboxylate (**2R,3S**)-(2.8) by Evans *et al*

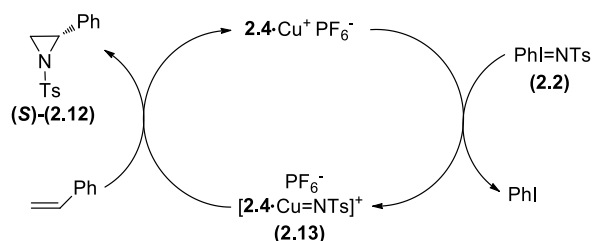
Investigating the mechanism of the reaction, Jacobsen *et al* performed an asymmetric synthesis of (*S*)-2-phenyl-1-tosylaziridine (*S*)-(2.12), starting from the same styrene (**2.11**), but using two different nitrene sources: (*N*-(*p*-toluenesulfonyl)imino)phenyliodinane (**2.2**) and *para*-toluenesulfonyl azide (**2.9**) (**Scheme 2.5**).³⁶



Scheme 2.5. Synthesis of (*S*)-2-phenyl-1-tosylaziridine (*S*)-(2.12) by Jacobsen *et al*

Under photochemical conditions, *para*-toluenesulfonyl azide (**2.9**) was converted to the nitrene intermediate (**2.10**), *via* nitrogen gas elimination (**Scheme 2.5**). In the presence of catalytic amounts of the copper(I) hexafluorophosphate and chiral

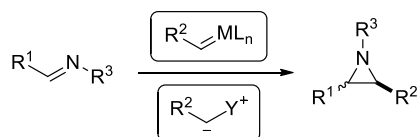
non-racemic (1*S*,2*S*)-bis((2,6-dichlorobenzylidene)diamino)cyclohexane (1*S*,2*S*)-(2.4) ligand, (*S*)-2-phenyl-1-tosylaziridine (*S*)-(2.12) was synthesised with the same enantioselectivity (41% e.e.) obtained in the catalytic aziridination reaction, that employed (*N*-(*p*-toluenesulfonyl)imino)phenyliodinane (2.2) as a nitrene source. This study was an indication of the common copper-nitrene intermediate (2.13) and allowed the mechanism of the reaction to be proposed (Scheme 2.6).



Scheme 2.6. Proposed mechanism of the synthesis of (*S*)-2-phenyl-1-tosylaziridine (*S*)-(2.12) via the nitrene method by Jacobsen *et al*

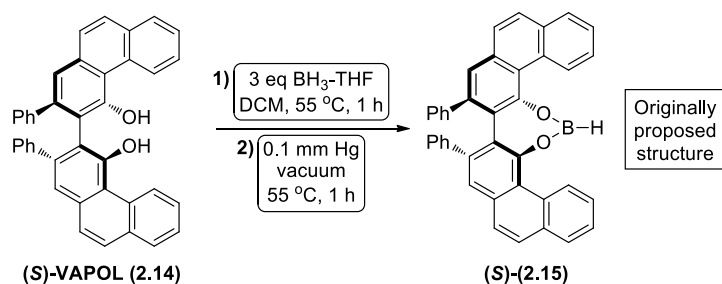
2.2.2. Carbene or ylid addition to imines

Carbene and ylid methods of aziridination involve a formation of one C–N bond and one C–C bond (Scheme 2.7).



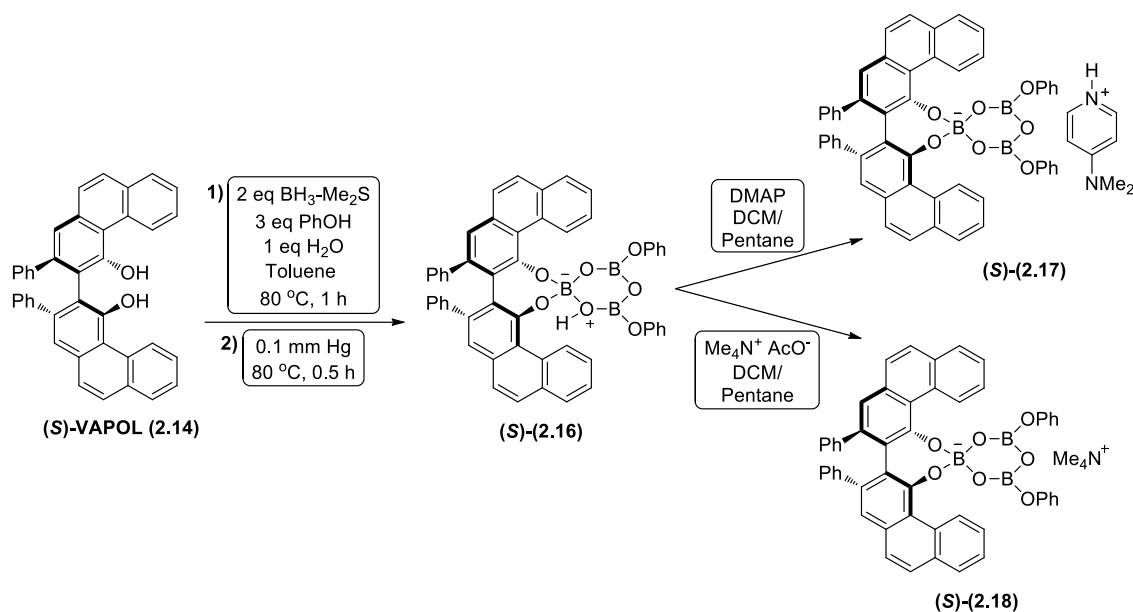
Scheme 2.7. Aziridination *via* a metal carbenoid or ylid addition to a generic imine

A plethora of methods employing metal carbenoids or ylids for the synthesis of chiral non-racemic aziridines has been reported, outlined in the review by Atkinson.³⁰ Wulff *et al* developed a robust catalytic asymmetric aziridination protocol providing chiral non-racemic alkyl *cis*-aziridine-2-carboxylates in high yields (up to 79%) and stereoselectivities (up to 99% e.e.).³⁷ The (*S*)-VAPOL-Boron complex (*S*)-(2.15) catalyst utilised in asymmetric aziridination reactions of *N*-substituted imines was originally reported to be a Lewis acid and was used previously by Wulff *et al* in asymmetric Diels-Alder reactions (Scheme 2.8).³⁸



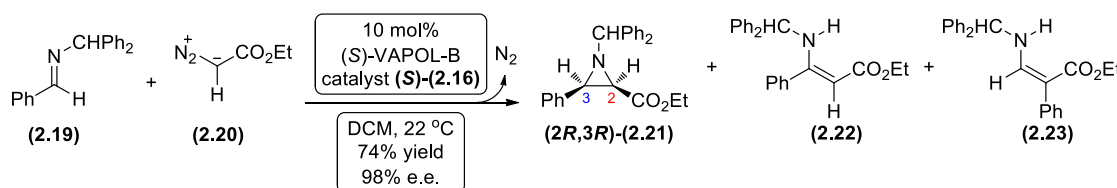
Scheme 2.8. Proposed structure the (*S*)-VAPOL-Boron complex (*S*)-(2.15) reported by Wulff *et al*

Although originally a Lewis acid nature of the catalyst was proposed, Wulff *et al* continued an investigation towards the active catalyst structure and succeeded in isolation of ion pair (S)-(2.17) and (S)-(2.18) (Scheme 2.9.). The X-ray diffraction analysis of these ion pairs allowed the structure of the active catalyst (S)-(2.16) to be deduced. These findings led to a conclusion that the boroxinate based (S)-VAPOL active catalyst (S)-(2.16) is not a Lewis acid, but in fact is a Brønsted acid of a singular structure.³⁹



Scheme 2.9. Active catalyst (S)-(2.16) structure determination via crystallisation of ion pairs (S)-(2.17) and (S)-(2.18) by Wulff *et al*

Utilising (S)-VAPOL-Boron complex (S)-(2.16) as a Brønsted acid in an asymmetric catalytic aziridination reaction between *N*-benzhydryl imine (2.19) and ethyl diazoacetate (2.20), ethyl (2*R*,3*R*)-*N*-benzhydryl-3-phenylaziridine-2-carboxylate (2*R*,3*R*)-(2.21) was afforded in 74% yield, after purification by silica gel chromatography, and greater than 50:1 *cis*- over *trans*-diastereoselectivity, determined by $^1\text{H-NMR}$ analysis of crude reaction mixture (Scheme 2.10.). The chiral HPLC analysis on a Chiralcel OD column displayed 98% e.e. Additionally, the $^1\text{H-NMR}$ analysis displayed only 4% of the acyclic by-products (2.22) and (2.23), that were obtained due to 1,2-hydride or 1,2-aryl shift respectively (Table 2.1. Entry 1).



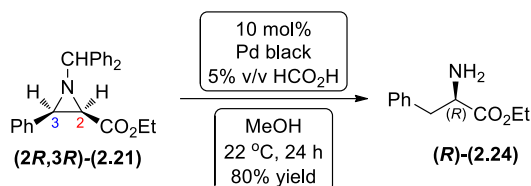
Scheme 2.10. Asymmetric aziridination of *N*-benzhydryl imine (2.19) with (S)-VAPOL-Boron catalyst (S)-(2.16) carried out by Wulff *et al*

Screening various catalysts, it was established that (*S*)-VAPOL-borate-complex (**(S)**-**(2.16)**) was superior to others listed in **Table 2.1**.⁴⁰ It was found that even despite the increase of the reaction time from 30 minutes to 16 hours, 1 mol% of the catalyst (**(S)**-**(2.16)**) was still effective to afford ethyl (*2R,3R*)-1-benzhydryl-3-phenylaziridine-2-carboxylate (**(2R,3R)**-**(2.21)**) in 72% yield and 99% e.e. (**Table 2.1**: Entry 2).

Entry	Catalyst	Loading (mol%)	Time (h)	Yield (%) <i>cis</i> - (2.21)	e.e. (%) <i>cis</i> - (2.21)	Ratio <i>cis</i> : <i>trans</i> - (2.21)	Yield (%) (2.22)	Yield (%) (2.23)
1	(<i>S</i>)-VAPOL-borate-complex	10	0.5	74	98	>50:1	2	2
2	(<i>S</i>)-VAPOL-borate-complex	1	16	72	99	42:1	4	2.5
3	(<i>S</i>)-BINOL-borate-complex	10	20	42	17	8:1	8	10
4	(<i>S</i>)-VAPOL-BH ₂ Br-complex	10	20	53	66	>50:1	13	6
5	(<i>S</i>)-VAPOL-Et ₂ AlCl-complex	10	18	41	5	>50:1	17	14

Table 2.1. Screening of catalysts prepared from vaulted biaryls in the asymmetric aziridination reaction by Wulff *et al*

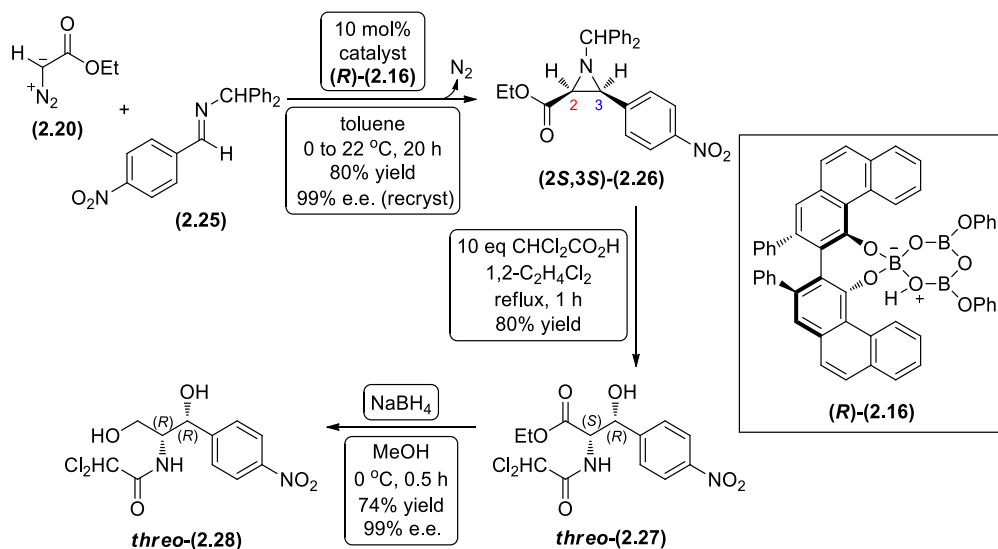
The absolute configuration of ethyl (*2R,3R*)-1-benzhydryl-3-phenylaziridine-2-carboxylate (**(2R,3R)**-**(2.21)**) was confirmed by the reductive ring opening to (*R*)-phenylalanine ethyl ester (**(R)**-**(2.24)**) (**Scheme 2.11**). The optical rotation of this material was found to be $[\alpha]_D^{25} -23.0$ (c 3.2 EtOH), which corresponds well to the reported value for (*S*)-phenylalanine ethyl ester $[\alpha]_D^{25} +23.8$ (c 3.2 EtOH).⁴¹



Scheme 2.11. Reductive ring-opening of (*2R,3R*)-1-benzhydryl-3-phenylaziridine-2-carboxylate *cis*-**(2.21)** by Wulff *et al*

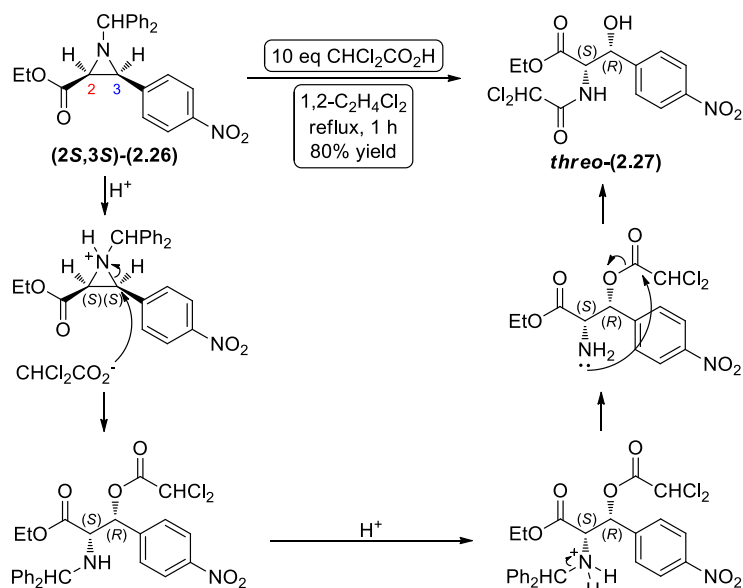
Chloramphenicol is one of the oldest antibacterial agents, which was first isolated from *Streptomyces Venezuelae* in 1947.⁴² In 2001 Wulff *et al* reported an asymmetric synthesis of optically pure (-)-(*R,R*)-chloramphenicol **threo**-**(2.28)** via asymmetric catalytic aziridination reaction of the corresponding *N*-benzhydryl imine (**(2.25)**). The synthesis of enantiomerically pure (-)-(*R,R*)-chloramphenicol **threo**-**(2.28)** was achieved in four steps from commercially available starting materials in 38% overall yield (**Scheme 2.12**). Initially commercially available *p*-nitrobenzaldehyde was converted to the corresponding *N*-benzhydryl imine (**(2.25)**), which was subsequently

reacted with ethyl diazoacetate (**2.20**). This asymmetric aziridination reaction was catalysed by 10 mol% (*R*)-VAPOL-borate-complex (**R**)-(**2.16**) and afforded ethyl (*2S,3S*)-1-benzhydryl-3-(4-nitrophenyl)aziridine-2-carboxylate (**2S,3S**)-(**2.26**) in 80% yield, 96% e.e. and 30:1 *cis*- over *trans*-stereoselectivity. Single crystallisation from hexane/methylene chloride improved the enantiomeric purity to 99% (84% yield, first crop).



Scheme 2.12. Asymmetric synthesis of (-)-(*R,R*)-chloramphenicol *threo*-(**2.40**) by Wulff *et al*

Treatment of *cis*-aziridine-2-carboxylate (**2S,3S**)-(**2.26**) with ten equivalents of dichloroacetic acid promoted an S_N2 -like ring-opening with an inversion of configuration at the C-3 centre to afford (*2S,3R*)-ethyl 2-(2,2-dichloroacetamido)-3-hydroxy-3-(4-nitrophenyl)propanoate *threo*-(**2.27**) in 80% yield as a single *threo*-diastereoisomer (**Scheme 2.13**).

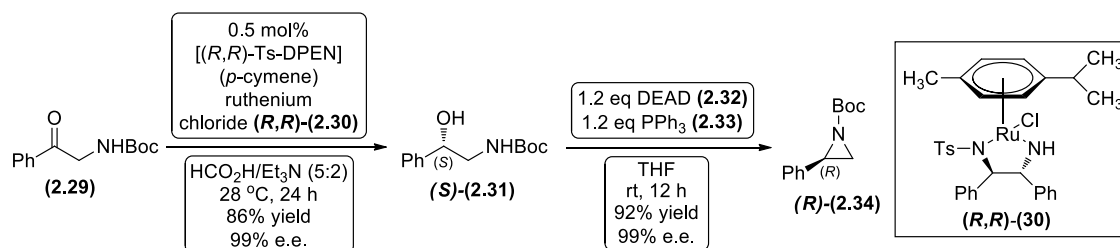


Scheme 2.13. Ring-opening of ethyl (*2S,3S*)-1-benzhydryl-3-(4-nitrophenyl)aziridine-2-carboxylate *cis*-(**2.26**) with dichloroacetic acid

Reduction of the ethyl ester functionality with sodium borohydride furnished (-)-(*R,R*)-chloramphenicol *threo*-(**2.28**) in 74% yield and 99% e.e. The optical rotation of this material was found to be $[\alpha]_{\text{D}}^{25}$ -25.4 (c 1.0 EtOAc), which compares favourably with the values $[\alpha]_{\text{D}}^{25}$ -24.2 (c 1.1 EtOAc) reported previously by Rao *et al.*⁴³

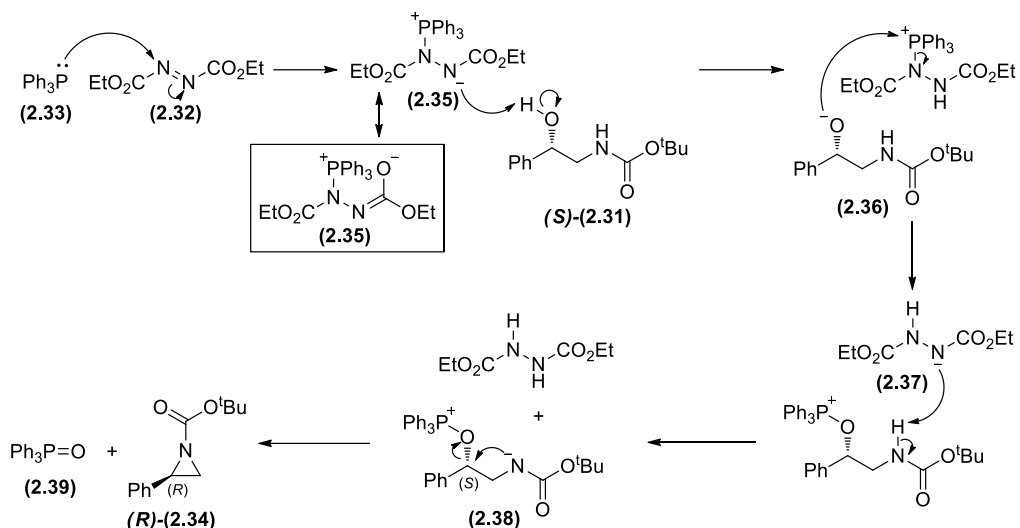
2.2.3. Cyclisation reactions

Cyclisation method of aziridination involves a ring-closure of 1,2-amino alcohols or 1,2-amino halides. Wills *et al* reported a synthesis of chiral non-racemic aziridines starting with optically pure 2-amino alcohols derived from the enantioselective reduction of *N*-Boc protected α -amino ketones (**Scheme 2.14**).⁴⁴ The enantioselective reduction of 2-(*N*-*tert*-butoxycarbonyl-amino)acetophenone (**2.29**) with [(*R,R*)-Ts-DPEN](*para*-cymene)ruthenium chloride (***R,R***-(**2.30**)) and formic acid/triethylamine as the hydrogen source afforded (*S*)-2-*N*-*tert*-butoxycarbonyl-amino-1-phenylethanol (***S***-(**2.31**)) in 86% yield and 99% e.e. as the product. The treatment of *N*-Boc protected 2-amino alcohol (***S***-(**2.31**)) with diethyl azodicarboxylate (DEAD) (**2.32**) and triphenylphosphine (**2.33**) in tetrahydrofuran, under Mitsunobu conditions, led to the formation of (*R*)-*N*-Boc-2-phenylaziridine (***R***-(**2.34**)) in 92% yield and 99% e.e.



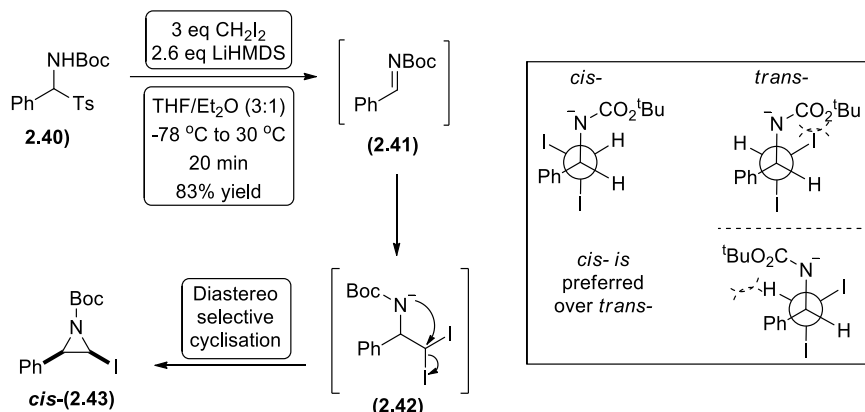
Scheme 2.14. Aziridination *via* cyclisation of (*S*)-2-*N*-*tert*-butoxycarbonyl-amino-1-phenylethanol (***S***-(**2.31**)) by Wills *et al*

Mitsunobu reaction is a powerful way to replace an alcohol group by a nucleophile with inversion of configuration due to an $\text{S}_{\text{N}}2$ type reaction (**Scheme 2.15**). In the first step, the phosphine (**2.33**) adds to the $\text{N}=\text{N}$ bond of DEAD (**2.32**) to give an anion (**2.35**) stabilised by one of the ester groups. After alcohol (***S***-(**2.31**)) deprotonation, the anion (**2.36**) attacks the positively charged phosphorus, due to a very strong affinity between oxygen and phosphorus. Finally, DEAD anion (**2.37**) generates the active nucleophile (**2.38**), that attacks the phosphorus derivative of the alcohol at the (*S*)-carbon centre in a $\text{S}_{\text{N}}2$ type reaction with the phosphine oxide (**2.39**) as the leaving group. $\text{S}_{\text{N}}2$ reactions lead to inversion of configuration, therefore the product (***R***-(**2.34**)) is afforded as the (*R*)-enantiomer.



Scheme 2.15. Proposed mechanism of the synthesis of *(R)*-*N*-Boc-2-phenylaziridine *(R)*-(2.34) via Mitsunobu reaction by Wills *et al*

Bull *et al* reported *cis*-selective synthesis of iodo-aziridines *via* cyclisation of 1,2-amino halides by using diiodomethyl lithium and *in situ* generated *N*-Boc-imines (**Scheme 2.16**).⁴⁵ The reaction proceeds in one-pot *via* a highly diastereoselective cyclisation of an amino gem-diiodide intermediate, analogous to the aza-Darzens reaction.



Scheme 2.16. Cyclisation of *N*-Boc-gem-diiodide intermediate (2.42) affording *cis*-*N*-Boc-2-iodo-3-phenylaziridine *cis*-(2.43) by Wills *et al*

N-Boc-protected phenyl(tosyl)methanamine (**2.40**) was examined, generating the corresponding *N*-Boc-protected imine (**2.41**) *in situ* by deprotonation with excess base. An addition of diiodomethyl lithium to phenyl *N*-Boc-protected imine at -78 °C afforded *N*-Boc-gem-diiodide intermediate (**2.42**), which was stable at -78 °C. Warming the intermediate to 30 °C, promoted a ring-closure to afford *cis*-*N*-Boc-2-iodo-3-phenylaziridine *cis*-(**2.43**) in 83% yield and more than 95:5 *cis*-selectivity, which was detected by ¹H-NMR analysis.

2.3. Natural products with an aziridine motif

Apart from being used as precursors to valuable organic entities, aziridines can serve as intermediates in the course of the natural product synthesis (see example of (-)-(R,R)-chloramphenicol *threo*-(2.28) synthesis, pages 11-13) or be present in the natural product itself (*vide infra*).⁴⁶

2.3.1. Mitomycins

In 1956 mitomycins A (2.44) and B (2.45) were isolated from *Streptomyces caespitosus* by Hata *et al* in Japan (Figure 2.4).⁴⁷ Two years later mitomycin C (2.46) was isolated from the same organism by Wakaki and co-workers.⁴⁸ Although mitomycins A (2.44) and B (2.45) are highly active against tumours (e.g. Ehrlich carcinoma), they do possess a very high toxicity (LD₅₀ i.v. in mice: 2 mg/kg and 3 mg/kg respectively).⁴⁹ Mitomycin C (2.46) was found to be the least toxic among mitomycins (LD₅₀ i.v. in mice: 9 mg/kg), yet potent against a range of tumours as well as gram-positive and gram negative bacteria (e.g. *Staphylococcus aureus*, *E. coli*).^{50,51}

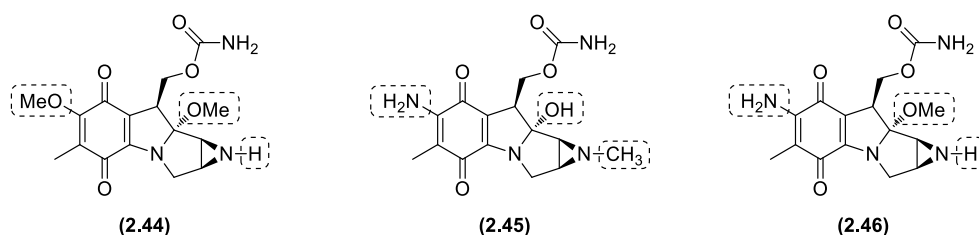
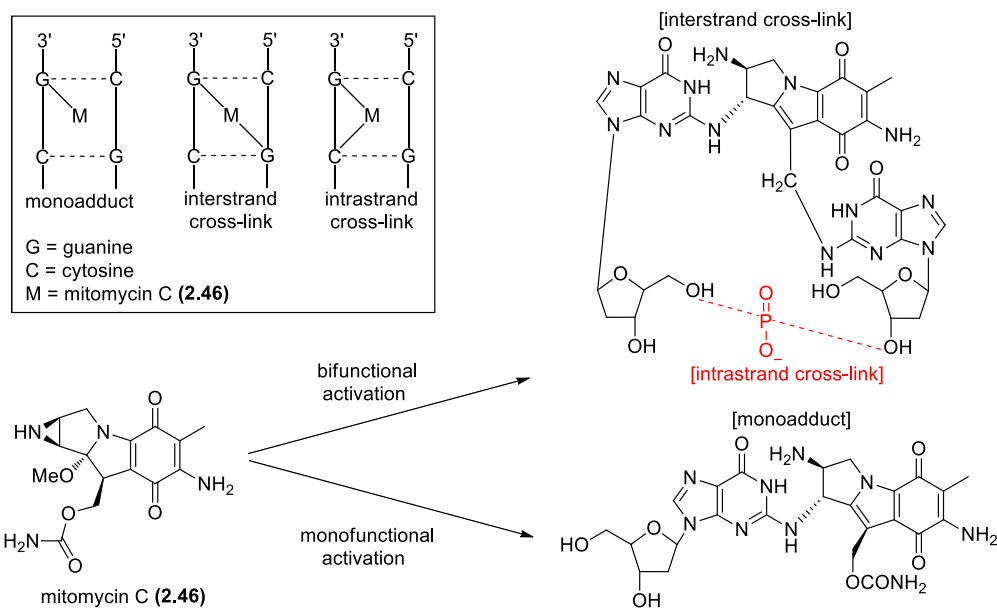


Figure 2.4. Mitomycins A (2.44) and B (2.45) were isolated by Hata *et al*. Mitomycin C (2.46) was isolated by Wakaki *et al*

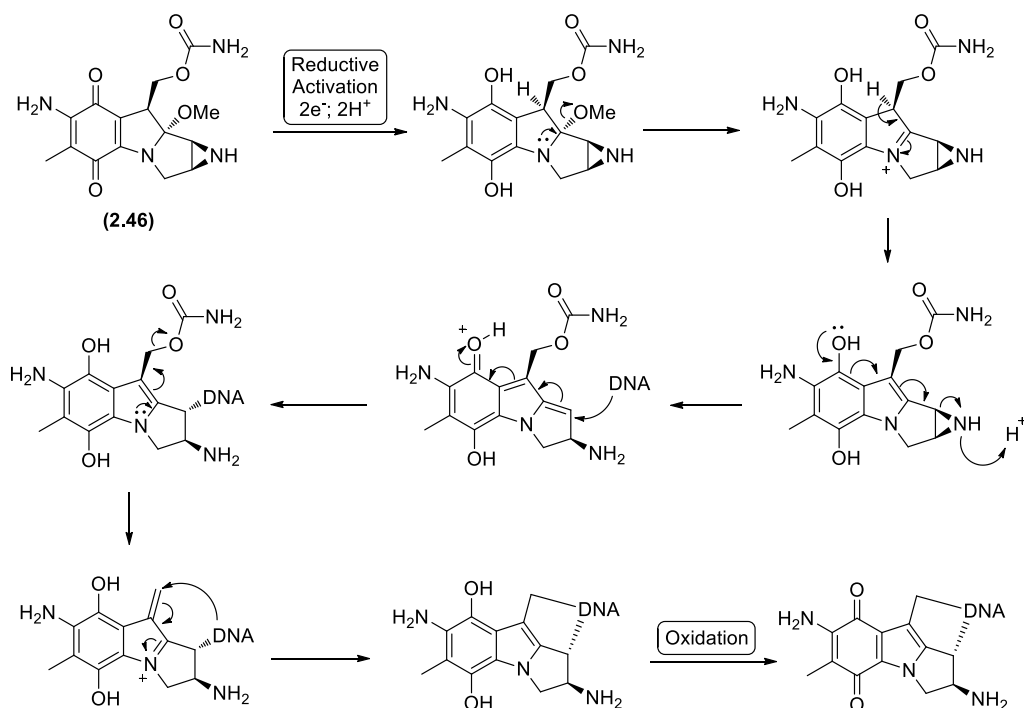
Tomacz *et al* reported that mitomycin C (2.46) reacts covalently with DNA, *in vivo* and *in vitro*, forming cross-links with the complementary strands of guanine (Scheme 2.17).⁵² Their work has demonstrated that aziridine functionality is directly involved into the inhibition of the DNA replication.⁵³

Investigations towards the mechanism of action of mitomycins revealed that mitomycins do not react directly with DNA, but require prior activation (Scheme 2.18.). Such activation is initialised *via* the quinone functionality reduction.⁵⁴ The reduction can be induced by both reductive enzymes and chemical reducing agents. The enzymes that can activate mitomycin C (2.46) include: cytochrome P450, cytochrome *c* reductase, DT-diaphorase or xanthine dehydrogenase.⁵⁵ Chemical reductants that can activate mitomycin C (2.46) include: sodium dithionite, catalytic hydrogenation, formate radicals or sodium borohydride.⁵⁶



Scheme 2.17. Guanine and mitomycin C (2.46) adducts

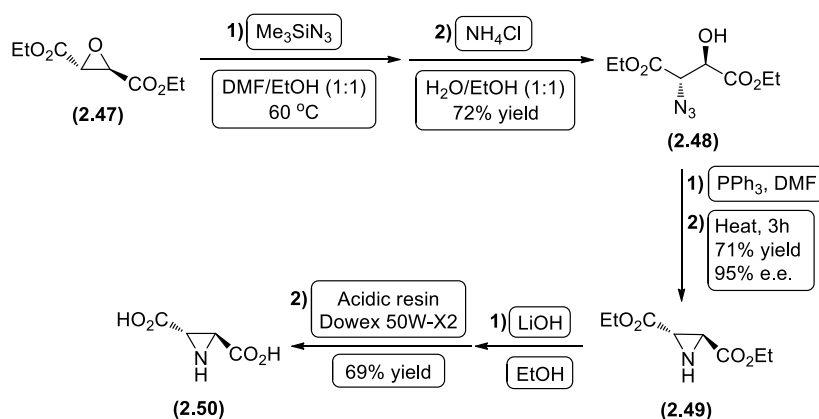
Many solid tumours contain less oxygen compared to a normal tissue, resulting from an imbalance between oxygen supply and consumption. This imbalance is caused by abnormal structure and function of the microvessels supplying the tumour, increased diffusion distances between the blood vessels and the tumour cells, and reduced oxygen transport capacity of the blood due to the anemia.⁵⁷ Therefore, reductive activation of the mitomycins can proceed in tumours, while it is suppressed by the oxidizing environments in normal tissues.



Scheme 2.18. Proposed mechanism of DNA cross-linking by mitomycin C (2.46) by Tomacz *et al*

2.3.2. (2*S*,3*S*)-(+)-Aziridine-2,3-dicarboxylic acid (2.50)

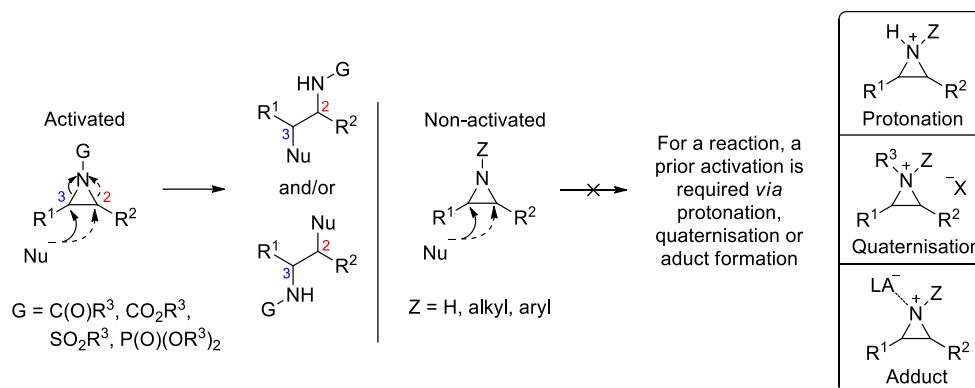
The only known example of naturally occurring 2,3-dicarboxylic acid containing aziridine functionality is (2*S*,3*S*)-(+)-aziridine-2,3-dicarboxylic acid (**2.50**), which was isolated from a cultured broth of a *Streptomyces* MD398-A1 by Naganawa and co-workers.⁵⁸ Schirmeister *et al* evaluated aziridine-2,3-dicarboxylates and *N*-acylated derivatives as potential irreversible inhibitors of the cysteine proteinases.⁵⁹ Evidence has been found for potential therapeutic effects of cysteine protease inhibitors against muscular dystrophy, arthritis, myocardial infarct, cancer, Alzheimer's disease, and cataracts.^{60,61} Legters *et al* reported the asymmetric synthesis of (2*S*,3*S*)-(+)-aziridine-2,3-dicarboxylic acid (**2.50**) starting from diethyl (2*R*,3*R*)-(-)-oxirane-2,3-dicarboxylate (**2.47**) (Scheme 2.19).⁶² Treatment of diethyl (2*R*,3*R*)-(-)-oxirane-2,3-dicarboxylate (**2.47**) with trimethylsilyl azide, resulted in a ring-opening of the three-membered ring and afforded *O*-silyl protected *anti*-vicinal azido alcohol. Addition of ammonium chloride cleaved the silyl protecting group and afforded diethyl (2*S*,3*R*)-2-azido-3-hydroxysuccinate (**2.48**) in 72% yield over two steps. Reaction with triphenylphosphine, under Mitsunobu conditions, generated diethyl (2*S*,3*S*)-(+)-aziridine dicarboxylate (**2.49**) in 71% yield and 95% e.e., which was determined by a ¹⁹F-NMR analysis of its Mosher derivative. Hydrolysis of diethyl (2*S*,3*S*)-(+)-aziridine dicarboxylate (**2.49**) with lithium hydroxide afforded the dilithio salt, which was subsequently passed through a strongly acidic sulfonic acid ion exchange resin (Dowex 50W-X2) to generate (2*S*,3*S*)-aziridine-2,3-dicarboxylic acid (**2.50**). The impure material was re-crystallised from water to afford pure (2*S*,3*S*)-aziridine-2,3-dicarboxylic acid (**2.50**) as a crystalline solid in 69% yield. The optical rotation was found to be $[\alpha]_D^{20} +51.4$ (c 0.5 H₂O), which is in good agreement with that of the natural product $[\alpha]_D^{24} +54.0$ (c 0.5 H₂O).⁵⁸



Scheme 2.19. Synthesis of (2*S*,3*S*)-(+)-aziridine-2,3-dicarboxylic acid (**2.50**) by Legters *et al*

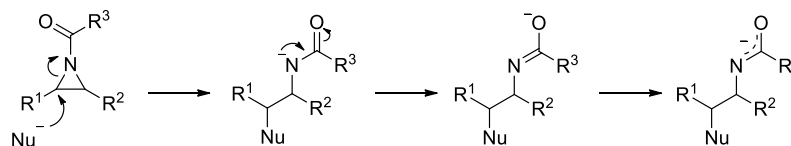
2.4. Ring opening of aziridines

Depending on the substituent on the nitrogen atom, aziridines can be classified as activated (oxygenated substituent such as carbonyl, sulfonyl or phosphoryl group) or non-activated (alkyl, aryl or hydrogen atom as a substituent) (**Scheme 2.20.**). Non-activated aziridines undergo ring-opening only after protonation, quaternisation or formation of a Lewis acid adduct.^{63,24}



Scheme 2.20. Ring-opening of activated and non-activated aziridines

Activated aziridines contain a substituent on the nitrogen atom, that can conjugatively stabilise the negative charge during a nucleophilic ring-opening (**Scheme 2.21.**)²⁴



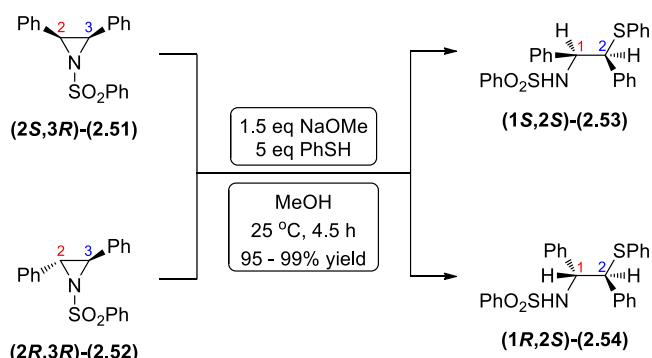
Scheme 2.21. Negative charge stabilisation by the activating substituent

As a consequence of the ring-strain present in aziridines, ring-opening reactions are a dominant feature of their chemistry, allowing access to α - and β -amino derivatives. For example, a nucleophilic attack at C-2 of an aziridine-2-carboxylates affords β -amino acid derivatives, whereas a ring-opening at C-3 results in α -amino acid derivatives. Although most nucleophiles reported would preferentially attack the less hindered site, regioselectivity highly depends on the ring substituents and a nucleophile. Some nucleophiles might afford mixtures of α - and β -amino derivatives.

2.4.1. Ring opening of activated aziridines

Mall and Stamm conducted an investigation towards a mechanism of a nucleophilic ring-opening of monocyclic activated aziridines and demonstrated that it occurs by an $\text{S}_{\text{N}}2$ -like mechanism with an inversion of configuration (**Scheme 2.22.**)⁶⁴

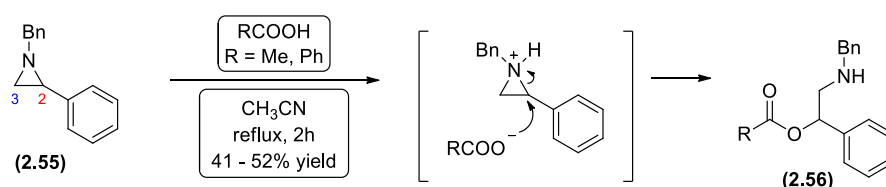
Activated *cis*-(2*S*,3*R*)-2,3-diphenyl-1-(phenylsulfonyl)aziridine (**2S,3R**)-(2.51) and *trans*-(2*S*,3*R*)-2,3-diphenyl-1-(phenylsulfonyl)aziridine (**2R,3R**)-(2.52) were reacted with thiophenol to afford corresponding *N*-((1*S*,2*S*)-1,2-diphenyl-2-(phenylthio)ethyl) benzenesulfonamide (**1S,2S**)-(2.53) and *N*-((1*R*,2*S*)-1,2-diphenyl-2-(phenylthio)ethyl) benzenesulfonamide (**1R,2S**)-(2.54) respectively. The sole product from the *cis*- isomer was always observed as a diastereoisomer of the sole product from the *trans*- isomer, therefore, in accordance with complete Walden inversion, these ring-opening reactions were interpreted as an S_N2 type.



Scheme 2.22. Nucleophilic ring-opening of activated *cis*- and *trans*-aziridines via an S_N2-like mechanism by Mall and Stamm

2.4.2. Ring opening of non-activated aziridines via protonation

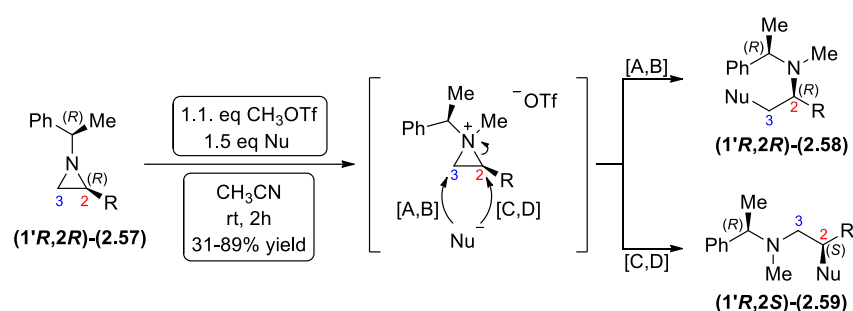
In order to ring-open non-activated aziridines, a prior activation is required. Singh *et al* demonstrated a ring-opening of 1-benzyl-2-phenylaziridine (**2.55**) with aromatic and aliphatic carboxylic acids using a protonation activation mode (Scheme 2.23).⁶⁵ A nucleophilic attack of the corresponding carboxylate anion at the C-2 benzylic position of aziridinium species afforded 2-(benzylamino)-1-phenylethyl acetate/benzoate (**2.56**). The direction of opening of aziridines is mainly affected by electronic factors because the acetoxy group preferentially attacks the carbon atom best able to accommodate some carbocation character.⁶⁶



Scheme 2.23. A C-2 directed ring-opening of 1-benzyl-2-phenylaziridine (**2.55**) with carboxylic acids by Singh *et al*

2.4.3. Ring opening of non-activated aziridines *via* quaternisation

Lee *et al* treated (2*R*)-[(1*R*)-Phenylethyl]methoxymethylaziridine (**(1'*R*,2*R*)-(2.57)**) with methyl trifluoromethanesulfonate, followed by reaction with the corresponding nucleophile to yield a single regioisomer (determined by ¹H-NMR analysis) of C-3 ring-opening product 2-amino-propane (**(1'*R*,2*R*)-(2.58)**) (Scheme 2.24).⁶⁷ When 2-benzyloxy substituent was introduced, identical regioselectivity was observed, with the cleavage of the bond between C-3 and the ring nitrogen. However, when the same ring-opening procedure was applied to aziridines containing carboxylate and acrylate substituents at C-2, the opposite regioselectivity was observed, with a nucleophile attacking the C-2 carbon of an aziridine, affording (**(1'*R*,2*S*)-(2.59)**).



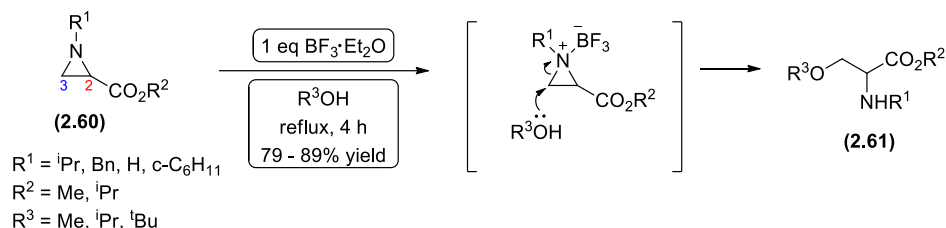
Entry	Substrate/path	R	Nu	Product	Yield (%)
1	(1'<i>R</i>,2<i>R</i>)-(2.57) A	CH ₂ OMe	NaN ₃	(1'<i>R</i>,2<i>R</i>)-(2.58)	89
2			NaOAc		75
3			NaCN		80
4	(1'<i>R</i>,2<i>R</i>)-(2.57) B	CH ₂ OBn	NaN ₃	(1'<i>R</i>,2<i>R</i>)-(2.58)	76
5			NaOAc		79
6			NaCN		81
7	(1'<i>R</i>,2<i>R</i>)-(2.57) C	CO ₂ Et	NaN ₃	(1'<i>R</i>,2<i>R</i>)-(2.59)	87
8			NaOAc		72
9			NaCN		86
10	(1'<i>R</i>,2<i>R</i>)-(2.57) D	CH=CHCO ₂ Et	NaN ₃	(1'<i>R</i>,2<i>R</i>)-(2.59)	71
11			NaOAc		87
12			NaCN		72

Scheme 2.24. Aziridine C-2 substituent dependent regioselectivity of ring-opening by Lee *et al*

The rationale for the C-2 regioselectivity can be attributed to the fact that when acyl or vinyl substituents are present at the C-2 position of an aziridine, the bond between the C-2 carbon and the ring nitrogen is activated towards approaching nucleophiles, as the π -system of the adjacent double bond stabilises the transition state by conjugation.²⁹

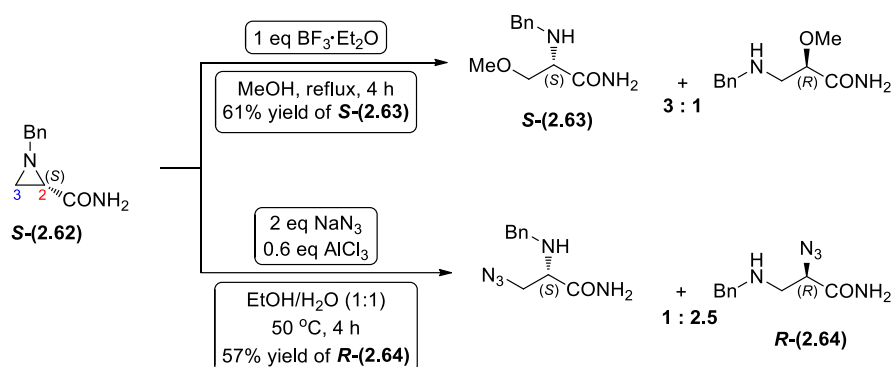
2.4.4. Ring opening of non-activated aziridines *via* an adduct formation

Vessiere *et al* demonstrated that boron trifluoride activated ring-opening reactions of *N*-alkyl-2-alkoxycarbonylaziridines (**2.60**) with aliphatic alcohols afford corresponding α -amino esters (**2.61**) (Scheme 2.25.). The reaction proceeded through a nucleophilic attack at the less hindered side of the aziridinium moiety.⁶⁸



Scheme 2.25. A C-3 directed ring-opening of *N*-alkyl-2-alkoxycarbonylaziridines (**2.60**) with aliphatic alcohols by Vessiere *et al*

Gotor *et al* reported a ring-opening of (*S*)-1-benzyl-aziridine-2-carboxamide **S**-(**2.62**) with methanol under boron trifluoride activation, affording predominantly α -amino carboxamide **S**-(**2.63**) (Scheme 2.26.).⁶⁹ The results have matched the ones reported previously by Vessiere *et al*. However, Gotor *et al* observed a Lewis acid and nucleophile dependent regioselectivity, when aluminium trichloride activated (*S*)-1-benzyl-aziridine-2-carboxamide **S**-(**2.62**) was reacted with sodium azide to afford β -amino carboxamide **R**-(**2.64**) as a major regioisomer.



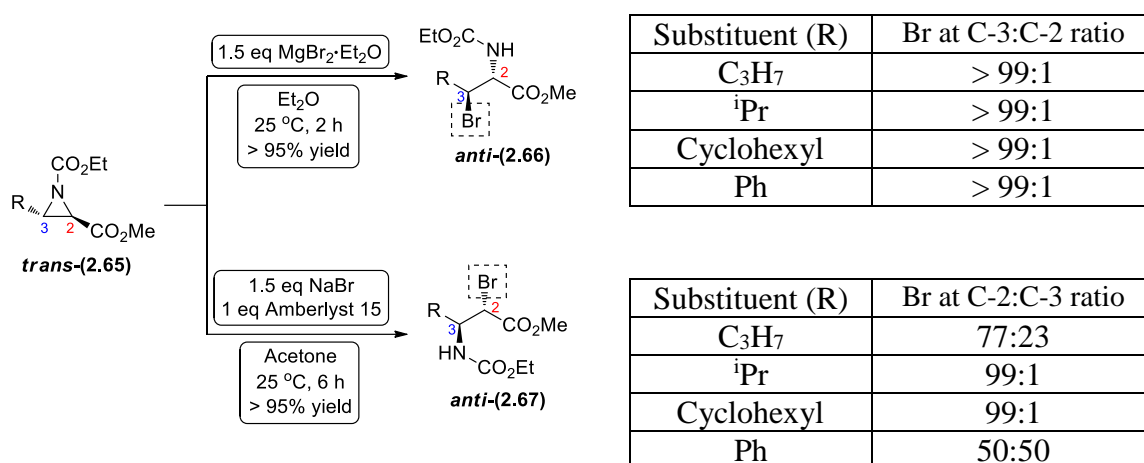
Scheme 2.26. Activation mode and nucleophile dependent regioselectivity of ring-opening of (*S*)-1-benzyl-aziridine-2-carboxamide **S**-(**2.62**) by Gotor *et al*

It was postulated that a complexation effect between aluminium trichloride and a carbonyl group at the C-2 position directed the incoming nucleophile to the proximal C-2 carbon.⁷⁰ Similar effect has been demonstrated by Tanner *et al* (see page 22).

Additional examples of regioselective ring-opening of aziridines are presented below that demonstrate that a choice of a substrate, activation mode and reagents can control exclusive C-2 or C-3 bond cleavage.

2.4.5. Regioselective control of an aziridine ring-opening with halogen nucleophiles

Ring-opening of aziridine-2-carboxylates with halogen nucleophiles affords α - or β -halo-substituted amino acid derivatives. Righi *et al* demonstrated a ring-opening of activated racemic methyl *trans*-aziridine-2-carboxylates **trans**-(**2.65**) with magnesium bromide at the C-3 position, affording α -amino acid derivatives *anti*-(**2.66**) (Scheme 2.27.). When the same starting material was reacted with sodium bromide-Amberlyst15 complex, the bond between the C-2 carbon and ring nitrogen was cleaved affording β -amino acid derivatives *anti*-(**2.67**).⁷¹



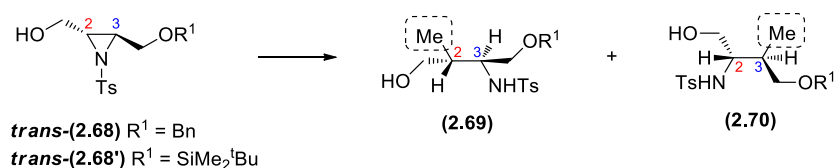
Scheme 2.27. Regioselective ring-opening of methyl *trans*-aziridine-2-carboxylates **trans**-(**2.65**) with magnesium bromide and sodium bromide-Amberlyst15 by Righi *et al*

When magnesium bromide is used as a reagent, the C-3 regioselectivity can be rationalised through a chelated complex between the magnesium metal and the two heteroatoms: a ring nitrogen and an oxygen in the C-2 carbonyl group (further discussion can be found in 5.17. Ring opening of *N*-aryl aziridines with magnesium bromide diethyl etherate, page 80).

2.4.6. Regioselective control of an aziridine ring-opening with carbon nucleophiles

Tanner *et al* investigated a nucleophilic ring-opening of *trans*-aziridino alcohols by methyl-transfer reagents such as trimethylaluminium and Gilman cuprate: lithium dimethyl cuprate (Scheme 2.28).⁷² In general, lithium dimethyl cuprate demonstrated excellent C-2 selectivity and the results can be interpreted in terms of directive effects exerted by the C-1 hydroxyl group, which allows intramolecular methyl transfer.⁷³ On the contrary, complete C-3 selectivity was observed in the reactions of **trans**-(**2.68**) and

trans-(**2.68'**) with trimethylaluminium, indicating a complexation effect of the C-4 benzyloxy or silyloxy groups in those cases.



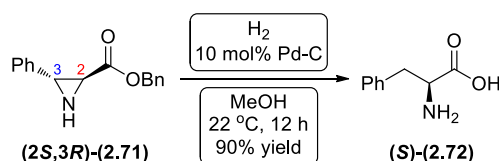
Entry	Substrate	Reagent/conditions	Ratio (2.69):(2.70)	Yield (%)
1	<i>trans</i> -(2.68)	3 eq LiMe ₂ Cu, Et ₂ O, -20 °C, 4 h	> 99:1	80
2	<i>trans</i> -(2.68')	3 eq LiMe ₂ Cu, Et ₂ O, -20 °C, 4 h	> 99:1	98
3	<i>trans</i> -(2.68)	6 eq AlMe ₃ , toluene, 75 °C, 12 h	< 1:99	71
4	<i>trans</i> -(2.68')	6 eq AlMe ₃ , toluene, 75 °C, 12 h	15:85	82

Scheme 2.28. Regioselective ring-opening of *trans*-aziridino alcohols *trans*-(**2.68**) and *trans*-(**2.68'**) by Tanner *et al*

It was proposed that a first equivalent of trimethylaluminium removes the hydroxyl proton from *trans*-(**2.68**) and *trans*-(**2.68'**) to form an aluminium alcoholate, from which methyl-transfer is expected to be slower than from a trialkylaluminium species. A second equivalent of trimethylaluminium then forms a Lewis acid-base complex with the C-4 benzyloxy group, thus allowing for intramolecular methyl-transfer to C-3. The lower C-3 selectivity for *trans*-(**2.68'**) substrate is expected due to steric bulk and the lower Lewis basicity of the *tert*-butyldimethylsilyloxy group. The oxygen basicity decreases upon replacement of alkyl groups by silyl groups because the HOMO orbital becomes less localised on an oxygen atom. Consequently, the key interaction between the ether HOMO and the LUMO of an electrophile is less stabilizing for silyl than for alkyl ethers.⁷⁴

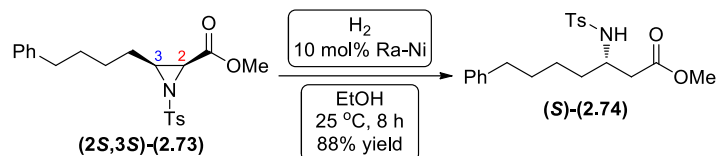
2.4.7. Reductive ring opening

Reductive ring opening of non-activated aziridines with C-3 aryl substituents usually affords α -amino acid derivatives.⁷⁵ Hruby *et al* reported that hydrogenation of (*2S,3R*)-benzyl 3-phenylaziridine-2-carboxylate (*2S,3R*)-(**2.71**) with 10 mol% Pd/C in methanol afforded (*S*)-phenylalanine (*S*)-(**2.72**) in 90% yield (Scheme 2.29).⁷⁶



Scheme 2.29. Synthesis of (*S*)-phenylalanine (*S*)-(**2.72**) via a C-3 ring-opening of (*2S,3R*)-benzyl 3-phenylaziridine-2-carboxylate (*2S,3R*)-(**2.71**) by Hruby *et al*

Davis *et al* demonstrated a Raney-nickel promoted ring-opening of activated *N*-tosyl aziridine (**(2*S*,3*S*)-(2.73)**) with an aliphatic group present at the C-3 position. Hydrogenolysis of the aziridine ring occurred at the C-2 carbon, affording the corresponding β -amino ester (**(*S*)-(2.74)**) (**Scheme 2.30**).⁷⁷



Scheme 2.30. C-2 ring-opening of *N*-tosyl aziridine (**(2*S*,3*S*)-(2.73)**) by Davis *et al*

2.5. Chapter conclusion

Aziridines are extensively used as ‘core’ heterocycle building blocks, that can be readily transformed into alternative structure and function diverse derivatives (e.g. α - and β -amino acids).⁷⁸ Aziridines are used during the synthesis of numerous drugs, biologically active natural products and their derivatives. Over 100 biologically active aziridine-containing compounds have anticancer and/or antibacterial activity against selected cancer cells and/or pathogenic bacteria with the strong indication that aziridine functionality is essential for the properties above.⁷⁹ Additionally, aziridines and their derivatives are produced commercially and are employed in plastic, coating, textile and other industries.⁸⁰

Chapter 3. Glycopeptide antibiotics

3.1. Definition of antibiotics

Antibiotics are natural compounds produced mostly by plant micro-organisms.⁸¹ A term “antibiotic,” was proposed by Selman Waksman, who performed multiple screenings of soils for the presence of biologically active compounds.⁸² The term was introduced to describe the compounds that were produced by microbes and could be used against other microbes, therefore countering infectious diseases.⁸³

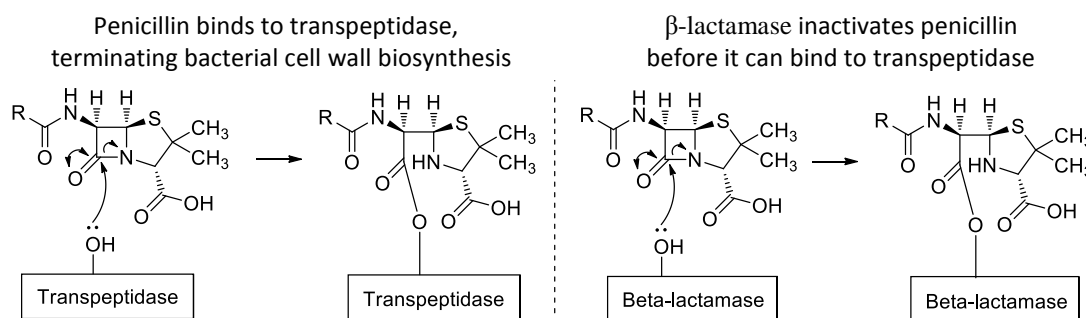
3.2. Classes

Antibiotics can be classified according to their biochemical target (**Table 3.1**).⁸⁴ Depending on the mode of action, antibiotics can suspend bacterial cell growth or kill the bacterial cells entirely. The majority of these antibiotics were discovered by screening bacteria found in soil.

Antibiotic Class	Examples	Target	Mode of Resistance
β -lactams	Penicillins (ampicillin)	Peptidoglycan biosynthesis	Hydrolysis Altered target
Aminoglycosides	Streptomycin	Translation	Phosphorylation
Glycopeptides	Vancomycin Teicoplanin	Peptidoglycan biosynthesis	Reprogramming of peptidoglycan biosynthesis
Phenicol	Chloramphenicol	Translation	Altered target
Quinolones	Ciprofloxacin	DNA replication	Acetylation Altered target

Table 3.1. Antibiotics in clinical use and modes of resistance

Antibiotics like penicillin and vancomycin are effective against Gram-positive bacteria, because they interfere with enzymes required for the bacterial cell wall synthesis.⁸⁵ Structurally penicillin is very similar to the -D-alanyl-D-alanine sequence, found in the bacterial cell wall (**Scheme 3.1**). Therefore, when the transpeptidase enzyme binds penicillin instead of -D-alanyl-D-alanine sequence, the bacterial cell wall synthesis is terminated and the bacteria die.⁸⁶



Scheme 3.1. Mode of action of penicillin (left) and inactivation by β -lactamase (right)

However, not long after penicillin was introduced, some bacteria developed an enzyme β -lactamase, that would ring-open penicillin, thus making it inactive.⁸⁷ Although semi-synthetic penicillins, such as methicillin, were developed, the bacterial resistance to these antibiotics had emerged as well. With the rising bacterial resistance, especially methicillin-resistant *Staphylococcus aureus* (MRSA), which was resistant to the most of the antibiotics in clinical use, it was required to find antibiotics that were effective. The vancomycin group of glycopeptide antibiotics was found to be one of the very few groups of antibiotics that were effective against MRSA.

3.3. Vancomycin and teicoplanin glycopeptide antibiotics

Vancomycin (**3.1**) was isolated in 1956 in the Eli Lilly Research Laboratories from *Streptomyces orientalis* from a soil sample obtained in Indonesia.⁸⁸ Vancomycin has a low toxicity (LD₅₀ i.v. in mice: 489 mg/kg, in rats: 319 mg/kg) displays potent activity against a range of Gram-positive bacteria, with an *in vitro* minimum inhibitory concentration (MIC) of 0.25-1.0 mg/L against MRSA.^{89,90,91}

Perkins demonstrated that vancomycin disrupts the bacterial cell wall synthesis, by terminating the sequence -D-alanyl-D-alanine.⁹² Williams *et al* published a proposed hydrogen bonding interaction between vancomycin and bacteria (**Figure 3.1**).⁹³ Teicoplanin (**3.2**) was isolated in 1978 from *Actinoplanes teichomyceticus* and belongs to the same glycopeptide group of antibiotics as vancomycin.⁹⁴ Although structurally, teicoplanin and vancomycin are very close, teicoplanin possesses additional F-O-G arylglycine biaryl subunit and a lipid attachment (**Figure 3.1. dotted box**)

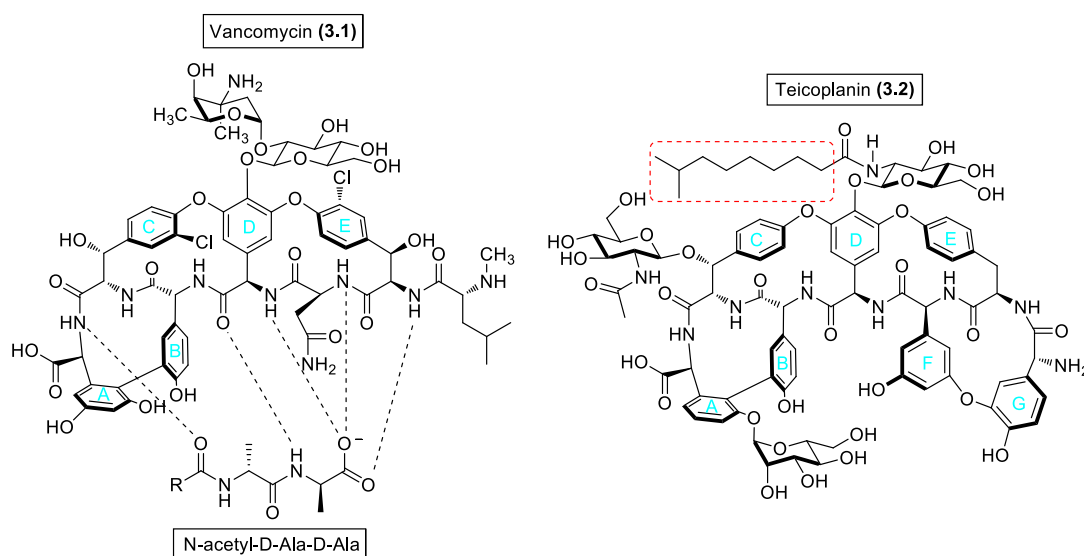


Figure 3.1. The interactions between vancomycin (**3.1**) and bacterial cell wall analogue through hydrogen bonding represented by the dotted lines (left). Structure of teicoplanin (**3.2**) (right)

3.4. α -Arylglycines

α -Arylglycine derivatives constitute a very important class of α -amino acids, because they are found in a wide range of bioactive compounds (**Figure 3.2.**):^{95,96}

- antiplatelet agents to prevent blood clots such as vicagrel and clopidogrel
- β -lactam antibiotics such as amoxicillin, cefadroxil and nocardicin A
- glycopeptide antibiotics such as vancomycin and teicoplanin

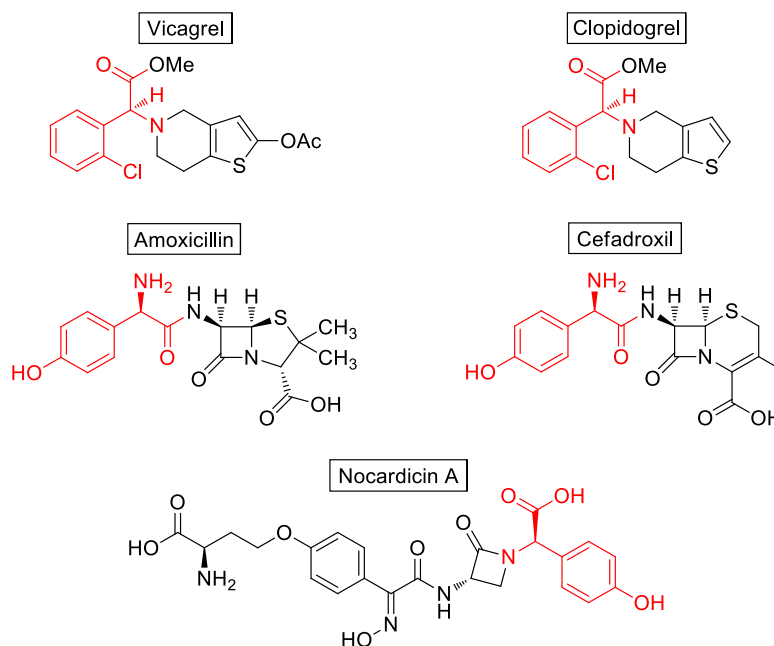


Figure 3.2. Bioactive compounds with α -arylglycine motif (highlighted red)

Several substituted phenylglycine derivatives, including 3-hydroxyphenylglycine, have been described as potent and selective agonists or antagonists of glutamate receptors of the central nervous system (CNS).⁹⁷ Arylglycinols constitute a class of α -amino- β -alcohols, which are also valuable structural units in synthetic and natural compounds.⁹⁸

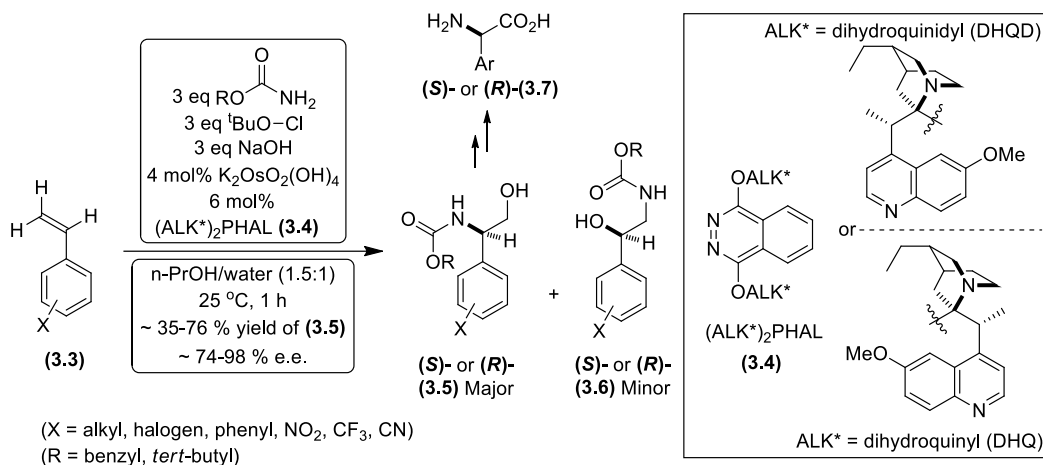
3.5. α -Arylglycine structural motif in glycopeptide antibiotics

Vancomycin and related glycopeptide antibiotics contain a number of arylglycines (**3.7**) within the heptapeptide backbone. Evans *et al* reported that any attempt to synthesize any member of this family of natural products must incorporate a methodology for the construction of these non-proteinogenic arylglycines.⁹⁹

Additionally, arylglycines are easily racemised under basic conditions, because the alpha proton is benzylic, therefore can be easily abstracted.¹⁰⁰

3.6. Aminohydroxylation reaction to afford arylglycines *via* aminoalcohols

In 1998 Sharpless and Reddy reported the osmium catalysed asymmetric aminohydroxylation (AA) reaction, which provided either (*R*)- or (*S*)- α -aryl-*N*-Cbz- or *N*-Boc- protected (*R*)- or (*S*)- α -amino- β -alcohols (**R**)- or (**S**)-(**3.5**) from styrene (**3.3**) (Scheme 3.2).¹⁰¹ The enantioselectivities were generally excellent and a subsequent oxidation step yielded the corresponding α -arylglycine derivatives (**R**)- or (**S**)-(**3.7**).



Scheme 3.2. Asymmetric aminohydroxylation reaction of substituted styrenes by Sharpless and Reddy

It was observed that the regioselectivity was highly dependent on the nature of the styrene (**3.3**) as well as the choice of ligand, solvent, and ligand-solvent combination. Phthalazine ligands (**3.4**) such as (DHQ)₂PHAL or (DHQD)₂PHAL in *n*-PrOH strongly favoured the benzylic amine (**R**)- or (**S**)-(**3.5**) over the benzylic alcohol (**R**)- or (**S**)-(**3.6**) regioisomer. The optimal experimental conditions employed 4 mol% potassium osmate catalyst [K₂OsO₂(OH)₄], 6 mol% alkaloid ligand (DHQ)₂PHAL or (DHQD)₂PHAL, 3.0 equivalents of benzyl carbamate salt [BnOC(O)NNaCl] and *n*-PrOH/H₂O solvent mixture (1.5:1) at 25 °C in order to obtain the corresponding α -arylglycinol (**R**)- or (**S**)-(**3.5**) product.

3.7. Bacterial resistance and overcoming the problem

The vancomycin resistant enterococci (VRE) were first reported in 1989.¹⁰² It appears that these enterococci have been able to obtain genes from other bacteria such that the precursor from which their cell wall is built no longer terminates in -D-alanyl-D-alanine, but rather terminates in -D-alanyl-D-lactate (-D-Ala-D-Lac) (Figure 3.3).^{103,104} As a consequence, the hydrogen bond which is normally made between the NH of the terminal D-alanine group and a carbonyl group of the antibiotic can no longer

be made. Instead, it is replaced by a repulsive interaction between the oxygen of the C-terminal D-lactate group and the carbonyl group of the antibiotic.

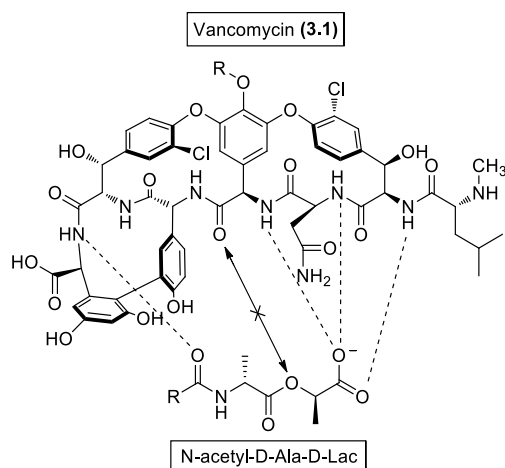


Figure 3.3. The repulsive interaction between vancomycin (3.1) and N-acetyl-D-Ala-D-Lac

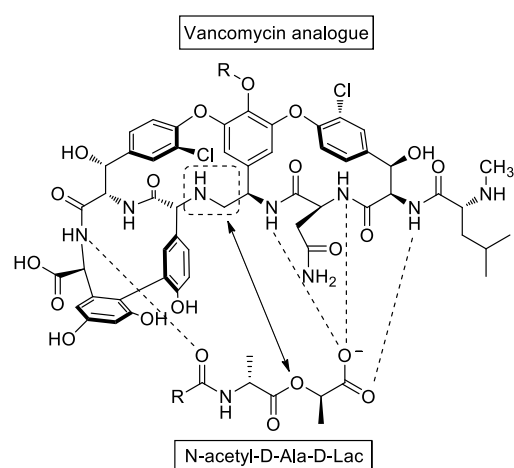


Figure 3.4. Elimination of the repulsive interaction between vancomycin analogue and N-acetyl-D-Ala-D-Lac

The emergence of bacterial strains, resistant to antibiotics, stimulated the synthesis of the individual natural products. In 1998 Evans *et al* reported the first total synthesis of the vancomycin aglycon and the eremomycin aglycon.¹⁰⁵ The group of Boger succeeded in the total synthesis of vancomycin and subsequent modifications to overcome the bacterial resistance with the D-Ala-D-Lac sequence (**Figure 3.4**).¹⁰⁶ By removing the carbonyl group, a repulsive interaction with the oxygen atom of the D-Ala-D-Lac moiety of resistant bacteria was eliminated, thereby restoring the affinity towards the target.

Scientists at Lilly laboratories demonstrated a different approach of overcoming the problem. Instead of modifying the peptide backbone, the periphery was functionalised with hydrophobic groups (**Figure 3.5**). The new derivatives successfully restored activity against resistant bacteria.^{107,108}

The original rationale behind this modification came from a comparison of vancomycin and teicoplanin. Teicoplanin possesses an acyl-linked aliphatic moiety (**Figure 3.1, dotted box**) that is believed to affect pharmacokinetic properties, such as longer serum half-life. Additionally, teicoplanin shows greater potency than vancomycin against many Gram-positive bacteria.¹⁰⁹

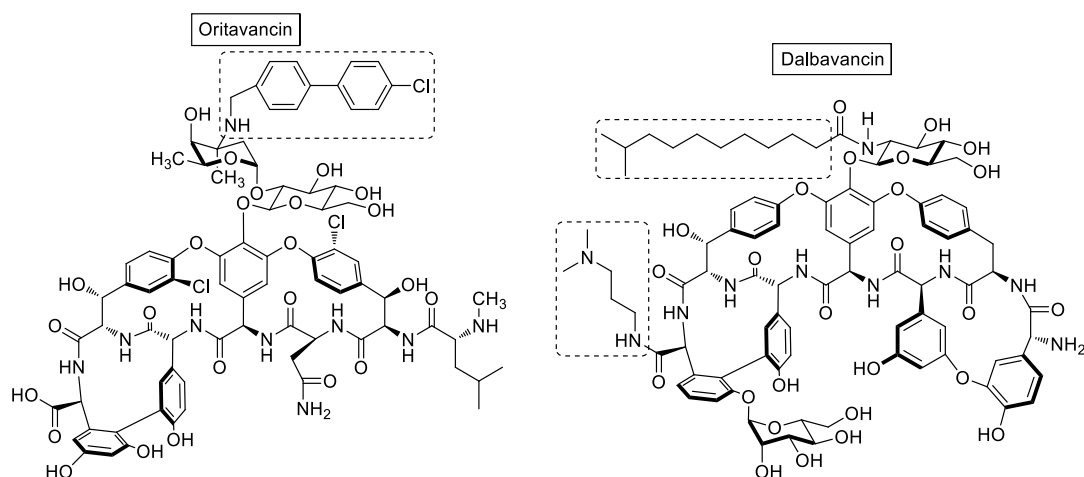


Figure 3.5. Lipid attachments (dotted boxes) promoted membrane anchoring and dimerisation

Williams and co-workers proposed that lipid attachments on glycopeptides were acting like anchors to the bacterial cell membrane (**Figure 3.6**).¹¹⁰ Without lipid groups, glycopeptides were distributed more broadly in the peptidoglycan layers. Due to anchoring, teicoplanin was able to insert itself into the membrane, in a very close proximity to D-Ala-D-Lac sequence. The interaction between the two was proposed to become intramolecular, which was more favourable than intermolecular.

The group of Williams demonstrated that dimerisation of the antibiotics enhanced the binding affinities to their cellular targets by preferential location of the antibiotic near the site of cell wall biosynthesis. Williams *et al* hypothesised that the binding of a dimer to two cell wall peptides involves only one bimolecular process, whereas in the binding of two equivalents of monomeric antibiotic, two bimolecular steps are involved, which is less favourable.¹¹¹

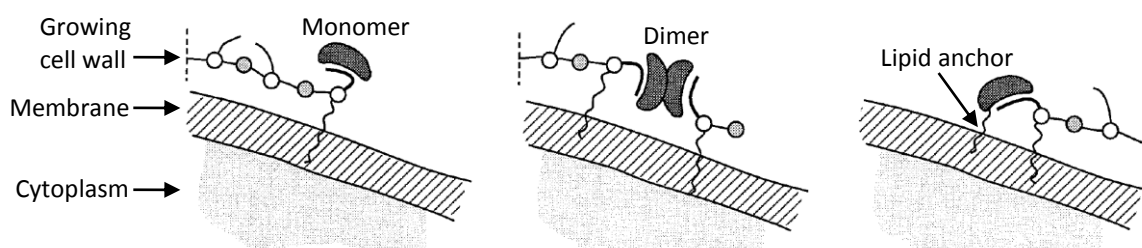


Figure 3.6. The binding bacteria and antibiotic monomer (left), dimer (middle) and via the lipid anchor (right) adopted from the publication by Williams *et al*¹¹¹

3.8. Chapter conclusion

In 2013 Bauer and Brönstrup published a review about industrial drug discovery and development based on the natural products.¹¹² They reported that modification of glycopeptides with hydrophobic side chains created a sub-class called “lipoglycopeptides”. The structural modifications resulted in the improved properties:

- Lipid chains promoted the membrane anchoring, positioning the glycopeptide in the close proximity to its target.
- The side chains enhanced the dimerisation of the lipoglycopeptides, which resulted in a much tighter binding to the peptidoglycan layer.
- The increased hydrophobicity also led to higher protein binding compared to vancomycin, resulting in longer *in vivo* half-life of the drug.

In summary, successful total synthesis of the desired antibiotics allowed to elucidate their mode of action and study their biological properties. Careful modifications of the antibiotics fine-tuned the physicochemical properties, which restored efficacy against resistant pathogens and improved pharmacokinetic properties.

Chapter 4. Properties and applications of compounds labelled with stable isotopes

4.1. Discovery of isotopes

Frederick Soddy was one of the pioneering scientists who investigated the chemistry of radioactive substances and the nature of isotopes. In 1910, Soddy demonstrated that mesothorium, the first product of the thorium disintegration series, was chemically inseparable from radium.¹¹³ He developed a concept that some atoms can be chemically identical and yet have different atomic weights. To describe such a phenomenon, the term "isotope" was introduced (Greek for ἴσος [isos] "**equal**" and τόπος [topos] "**place**"), because these related atoms occupied the same place in the periodic table of the elements.

The discovery of isotopes of stable elements was made by Thomson in 1912.¹¹⁴ He used positive ray apparatus to determine the atomic weight of the gases in the discharge tube. Each atom produced a separate parabola on the photographic plate. When analysing the sample of neon, two parabolas corresponding to atomic weights 20 and 22 were observed. The first one was assigned to neon (atomic weight 20), whereas the second could not be assigned as any known gas. Thomson's student Francis Aston attempted to separate this unknown gas from neon, but was unsuccessful. Thomson and Aston believed that the two gases, although of different atomic weights, had identical chemical properties.

Unfortunately, the "parabola method" had limitations.¹¹⁵ Aston noticed that many rays were lost due to collisions in the narrow canal-ray tube. As a result, Aston had to re-design and build a different version of the apparatus, improving the materials, vacuum and slit system. The new apparatus was found to work satisfactorily after successfully referencing it to the oxygen and carbon mass spectra data. When analysing a sample of neon, using the new equipment, similar results were obtained, confirming that neon is a mixture of two isotopes of atomic weights 20 and 22.

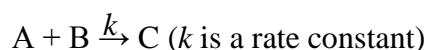
Conversely, Aston did not identify any isotopes of hydrogen, he only reported hydrogen itself with atomic weight of one. In 1931, Birge and Menzel noticed a difference in the atomic weights of hydrogen when determined chemically and by mass spectrometry.¹¹⁶ They made a hypothesis about the existence of an isotope of hydrogen with a mass of two. Urey *et al* performed a concentration experiment in order to obtain a sample of heavy isotope of hydrogen.¹¹⁷ The initial experiment involved distillation of liquid hydrogen near its triple point and was a success. The isotope of hydrogen of atomic weight of two was obtained and named deuterium (Greek for δεύτερος

[deuterios] "**second**").¹¹⁸ Later on, Urey and Washburn developed an electrolytic method of separation of the isotopes of hydrogen.

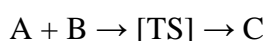
4.2. Deuterium, kinetic isotope effect

Compared to the hydrogen nucleus (the proton), with an atomic mass 1.008 AMU, the deuterium nucleus (the deuteron) contains an additional neutron, which results in a near two-fold increase of the atomic mass (2.014 AMU).¹¹⁹ Due to the greater atomic mass of deuterium, a carbon-deuterium (C–D) bond has a lower zero-point energy (vibrational ground state energy) than the corresponding carbon-hydrogen (C–H) bond. This results in a higher activation energy for C–D bond cleavage and a slower reaction rate (represented by rate constant k). The effect on rate is known as the primary deuterium isotope effect (DIE), which is expressed as the ratio of the reaction rate constants of C–H versus C–D bond cleavage: $\text{DIE} = k_{\text{H}}/k_{\text{D}}$.¹²⁰

Apart from deuterium, other isotopes can affect the bond energy of a labelled compound. The effect of isotopic substitution on a rate constant is referred to as a kinetic isotope effect (KIE).^{121,122} For example, in the reaction:



the effect of isotopic substitution in reactant A is expressed as the ratio of rate constants $k_{\text{l}}/k_{\text{h}}$, where the subscripts "l" and "h" represent reactions in which A contains the light and heavy isotopes, respectively. Within the framework of transition state theory the reaction can be rewritten as:



Primary KIE arises from the direct breaking, or formation, of a bond to, or from, isotopically substituted atom in the rate-controlling step of a specified reaction. Secondary KIE arises when the bond to the isotopically substituted atom is not cleaved during the reaction.

The effect of isotopic substitution on molecular vibration can be understood by considering a diatomic model, which can be represented as two masses connected by a spring.¹²³ Each mass represents one atom of the molecule and the spring represents a chemical bond (**Figure 4.1.**).

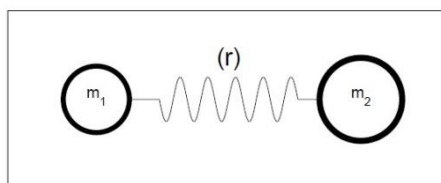


Figure 4.1. A diatomic model: two masses connected by a spring

The vibrational energy in the ground state (zero-point energy, E_0) depends on the frequency of the bond stretch (ν), which in turn is dependent on the reduced mass of the two connected atoms (μ) (**Figure 4.2.**)¹²⁴

$$E_0 = 1/2 h \nu$$

$$\nu = \frac{1}{2\pi} \sqrt{\frac{k_f}{\mu}}$$

$$\mu = m_1 m_2 / (m_1 + m_2)$$

(k_f and h are constants)

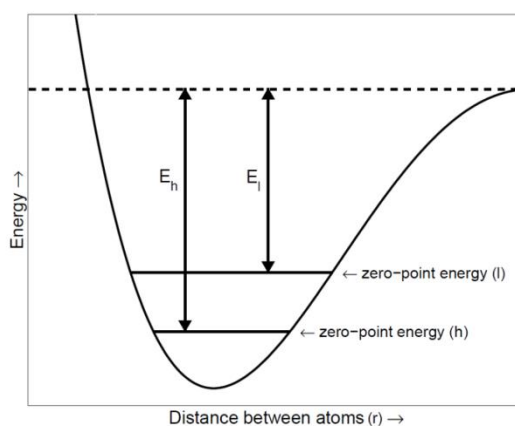


Figure 4.2. Activation energies (E_h and E_l) required for dissociation of heavy and light atoms

In summary, due to the higher mass, and thus lower vibrational frequency of the molecule that contains the heavy isotope, its ground state energy (also called the zero point energy) is generally lowered. Complete dissociation of a bond with the isotopically substituted atom consequently requires more energy ($E_h > E_l$) than that for a corresponding "lighter" bond in the same environment.

The increased bond stability to isotopically substituted atom may lead to changes of properties of a drug. By altering the metabolic pathways of the compound, its biological activity may be enhanced, reduced or prolonged. By carefully fine-tuning the pathway, the formation of an active metabolite may be achieved or the formation of a toxic one may be avoided.¹²⁵

Initial studies demonstrated that the physical properties of deuterium oxide were different to those of normal water (**Table 4.1.**)^{45,126}

Property	H ₂ O	D ₂ O
Melting point	0 °C	3.8 °C
Boiling point	100 °C	101.42 °C
Density	0.9982	1.1056

Table 4.1. Physical properties of deuterium oxide and hydrogen oxide

4.3. Application of isotopes

In 1969, Jones reported that since 1960 there has been a reawakening of interest in stable isotopes. This may be attributed to developments in the analytical equipment (MS and NMR in particular) that allow researchers to trace and study desired labelled compounds.¹²⁷

Non-radioactive isotopes, also known as stable isotopes, are used extensively in industry and academia. Compounds labelled with one or multiple stable isotopes (e.g. ^{13}C , ^{15}N , ^2H , etc) combined with analytical techniques (NMR, GS, MS, IR) can provide a valuable information in the elucidation of reaction mechanisms and metabolic research.¹²⁸

The increase in the use of deuterium labelling can be explained by the central position which hydrogen holds in chemistry and its role in proton transfer reactions. Initial studies of deuterated water, established its low toxicity towards mammalian cells.¹²⁹ Safety is one of the benefits of stable isotopes, which enables their use for *in vivo* human studies.¹³⁰ Deuteration may change the pathway of drug metabolism, which is called metabolic switching. This may lead to increased duration of action and lower toxicity.

The shape of the molecule depends on its atoms and the interactions of their electron clouds. Due to the fact that deuterated and non-labelled analogues have the same number of electrons, the shapes and sizes of the compounds are very similar (Figure 4.3).¹³¹

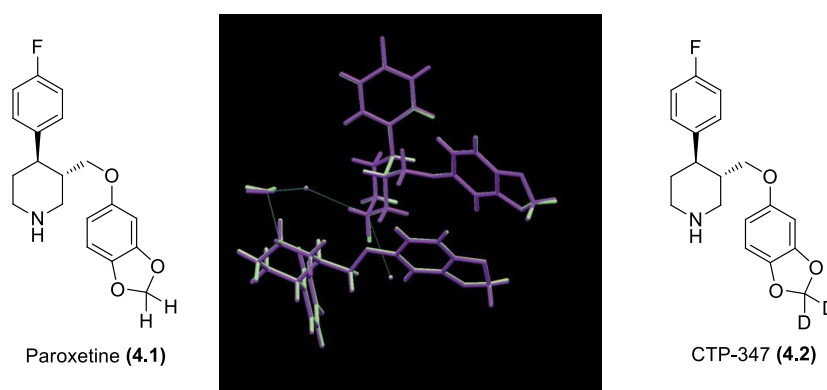
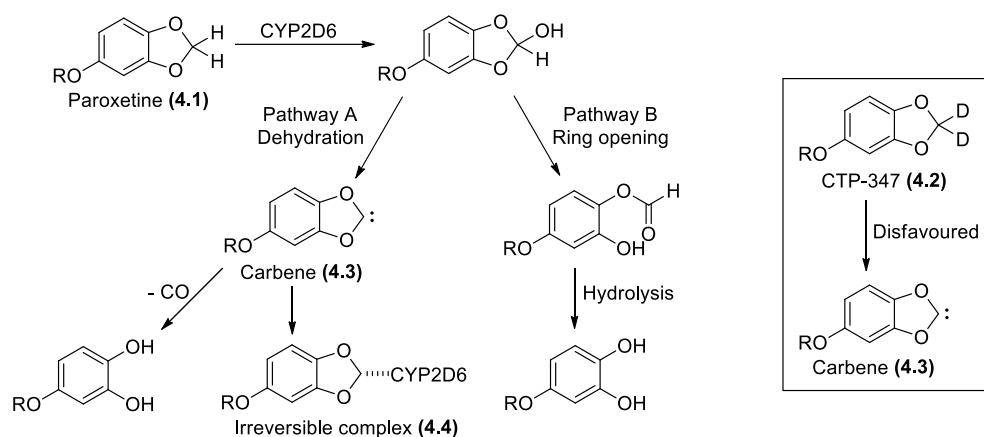


Figure 4.3. An overlay of the crystal structures of CTP-347 (4.2) hydrochloride hemihydrate (purple) and paroxetine (4.1) hydrochloride hemihydrate (green)

Concert Pharmaceuticals developed a compound called CTP-347 (4.2), a selectively deuterated analogue of paroxetine (4.1), for the treatment of hot flashes.¹³² Modification was required, because paroxetine (4.1) irreversibly inactivates the liver enzyme CYP2D6, leading to various side effects when used in combination with other

medications. The proposed mechanism (**Scheme 4.1.**) shows the covalent binding between paroxetine metabolite and the active site of CYP2D6, forming irreversible complex (**4.4**).¹³³ On the contrary, CTP-347 (**4.2**) demonstrated little to no CYP2D6 inactivation, when the experiments were performed *in vitro*. It is believed that selective deuteration prevents the formation of the undesired carbene metabolite (**4.3**).



Scheme 4.1. Proposed mechanism of CYP2D6 inactivation by the carbene metabolite (4.3) of paroxetine (4.1)

CTP-347 (**4.2**) was subsequently studied in a patient clinical trial. Along with CTP-347, dextromethorphan was administered, which acts as a selective probe for CYP2D6 activity. Subjects receiving CTP-347 were able to metabolise dextromethorphan better than the patients who received paroxetine. This demonstrated the benefit of using deuterium over hydrogen in order to overcome undesired drug-drug interactions, potentially enabling the broader use of CTP-347 with other drugs.

Despite the change in the metabolic pathway, CTP-347 has the same inhibition and selectivity as paroxetine. In the enzyme assays the two drugs were essentially identical. Human assays proved that CTP-347 did not form any unwanted metabolites compared to paroxetine.

Auspex Pharmaceuticals announced that a deuterated version of venlafaxine causes fewer side effects and stays in the bloodstream longer than the non-deuterated version, which prolongs the action of the drug.¹³⁴

4.4. Magnetic properties of atomic nuclei

Many atoms (^1H , ^{13}C , ^{15}N , etc) have positively charged nuclei that will resonate and spin, when placed in a strong magnetic field (**Figure 4.4**).¹³⁵ Due to angular momentum, the nucleus spins in a circular motion called the precession rate:

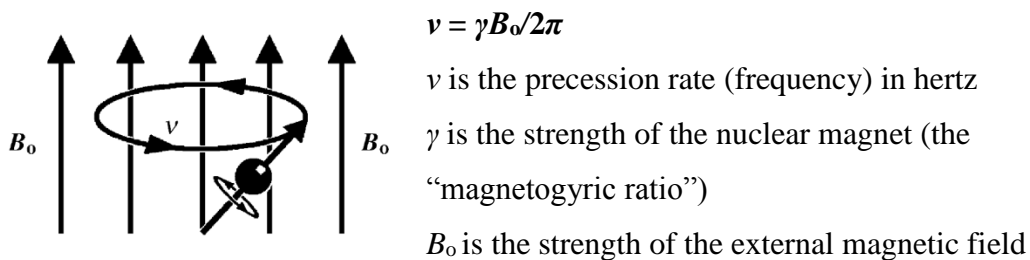


Figure 4.4. Model of spinning nucleus in an external magnetic field

Measuring the resonant frequency of an atom gives us detailed information about the molecular structure. A selection of some NMR active nuclei is shown below (**Table 4.2.**).¹³⁶ The magnetogyric ratio is a constant for any particular type of nucleus and is directly proportional to the strength of the nuclear magnet and therefore to the NMR signal strength (proton NMR has got the strongest signal).

Nucleus	Spin: I	Abundance (%)	Magnetogyric ratio: γ ($10^6 \text{ rad s}^{-1} \text{ T}^{-1}$)
^1H	$\frac{1}{2}$	~100	267.522
^2H	1	0.015	41.066
^{13}C	$\frac{1}{2}$	1.1	67.283
^{15}N	$\frac{1}{2}$	0.37	19.338
^{19}F	$\frac{1}{2}$	~100	251.815
^{31}P	$\frac{1}{2}$	~100	108.394

Table 4.2. Properties of some NMR active nuclei

NMR-active nuclei, located in the bonding network, do interact with each other, creating spin-spin splitting. The value of the splitting constant (J) will depend on the nuclei involved in the interaction. By labelling a compound with selected isotopes it is possible to achieve enhancement of some signals (e.g. ^{13}C label displays strong peak in ^{13}C -NMR) or masking of others (e.g. replacing ^1H with ^2H therefore removing proton signals). Additionally, specific NMR experiments can provide information about shape and configuration of the molecule and the interactions between molecules.

4.5. Synthesis of isotopically labelled compounds

Incorporation of stable isotopes into organic compounds can be achieved by two methods: synthetic and exchange.¹³⁷

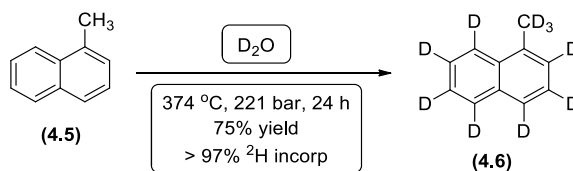
Synthetic method involves a synthesis of ^2H -labelled compounds (also ^{13}C , ^{15}N , etc) *via* a series of chemical reactions, starting from commercially available stable isotope-labelled precursors. Using this method a highly selective incorporation of the isotopic label at the desired position can be achieved. However, long synthetic routes and the high costs of some isotopically labelled starting materials (e.g. ^{13}C and ^{15}N)

must often be taken into account. Up to date, ^{13}C and ^{15}N -labelled compounds are commercially available (> 2000 compounds available from Sigma-Aldrich, May 2015) and can be used as synthons during the synthesis of a desired target molecule.

Exchange method offers a direct exchange of a hydrogen atom (bonded to a carbon atom) by a deuterium atom in the desired compound. These exchange reactions can be carried out directly on the target molecule using reagents such as D_2O or D_2 gas as the deuterium source. This method is particularly efficient if carried during the final stage of the synthetic sequence, because introduction of the isotopes early in the synthesis may lead to the loss of the label. However, poor selectivity and incomplete deuteration can be among the disadvantages of the above method. Exchange method is also applicable to the ^{18}O isotope.¹³⁸

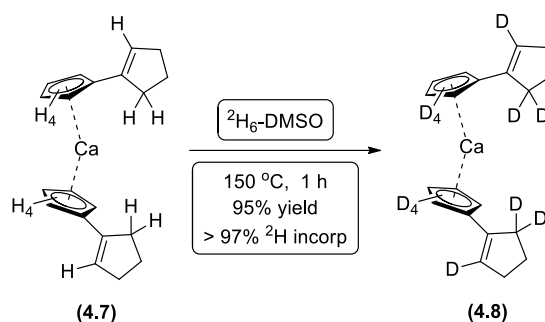
4.5.1. H/D exchange without the addition of acid or base

Junk and Catallo demonstrated that H/D exchange can be carried out in supercritical media by performing a deuteration of arenes with D_2O in autoclaves above $370\text{ }^\circ\text{C}$.¹³⁹ Thus, an almost complete incorporation of deuterium was achieved (> 97% ^2H incorporation) of (4.6) in the exchange reaction between 1-methylnaphthalene (4.5) and D_2O (Scheme 4.2.).



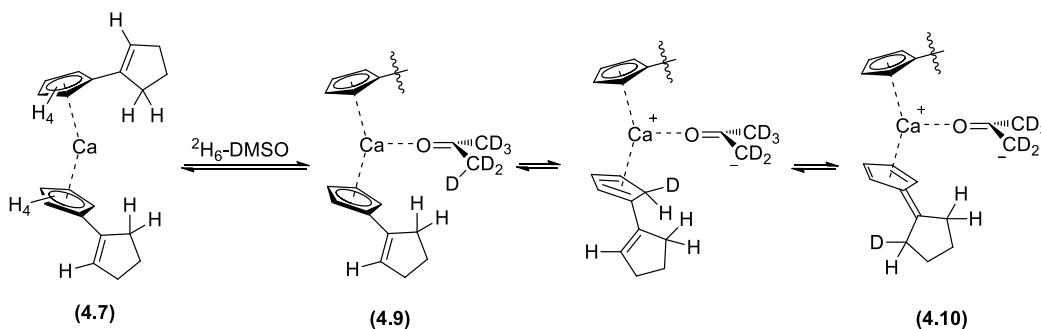
Scheme 4.2. H/D exchange of 1-methylnaphthalene (4.5) under supercritical conditions by Junk and Catallo

Shapiro *et al* reported a method for deuterating cyclopentadienyl (Cp) ligands in calcocenes (Scheme 4.3.).¹⁴⁰ The four hydrogen atoms of Cp ligands were exchanged for deuterium in $^2\text{H}_6$ -DMSO by heating a closed vessel at $150\text{ }^\circ\text{C}$ for 1 hour (> 97% ^2H incorporation). Furthermore, it was possible to deuterate substituents on the Cp rings at those positions that are π -conjugated with the cyclopentadiene moiety through a fulvene tautomer (Scheme 4.4.).



Scheme 4.3. H/D exchange of Cp_2Ca (4.7) by Shapiro *et al*

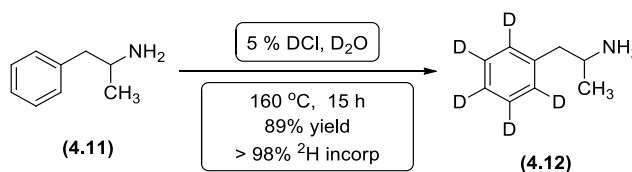
Shapiro *et al* proposed that H/D exchange proceeded by the coordination of $^2\text{H}_6$ -DMSO to the calcium (4.9). Labelling of the 2,5-positions of the cyclopentenyl substituents was proposed to occur *via* a fulvene intermediate (4.10).



Scheme 4.4. Proposed mechanism of H/D exchange of Cp_2Ca (4.7) by Shapiro *et al*

4.5.2. Acid-catalysed H/D exchange

Aromatic compounds can undergo H/D exchange when treated with acids. Ingold *et al* demonstrated deuteration of benzene to afford $^2\text{H}_6$ -benzene *via* D_2SO_4 catalysed exchange.¹⁴¹ Additionally, milder system $\text{BF}_3 \cdot \text{D}_2\text{O}$ was reported to yield deuterated aromatic compounds.¹⁴² The group of Leis synthesised $^2\text{H}_5$ -amphetamine (4.12) in 89% yield by treating amphetamine (4.11) with 5% DCl in D_2O for 15 hours at 160 °C (Scheme 4.5).¹⁴³

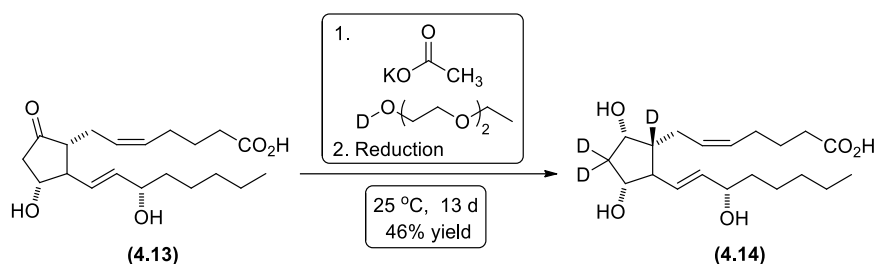


Scheme 4.5. H/D exchange of amphetamine (4.11) under acidic conditions by Leis *et al*

4.5.3. Base-catalysed H/D exchange

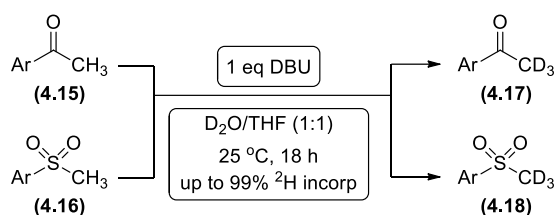
Base-catalysed H/D exchange may be useful when the compound is acid-sensitive. Falardeau *et al* reported a synthesis of the methyl ester of [8,10,10- $^2\text{H}_3$]PGF_{2α} (4.14) (Scheme 4.6).¹⁴⁴ Prostaglandin E₂ (4.13) was treated with deuterium-labeled

carbitol in the presence of anhydrous potassium acetate and underwent α -H/D exchange *via* an intermediate enolate. Subsequent reduction afforded the desired deuterated product (**4.14**).



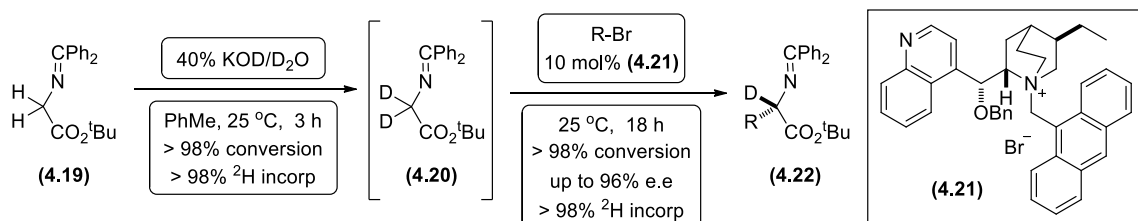
Scheme 4.6. H/D exchange of PGE₂ (**4.13**) under basic conditions by Falardeau *et al*

Berthelette *et al* developed a method of labelling aryl methyl sulfones (**4.16**) and aryl methyl ketones (**4.15**) with deuterium (**Scheme 4.7.**)^{145,146} 1,8-Diazabicyclo[5.4.0]undec-7-ene (DBU) was found to be the most suitable base in the D₂O/THF (1:1) solvent system. The desired products (**4.17**) and (**4.18**) were afforded with up to 99% ²H incorporation.



Scheme 4.7. H/D exchange of (**4.15**) and (**4.16**) under basic conditions by Berthelette *et al*

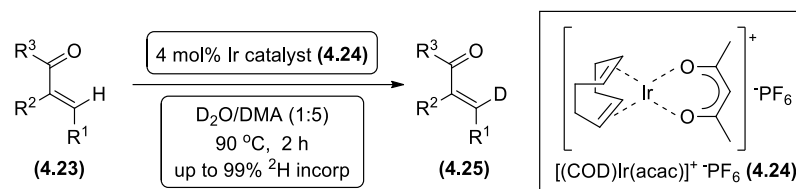
Lygo and Humphreys developed a method for the synthesis of deuterium labelled L- α -amino acid precursors (**4.22**) *via* asymmetric alkylation of a benzophenone-derived glycine imine (**4.19**) (**Scheme 4.8.**). The key alkylation step employs a chiral quaternary ammonium salt (**4.21**) derived from cinchonidine in conjunction with KOD in D₂O, enabling both side-chain and isotopic label to be incorporated in a single reaction step *via* the intermediate (**4.20**).¹⁴⁷



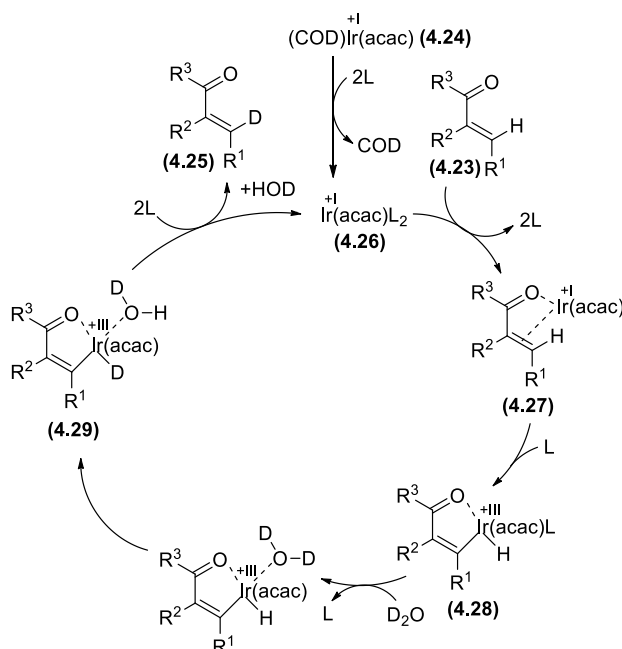
Scheme 4.8. H/D exchange of the glycine derived imine (**4.19**) under basic conditions by Lygo and Humphreys

4.5.4. Homogeneous metal catalysts

Fels *et al* demonstrated Iridium-catalysed H/D exchange reaction in aromatic and non-aromatic double bonds if an electron-donating group was in a 1,4-relation with the carbon where the H/D exchange occurred (**Scheme 4.9**).¹⁴⁸



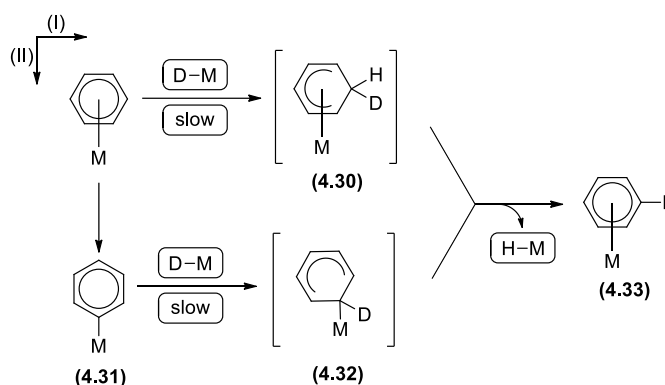
Fels and co-workers demonstrated that cyclooctadiene ligand was replaced by solvent molecules, *N,N*-dimethylacetamide (DMA), to form the real catalytically active compound (**4.26**) (**Scheme 4.10**). In the mechanism proposed by Fels *et al*, coordination of the substrate to the iridium catalyst occurs first, forming the complex (**4.27**). This is followed by the oxidative insertion of iridium into the C–H bond (**4.28**). Subsequently, coordination of D₂O promoted H/D exchange (**4.29**). The reductive elimination afforded a regeneration of the catalyst (**4.26**) and the labelled product (**4.25**). This proposed mechanism reflects the preferred square-planar coordination sphere for Ir(I) and the octahedral coordination for Ir(III).



4.5.5. Heterogeneous catalysts

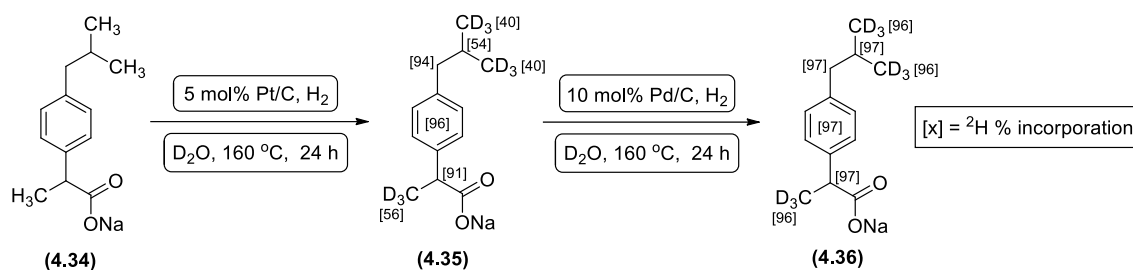
An important technical advantage of heterogeneous catalysis over homogeneous is the possibility to remove the catalyst by simple filtration at the end of the reaction. High activity for H/D exchange has been found with palladium, platinum, rhodium, nickel, and cobalt catalysts.¹⁴⁹

In 1964 Garnett and co-workers postulated that a π -complex mechanism had to be involved in heterogeneously catalysed H/D exchange.¹⁵⁰ Kinetic investigations indicated that, in addition to an associative mechanism, a competing dissociative π -complex mechanism was also involved (**Scheme 4.11.**). In the associative mechanism (**I**), direct substitution of a hydrogen atom by a deuterium atom bound to the metal centre takes place (**4.30**). In the dissociative mechanism (**II**), a proton of the initially formed π -complex is substituted by the metal atom to form a carbon-metal σ -bond (**4.31**). In the second step (**4.32**) a substitution of the metal atom by a deuterium atom takes place to form the product (**4.33**).



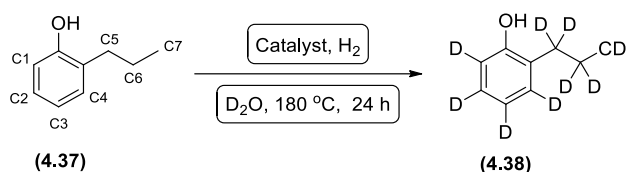
Scheme 4.11. Proposed associative (**I**) and dissociative mechanism (**II**) of the heterogeneous H/D exchange of aromatic substrates by Garnett *et al*

It has been demonstrated by comparative studies of Sajiki and co-workers that palladium catalysts were able to promote the H/D exchange reactions in inactive alkyl chains, while platinum catalysts were superior at deuteration of aromatic positions. Sajiki *et al* reported excellent deuterium incorporation (min 96%) of ibuprofen (**4.34**), an anti-inflammatory drug (**Scheme 4.12.**).¹⁵¹ The non-labelled compound (**4.34**) was subjected to the deuteration procedure catalysed by 5 mol% Pt/C, which resulted in the high levels of the deuterium incorporation at the aromatic and benzylic positions (**4.35**). Subsequent 10 mol% Pd/C-catalysed H/D exchange afforded excellent deuterium incorporation in the non-activated alkyl chains (**4.36**).



Scheme 4.12. Sequential deuteration of ibuprofen (4.34) by Sajiki *et al*

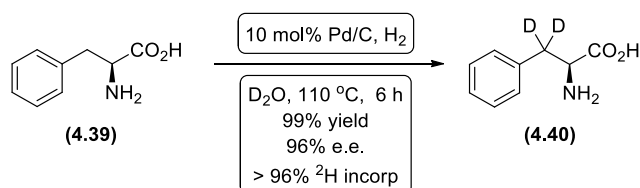
Sajiki *et al* extended the methodology to overcome the low levels of deuteration at sterically hindered positions. Attempted deuteration of 2-*n*-propylphenol (4.37) with either palladium or platinum afforded only moderate deuterium incorporation at the C-4 position of (4.38) which has steric hindrance of the alkyl chain (Scheme 4.13. Entry 1 and 2).¹⁵² However, when combined palladium and platinum complexes were used as a catalyst, fully deuterated ²H₁₁-2-*n*-propylphenol (4.38) was obtained (Scheme 4.13. Entry 3). This result indicates that a more dispersed catalyst has a higher activity in the H/D exchange reaction and demonstrates the presence of a synergistic effect between the platinum and palladium complexes.



Entry	Catalyst (wt%)	² H Content [%]							Yield [%]
		C1	C2	C3	C4	C5	C6	C7	
1	10% Pd/C (10%)	99	98	99	48	98	97	97	84
2	5% Pt/C (20%)	98	98	98	38	72	42	28	62
3	5% Pd/C (20%) + 5% Pt/C (20%)	99	99	98	97	98	98	98	84

Scheme 4.13. Synergistic effect of palladium and platinum in H/D exchange of (XX) by Sajiki *et al*

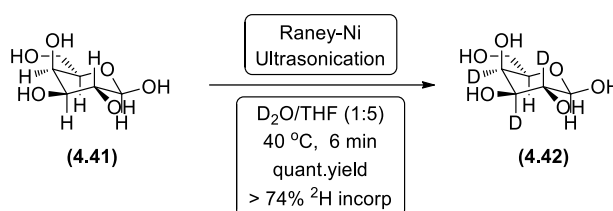
Sajiki *et al* demonstrated a selective deuteration of the β-position of L-phenylalanine (4.39) by using Pd/C-H₂/D₂O system (Scheme 4.14).¹⁵³ The deuterated analogue (4.40) was afforded in 99% yield, 96% ²H incorporation and more importantly without any racemisation.



Scheme 4.14. Palladium-catalysed H/D exchange of (4.39) by Sajiki *et al*

Cioffi and co-workers developed a deuteration of carbohydrates with Raney-nickel catalyst, which proceeded with a retention of configuration (Scheme 4.15).¹⁵⁴

Methyl- β -D-galactopyranoside (**4.41**) was subjected to ultrasonication conditions, that afforded the desired product (**4.42**) in quantitative yield and more than 74% ^2H incorporation.¹⁵⁵



Scheme 4.15. Raney-nickel-catalysed H/D exchange of (**4.41**) by Cioffi *et al*

4.6. Chapter conclusion

Non-radioactive isotopes, also known as stable isotopes, are used extensively in industry and academia in the research areas such as: drug metabolism, toxicology, pharmacokinetics and reaction mechanisms.^{156,157,158,159} Compounds labelled with one or multiple stable isotopes can provide a valuable information, which would be unavailable if only non-labelled compounds are studied. With the advent of peptides and proteins, it is important to study them rigorously to understand and improve drug treatment.

Section 2. Results **and Discussion**

Chapter 5. Synthesis and applications of chiral non-racemic aziridines labelled with stable isotopes

5.1. Chapter introduction

Up to date numerous methods have been reported for the synthesis of ^2H -, ^{13}C -, ^{15}N - and ^{18}O -labelled proteinogenic and non-proteinogenic α -amino acids covered in the review by Kelly *et al* and publications by Veglia *et al* and Geierstanger *et al*.^{160,161,162} However, some methods suffer from harsh reaction conditions (high temperatures, strong acids or bases), toxic and environmentally unfriendly metal salts, multi-step inefficient protocols or formation of inseparable by-products.¹⁶³ Furthermore, relatively low yields and/or reduced levels of ^2H incorporation are among common drawbacks.

Optically active aziridines are well-known precursors for chiral α - and β -amino acids. Thus, we were looking to develop an atom-efficient, multi-component, organocatalytic protocol to access structurally diverse optically active aziridines labelled with stable isotopes. Employing readily generated isotopically labelled aldehydes, amines and alkyl diazoacetates as building blocks, we aimed to maximise the number and type of isotope nuclei embedded within an aziridine, without additional reaction optimisation.

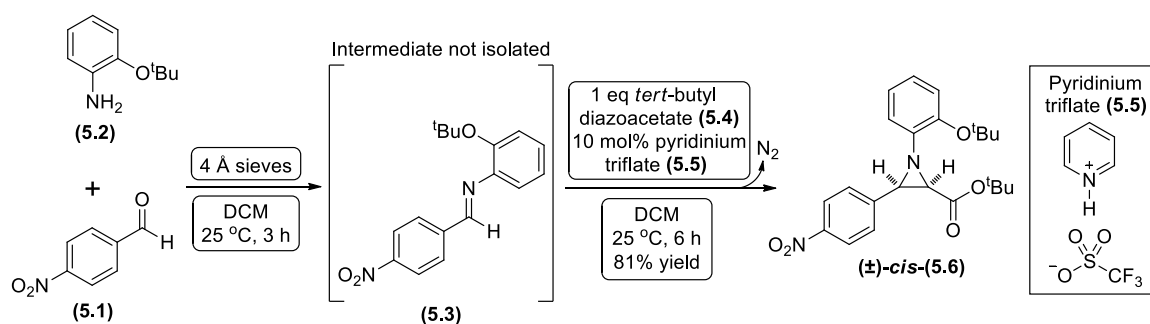
Initially, we performed model organocatalytic aziridination reactions to generate non-labelled racemic and chiral non-racemic *cis*-aziridines. By establishing optimal reaction conditions, we aimed to synthesise chiral non-racemic *cis*-aziridines, labelled with stable isotopes, *via* an organocatalytic asymmetric aziridination reaction.

5.2. Studies towards a racemic aziridination protocol

The work that was previously carried out within the Bew group, focused on developing novel aziridination reaction protocols. This work demonstrated that a Brønsted acid, pyridinium triflate (**5.5**), catalysed a reaction between ethyl or *tert*-butyl diazoacetate and *N*-alkyl or *N*-arylimine.¹⁶⁴ Using this simple organocatalyst, racemic (\pm) *N*-aryl-, *N*-alkyl- and *NH*- $\text{C}_{2,3}$ -disubstituted aziridines were generated in good yields (up to 92%) and diastereoselectivities (*cis*- predominantly over *trans*-). The selection of the catalyst (**5.5**) was based on the work of Johnston *et al*, who employed various Brønsted acids (e.g. acetic acid [$\text{p}K_{\text{a}}$ 4.75], trifluoroacetic acid [$\text{p}K_{\text{a}}$ 0.5], triflic acid [$\text{p}K_{\text{a}}$ -14]) as catalysts for ethyl *cis*-aziridine-2-carboxylates formation.¹⁶⁵ He reported that lower $\text{p}K_{\text{a}}$ resulted in a better catalytic activity in terms of a shorter reaction time

and higher product yields. However, triflic acid is extremely hygroscopic, making it difficult to handle and store. Furthermore, the use of such strong acid prevents chemistry on substrates that have acid-sensitive functional and/or protecting groups. Additionally, good yields (53-89%) and diastereoselectivities (>95:5 *cis:trans*) were achieved only when reactions were performed at -78 °C and reasonably high 25 mol% loading of triflic acid catalyst. Using pyridinium triflate as a catalyst in aziridination reactions has got several advantages over triflic acid. As a stable solid, pyridinium triflate is easily weighed and handled, inexpensive, non-hygroscopic, requires no drying or crystallisation and its mildly acidic nature allows incorporation of acid-sensitive groups.

As part of our preliminary investigation towards the synthesis of (\pm)-*cis*-aziridines, a one-pot procedure was attempted, with the desired imine (**5.3**) pre-formed *in situ* (Scheme 5.1).



Scheme 5.1. Synthesis of (\pm)-*cis*-(5.6**) via a one-pot aziridination reaction with the intermediate imine (**5.3**)**

A slight excess (10%) of 4-nitrobenzaldehyde (**5.1**) ensured that all of the 2-*tert*-butoxyaniline (**5.2**) was consumed and the corresponding imine (**5.3**) was formed. If any of the unreacted amine is present, it will react with the catalyst (**5.5**), competing with the imine. This reactivity can be rationalised by considering the molecular orbital effect on acidity/basicity. The more "s" character the orbital possesses, the closer the electrons are held to the nucleus and therefore the acidity of a bond increases.¹⁶⁶ If the lone pair is in an sp^2 or sp orbital, it is held closer to the nucleus and is more difficult to protonate than if it is in an sp^3 orbital. For example, cyclohexanimine has pK_a of 9.2 (nitrogen lone pair is in sp^2 orbital) and is less basic (thus more acidic) than cyclohexylamine, which has pK_a of 10.6 (nitrogen lone pair is in sp^3 orbital).

Activated (flame dried) 4 Å molecular sieves were used to trap the generated water in the condensation reaction between 4-nitrobenzaldehyde (**5.1**) and 2-*tert*-butoxyaniline (**5.2**) and shift the reaction equilibrium towards the imine (**5.3**) formation.

After three hours stirring at room temperature, an aliquot was taken out and submitted to $^1\text{H-NMR}$ analysis; this confirmed the imine (**5.3**) formation (**Figure 5.1**). New singlet was observed at δ 8.58 ppm, which was assigned to the proton on the α -carbon of the imine (**5.3**). Residual, due to 10% excess, aldehyde (**5.1**) singlet was observed at δ 10.15 ppm (17% detected by $^1\text{H-NMR}$ analysis).

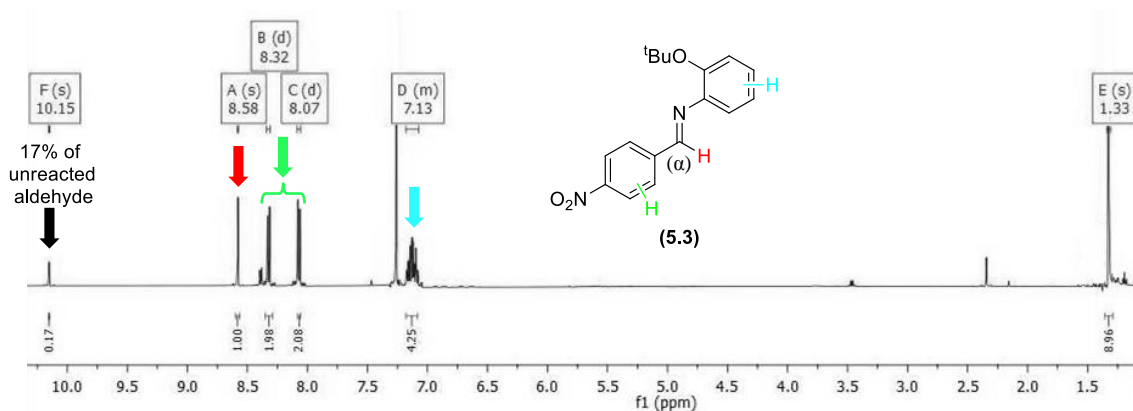


Figure 5.1. $^1\text{H-NMR}$ (500 MHz, CDCl_3) spectrum of imine (**5.3**)

Imine (**5.3**) was not isolated and was directly submitted to the aziridination reaction. After addition of 10 mol% pyridinium triflate (**5.5**) catalyst and *tert*-butyl diazoacetate (**5.4**) a rapid gas evolution was observed in the vial, which was hypothesised to be molecular nitrogen elimination, during the aziridine ring closing step (**5.7**) (see **Scheme 5.2.**, page 50). After 6 hours at room temperature, $^1\text{H-NMR}$ (500 MHz, CDCl_3) analysis of an aliquot indicated a complete disappearance of the characteristic imine singlet at δ 8.58 ppm (**Figure 5.2**).

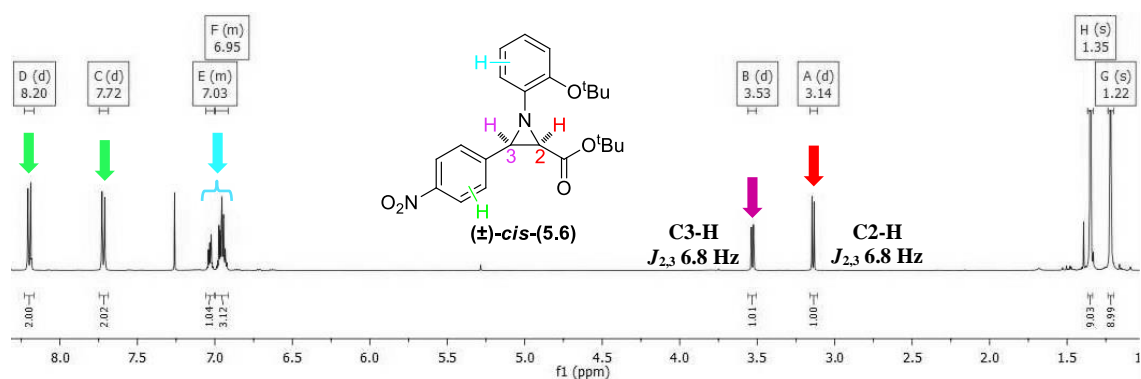


Figure 5.2. $^1\text{H-NMR}$ (500 MHz, CDCl_3) spectrum of (\pm)-*cis*-(**5.6**)

Purification by flash chromatography on silica gel, eluting with 20% diethyl ether in 40-60 petroleum ether, afforded (\pm)-*cis*-(**5.6**) as an orange oil in a 81% yield. The *cis*-configuration of the product was assigned on the basis of the vicinal proton-proton coupling constants ($J_{2,3}$ 6.8 Hz) of the doublets, corresponding to the protons at

C-3 (δ 3.53 ppm) and C-2 (δ 3.14 ppm).^{167,168} Our results were in good agreement with the work of Templeton *et al*, who reported *cis*-aziridine formation over *trans*- in the reactions between *N*-substituted aryl imines with ethyl diazoacetate, catalysed by Lewis acids.¹⁶⁹

The observed magnitude of the coupling constants in *cis*-aziridines can be rationalised using the research by Martin Karplus, who established a relationship between the dihedral angle and vicinal coupling constant applicable to the structural analysis of organic molecules (**Figure 5.3.**).¹⁷⁰ In the *trans*-aziridines, the dihedral angle ϕ is ~ 120 degrees, thus a coupling constant 3J is $\sim 2 - 5$ Hz. In the *cis*-configuration of aziridines, the dihedral angle ϕ is close to 0 (zero) degrees, therefore affording 3J in the range of $\sim 5 - 9$ Hz.

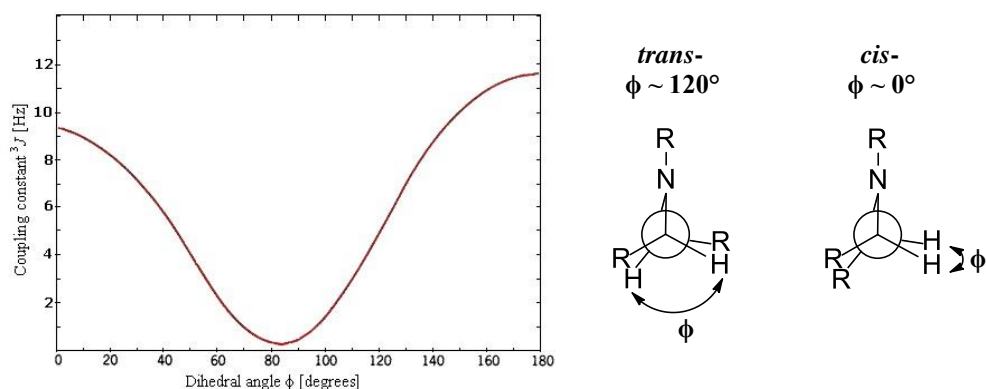
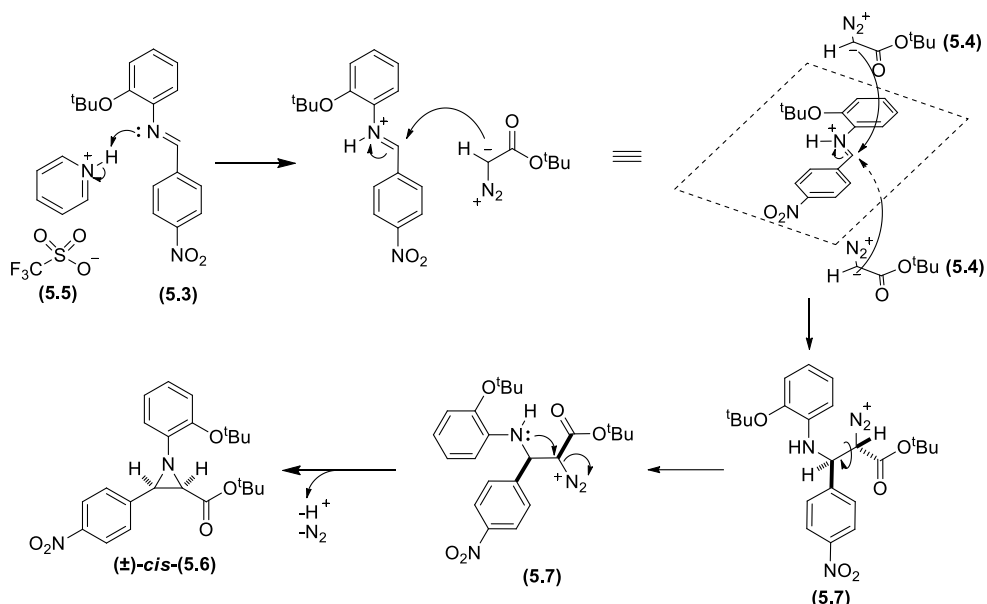


Figure 5.3. Aziridine coupling constant (3J) dependence on the dihedral angle (ϕ)

A literature search on the aziridination reaction mechanism afforded several publications by Wulff *et al*, who proposed that the diazo- group should be in antiperiplanar conformation to the nitrogen that ends up in the aziridine ring for the elimination of the dinitrogen leaving group to occur in the ring closing step (**5.7**) (**Scheme 5.2.**).¹⁷¹ Based on this research, we proposed a mechanism of the reaction generating (\pm)-*cis*-(**5.6**), which is racemic, because using achiral catalyst such as pyridinium triflate (**5.5**), allows *tert*-butyl diazoacetate (**5.4**) to attack imine (**5.3**) equally from both faces. *Cis*- selectivity was rationalised considering the fact that bulky *tert*-butyl group of the diazoacetate occupies the least sterically hindered position relative to the aromatic groups of the imine, setting the stereochemistry in the first irreversible step.



At this point it was considered important to confirm the *cis*-character of the aziridines synthesised *via* the methodology discussed previously. Up to this point, *cis*-character of the aziridines had only been proven by the characteristic coupling constants of in the range 5 - 9 Hz of the C-2-*H* and C-3-*H* peaks within ¹H-NMR spectra of the products. After much experimentation, a further confirmation of the *cis*-relationship at the C-2 and C-3 positions was achieved *via* single-crystal structure analysis of (±)-*cis*-(5.8) (Figure 5.4). Compound (±)-*cis*-(5.8) was generated using identical procedure utilised in the synthesis of (±)-*cis*-(5.6) and it was identified that (±)-*cis*-(5.8) possessed the doublets at δ 3.59 ppm and δ 3.19 ppm with *J*_{2,3} being 6.8 Hz. A successful crystallisation of (±)-*cis*-(5.8) was achieved from pentane/diethyl ether 2:1 mixture, with the crystals obtained as pale yellow needles. The X-ray crystal structure confirmed the *cis*-relationship at the C-2 and C-3 positions (see below the conformation of the carbon sequence C15-C14-C7-C8).

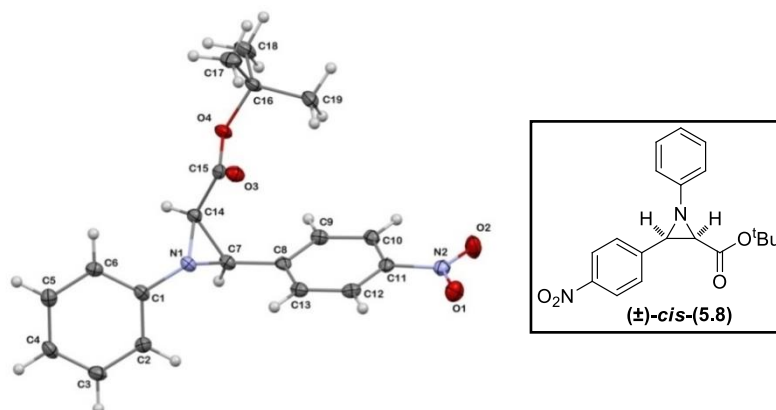
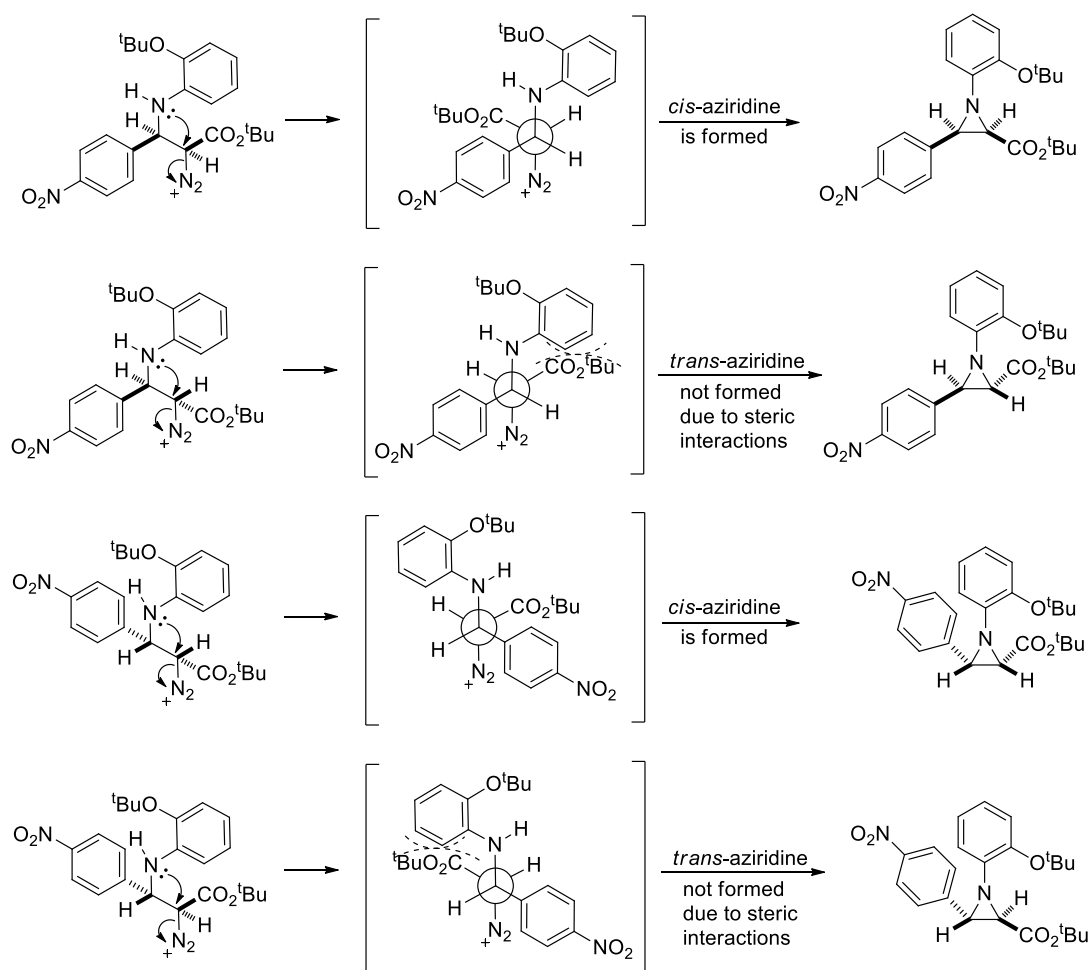


Figure 5.4. Oak Ridge Thermal Ellipsoid Plot (ORTEP) representation of the X-ray crystal structure of (±)-*cis*-(5.8) displaying *cis*-stereochemistry at the C-2 and C-3 positions

Obtaining the confirmation of *cis*-configuration of aziridines synthesised, we attempted to rationalise the diastereoselectivity by considering steric effects during the ring-closing step (**Scheme 5.3**). Additionally to this argument, Wulff *et al* conducted an extensive research into the stereoselectivity of the asymmetric aziridination reaction, by using a combination of experimental kinetic isotope effects and theoretical calculations.¹⁷² A comparison of theoretical Gibbs free energies in the transition state for the S_N2-like ring closure led to the conclusion that the *cis*-aziridination pathway (21.3 kcal/mol) has lower energy than *trans*- (22.6 kcal/mol) and is therefore more energetically favourable. This is in reasonable agreement with the experimental > 50:1 *cis*-/*trans*- ratio observed by Wulff *et al* for this reaction and our data, which suggest predominantly *cis*-aziridine formation over *trans*-.



Scheme 5.3. Newman projections to justify the *cis*-stereoselectivity of (\pm)-*cis*-(5.6)

Our preliminary investigations into a racemic aziridination protocol resulted in a successful synthesis of (\pm)-*cis*-(5.6) and (\pm)-*cis*-(5.8). A *cis*-configuration of the generated aziridines was confirmed on a basis of crystal structure and aziridine ring coupling constants. Using the results obtains, we proceeded with an investigation towards asymmetric aziridination reactions.

5.3. Studies towards an asymmetric aziridination protocol

Within the work of Pesce, it was demonstrated that chiral non-racemic Brønsted acid catalysts derived from (*S*)-1,1'-binaphthyl-2,2'-diol (BINOL) proved effective in providing excellent asymmetric inductions in aziridination reactions (**Figure 5.5**).¹⁷³ The catalyst of choice was (*S*)-BINOL derived phosphoryl *N*-trifluoromethane sulfonamide functionalised with two 9-anthryl substituents (**(S)**-**(5.9)**) at the 3- and 3'-positions. The selection was based on the work of Yamamoto *et al*, who utilised (*S*)-BINOL-based chiral *N*-triflyl phosphoramidate as a catalyst in a highly enantioselective Diels-Alder reaction of an α,β -unsaturated ketone with silyloxydienes.¹⁷⁴

Using Molecular Mechanics 2 (MM2) software, Pesce demonstrated that two 9-anthryl substituents of the catalyst (**(S)**-**(5.9)**) create a "box" cavity with the phosphoryl *N*-trifluoromethane sulfonamide group in the centre. The activation of an imine occurs *via* protonation by the acidic proton NH of the catalyst. Additionally the transition state is stabilised by phosphoryl oxygen *via* bonding to the hydrogen atom on the α -carbon of the *N*-aryl imine. Similar transition state was observed by Gridnev *et al* between (*S*)-BINOL derived phosphoric acid and *N*-Boc imine and a crystal structure was obtained as the evidence.¹⁷⁵

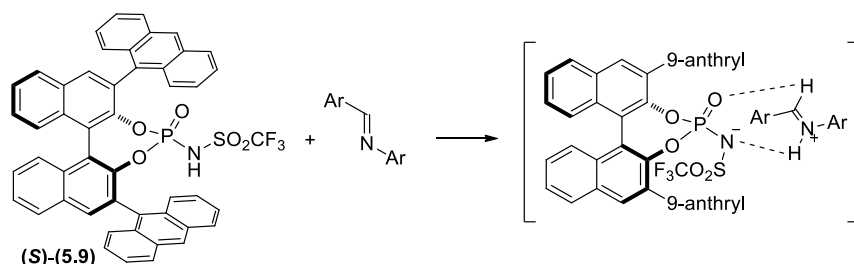
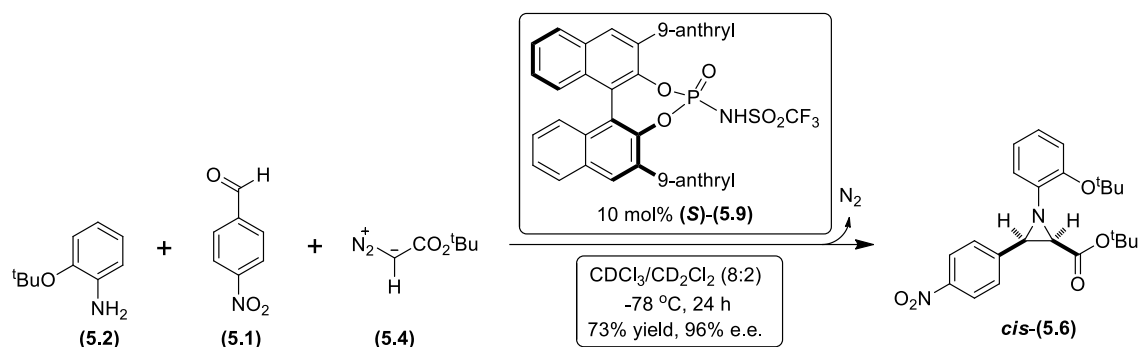


Figure 5.5. Proposed model of the transition state between the catalyst (**(S)**-**(5.9)**) and a generic imine

Following the procedure reported by Pesce, our initial attempt towards a one-pot asymmetric aziridination reaction utilised 10 mol% (*S*)-3,3'-bis(anthracen-9-yl)-[1,1']-binaphthalen-2,2'-yl *N*-triflyl phosphoramidate catalyst (**(S)**-**(5.9)**), *tert*-butyl diazoacetate (**(5.4)**) and *N*-substituted imine, generated *in situ* from 4-nitrobenzaldehyde (**(5.1)**) and 2-*tert*-butoxyaniline (**(5.2)**) (**Scheme 5.4**).

Deuterated chloroform/deuterated dichloromethane (8:2) solvent system allowed reaction monitoring directly by ¹H-NMR analysis, without obscuring the spectrum by any additional solvent peaks. Additionally, this system was one of the cheapest deuterated solvent combinations, that allowed reactions to be carried at -78 °C, without freezing. The freezing point of chloroform is -63.5 °C, dichloromethane is -97 °C.¹⁷⁶



The reaction was kept at $-78\text{ }^{\circ}\text{C}$ and monitored by thin layer chromatography and $^1\text{H-NMR}$ analysis. After circa 24 hours, the characteristic imine peak at $\delta\ 8.58\text{ ppm}$ was no longer observed. Two new doublets were observed at $\delta\ 3.53$ ($J_{2,3}\ 6.8\text{ Hz}$) and 3.14 ppm ($J_{2,3}\ 6.8\text{ Hz}$), matching with the racemic sample (\pm)-*cis*-(5.6). To determine the enantiopurity of *cis*-(5.6), a chiral HPLC analysis was performed. The chiral non-racemic sample was run against the corresponding racemic aziridine and e.e. was calculated to be 96% (**Table 5.1**).

Compound	Chiral HPLC spectrum
<p style="text-align: center;">(\pm)-<i>cis</i>-(5.6)</p> <p>$R_t = 6.27, 10.41\text{ min}$ racemic</p>	
<p style="text-align: center;"><i>cis</i>-(5.6)</p> <p>$R_t = 6.25, 10.38\text{ min}$ 96% e.e.</p>	
Conditions: Chiralpak AD-H HPLC column, 95% <i>iso</i> -hexane : 5% <i>iso</i> -propanol, flow rate: 1 mL / min	

Table 5.1. Chiral HPLC spectra of (\pm)-*cis*-(5.6) and *cis*-(5.6)

With the synthesis of chiral non-racemic *cis*-(**5.6**), accomplished, chiral non-racemic *cis*-(**5.8**) was generated *via* the asymmetric aziridination protocol described above, utilising aniline instead of 2-*tert*-butoxyaniline. This reaction was designed to test the differences in yield and, most importantly, e.e., which occur upon changing the amine substituent within the one-pot reaction asymmetric aziridination reaction. It was observed that without 2-*tert*-butoxy group e.e. decreased from 96% to 92% (**Table 5.2**). This can be attributed to the fact that bulky 2-*tert*-butoxy group provides additional steric influence, blocking one face of the imine during *tert*-butyl diazoacetate approach.

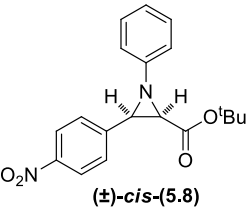
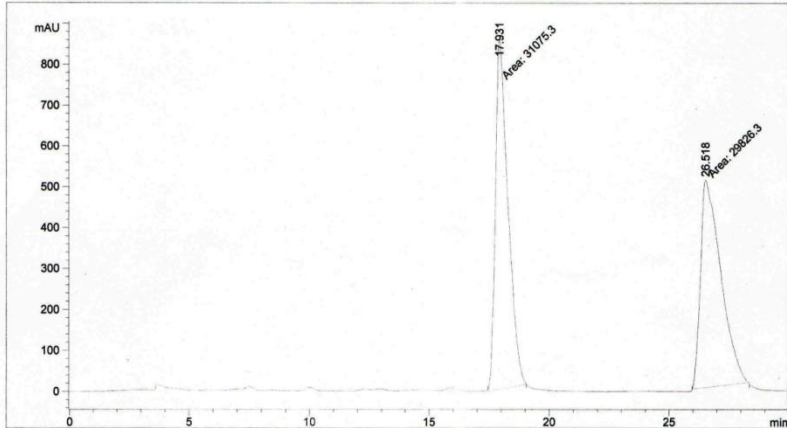
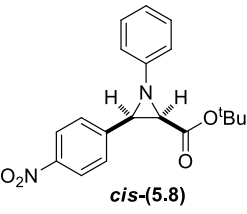
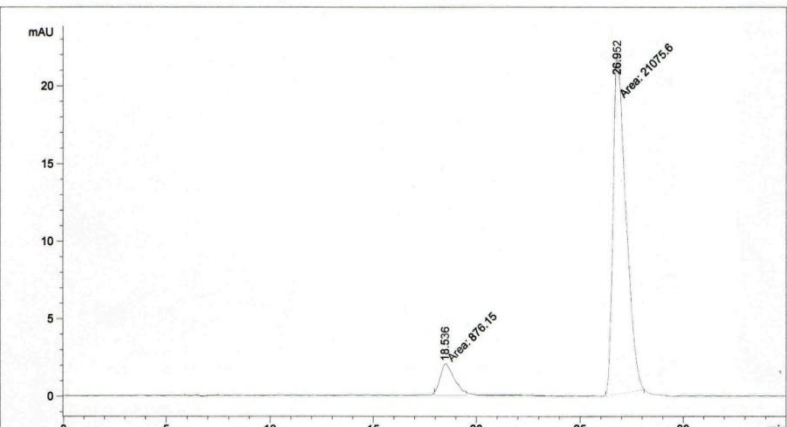
Compound	Chiral HPLC spectrum
 <p>(±)-<i>cis</i>-(5.8)</p> <p>$R_t = 17.93, 26.52$ min racemic</p>	
 <p><i>cis</i>-(5.8)</p> <p>$R_t = 18.53, 26.95$ min 92% e.e.</p>	
<p>Conditions: Phenomenex Lux Cellulose-1 HPLC column, 99% <i>iso</i>-hexane : 1% <i>iso</i>-propanol, flow rate: 1 mL / min</p>	

Table 5.2. Chiral HPLC spectra of (±)-*cis*-(**5.8**) and *cis*-(**5.8**)

Although chiral HPLC analysis allowed the enantiopurity of aziridines to be established, no confirmation of the absolute stereochemistry was obtained. Unfortunately, no similar examples were found within the literature in order to compare the specific rotation values. Thus, the stereochemistry of enantiomerically enriched aziridines throughout this thesis should be considered as the relative stereochemistry. However, Freedman *et al* reported that chiro-optical methods, such as vibrational

circular dichroism (VCD) can be used to determine the absolute configuration of the molecule.¹⁷⁷ VCD utilises the differential interaction of a chiral molecule with left *versus* right circularly polarized light. Felipe *et al* demonstrated that absolute configuration of several natural products was assigned using VCD spectroscopy.¹⁷⁸ Therefore, the subject of our future investigations will be the measurement of VCD spectra of enantiomerically enriched aziridines and elucidation of their absolute configuration.

By synthesising non-labelled racemic aziridines (\pm)-*cis*-(**5.6**) and (\pm)-*cis*-(**5.8**) and non-labelled enantiomerically enriched *cis*-(**5.6**) and *cis*-(**5.8**) the aziridination protocols (racemic and asymmetric) have been established. Thus, it was necessary to generate a suite of starting materials, such as aldehydes, amines, diazoacetates, labelled with stable isotopes so we could investigate the synthesis of the corresponding labelled optically active aziridines.

A literature search on the synthesis of isotopically labelled aziridines was, surprisingly, rather limited. Beresford and Young reported synthesis of labelled aziridine-2-carboxylates, which were subsequently used as synthons for preparation of L-amino acids, labelled at the β -carbon atom.¹⁷⁹ Davies *et al* used ²H- or ¹³C-formyl labelled aromatic aldehydes to generate corresponding C-3 labelled *N*-tosyl-3-aryl-2-alkynyl aziridines, that were subsequently converted into 2,4-disubstituted pyrroles *via* gold-catalysed 1,2-aryl shift.¹⁸⁰ Although reaxys and scifinder searches afforded several hits on ¹⁵N-labelled aziridines, these compounds were mainly generated for spectroscopic studies.^{181,182}

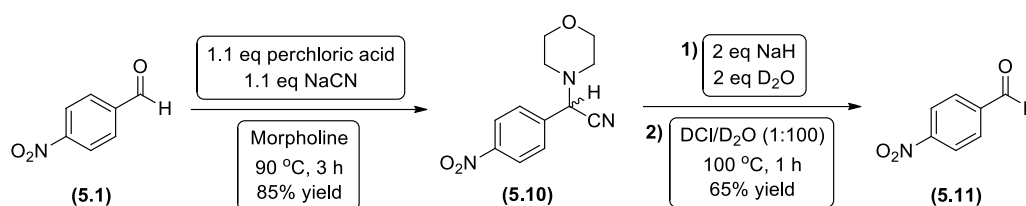
We envisaged the introduction of stable isotopes into an aziridine ring and its subsequent ring-opening, generating high-value compounds such as optically active α - and β -amino acid derivatives, labelled with stable isotopes. An aziridine ring itself is a desirable target for labelling, because protons and carbons within the ring display very specific NMR signals, in the region, not obstructed by other signals. This allows straightforward identification and characterisation of the changes induced by the isotopic incorporation, such as loss of a signal if a proton has been substituted with a deuteron or enhancement of a signal when ¹³C is used instead of ¹²C.

Although this chapter is dedicated to the production of chiral non-racemic aziridines labelled with stable isotopes, the author feels that the background development of isotopically labelled starting materials is worthy of note. Detection and analysis of isotopic splitting patterns in starting materials provides valuable information during product characterisation.

5.4. Synthesis of α - ^2H -aldehydes

A literature search on the aldehyde deuteration at the formyl group afforded a publication by Kirby *et al*, who published a procedure of introducing deuterium or tritium labels at the formyl group of aromatic aldehydes, *via* the readily accessible morpholino-acetonitrile intermediates, such as **(5.10)**.¹⁸³

Following the method published by Kirby *et al*, 4-nitrobenzaldehyde (**(5.1)**) was treated with perchloric acid and potassium cyanide in morpholine as a solvent to afford 2-morpholino-2-(4-nitrophenyl)acetonitrile (**(5.10)**) (**Scheme 5.5**).



The ^1H -NMR (500 MHz, CDCl_3) analysis of **(5.10)** revealed a complete absence of aldehyde peak ($\sim \delta$ 10 ppm) and a new singlet at δ 4.90 ppm related to the proton on the α -carbon of **(5.10)**, as well as the multiplets at δ 3.75 ppm and δ 2.61 ppm corresponding to the protons on the morpholino-group (**Figure 5.6**). FT-IR analysis indicated the absence of the carbonyl group at 1705 cm^{-1} and the presence of the new peak at 2226 cm^{-1} , corresponding to the cyano group.

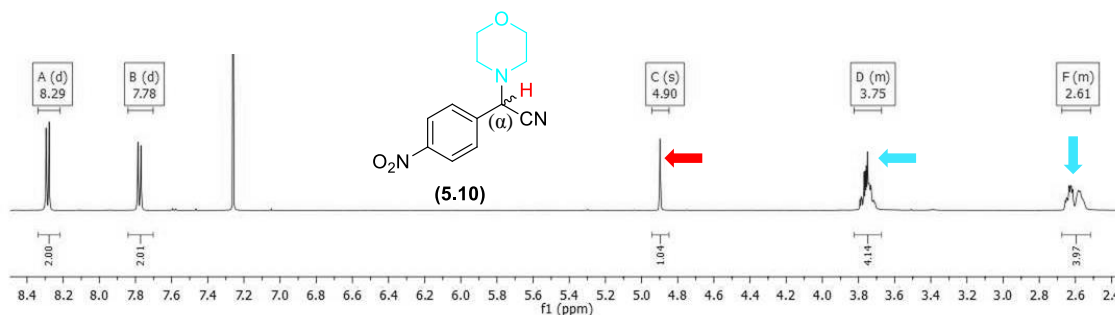


Figure 5.6. ^1H -NMR (500 MHz, CDCl_3) spectrum of morpholino-acetonitrile derivative (**(5.10)**)

Hanson reported that in the morpholino-acetonitrile derivatives the presence of the nitrile group, increases the acidic character of the proton attached to the α -carbon.¹⁸⁴ Following the procedure by Kirby *et al*, a deprotonation of **(5.10)** with sodium hydride was performed, followed by subsequent quenching of the resulting anion with deuterium oxide to install the deuterium atom on the α -carbon of **(5.10)**. Sodium hydride was selected, because of its ability to remove the desired proton irreversibly, generating hydrogen gas, which is the driving force of the reaction. The ^2H -labelled morpholino-acetonitrile derivative (not shown) was hydrolysed under the mildly acidic

conditions (1% DCl in D₂O) under a reflux to afford ²H-formyl 4-nitrobenzaldehyde (**5.11**) without any loss of the deuterium label (²H incorporation remained > 95%). Deuterium incorporation level was determined by analysing the ¹H-NMR spectra of (**5.1**) and (**5.11**) and comparing the integration of the formyl proton (**Figure 5.7**). Deuterium incorporation in all subsequent examples discussed throughout this dissertation was established using this procedure: direct comparison of the integration values between the proton in a non-labelled sample and a residual proton in a deuterated material.

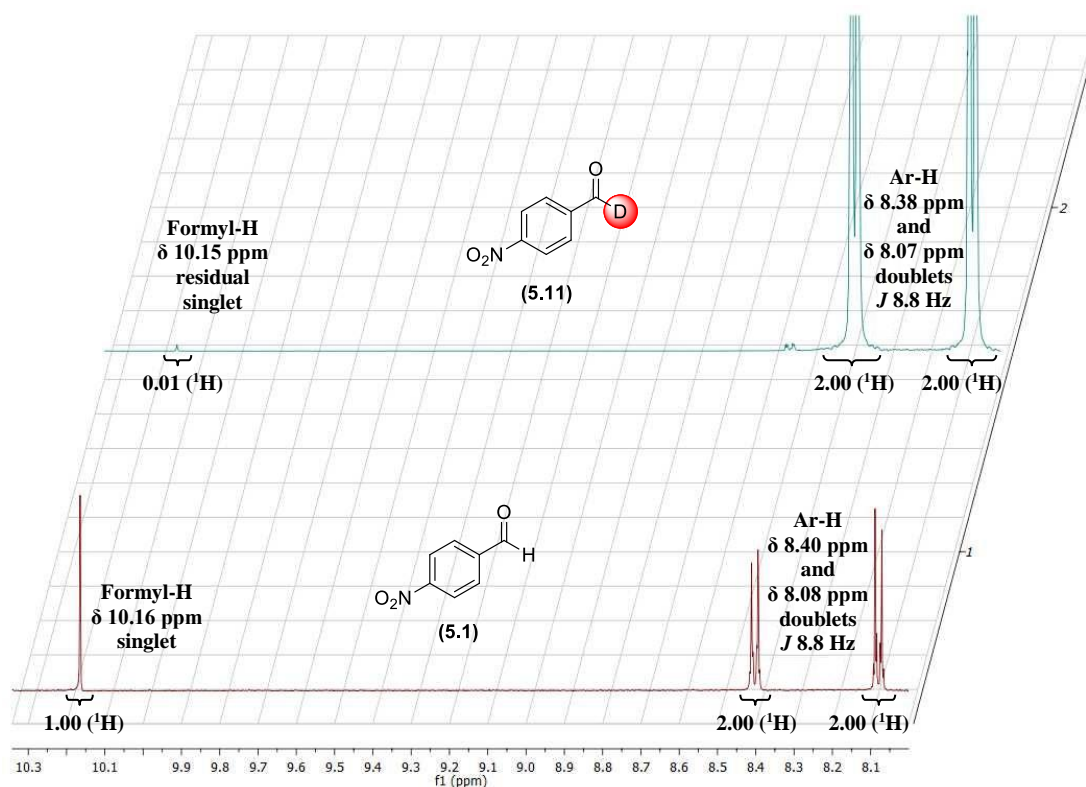


Figure 5.7. Stacked ¹H-NMR (500 MHz, CDCl₃) spectra of α -²H-4-nitrobenzaldehyde (**5.11**) (top) and 4-nitrobenzaldehyde (**5.1**) (bottom)

²H-NMR (500 MHz, DCM) analysis of (**5.11**) displayed a broad singlet at δ 10.11 ppm, which corresponded to the signal of the deuterium atom (**Figure 5.8**). All ²H-NMR experiments were performed in the "unlocked" mode in a non-deuterated solvent (e.g. DCM) with a drop of CDCl₃ and/or CD₂Cl₂ as a chemical shift reference.

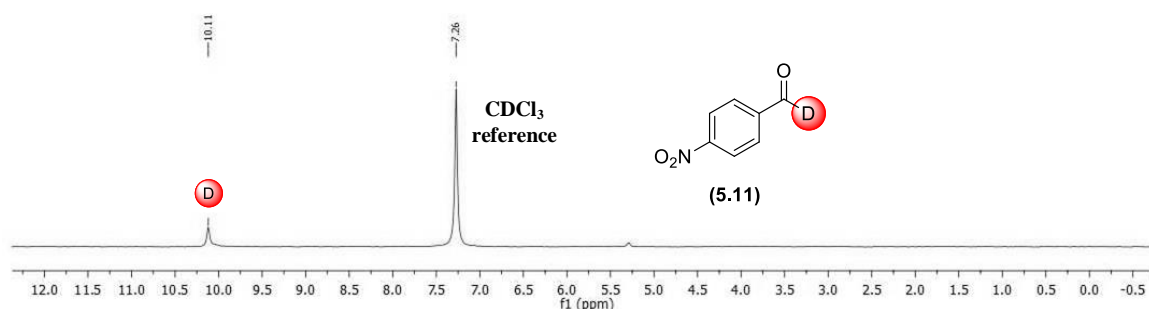


Figure 5.8. ²H-NMR (77 MHz, DCM) spectrum of α -²H-4-nitrobenzaldehyde (**5.11**)

Furthermore, within the ^{13}C -NMR (126 MHz, CDCl_3) spectrum of (**5.11**), the carbonyl signal was observed as a triplet at δ 190.2 ppm with $J_{\text{C-D}}$ 27.4 Hz (**Figure 5.9**). This splitting pattern was accounted for the fact that the ^{13}C -NMR spectrum was *not* deuterium decoupled. Deuterium has a spin of 1, with three spin states possible: spin 1, 0, and -1.¹³⁵ A ^2H nucleus splits the ^{13}C signal into three equally spaced peaks (1:1:1 ratio due to the nearly equal populations of the three ^2H spin states) and this results in lower intensities of the peaks. In addition, the reduced carbonyl signal intensity was observed, because carbons are much slower to relax when bound to ^2H (relative to ^1H), due to the smaller nuclear magnet (magnetogyric ratio) of deuterium (see page 37). The *ipso*-carbon was observed at δ 140.1 ppm as a triplet as well, however with a smaller magnitude of the coupling constant ($^2J_{\text{C-D}}$ 3.5 Hz).

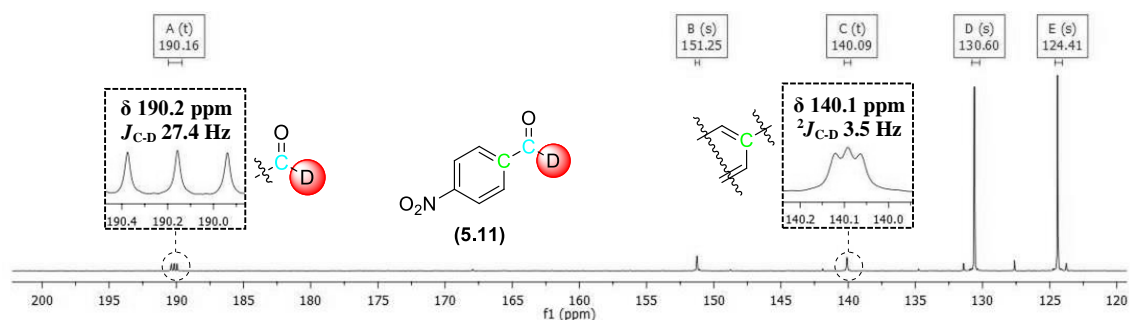


Figure 5.9. ^{13}C -NMR (126 MHz, CDCl_3) spectrum of α - ^2H -4-nitrobenzaldehyde (**5.11**)

Using the method outlined above, a library of deuterated aldehydes has been generated, including ^2H -formyl 4-nitrobenzaldehyde (**5.11**), ^2H -formyl 4-cyanobenzaldehyde (**5.12**), ^2H -formyl 4-fluorobenzaldehyde (**5.13**), ^2H -formyl 4-bromobenzaldehyde (**5.14**) and ^2H -formyl 2-naphthaldehyde (**5.15**) (**Table 5.3**). Their synthesis proceeded exceptionally well on a multi-gram scale and, more importantly, with excellent deuterium incorporation levels (> 95% ^2H incorporation). Reactions were cost effective, due to commercially available inexpensive starting materials. Furthermore, morpholino-acetonitrile intermediates are highly crystalline solids, which is convenient for their handling and storage. The functional groups were chosen on a basis of electronic character and utilisation in any subsequent transformations. Nitro and cyano groups are strongly deactivating substituents towards electrophilic aromatic substitution, fluoro and bromo substituents are weakly deactivating and 2-naphthyl group is weakly activating. Nitro and cyano groups can be reduced to the corresponding amines, that can be used in peptide coupling or transformed into other groups *via* diazonium salts.¹⁸⁵ Additionally, the cyano group can be hydrolysed to an amide or a

carboxylic acid derivative. Bromo substituent can be used in cross-coupling reactions and fluorine nucleus is an excellent NMR probe, often used for studies of chemical and biological systems (see example of *cis*-(**5.37**) page 72).¹⁸⁶

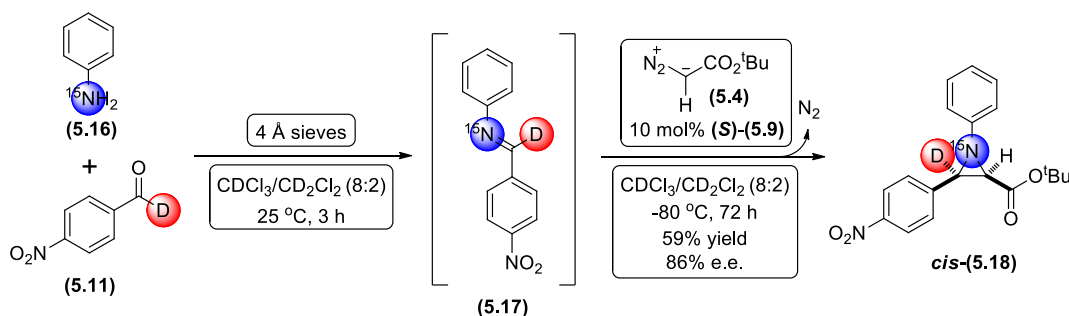
65% yield (5.11)	72% yield (5.12)	71% yield (5.13)	68% yield (5.14)	78% yield (5.15)
----------------------------------	----------------------------------	----------------------------------	----------------------------------	----------------------------------

Table 5.3. Generated library of α -²H-aldehydes

With isotopically labelled starting materials in hand, we attempted to introduce stable isotope labels into the corresponding aziridines, following the asymmetric protocol discussed previously.

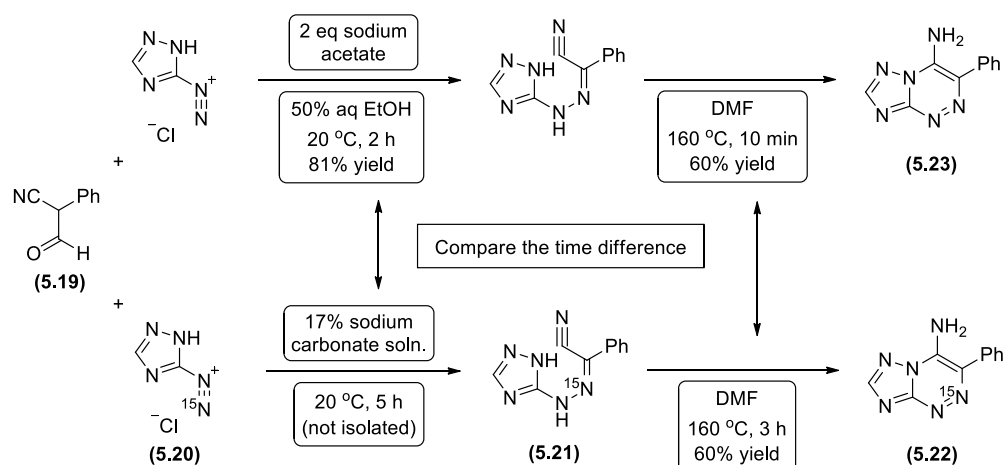
5.5. Asymmetric synthesis of 1-¹⁵N-3-²H-*tert*-butyl 3-(4-nitrophenyl)-1-phenyl aziridine-2-carboxylate *cis*-(**5.18**)

The first isotope incorporating aziridination reaction, utilising the asymmetric protocol discussed previously employed α -²H-4-nitrobenzaldehyde (**5.11**) and commercially available ¹⁵N-aniline (**5.16**). Imine (**5.17**) was pre-formed *in situ* at room temperature, which was confirmed by ¹H- and ²H-NMR spectroscopy (**Scheme 5.6**). (*S*)-3,3'-Bis(anthracen-9-yl)-[1,1']-binaphthalen-2,2'-yl *N*-triflyl phosphoramidate (10 mol%) catalyst (**S**)-(**5.9**) was added and the reaction vessel was cooled to -80 °C. *tert*-Butyl diazoacetate (**5.4**) was syringed through the septum of the reaction vessel and the reaction mixture was stirred at -80 °C, monitoring by ¹H-NMR and TLC until the reaction was deemed complete (~ 72 hours).



The rate of the above reaction was observed to be significantly slower (72 h vs 24 h) compared to the aziridination to form chiral non-racemic *cis*-(**5.8**), when no isotopes were incorporated. The decrease of the reaction rate to form *cis*-(**5.18**) can be attributed to a kinetic isotope effect (KIE).¹⁸⁷ A primary KIE arises from bond breaking/making to the ¹⁵N atom. When isotopes are remote from the reaction centre, a secondary KIE may be observed. In the compound *cis*-(**5.18**), deuterium was not involved directly in the bond breaking/making, however, it was attached to the carbon participating in the bond formation, potentially contributing to the secondary KIE.

A literature search of the comparison of the reaction rates between labelled and non-labelled compounds afforded a publication by Chupakhin *et al*, who reported a reaction between 7-¹⁵N-1H-1,2,4-triazole-5-diazonium chloride (**5.20**) and α -formyl- α -phenylacetonitrile (**5.19**) affording 2-¹⁵N-3-phenyl-[1,2,4]triazolo[5,1-c][1,2,4]triazin-4-amine (**5.22**).¹⁸⁸ The first step involved a nucleophilic addition to the *sp* hybridised ¹⁵N affording hybridisation change to *sp*².¹⁸⁹ Second step proceeded via cyclisation of six-membered ring of (**5.21**), without any ¹⁵N-hybridisation changes, but with a rearrangement of bonds connected to ¹⁵N. During both steps, the reaction with ¹⁵N-labelled compound proceeded with a much *slower rate*, compared to the non-labelled equivalent (**5.23**).¹⁹⁰



Scheme 5.7. Direct comparison of the reaction rates during formation of 2-¹⁵N-3-phenyl-[1,2,4]triazolo[5,1-c][1,2,4]triazin-4-amine (5.22**) and 3-phenyl-[1,2,4]triazolo[5,1-c][1,2,4]triazin-4-amine (**5.23**) by Chupakhin *et al***

Purification by flash chromatography on silica gel afforded *cis*-(**5.18**) as a yellow solid in 59% yield and 86% e.e. (determined by chiral HPLC). Subsequent ¹H-NMR (500 MHz, CDCl₃) analysis of *cis*-(**5.18**) revealed the absence of the signal from the proton at the C-3 position, because it had been replaced with deuterium

(**Figure 5.10.**) The proton at the C-2 position was expected to be observed as a triplet due to a spin coupling with an adjacent deuterium atom at the C-3 position. However, the actual signal was observed at δ 3.19 ppm as a singlet. This fact is attributed to the differences in the magnetogyric ratios of a proton and a deuterium (see **Table 4.2. Properties of some NMR active nuclei**, page 37). The coupling constants for ^1H - ^2H couplings are proportional to those of ^1H - ^1H coupling and are reduced by a factor of ~ 7 . Thus, a *cis*-coupling constant of the proton at C-2 is expected to be less than 1.0 Hz. Couplings this small are sometimes not observed within ^1H -NMR and the triplet appears as a singlet, which is slightly broad near the baseline. In the ^2H -NMR (77 MHz, DCM) spectrum of *cis*-(**5.18**) a broad singlet was observed at δ 3.54 ppm corresponding to the deuterium atom installed at C-3.

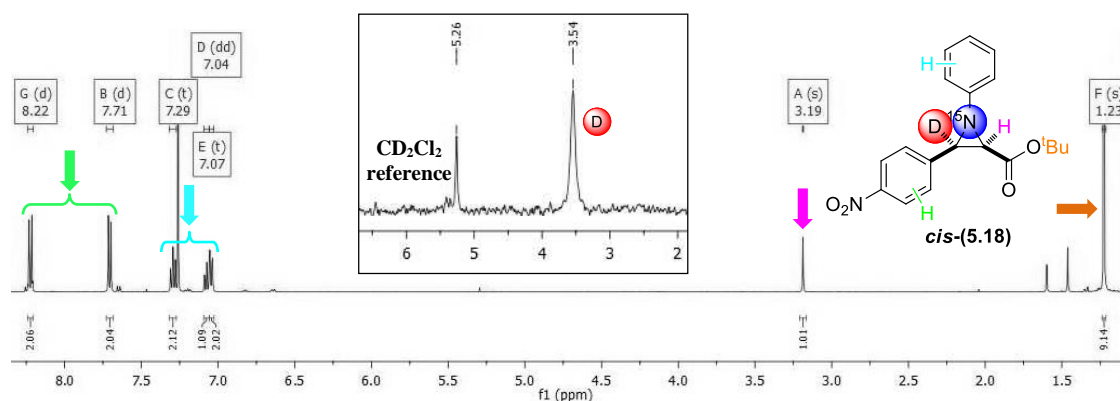


Figure 5.10. ^1H -NMR (500 MHz, CDCl_3) spectrum of *cis*-(**5.18**) with ^2H -NMR (77 MHz, DCM) insert

Although no crystal structure was obtained for *cis*-(**5.18**), ^1H -NMR analysis was used to confirm deuterium incorporation and a *cis*-configuration (**Figure 5.11**). ^1H -NMR (500 MHz, CDCl_3) analysis of *cis*-(**5.18**) revealed a signal at δ 3.59 ppm from the residual proton at the C-3 position with the integration of 0.01, therefore deuterium incorporation was recorded above 95%. The coupling constant of this proton was recorded as $J_{2,3}$ 6.8 Hz. Chemical shift and the coupling constant ($J_{2,3}$) of the C3-residual proton have matched the ones obtained from the racemic sample (\pm)-*cis*-(**5.8**), therefore a *cis*-configuration of *cis*-(**5.18**) was confirmed.

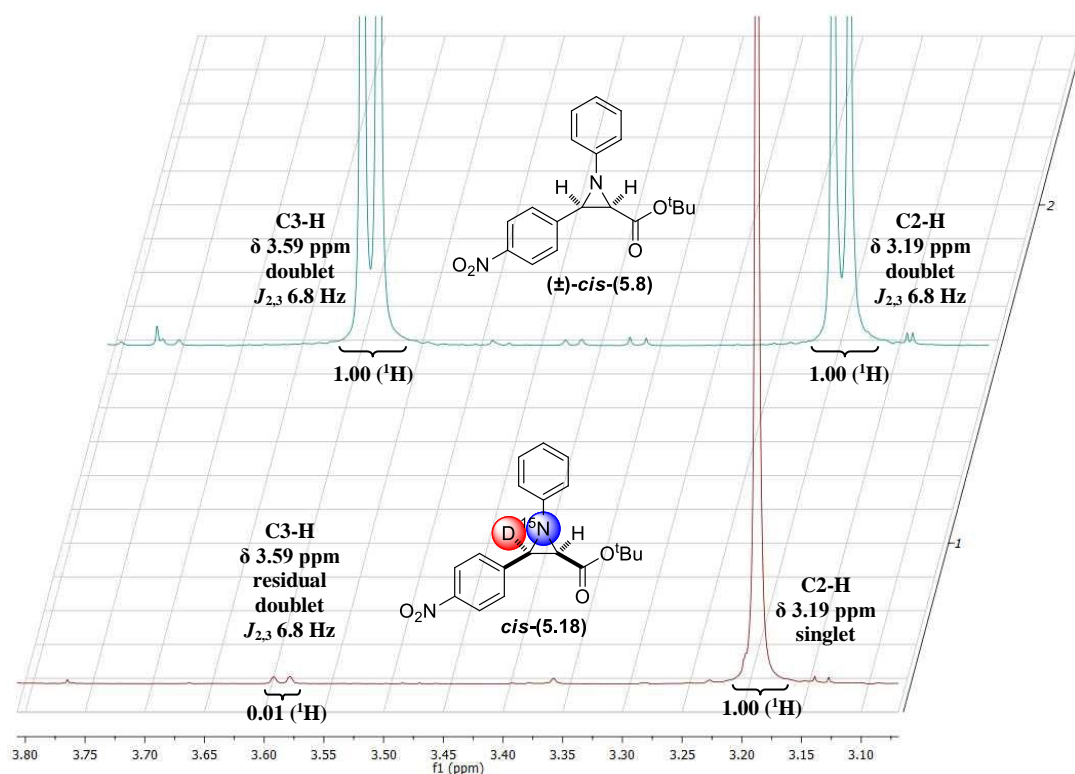


Figure 5.11. ^1H -NMR (500 MHz, CDCl_3) spectra of (\pm) -*cis*-(5.8) (top) and *cis*-(5.18) (bottom)

While examining the ^{13}C -NMR (126 MHz, CDCl_3) spectrum of *cis*-(5.18), a complex splitting pattern was observed, mainly arising from the fact that a ^{15}N nucleus is NMR-active. (Figure 5.12.). Signal from the C-2 position appeared at δ 46.6 ppm as a doublet ($J_{\text{C-N}}$ 6.8 Hz), which was attributed to the coupling to the ^{15}N nucleus. Likewise, carbon at the C-3 position was split by both ^2H and ^{15}N , therefore a triplet of doublets splitting pattern was observed at δ 45.7 ppm ($J_{\text{C-D}}$ 25.5 Hz, $J_{\text{C-N}}$ 6.8 Hz). The strength of the NMR magnet and the concentration of the sample allowed to observe other carbons to be split by ^{15}N as well. Carbonyl peak at δ 166.1 ($J_{\text{C-N}}$ 4.8 Hz) ppm appeared as a doublet, as well as aromatic carbons at δ 151.8 ($J_{\text{C-N}}$ 2.6 Hz), δ 142.5 ($J_{\text{C-N}}$ 4.1 Hz), δ 128.9 ($J_{\text{C-N}}$ 1.8 Hz) and δ 120.0 ppm ($J_{\text{C-N}}$ 3.3 Hz). The coupling constants of similar magnitude were reported by Beller *et al*, who characterised ^{15}N -labelled *N*-benzylaniline.¹⁹¹

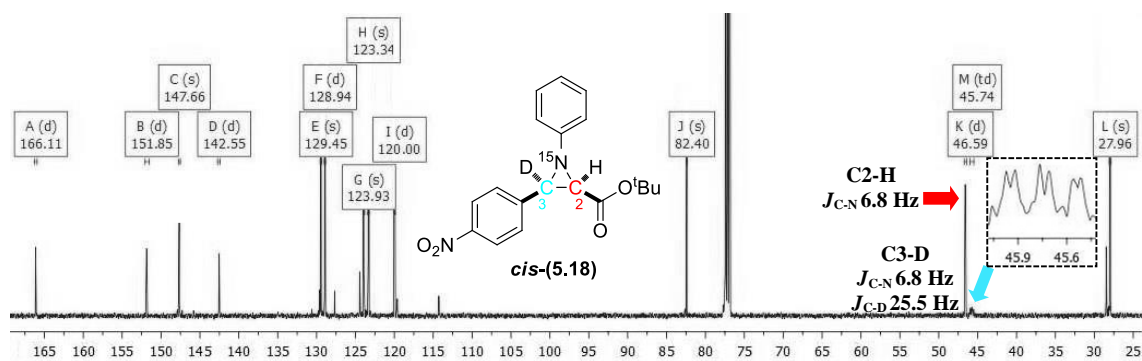


Figure 5.12. ^{13}C -NMR (126 MHz, CDCl_3) spectrum of *cis*-(5.18)

The HRMS analysis provided a confirmation of the synthesis of *cis*-(**5.18**) with $[M+H]^+$ ions found at the required m/z (found: 343.1526, required: 343.1529) (**Figure 5.13**). No peaks were detected corresponding to the 342.1529 fragment (M^+-1) or 342.1529 fragment (M^+-2) which confirms no ^2H or ^{15}N "loss" occurred, suggesting the deuterium and ^{15}N incorporation level to be above 95%.

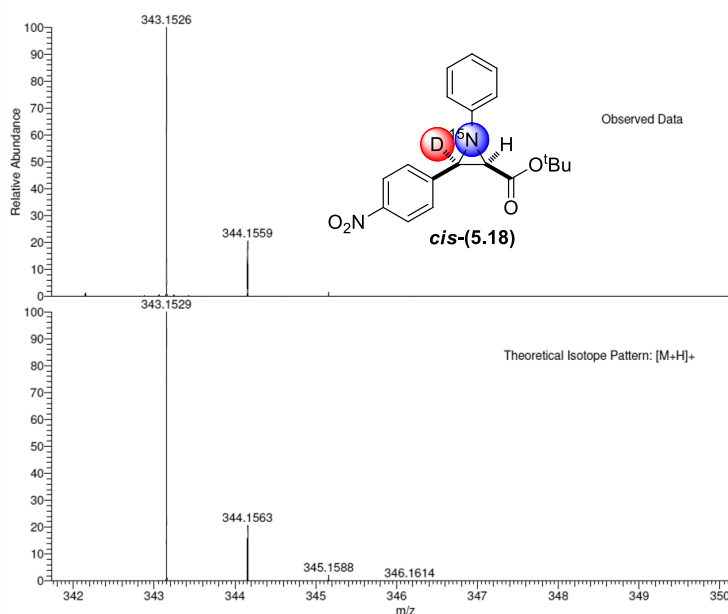
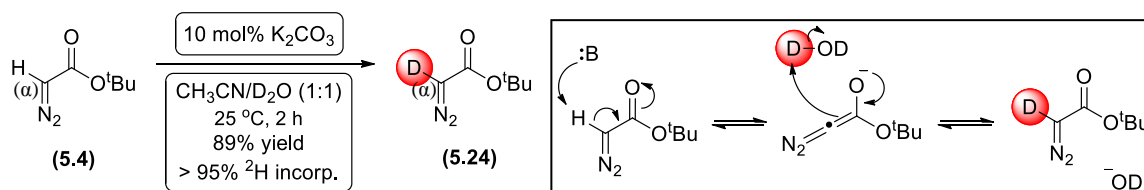


Figure 5.13. HRMS (HASP) spectrum of *cis*-(**5.18**)

With accomplished synthesis of *cis*-(**5.18**), we wanted to extend the scope of our investigation by introducing additional isotopic labels into aziridines and examine subsequent impact on enantiomeric excess, yield and isotopic incorporation levels.

5.6. Synthesis of α - ^2H -*tert*-butyl diazoacetate (**5.24**)

Diazo compounds are remarkably versatile building blocks in organic synthesis, that are utilised in reactions such as: aziridination, cyclopropanation and formation of lactams.¹⁹² Previously, within the Bew group, a methodology has been developed, that employs a one-pot-one-cycle procedure to obtain aryl and alkyl diazoacetates with deuterium installed at the α -position (**Scheme 5.8**).¹⁹³



Scheme 5.8. Synthesis and a proposed mechanism of a formation of α - ^2H -*tert*-butyl diazoacetate (**5.24**)

The high levels of deuterium incorporation (> 95%) were achieved employing commercially available, inexpensive starting materials and very mild conditions. Treating *tert*-butyl diazoacetate with 10 mol% of potassium carbonate in homogenous acetonitrile-deuterium oxide 1:1 mixture at ambient temperature afforded the desired α - ^2H -*tert*-butyl diazoacetate. ^1H -NMR (500 MHz, CDCl_3) analysis revealed the absence of the alpha proton singlet at δ 4.59 ppm (determined from the starting material), whereas a signal of the *tert*-butyl group remained intact (**Figure 5.14**).

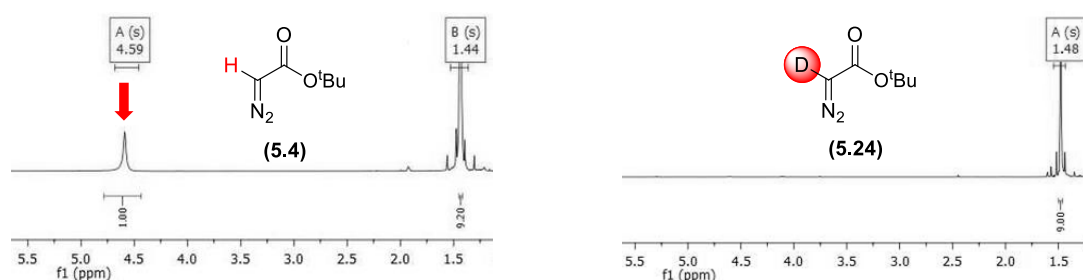


Figure 5.14. ^1H -NMR (500 MHz, CDCl_3) spectra of *tert*-butyl diazoacetate (5.4) (left) and α - ^2H -*tert*-butyl diazoacetate (5.24) (right)

Within the ^{13}C -NMR (126 MHz, CDCl_3) spectrum of *tert*-butyl diazoacetate (5.4) the signal from the α -carbon was observed as a singlet at δ 46.7 ppm, because the ^{13}C -NMR spectrum was proton decoupled (**Figure 5.15**). However, in the ^{13}C -NMR (126 MHz, CDCl_3) spectrum of α - ^2H -*tert*-butyl diazoacetate (5.24) the signal of the α -carbon was observed as a triplet ($J_{\text{C-D}}$ 29.9 Hz). This was attributed to the deuterium nucleus splitting the carbon, its attached to, into three peaks of equal intensity. Identical pattern was observed when a deuterium label was incorporated into the formyl group of aromatic aldehydes (see **5.4. Synthesis of α - ^2H -aldehydes**, page 56).

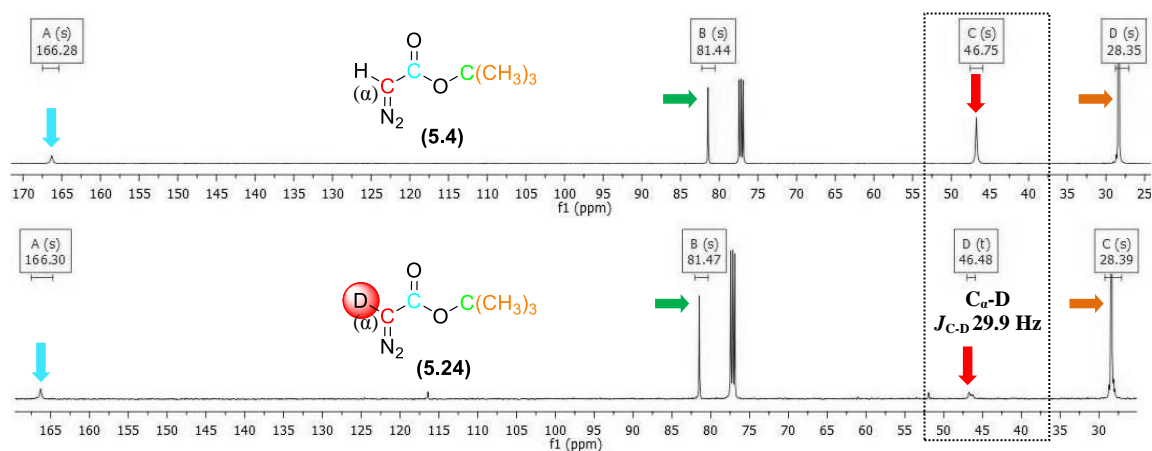
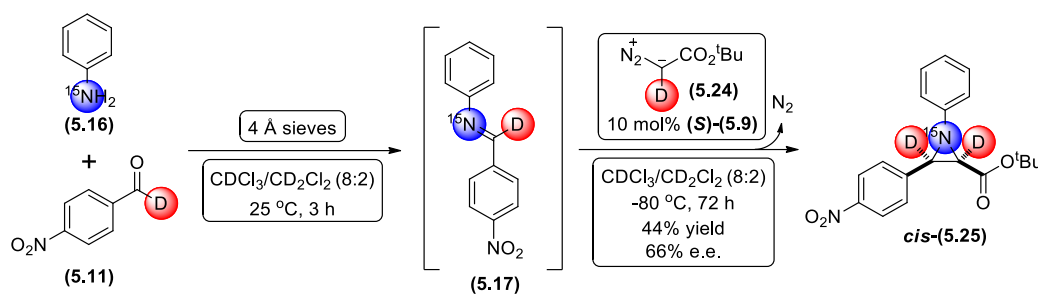


Figure 5.15. ^{13}C -NMR (126 MHz, CDCl_3) spectrum of *tert*-butyl diazoacetate (5.4) (top) α - ^2H -*tert*-butyl diazoacetate (5.24) (bottom)

Following a successful synthesis of *cis*-(**5.18**) with a deuterium label at the C-3 position, we attempted incorporation of a ^2H -label at the C-2 position as well, using α - ^2H -*tert*-butyl diazoacetate (**5.24**).

5.7. Asymmetric synthesis of 1- ^{15}N -2,3- ^2H -*tert*-butyl 3-(4-nitrophenyl)-1-phenyl aziridine-2-carboxylate *cis*-(**5.25**)

With ^2H -*tert*-butyl diazoacetate (**5.24**) in hand, the synthesis of *cis*-(**5.25**) was attempted, incorporating ^2H -labels at both C-3 and C-2 positions as well as ^{15}N -ring nitrogen, utilising the same method as described in the synthesis of *cis*-(**5.18**). Purification by flash chromatography on silica gel afforded *cis*-(**5.25**) as a yellow solid in 44% yield and 66% e.e. (determined by chiral HPLC) (Scheme 5.9).



Scheme 5.9. Asymmetric synthesis of *cis*-(**5.25**)

Subsequent ^1H -NMR (500 MHz, CDCl_3) analysis of *cis*-(**5.25**) revealed the absence of the aziridine proton signals, that were expected in the δ 3 - 4 ppm range by comparison with the non-labelled sample (Figure 5.16.). The ^2H -NMR (77 MHz, DCM) spectrum of *cis*-(**5.25**) displayed broad singlets at δ 3.54 and δ 3.14 ppm corresponding to the deuterium atoms installed at C-3 and C-2 positions (> 95% ^2H incorporation).

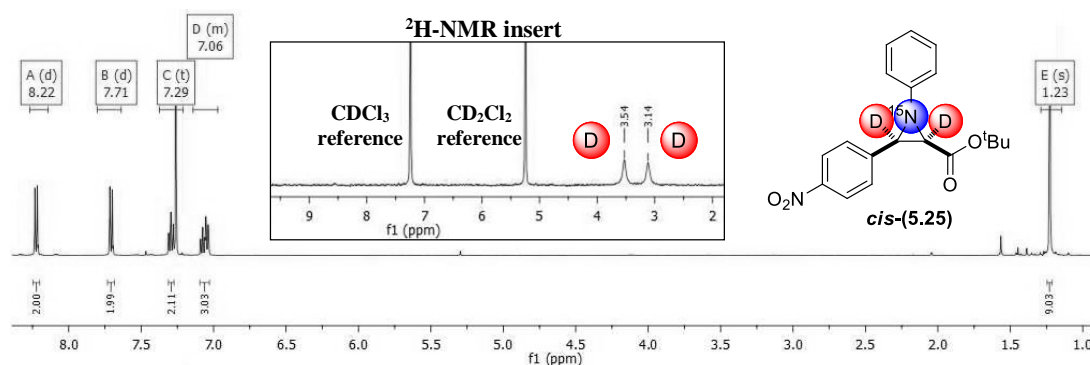


Figure 5.16. ^1H -NMR (500 MHz, CDCl_3) spectrum of *cis*-(**5.25**) with ^2H -NMR (77 MHz, DCM) insert

As expected, the ^{13}C -NMR (126 MHz, CDCl_3) spectrum of *cis*-(**5.25**) revealed the carbon signals from C-2 and C-3 to be very close to the baseline due to deuterium splitting and the effect of relaxation. Unfortunately, due to low intensity, the peaks were not resolved and appeared as multiplets at δ 46.4 and 45.7 ppm.

^{15}N -NMR (51 MHz, CDCl_3) spectra of *cis*-(**5.18**) and *cis*-(**5.25**) correlated well with each other (**Figure 5.17**). Signals were observed as singlets at δ 66.41 ppm and δ 66.22 ppm respectively.

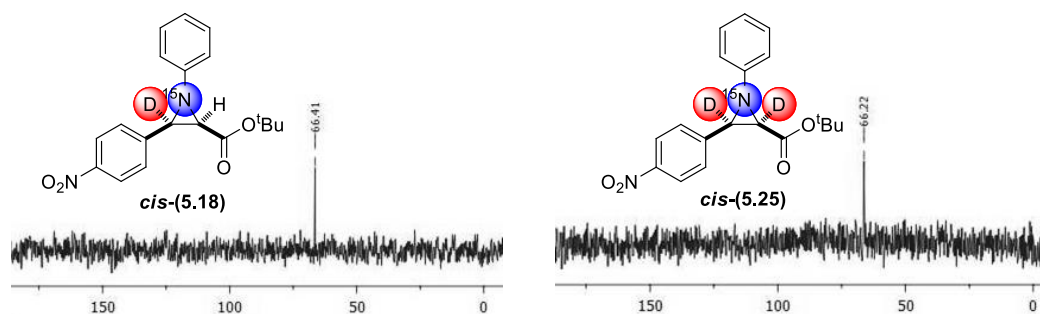


Figure 5.17. ^{15}N -NMR (51 MHz, CDCl_3) spectrum of *cis*-(**5.18**) (left) and *cis*-(**5.25**) (right)

Overall, both *cis*-(**5.18**) and *cis*-(**5.25**) were obtained successfully following a one-pot asymmetric aziridination protocol. Predominantly *cis*-aziridines were observed with little or no *trans*-. The yields of the aziridination reactions were moderate, however, mainly due to problems with purification. Most importantly, isotope incorporation levels above 95% were achieved, without any loss of label. Encouraged by the results of the aziridination reactions described above, incorporation of ^{13}C -stable isotope was attempted.

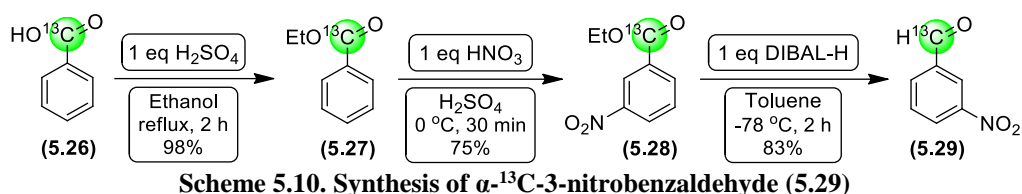
5.8. Synthesis of α - ^{13}C -3-nitrobenzaldehyde (**5.29**)

The natural abundance of the NMR active ^{13}C -isotope is 1.1%, with remaining 98.9% being ^{12}C -isotope, which is NMR inactive. Therefore, NMR sensitivity of the ^{13}C nucleus is very low. However, when enriched above natural abundance, the ^{13}C -isotope displays a very strong signal, which can provide a valuable information from the specific sites of a labelled compound. The chemical shift of the ^{13}C -isotope is sensitive to an isotope that is attached to it. Thus, a chemical shift of a ^{13}C - ^2H or a ^{13}C - ^{18}O signal appears at a slightly different position from the corresponding ^{13}C - ^1H or ^{13}C - ^{16}O signal.¹⁸⁴ Coupling with other NMR active nuclei has proved to be a valuable tool in the structure elucidation of chemical compounds. At natural abundance the statistical chance of having two ^{13}C -nuclei adjacent to each other is too low for the ^{13}C - ^{13}C

coupling to be observed. However, if enriched, two or more adjacent ^{13}C -nuclei will reveal a coupling pattern. If the ^{13}C - ^{13}C bond has been broken, the coupling is no longer present.

Hutton *et al* demonstrated a powerful technique called Triple-Resonance Isotope-Edited (TRIED) NMR for studying metabolism.¹⁹⁴ TRIED NMR uses through-bond (scalar) coupling between spins to select NMR signals from molecules having ^1H - ^{13}C - ^{15}N atom sequence. Natural-abundance background signals from molecules not containing such labelled atoms are effectively suppressed, with a suppression ratio of approximately $10^4:1$. This filtering allows labelled species to be detected and characterised without requiring extensive, time-consuming sample purification. Stark *et al* published a method to selectively detect ^1H - ^{13}C - ^{13}C fragments, that were biosynthetically introduced into the active site of heme proteins.¹⁹⁵ This method utilised nearly identical pulse sequence, described by Hutton *et al*. The only difference was the third atom in a fragment: ^{13}C instead of ^{15}N . The proton connected to ^{13}C - ^{13}C atoms was pulsed and a transfer of a magnetisation back to the ^1H nucleus allowed an enhanced proton signal to be observed.

α - ^{13}C -Benzoic acid (99 atom%) (**5.26**) was chosen as the starting material for generating a series of ^{13}C -labelled aldehydes, due to the combination of its price, commercial availability and straightforward transformation to the desired α - ^{13}C -labelled aldehydes. During the first stage of the synthesis, α - ^{13}C -benzoic acid (**5.26**) was converted to ethyl α - ^{13}C -benzoate (**5.27**) (**Scheme 5.10.**). Following the procedure reported by Baker and Hey, attempted nitration occurred at the *meta*-position of the aromatic ring, affording ethyl α - ^{13}C -3-nitrobenzoate (**5.28**), because the ester functional group is a strongly deactivating substituent and is *meta*-directing.¹⁹⁶ Reduction of the ester functional group of ethyl α - ^{13}C -3-nitrobenzoate (**5.28**) using diisobutylaluminium hydride (DIBAL-H) resulted in α - ^{13}C -3-nitrobenzaldehyde (**5.29**).¹⁹⁷ DIBAL-H is a reducing agent, commonly used for the reduction of esters to aldehydes.¹⁹⁸ DIBAL-H acts as an “electrophilic” reductant, coordinating a lone pair from the carbonyl oxygen (a nucleophile) to the aluminium (electrophile). After hydride transfer, a neutral hemiacetal intermediate is formed, that is stable at low temperatures ($-78\text{ }^\circ\text{C}$). Aqueous workup protonates the hemiacetal, releasing the desired aldehyde as the product. The by-products of the reaction are corresponding alcohol and aluminium salts. The temperature must be kept below $-70\text{ }^\circ\text{C}$ to prevent over-reduction of the aldehyde to the alcohol. The overall yield of the transformation of (**5.26**) to (**5.29**) was 61% over the three steps.



Within the $^1\text{H-NMR}$ (500 MHz, CDCl_3) spectrum of (5.29), the formyl proton was observed at δ 10.13 ppm as a doublet with a very large coupling constant ($J_{\text{C-H}} = 179.1$ Hz) (Figure 5.18.). This was attributed to the fact that the sample of (5.29) was enriched in ^{13}C -isotope (99 atom%), which is NMR active and therefore splits the attached proton into a doublet. An example of $^1\text{H-}^{13}\text{C}$ coupling was found within the literature, reported by Jones *et al*, who observed coupling constant values for ^{13}C -labelled benzaldehyde derivatives of ~ 160 Hz magnitude.¹⁹⁹ The $^{13}\text{C-NMR}$ (126 MHz, CDCl_3) analysis of (5.29) afforded a signal from the α -carbon at δ 189.8 ppm as a singlet, as the $^{13}\text{C-NMR}$ spectrum was proton decoupled. The intensity of the carbonyl signal was greatly enhanced compared to the aromatic non-labelled carbons due to the 99% enrichment of ^{13}C -isotope.

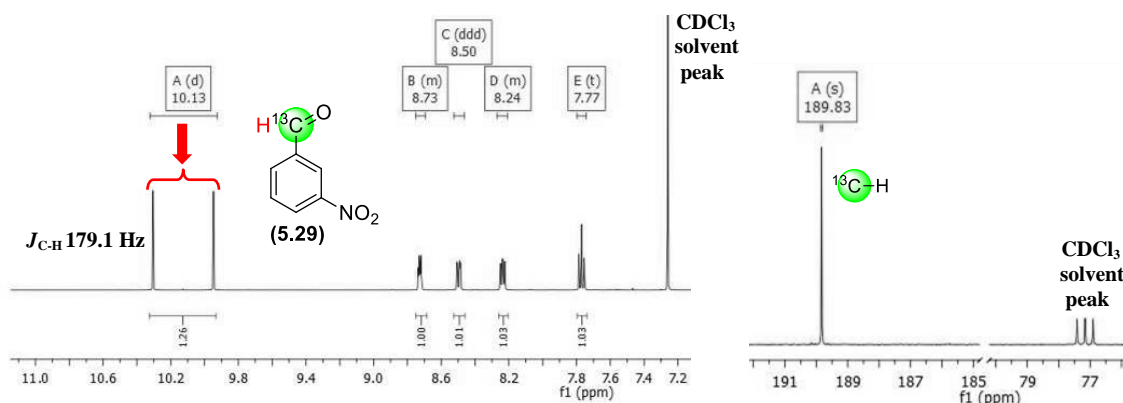
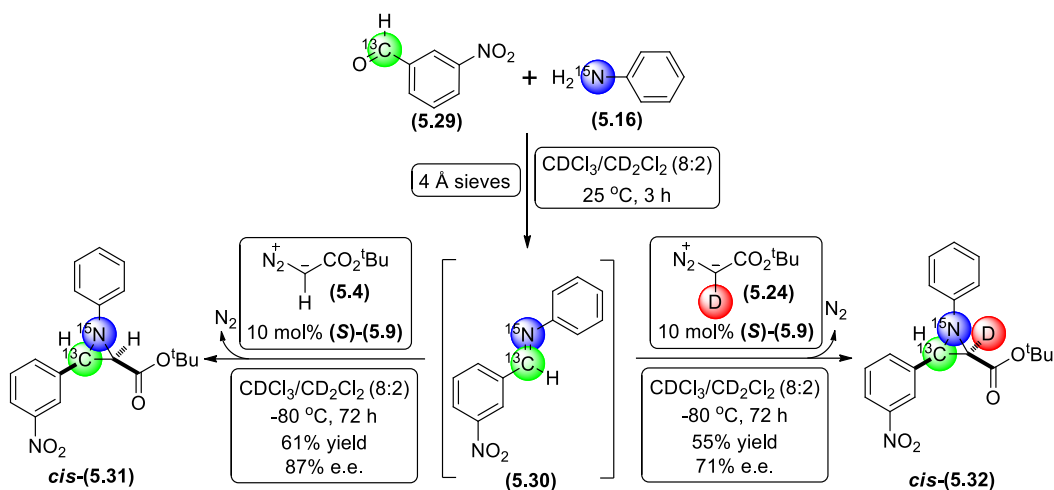


Figure 5.18. $^1\text{H-NMR}$ (500 MHz, CDCl_3) and $^{13}\text{C-NMR}$ (126 MHz, CDCl_3) spectra of (5.29)

5.9. Asymmetric synthesis of 1- ^{15}N -3- ^{13}C -*tert*-butyl 3-(3-nitrophenyl)-1-phenylaziridine-2-carboxylate *cis*-(5.31) and 1- ^{15}N -2- ^2H -3- ^{13}C -*tert*-butyl 3-(3-nitrophenyl)-1-phenylaziridine-2-carboxylate *cis*-(5.32)

Employing the asymmetric aziridination protocol discussed previously, α - ^{13}C -3-nitrobenzaldehyde (5.29) was mixed with ^{15}N -aniline (5.16), generating corresponding ^{15}N -aryl α - ^{13}C -imine (5.30) intermediate, that was reacted with the corresponding *tert*-butyl diazoacetates (5.4) and (5.24) affording aziridines *cis*-(5.31) and *cis*-(5.32) (Scheme 5.11.).



Scheme 5.11. Synthesis of *cis*-(5.31) and *cis*-(5.32)

Analysing the ¹H-NMR (500 MHz, CDCl₃) spectrum of *cis*-(5.31), it was noted that the proton at the C-3 position at δ 3.59 ppm was split by both the ¹³C-labelled carbon and the neighbouring proton at the C-2 carbon (dd, $J_{13\text{C-H}} = 169.0$ Hz; $J_{2,3} = 6.7$ Hz) (**Table 5.4**). The proton at the C-2 carbon at δ 3.17 ppm was split by the ¹⁵N, ¹³C and the proton at the C-3 position (ddd, $J_{2,3} = 6.7$ Hz; ${}^2J_{13\text{C-H}} = 2.5$ Hz; $J_{\text{N-H}} = 0.7$ Hz). Within the ¹H-NMR (500 MHz, CDCl₃) spectrum of *cis*-(5.32), no signal was observed from the proton at the C-2 carbon, as it had been replaced with a deuterium atom (> 95% ²H incorporation). The absence of the C-2 proton affected the splitting pattern of the C-3 proton, which was observed as a doublet ($J_{13\text{C-H}} = 169.0$ Hz), due to the splitting by the ¹³C-nucleus.

Both aziridines had ¹³C-labelled C-3 carbon, therefore the signal was greatly enhanced, suppressing the rest of the spectrum. The ¹³C-NMR (126 MHz, CDCl₃) spectrum of *cis*-(5.31) revealed the C-3 carbon at δ 45.9 ppm as a doublet due to ¹⁵N splitting ($J_{13\text{C-N}} = 7.0$ Hz). Similar splitting was observed within the ¹⁵N-NMR (51 MHz, CDCl₃) spectrum of *cis*-(5.31), where ¹⁵N signal was observed at δ 66.15 ppm as a doublet due to ¹³C splitting ($J_{13\text{C-N}} = 6.8$ Hz). Nearly identical results were observed within the ¹³C-NMR (126 MHz, CDCl₃) and the ¹⁵N-NMR (51 MHz, CDCl₃) spectra of *cis*-(5.32). The C-3 carbon was identified at δ 45.7 ppm as a doublet ($J_{13\text{C-N}} = 7.0$ Hz) and the ¹⁵N signal was observed at δ 65.98 ppm as a doublet ($J_{13\text{C-N}} = 6.8$ Hz).

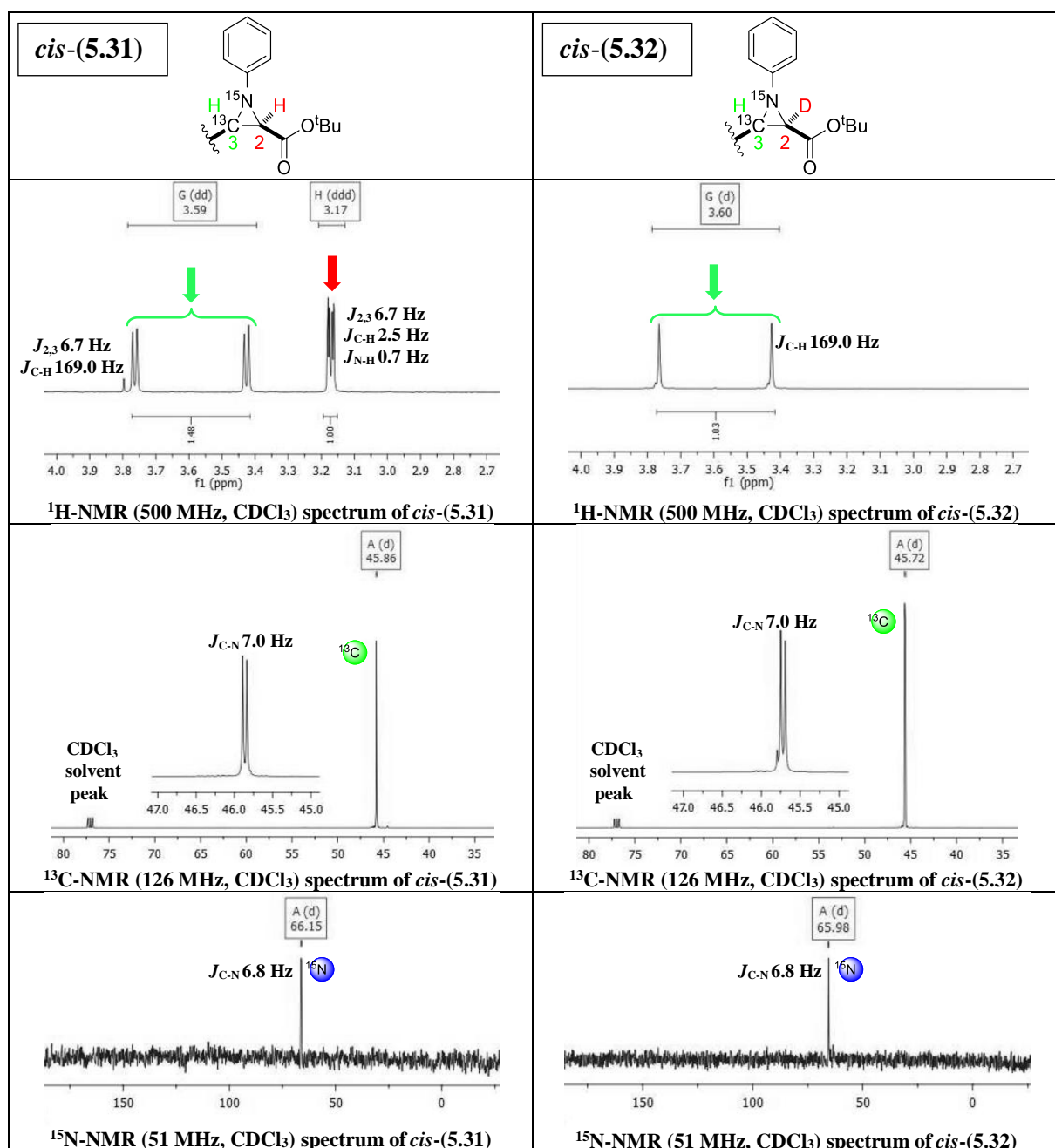


Table 5.4. Comparison of the ^1H -, ^{13}C - and ^{15}N -NMR data between *cis*-(5.31) and *cis*-(5.32)

Results obtained above demonstrate that, if enriched, ^{13}C -isotope can be used as an excellent NMR probe. The appearance of strongly enhanced ^{13}C -resonances permits assignment of the labelled positions. Additionally, coupling to other NMR active nuclei results in specific splitting patterns with unique coupling constants that can be used to gather information about a molecule as a whole or its fragments.

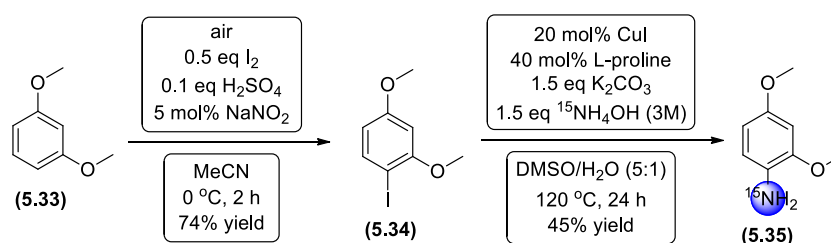
5.10. Synthesis of ^{15}N -2,4-dimethoxyaniline (5.35)

In order to obtain the desired NH-amino acid derivatives from the optically active aziridines synthesised, the nitrogen atom must contain a cleavable protecting

group. A search within the literature revealed a publication by Mayer *et al*, who demonstrated a deprotection of the *N*-*para*-methoxyphenyl (PMP) aziridine, using a readily available oxidant: ammonium cerium(IV) nitrate (CAN).²⁰⁰ Two equivalents of CAN cleaved the *N*-PMP group under mild conditions affording the corresponding *NH*-aziridine in a 82% yield.

Structurally, apart from an additional methoxy group at the 2-position, 2,4-dimethoxyphenyl is identical to PMP. Thus, we considered 2,4-dimethoxy phenyl to be a suitable nitrogen protecting group, that can be introduced in the form of 2,4-dimethoxyaniline.

¹⁵N-2,4-dimethoxyaniline (**5.35**) was synthesised in two steps from commercially available 1,3-dimethoxybenzene (**5.33**) (**Scheme 5.12**).



Scheme 5.12. Synthesis of ¹⁵N-2,4-dimethoxyaniline (**5.35**)

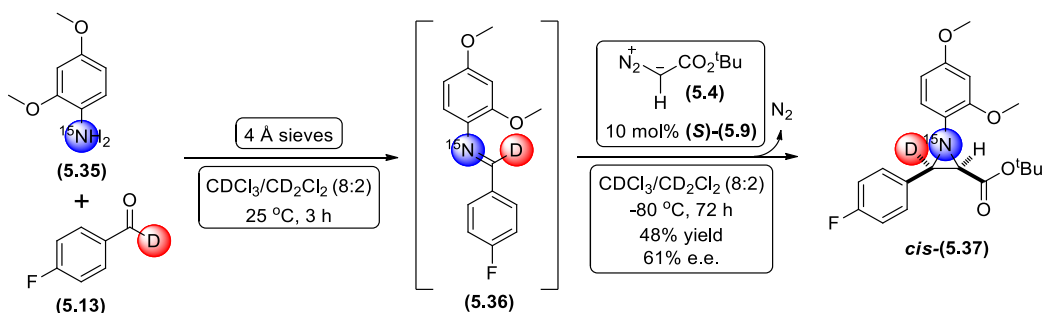
The procedure reported by Iskra *et al* was utilised to achieve a selective and efficient aerobic oxidative iodination of 1,3-dimethoxybenzene (**5.33**), using molecular iodine, air as the terminal oxidant, sodium nitrite as a catalyst and sulfuric acid as an activator of the overall catalytic process.²⁰¹ 1-Iodo-2,4-dimethoxybenzene (**5.34**) was afforded as a yellow liquid in a 74% yield after purification by flash chromatography on silica gel, eluting with 20% diethyl ether in 40-60 petroleum ether. Exploiting an Ullmann coupling, reported by Kim and Chang, ¹⁵N-2,4-dimethoxyaniline (**5.35**) was afforded in a 45% yield *via* a copper(I) iodide catalysed *N*-arylation of 1-iodo-2,4-dimethoxybenzene (**5.34**).²⁰² Ullmann coupling is discussed in more detail on page 93.

5.11. Asymmetric synthesis of 1-¹⁵N-3-²H-*tert*-butyl 1-(2,4-dimethoxy phenyl)-3-(4-fluorophenyl)aziridine-2-carboxylate *cis*-(**5.37**) with cleavable *N*-2,4-dimethoxy phenylprotecting group

Apart from cleavable *N*-protecting group, an installation of a ¹⁹F-nucleus was attempted, which is often used as an NMR probe for investigating the interactions of biological molecules, due to its NMR characteristics, small size, and near total absence from biology.²⁰³ Fluorine is often considered as isosteric with hydrogen because the van

der Waals radius of fluorine is 1.35 Å, similar to that of hydrogen, 1.2 Å, although a C–F bond is actually significantly longer (~ 1.4 Å) than a C–H bond (~ 1.0 Å). Nevertheless, fluorine can often replace hydrogen in small molecules with minimal effect on their binding to enzymes and proteins. The ^{19}F -nucleus has a spin of $\frac{1}{2}$ and exists in 100% natural abundance. Its NMR properties are very close to that of proton NMR: the large magnetogyric ratio translates into high sensitivity in NMR spectroscopy (83% sensitivity compared to ^1H). The chemical shift of ^{19}F -nucleus is very sensitive to changes in the local chemical environment. ^{19}F -chemical shift has a range of ~ 400 ppm, whereas ^1H chemical shift covers only ~ 15 ppm. Therefore, a wide range of changes affecting the local environment of a peptide or protein can be detected using simple ^{19}F -NMR techniques by incorporating suitably labelled residues at appropriate positions within the protein. Protein conformational changes, ligand binding, interactions with other proteins, nucleic acids or lipid membranes, solvent isotope effects can be detected via ^{19}F -NMR chemical shift changes.

With ^{15}N -2,4-dimethoxyaniline (**5.35**) prepared, a synthesis of *cis*-(**5.37**) was attempted, following the aziridination protocol developed previously, via the intermediate (**5.36**) starting from ^2H -formyl 4-fluorobenzaldehyde (**5.13**) (Scheme 5.13.). Purification by flash chromatography on silica gel afforded *cis*-(**5.37**) as a dark orange solid in 48% yield and 61% e.e.



Scheme 5.13. Asymmetric synthesis of *cis*-(**5.37**)

Subsequent ^1H -NMR (500 MHz, CDCl_3) analysis of *cis*-(**5.37**) revealed the absence of the signal from the proton at the C-3 position, because it had been replaced with deuterium (> 95% ^2H incorporation) (Figure 5.19.). Signal from the proton at the C-2 position was observed at δ 2.91 ppm as a singlet, due to the absence of the neighbouring proton at the C-3 position.

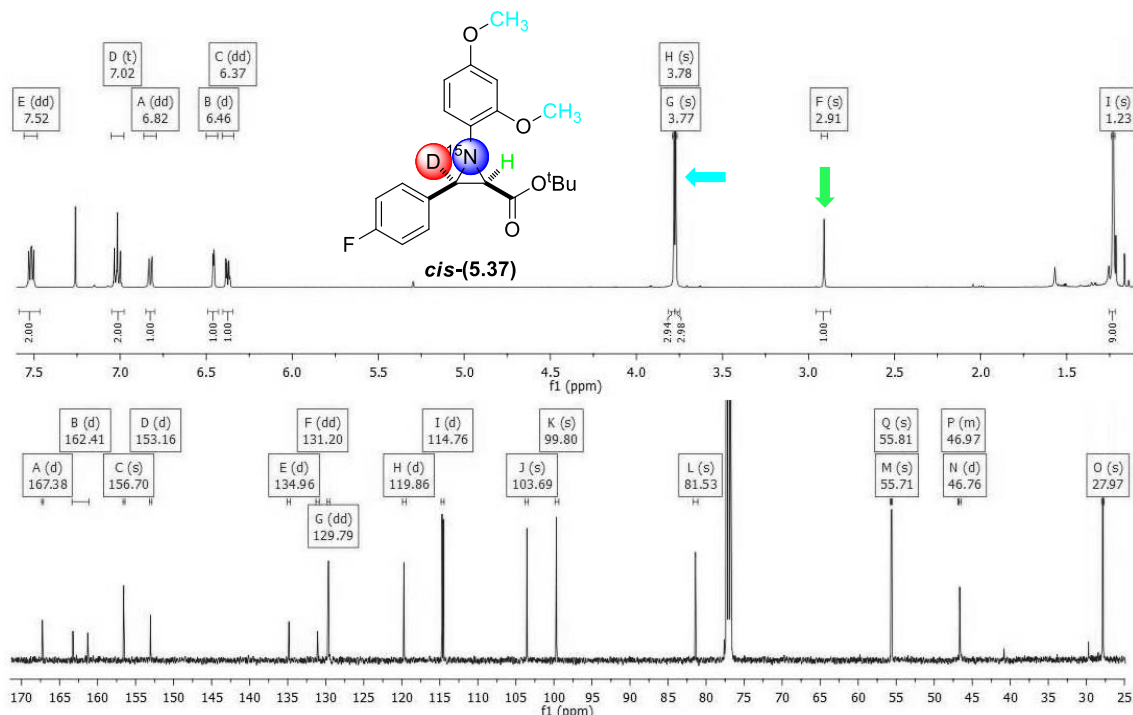


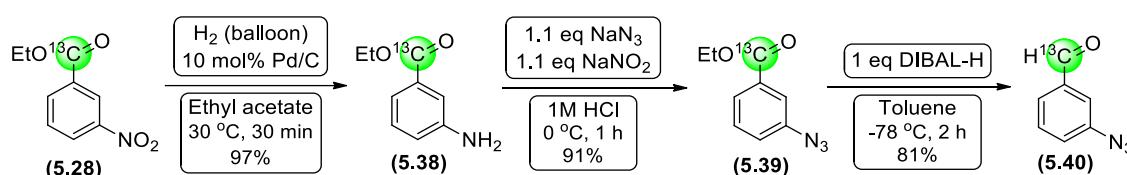
Figure 5.19. ^1H -NMR (500 MHz, CDCl_3) and ^{13}C -NMR (126 MHz, CDCl_3) spectra of *cis*-(**5.37**)

Because the ^{13}C -NMR (126 MHz, CDCl_3) spectrum of *cis*-(**5.37**) was not ^{19}F decoupled, fluorine-carbon couplings were observed. The *para*-carbon, with the fluorine atom directly attached to it, was observed at δ 162.4 ppm as a doublet with a large splitting constant $^1J_{\text{C-F}} = 245.2$ Hz. The *meta*-carbon was observed at δ 114.7 ppm (d, $^2J_{\text{C-F}} = 21.5$ Hz). The *ortho*-carbon was observed at δ 129.8 ppm as a doublet of doublets as it was split by both ^{19}F and ^{15}N nuclei ($^3J_{\text{C-F}} = 8.1$, $^3J_{\text{C-N}} = 1.7$ Hz). The *ipso*-carbon was observed at δ 131.2 ppm (dd, $^4J_{\text{C-F}} = 3.9$, $^2J_{\text{C-N}} = 3.2$ Hz), displaying four bond carbon-fluorine coupling and two bond carbon- ^{15}N coupling. The data matched favourably to the studies of Lichter and Wasylishen, who recorded the $J_{\text{C-F}}$ coupling constants of fluorobenzene to be 245 (1J), 21 (2J), 8 (3J), and 3 (4J) Hz.²⁰⁴ Carbonyl carbon was observed as a doublet at δ 167.4 ($^2J_{\text{C-N}} = 4.6$ Hz). The signal at δ 46.7 ppm (d, $^1J_{\text{C-N}} = 7.0$ Hz) was assigned to the carbon on the C-2 position. Unfortunately, the carbon on the C-3 position was not observed, possibly due to the low concentration of the sample and insufficient number of the scans. The remaining signals were recorded at δ 153.1 ppm (d, $^2J_{\text{C-N}} = 2.6$ Hz), 135.0 ppm (d, $^1J_{\text{C-N}} = 3.0$ Hz) and 119.8 ppm (d, $^3J_{\text{C-N}} = 1.8$ Hz) and assigned to the carbons from the dimethoxyphenyl aromatic ring. ^{19}F NMR (471 MHz, CDCl_3) spectrum of *cis*-(**5.37**) displayed a strong singlet at δ -115.24 ppm.

5.12. Synthesis of α - ^{13}C -3-azidobenzaldehyde (5.40)

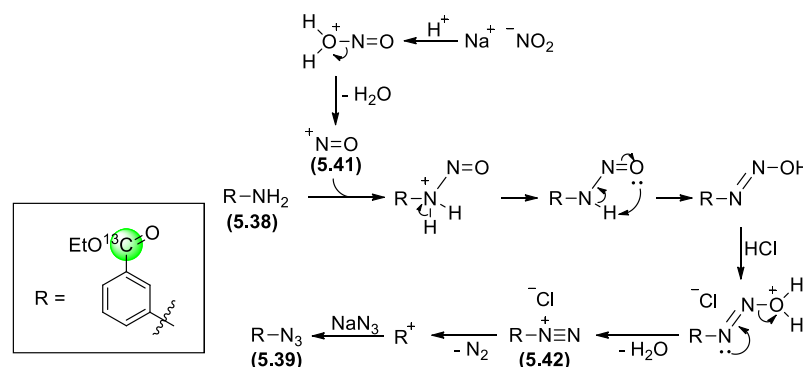
Organic azides possess diverse chemical reactivities.²⁰⁵ They undergo [3+2] cycloaddition with unsaturated bonds, such as those in alkynes and alkenes as well as carbonitriles to afford triazoles, triazolines and tetrazoles respectively. Organic azides can also be regarded as nitrene equivalents, that are capable of forming a new bond with the internal azido nitrogen and releasing molecular nitrogen as a leaving group. The azido group can also be used as a protecting group for primary amines in metathesis reactions, because primary amines displace the phosphine ligands in the first and second generation Grubbs catalysts.²⁰⁶

Due to high versatility of the azido functional group, a synthesis of α - ^{13}C -3-azidobenzaldehyde (5.40) was attempted starting from ethyl α - ^{13}C -3-nitrobenzoate (5.28), with the desired product achieved in 71% overall yield over three steps (Scheme 5.14.).



Scheme 5.14. Synthesis of α - ^{13}C -3-azidobenzaldehyde (5.40)

Following the procedure reported by Try *et al*, ethyl α - ^{13}C -3-nitrobenzoate (5.28) was converted to the corresponding ethyl α - ^{13}C -3-aminobenzoate (5.38) *via* nitro group reduction.²⁰⁷ Employing the conditions reported by Yao *et al*, the amine group was subjected to a nitrosation reaction using the nitrosyl cation (^+NO) (5.41), which was generated *in situ* from nitrous acid (HNO_2) (Scheme 5.15.).²⁰⁸ The diazonium intermediate (5.42) was reacted with sodium azide, affording ethyl α - ^{13}C -3-azidobenzoate (5.39).²⁰⁹ In the final step, the ester group of ethyl α - ^{13}C -3-azidobenzoate (5.39) was reduced with DIBAL-H (see synthesis of (5.29), page 67-68) affording α - ^{13}C -3-azidobenzaldehyde (5.40).



Scheme 5.15. Proposed mechanism of the nitrosation of the primary amine (5.38) and subsequent conversion to azide derivative (5.39)

Subsequent $^1\text{H-NMR}$ (500 MHz, CDCl_3) analysis of (**5.40**) revealed the proton at the α -carbon at δ 9.99 ppm to be a doublet with the coupling constant of 176.2 Hz (**Figure 5.20.**), similar to that of α - ^{13}C -3-nitrobenzaldehyde (**5.29**), which displayed the proton at the α -carbon at δ 10.13 ppm (d, $J_{^{13}\text{C-H}} = 179.1$ Hz) (see **Figure 5.18.**, page 68).

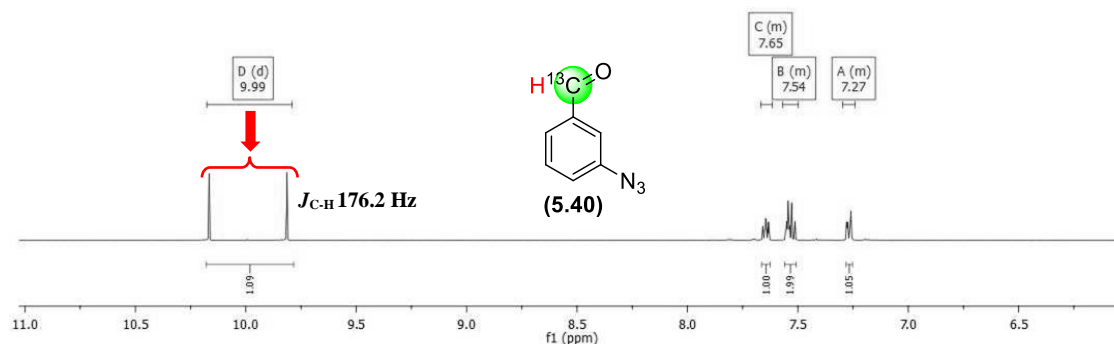


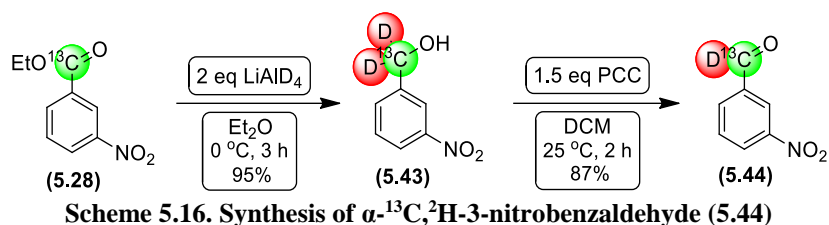
Figure 5.20. $^1\text{H-NMR}$ (500 MHz, CDCl_3) spectrum of (**5.40**)

The presence of the azide group was indicated by the FT-IR analysis with a strong peak at 2114 cm^{-1} . The HRMS analysis provided a final confirmation of the synthesis of (**5.40**) with $[\text{M}+\text{H}]^+$ ions found at the required m/z (found: 149.0535, requires: 149.0539). Synthesis of (**5.40**) allowed us to generate compounds such as chiral non-racemic aziridine *cis*-(**5.52**) and β -bromo- α -amino ester (**5.68**), suitable for further transformations such as "click" reaction or Staudinger reduction.²¹⁰

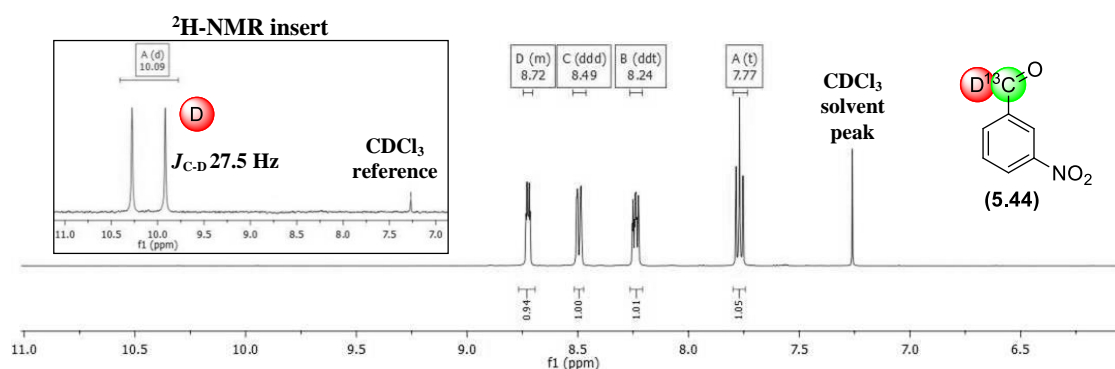
5.13. Synthesis of α - ^{13}C , ^2H -3-nitrobenzaldehyde (**5.44**)

It has been discussed previously that a chemical shift of a ^{13}C -isotope is sensitive to an isotope that is attached to it. To explore this property, and with α - ^{13}C -3-nitrobenzaldehyde (**5.29**) already generated, we attempted a synthesis of α - ^{13}C , ^2H -3-nitrobenzaldehyde (**5.44**) with a deuteron instead of a proton directly attached to a ^{13}C -nucleus.

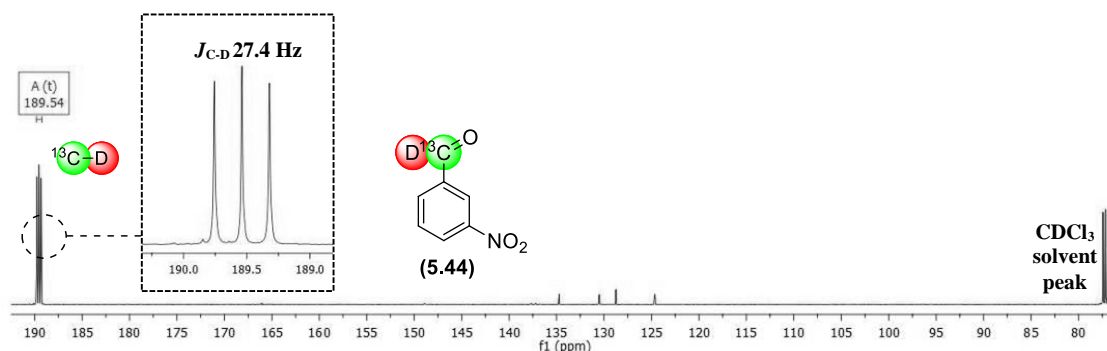
α - ^{13}C , ^2H -3-nitrobenzaldehyde (**5.44**) was synthesised in two steps from ethyl α - ^{13}C -3-nitrobenzoate (**5.28**) (**Scheme 5.16.**). The first step involved a reduction of ^{13}C -3-nitrobenzoate (**5.28**) with lithium aluminium deuteride, affording α -di- ^2H , ^{13}C -3-nitrobenzyl alcohol (**5.43**). Subsequent oxidation of this alcohol with pyridinium chlorochromate afforded α - ^{13}C , ^2H -3-nitrobenzaldehyde (**5.44**) in a 83% overall yield. The experimental procedure utilised was originally reported by Goss *et al*, who synthesised a α - ^2H -labelled benzaldehyde from ethyl benzoate in a 80% overall yield.²¹¹



Within the ^1H -NMR (500 MHz, CDCl_3) spectrum of α - ^2H , ^{13}C -3-nitrobenzaldehyde (**5.44**) no signal for the formyl proton was observed, as it had been replaced with deuterium (> 95% ^2H incorporation) (**Figure 5.21**). The ^2H -NMR (77 MHz, CDCl_3) spectrum of (**5.44**) displayed the deuterium signal at δ 10.09 ppm as a doublet ($J_{^{13}\text{C}-\text{D}} = 27.5$ Hz), due to the splitting by the NMR active ^{13}C -nucleus.

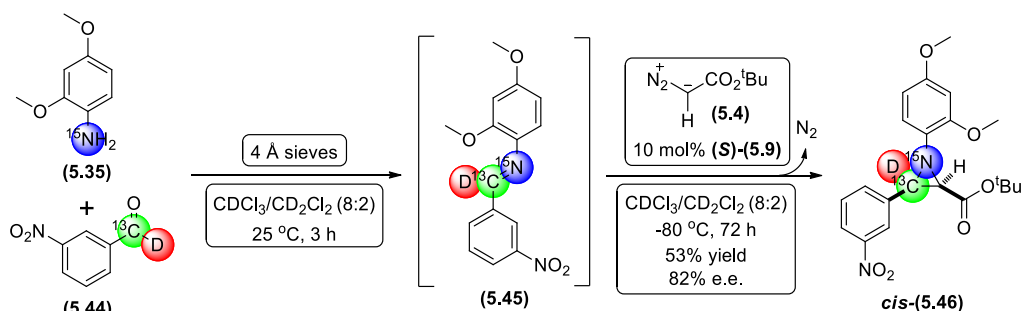


^{13}C -NMR (126 MHz, CDCl_3) analysis of (**5.44**) afforded a signal from the α -carbon at δ 189.5 ppm as a triplet ($J_{^{13}\text{C}-\text{D}} = 27.4$ Hz), due to ^2H - ^{13}C coupling (**Figure 5.22**). The effect of deuteration was also observed in the intensity of the peak, which was not as enhanced as the peak in the proteo-equivalent compound: α - ^{13}C -3-nitrobenzaldehyde (**5.29**), possessing a carbonyl peak at 189.8 ppm (see page 68). The chemical shift difference was attributed to the sensitivity of a ^{13}C -nucleus to a directly attached isotope, known as an isotope shift effect.



5.14. Synthesis of 1-¹⁵N-3-¹³C,²H-tert-butyl 1-(2,4-dimethoxyphenyl)-3-(3-nitrophenyl)aziridine-2-carboxylate *cis*-(**5.46**)

With α -²H,¹³C-3-nitrobenzaldehyde (**5.44**) prepared, a synthesis of *cis*-(**5.46**) was attempted, following the asymmetric aziridination protocol developed earlier *via* the intermediate (**5.45**) (Scheme 5.17.). Purification by flash chromatography on silica gel, afforded *cis*-(**5.46**) as a yellow oil in a 53% yield and 82% e.e.



Scheme 5.17. Asymmetric synthesis of *cis*-(**5.46**)

Analysing the ¹H-NMR (500 MHz, CDCl₃) spectrum of *cis*-(**5.46**), it was noted that the proton at the C-2 carbon at δ 3.02 ppm was split by the ¹³C-nucleus, which resulted in a doublet (²J_{13C-H} = 2.1 Hz) (Figure 5.23.). Similar coupling was observed in the compound *cis*-(**5.31**).

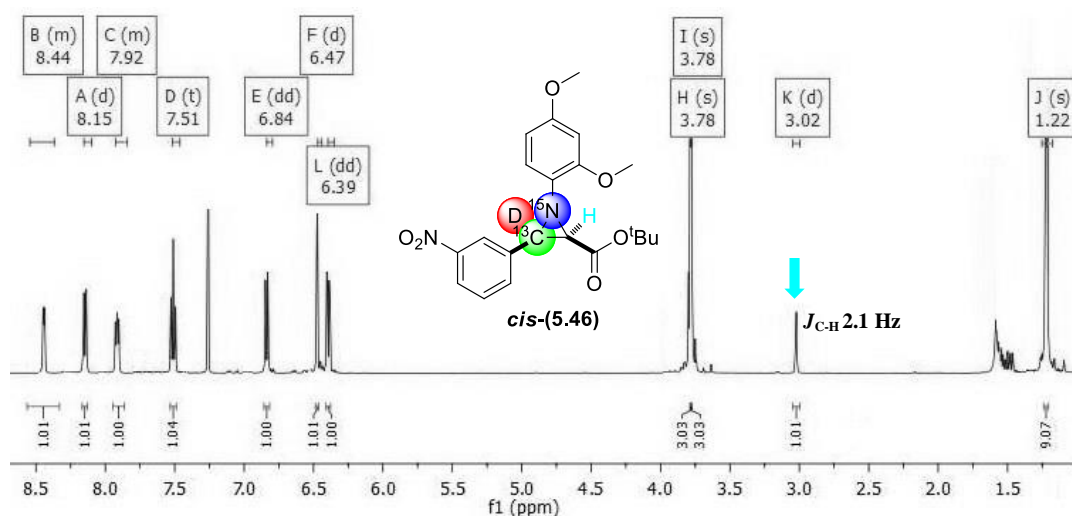


Figure 5.23. ¹H-NMR (500 MHz, CDCl₃) spectrum of *cis*-(**5.46**)

The ¹³C-NMR (126 MHz, CDCl₃) spectrum of *cis*-(**5.46**) displayed a signal from the α -carbon at δ 46.4 ppm as a triplet of doublets ($J_{13C-D} = 25.5$ Hz, $J_{13C-N} = 7.0$ Hz), as it has been split not only by the ²H-nucleus [as observed in the starting material (**5.44**)], but also by ¹⁵N (Figure 5.24.). The peak possessed low intensity and was not fully resolved due to the effect of the deuteration.

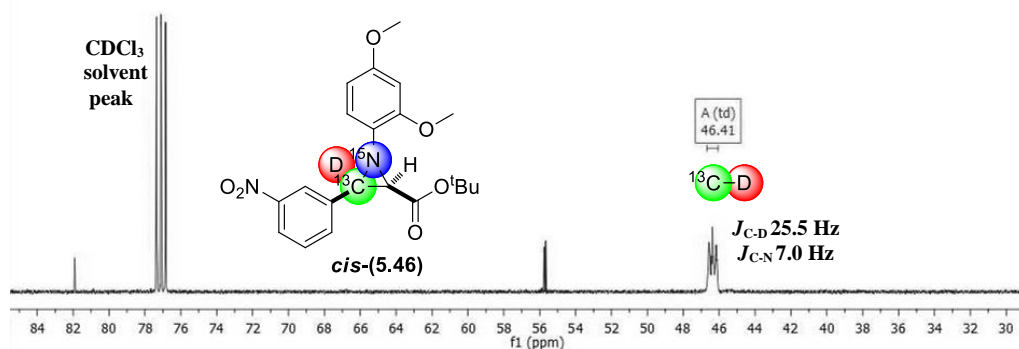


Figure 5.24. ^{13}C -NMR (126 MHz, CDCl_3) spectrum of *cis*-(5.46)

5.15. Summary table of enantiomerically enriched *N*-aryl aziridine-2-carboxylates labelled with stable isotopes

<p>67% yield 85% e.e.</p> <p><i>cis</i>-(5.18)</p>	<p>57% yield 86% e.e.</p> <p><i>cis</i>-(5.47)</p>	<p>49% yield 75% e.e.</p> <p><i>cis</i>-(5.48)</p>
<p>44% yield 66% e.e.</p> <p><i>cis</i>-(5.25)</p>	<p>61% yield 87% e.e.</p> <p><i>cis</i>-(5.31)</p>	<p>55% yield 71% e.e.</p> <p><i>cis</i>-(5.32)</p>
<p>51% yield 72% e.e.</p> <p><i>cis</i>-(5.49)</p>	<p>48% yield 61% e.e.</p> <p><i>cis</i>-(5.37)</p>	<p>66% yield 70% e.e.</p> <p><i>cis</i>-(5.50)</p>
<p>51% yield 80% e.e.</p> <p><i>cis</i>-(5.51)</p>	<p>44% yield 72% e.e.</p> <p><i>cis</i>-(5.52)</p>	<p>53% yield 82% e.e.</p> <p><i>cis</i>-(5.46)</p>

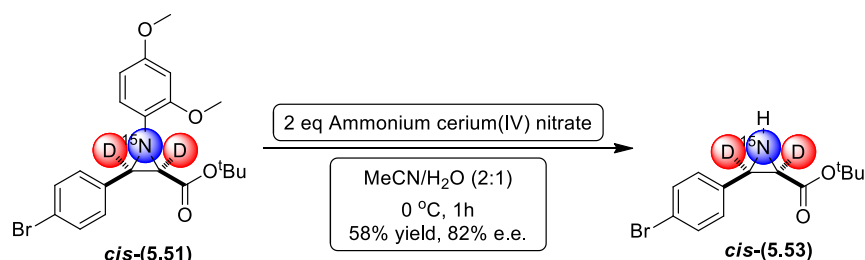
Table 5.5. Chiral non-racemic aziridine library

To summarise, during the course of this project a library of novel optically active aziridines has been generated (Table 5.5.). The aziridines were generated in 44 - 67% yield, 61 - 87% e.e. and were ^2H , ^{15}N and/or ^{13}C isotopically enriched. It was established that incorporation of stable isotopic labels led to increased reaction time, which could be attributed to the time required to break a stronger, isotopically

substituted bond, thus suggesting that the rate determining step is the addition of a diazoacetate derivative to an ^{15}N -labelled imine. Additionally, the energy difference between light and heavy atoms influences the approach of the diazoacetate derivative to an imine, which is reflected in the decreasing e.e. trend observed, thus making C-C bond formation a step where the stereochemistry is set. Furthermore, we wanted to investigate if any subsequent transformations of isotopically labelled aziridines such as ring-opening, *N*-terminus deprotection would result in a loss of label, decrease of e.e., lack of reactivity.

5.16. Oxidative cleavage of *N*-2,4-dimethoxyphenyl protecting group from 1- ^{15}N -2,3- ^2H -*tert*-butyl 3-(4-bromophenyl)-1-(2,4-dimethoxyphenyl)aziridine-2-carboxylate *cis*-(5.46)

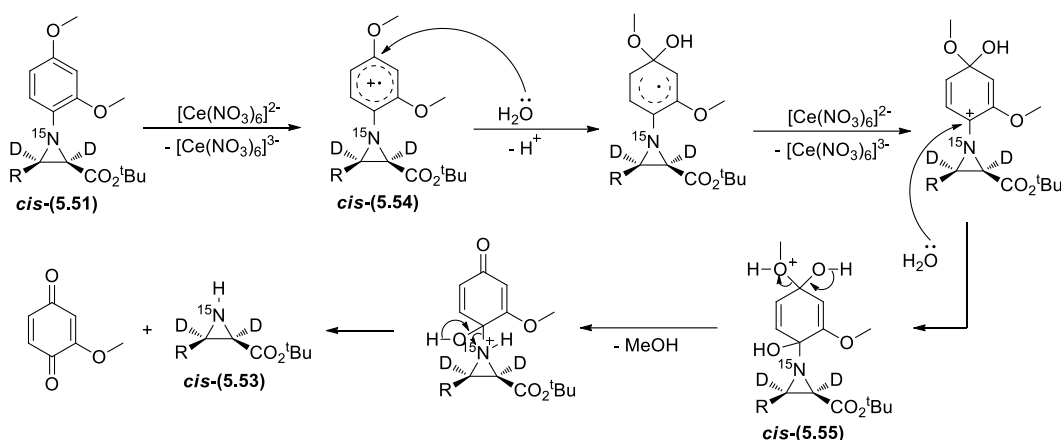
As discussed previously, a literature search afforded a publication by Mayer *et al*, who demonstrated a deprotection of the *N*-PMP group, using CAN, affording the corresponding *NH*-aziridine in a 82% yield (see page 71). Following this procedure we were able to demonstrate that *N*-2,4-dimethoxyphenyl group can be removed from *cis*-(5.51) under oxidative conditions, using CAN (Scheme 5.18.). Gratifyingly, *cis*-(5.53) was obtained in 58% yield and 82% enantiomeric excess, which confirmed that no racemisation occurred during the oxidative deprotection of the *N*-terminus.



Scheme 5.18. Synthesis of *cis*-(5.53)

Investigating a mechanism of the side-chain oxidation of alkylated aromatic hydrocarbons with CAN, Baciocchi *et al* established that the first step of the reaction was a formation of a radical cation.²¹² Jarrahpour and Zarei reported successful deprotection of PMP from the substituted β -lactams using CAN.²¹³ Their study indicated that a successful deprotection occurred only when at least two equivalents of CAN were present. By analogy with their results, we proposed a reaction of 1,4-dimethoxybenzene group of *cis*-(5.51) with CAN initially afforded a radical cation intermediate *cis*-(5.54), stabilised by electron donating substituents (Scheme 5.19.).²¹⁴ An aqueous media was required to promote a successful dissociation of CAN into $[\text{Ce}(\text{NO}_3)_6]^{2-}$ and NH_4^+ , as well as to allow the attack of a water molecule at the *para*-

position of *cis*-(**5.54**). Second equivalent of CAN promoted a water attack at the *ipso*-carbon of 1,4-dimethoxybenzene group. Elimination of methanol from *cis*-(**5.55**) and subsequent formation of 2-methoxy-1,4-benzoquinone generated *tert*-butyl 1-¹⁵NH-2,3-²H-3-(4-bromophenyl)aziridine-2-carboxylate *cis*-(**5.53**).



Scheme 5.19. Proposed mechanism of 2,4-dimethoxyphenyl group cleavage *via* CAN

The ¹H-NMR (500 MHz, CDCl₃) spectrum of *cis*-(**5.53**) displayed the signals from the *para*-bromophenyl group at δ 7.44 ppm (d, *J*_{H-H} = 7.9 Hz) and δ 7.22 ppm (d, *J*_{H-H} = 7.9 Hz) and a signal from the *tert*-butoxy group at δ 1.22 ppm as a singlet (**Figure 5.25**). Compared to the ¹H-NMR spectrum of starting material *cis*-(**5.51**) which displayed aromatic protons from the bromo-phenyl substituent at δ 7.49 - 7.38 ppm as a multiplet, a clear difference in chemical shift and a splitting pattern was observed.

Additionally it was confirmed that the oxidative deprotection did not affect neither e.e., which remained at 82% (determined by chiral HPLC), nor the deuterium incorporation level, which remained above 95% (determined from the non-labelled sample).

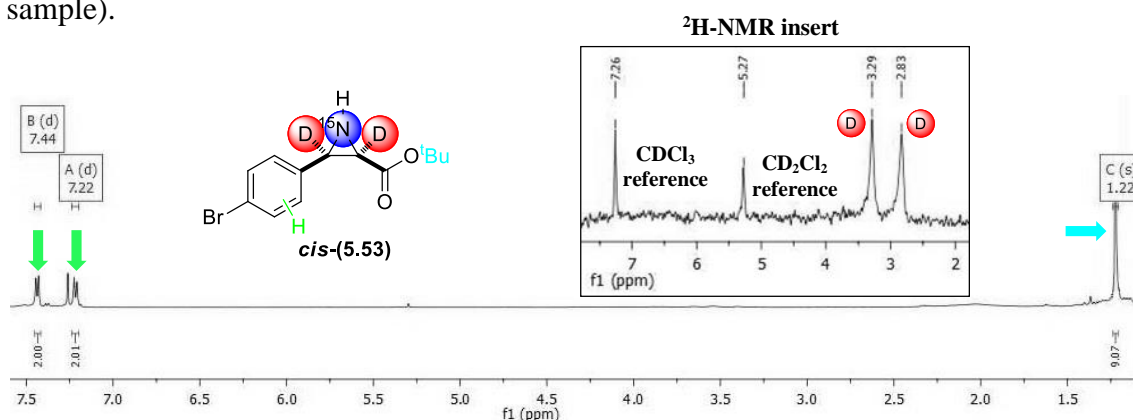
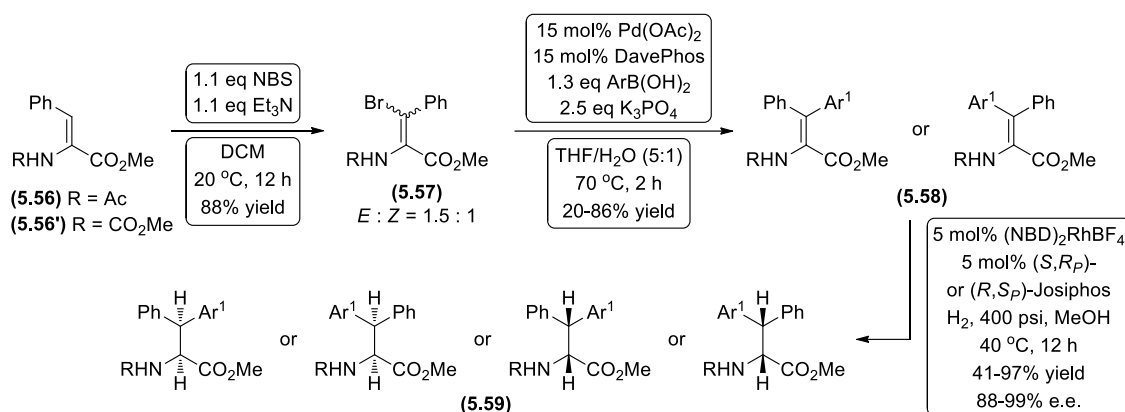


Figure 5.25. ¹H-NMR (500 MHz, CDCl₃) spectrum of *cis*-(**5.53**) with ²H-NMR (77 MHz, DCM) insert

5.17. Ring opening of *N*-aryl aziridines with magnesium bromide diethyl etherate

Molinaro *et al* reported an enantio- and diastereoselective route to novel non-symmetrically substituted *N*-protected β,β-diaryl-α-amino esters (**5.59**), through the

asymmetric hydrogenation of tetrasubstituted olefins (**5.58**) (Scheme 5.20).²¹⁵ The corresponding β -bromo- β -substituted dehydroamino esters (**5.57**) were prepared in 88% yield as a 1.5:1 mixture of *E*- and *Z*-isomers. The isomers were separable by flash chromatography and were individually coupled under Suzuki-Miyaura conditions with commercially available arylboronic acids. A catalytic complex of Pd(OAc)₂ and DavePhos provided alkenes (**5.58**) in 45-89% yields. The reaction conditions used bis(norbornadiene)rhodium(I) tetrafluoroborate [Rh(NBD)₂BF₄] and (*S,R_p*)- or (*R,S_p*)-Josiphos ligands and allowed outstanding control over the two vicinal stereogenic centers providing excellent enantioselectivities (88-99%) during the synthesis of (**5.59**).



Scheme 5.20. Synthesis of *N*-protected β,β -diaryl- α -amino esters (**5.59**) by Molinaro *et al*

The β,β -diarylalanine structural motif is an important pharmacophore in molecular agents that target many diseases, including atherosclerosis, cancer, diabetes, HIV and thrombosis (Figure 5.26). Fex *et al* synthesised a set of compounds such as (**5.60**) designed to bind to thrombin, a serine protease that is critically involved in blood coagulation by converting soluble fibrinogen into insoluble fibrin.²¹⁶ Additionally, this structural class appears in synthetic intermediates in natural product synthesis such as the intermediate of podophyllotoxin (**5.61**).²¹⁷

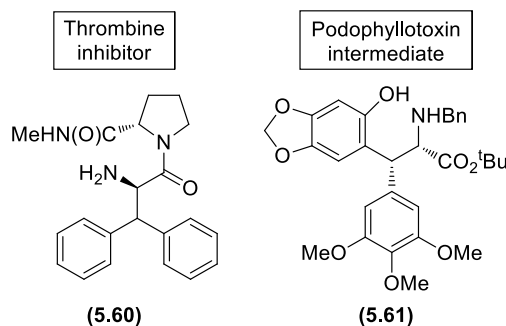


Figure 5.26. Bioactive compounds with β,β -diaryl- α -amino acid motif

Employing the procedure reported by Righi *et al* (see Scheme 2.22, page 22), we wanted to ring-open our optically active labelled aziridines in order to generate

corresponding β -bromo- α -amino esters, that are suitable for cross-coupling reactions, ultimately affording optically active β,β -diarylalanine derivatives, labelled with stable isotopes.

To test this methodology, racemic non-labelled aziridines were subjected to the ring-opening with magnesium bromide diethyl etherate (**Table 5.6**). Gratifyingly, the ring-opened products were generated in 61 - 80% yield, were easily purified by flash column chromatography on silica gel and were reasonably stable (no decomposition was observed after being left at room temperature for more than two months).

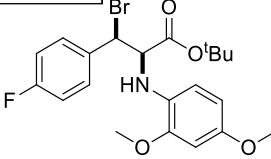
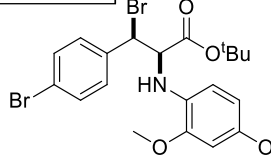
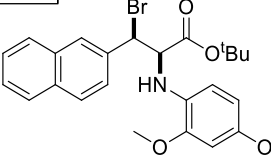
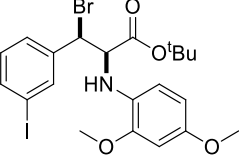
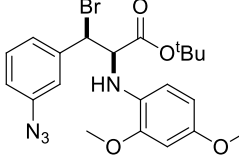
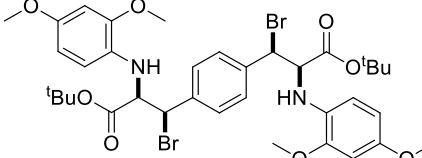
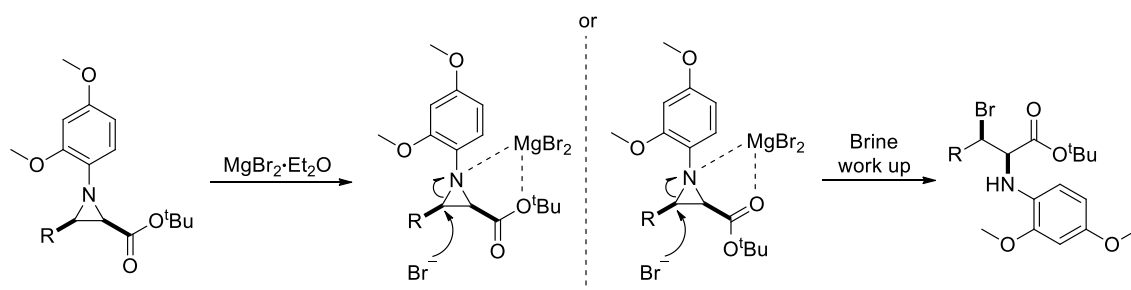
72% yield  (5.62)	64% yield  (5.63)	61% yield  (5.64)
73% yield  (5.65)	80% yield  (5.66)	68% yield  (5.67)

Table 5.6. Generated library of racemic aziridines ring-opened with magnesium bromide

Subsequent publications by the group of Righi included ring opening of epoxides using metal halides and elucidation of the ring-opening chelation control mechanism.^{218,219,220} Based on the mechanism, it was proposed that the magnesium metal coordinates to the nitrogen of the aziridine and one of the oxygens of the carbonyl group (**Scheme 5.21**). This blocks the approach of the bromine nucleophile to the C-2 position and ring-opens the aziridines at the C-3, affording β -bromo- α -amino acid derivatives.



Scheme 5.21. Proposed mechanism of aziridine ring-opening under MgBr_2 chelation control by Righi *et al*

At this point it was still unconfirmed whether the bromine atom occupied β -position affording the desired α -amino acid derivatives (**5.62**) - (**5.67**) or ring-opened aziridines at the C-2, yielding α -bromo- β -amino acid precursors. To establish the configuration of the ring-opened compounds, it was desired to obtain a crystal suitable for an x-ray analysis. After much experimentation, a further confirmation of the bromine atom at the β -position was achieved *via* single-crystal structure analysis (**Figure 5.27.**). A successful crystallisation of (**5.63**) was achieved from pentane/diethyl ether (2:1), with the crystal obtained as a colourless cube. The X-ray crystal structure confirmed the formation of the desired β -bromo- α -amino acid derivative.

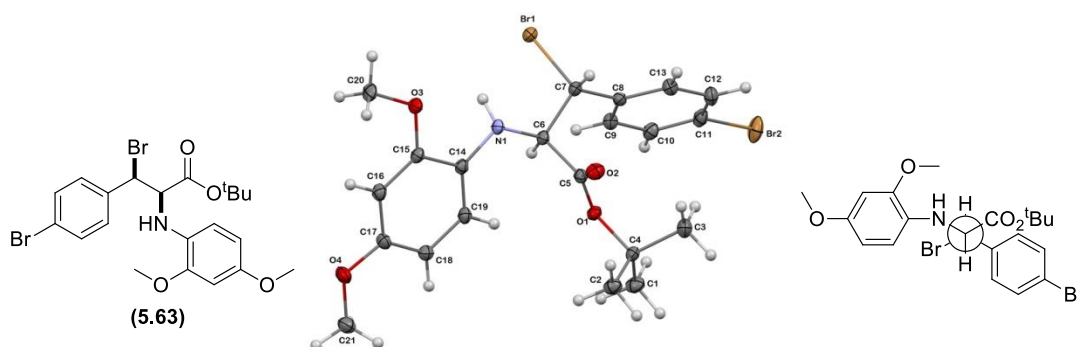
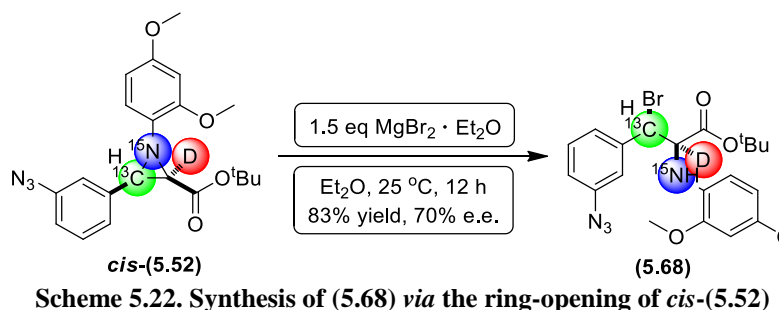


Figure 5.27. Oak Ridge Thermal Ellipsoid Plot (ORTEP) representation of the X-ray crystal structure of (**5.63**)

Encouraged by these results, we performed a ring-opening of chiral non-racemic aziridine *cis*-(**5.52**), investigating any possible negative impacts such as loss of e.e., label scrambling or loss. Following the procedure described above, *cis*-(**5.52**), which had 72% e.e. determined, was subjected to the ring opening with the magnesium bromide diethyl etherate (**Scheme 5.22.**). Purification by flash chromatography on silica gel afforded (**5.68**) in 83% yield and 70% e.e., which confirmed that the product did not fully racemise during the ring-opening step. A slight e.e. loss from 72% to 70% might be attributed to a very minor racemisation or an experimental error.



Analysing the $^1\text{H-NMR}$ (500 MHz, CDCl_3) spectrum of (**5.68**), it was noted that the proton at the β -carbon at δ 5.32 ppm was split into a double of doublets (**Figure 5.28.**). It was split by the ^{13}C -nucleus, which resulted in a coupling constant, $J_{\text{C-H}}$ to be

153.8 Hz. It was also split by a proton on the ^{15}N -atom, and the coupling constant was recorded as 3.2 Hz.

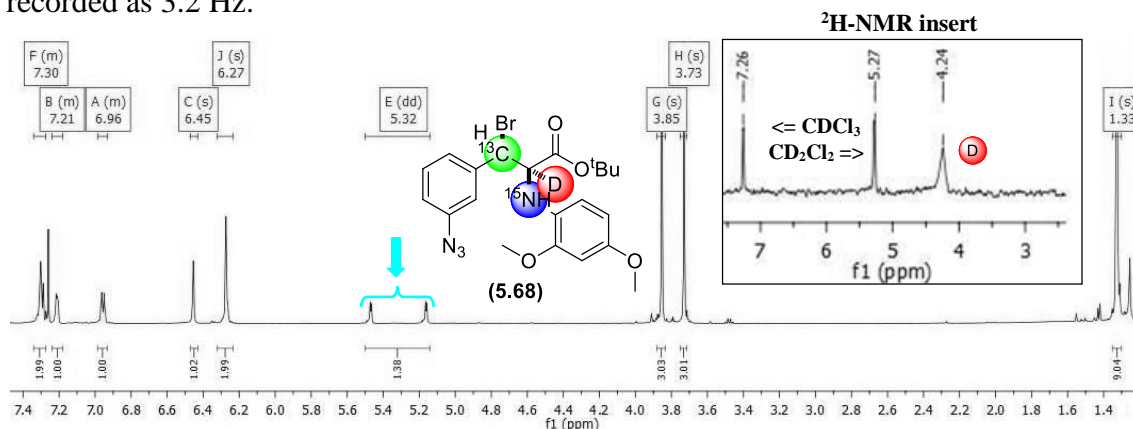


Figure 5.28. ^1H -NMR (500 MHz, CDCl_3) spectrum of (5.68) with ^2H -NMR (77 MHz, DCM) insert

Analysing the starting material of the above reaction, aziridine *cis*-(5.52), it was noticed that one bond ^{13}C - ^{15}N coupling constant was recorded to be ~ 7.0 Hz magnitude. After the ring-opening of *cis*-(5.52) and purification of the product (5.68), ^{13}C -NMR (126 MHz, CDCl_3) and ^{15}N -NMR (51 MHz, CDCl_3) spectra displayed the ^{13}C - ^{15}N coupling constant to be ~ 2.0 Hz (**Figure 5.29.**). A decrease of the magnitude suggests that ^{13}C and ^{15}N atoms are no longer bonded together and are separated by at least one atom. Conclusively, it was proposed that the ring opening resulted in the β -bromo- α -amino ester derivative (5.68).

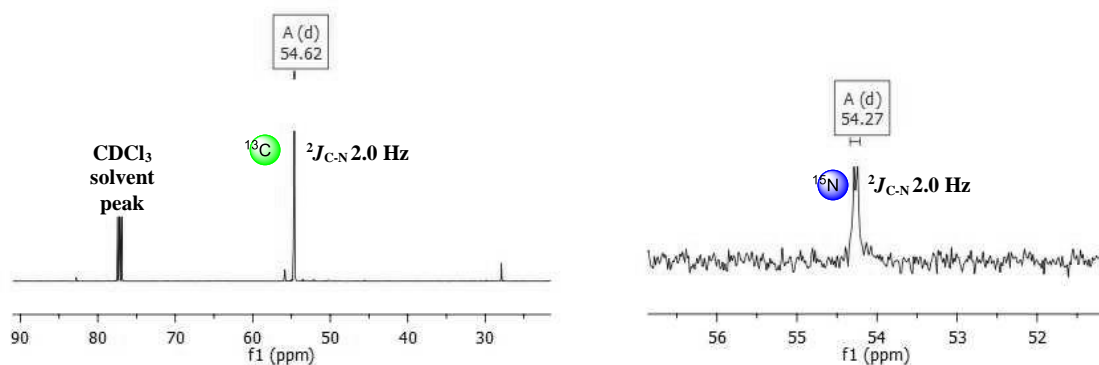


Figure 5.29. ^{13}C -NMR (126 MHz, CDCl_3) (left) and ^{15}N -NMR (51 MHz, CDCl_3) (right) spectra of (5.68)

The presence of the azide group was indicated by the FT-IR analysis with a strong peak at 2113 cm^{-1} . The HRMS analysis provided a final confirmation of the synthesis of (5.68) with $[\text{M}+\text{H}]^+$ ions found at the required m/z (found: 480.1187, required: 480.1199).

Although no cross-coupling reactions have been attempted and will be the subject of future investigations, optically active β -bromo- α -amino esters, labelled with

stable isotopes can provide a direct route towards corresponding β,β -diarylalanine derivatives.

5.18. Triple-Resonance Isotope-Edited (TRIED) NMR¹

With several compounds possessing the desired atom sequence for TRIED NMR analysis, we wanted to apply this method to achieve a signal enhancement. Recently, Sando *et al* demonstrated that *in situ* analysis of 8-¹³C-7-¹⁵N-theophylline (**5.69**) was achieved using a TRIED NMR experiment, which utilises through-bond (scalar) coupling between three NMR-active nuclei with different frequencies (**Figure 5.30**).²²¹ Theophylline is a pharmaceutical agent for treatment of respiratory diseases, such as chronic obstructive pulmonary disease and asthma.²²² The conventional ¹H-NMR spectrum of a 200 μ M sample of [8-¹³C-7-¹⁵N]-theophylline (**5.69**) in D₂O, containing excess amino acids (42.875 mM), displayed a barely visible proton signal in the sequence ¹H-¹³C-¹⁵N, due to strong background signals derived from the amino acids. However, when performing a ¹H-¹³C-¹⁵N TRIED NMR experiment, an enhanced singlet was observed around 8.0 ppm corresponding to proton connected to the ¹³C-¹⁵N atom sequence. This result suggests a high selectivity of the double-labelled probe under the triple resonance NMR conditions and allows a detection of the labelled compound in a crude biological sample. Most importantly, the labelled theophylline displayed identical biological properties of the non-labelled analogue, allowing the investigation towards its behaviour as a pharmaceutical agent.

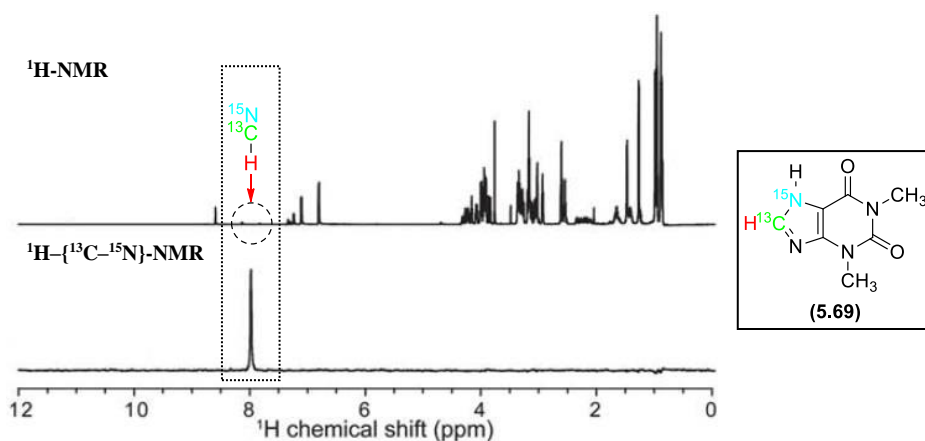


Figure 5.30. Conventional ¹H-NMR (top) and ¹H-¹³C-¹⁵N triple resonance NMR (bottom) spectra of [8-¹³C-7-¹⁵N]-labelled theophylline (**5.69**) (200 μ M) in D₂O containing excess amino acids (42.875 mM) recorded by Sando *et al*

¹ All TRIED data collection and processing for compounds *cis*-(**5.31**) and (\pm)-*cis*-(**5.64**) carried out by Dr Colin Macdonald, UEA, Norwich, UK

With a previously synthesised aziridine *cis*-(**5.31**) having desired atom sequence, it was decided to apply the TRIED analysis to determine if it can be used as a probe for the pharmacokinetic analysis (**Figure 5.31**). The conventional ^1H -NMR spectrum of *cis*-(**5.31**) revealed a signal (doublet, $J_{2,3}$ 6.7 Hz; $J_{^{13}\text{C}-\text{H}}$ 169.0 Hz) at δ 3.59 ppm corresponding to the proton in the ^1H - ^{13}C - ^{15}N sequence. The intensity was recorded as \sim 500 units (2.9 mM in CDCl_3). Performing the ^1H - $\{^{13}\text{C}$ - $^{15}\text{N}\}$ triple resonance NMR experiment, a single peak was observed at δ 3.64 ppm, which corresponded to the proton at the C-3 position, connected to the ^{13}C - ^{15}N atom sequence. The intensity of the peak was recorded to be \sim 250000 units (2.9 mM concentration in CDCl_3), which was 500 times higher than the intensity of the proton peak in the conventional ^1H -NMR spectrum. This result confirmed that the signal of the proton in the ^1H - ^{13}C - ^{15}N sequence was greatly enhanced, while the rest of the signals were suppressed.

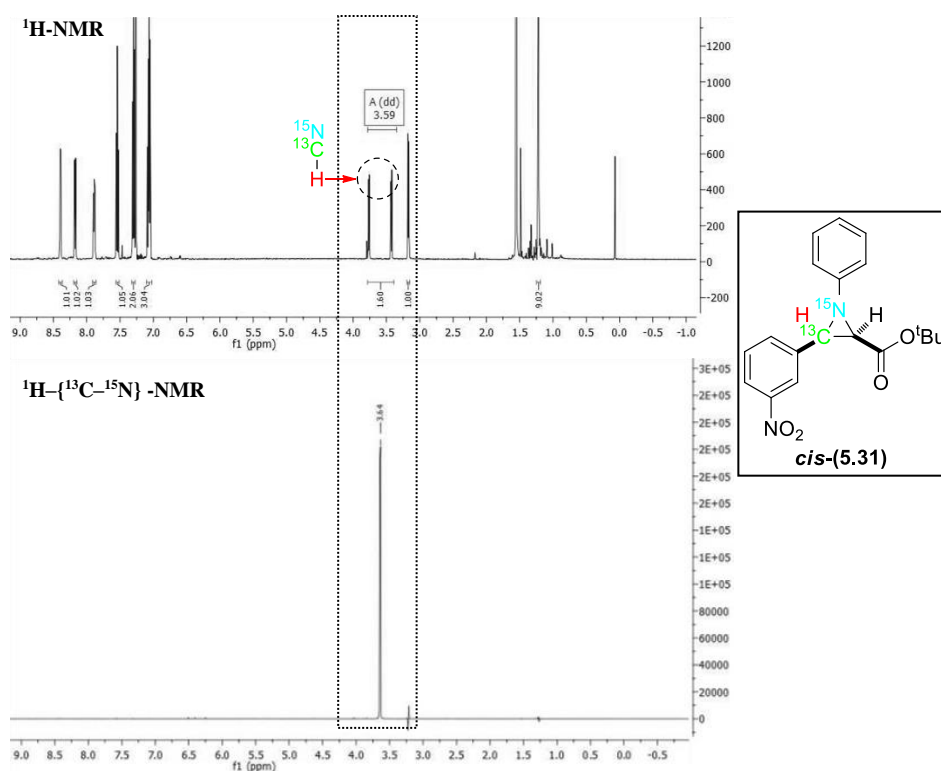


Figure 5.31. Conventional ^1H -NMR (top) and ^1H - $\{^{13}\text{C}$ - $^{15}\text{N}\}$ triple resonance NMR (bottom) spectra of *cis*-(**5.31**) (2.9 mM) in CDCl_3

After successful testing of the ^1H - $\{^{13}\text{C}$ - $^{15}\text{N}\}$ triple resonance technique, it was hypothesised that ^2H - $\{^{13}\text{C}$ - $^{15}\text{N}\}$ experiment would enhance a deuterium signal. After much experimentation a successful result was obtained using compound (\pm)-*cis*-(**5.64**).

The conventional ^2H -NMR spectrum of (\pm)-*cis*-(**5.64**) revealed a signal (doublet, $J_{\text{C-D}}$ 25.1 Hz) at δ 3.47 ppm, which was assigned to the deuterium atom in the ^2H - ^{13}C - ^{15}N sequence (**Figure 5.32**). The intensity was recorded to be \sim 7 units (3.3 mM in

CH₂Cl₂). Analysing the ²H-¹³C-¹⁵N} triple resonance NMR experiment, a single peak was observed at δ 3.47 ppm. This signal was assigned to the deuterium atom at the C-3 position, which was connected to the ¹³C-¹⁵N atom sequence. The intensity of the peak was recorded to be ~ 350 units (3.3 mM in CH₂Cl₂), which was 50 times higher than the intensity of the deuterium peak in the conventional ²H-NMR spectrum.

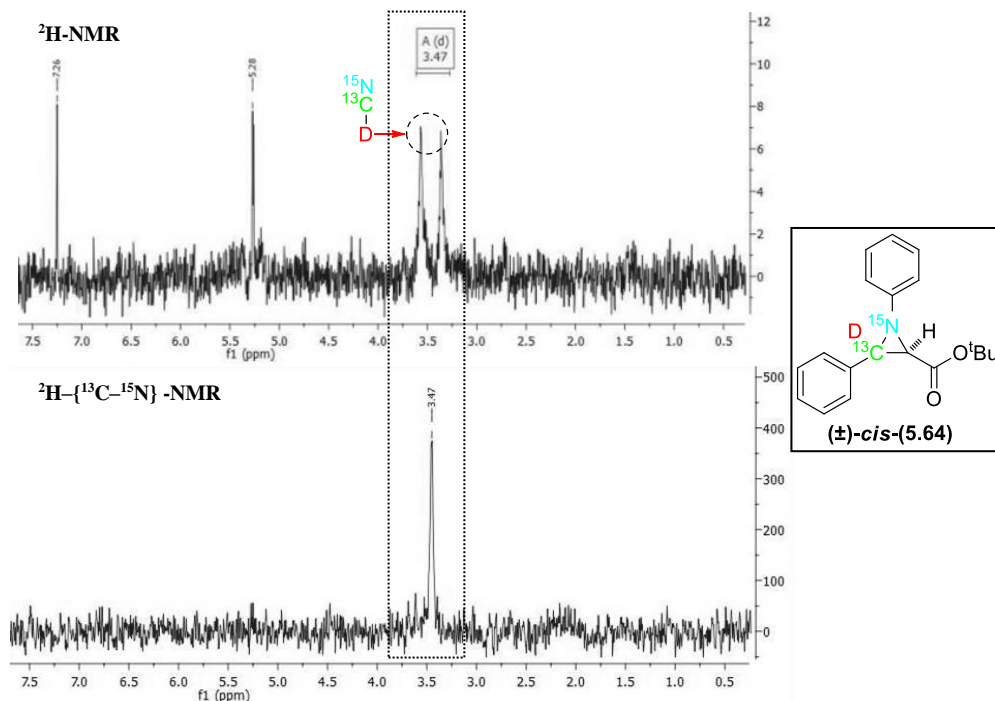


Figure 5.32. Conventional ²H-NMR (top) and ²H-¹³C-¹⁵N} triple resonance NMR (bottom) spectra of (±)-cis-(5.64) (3.3 mM) in CH₂Cl₂

Although, the enhancement of the deuterium signal had 10 fold decrease in magnitude compared the proton signal enhancement, it was demonstrated that deuterium could act as a probe for selective NMR detection by triple resonance analysis. Attaching a proton or deuteron to the ¹³C-¹⁵N sequence greatly improves the signal of the pulsed atom: proton - up to 500 times and deuteron - up to 50 times.

In conclusion the TRIED NMR technique discussed above provides a powerful approach for a detection of organic molecules containing ¹H-¹³C-¹⁵N atom sequence and their analysis without any purification. With H-C-N atom sequence being very common in amino acids, TRIED NMR technique can be used as a tool in protein characterisation. Within this chapter, only proton and deuterium enhancement has been explored so far, with plenty of other potential candidate molecules to be investigated in the future. It well may be the case that other NMR active nuclei can provide even better signal enhancement.

5.19. Chapter conclusion

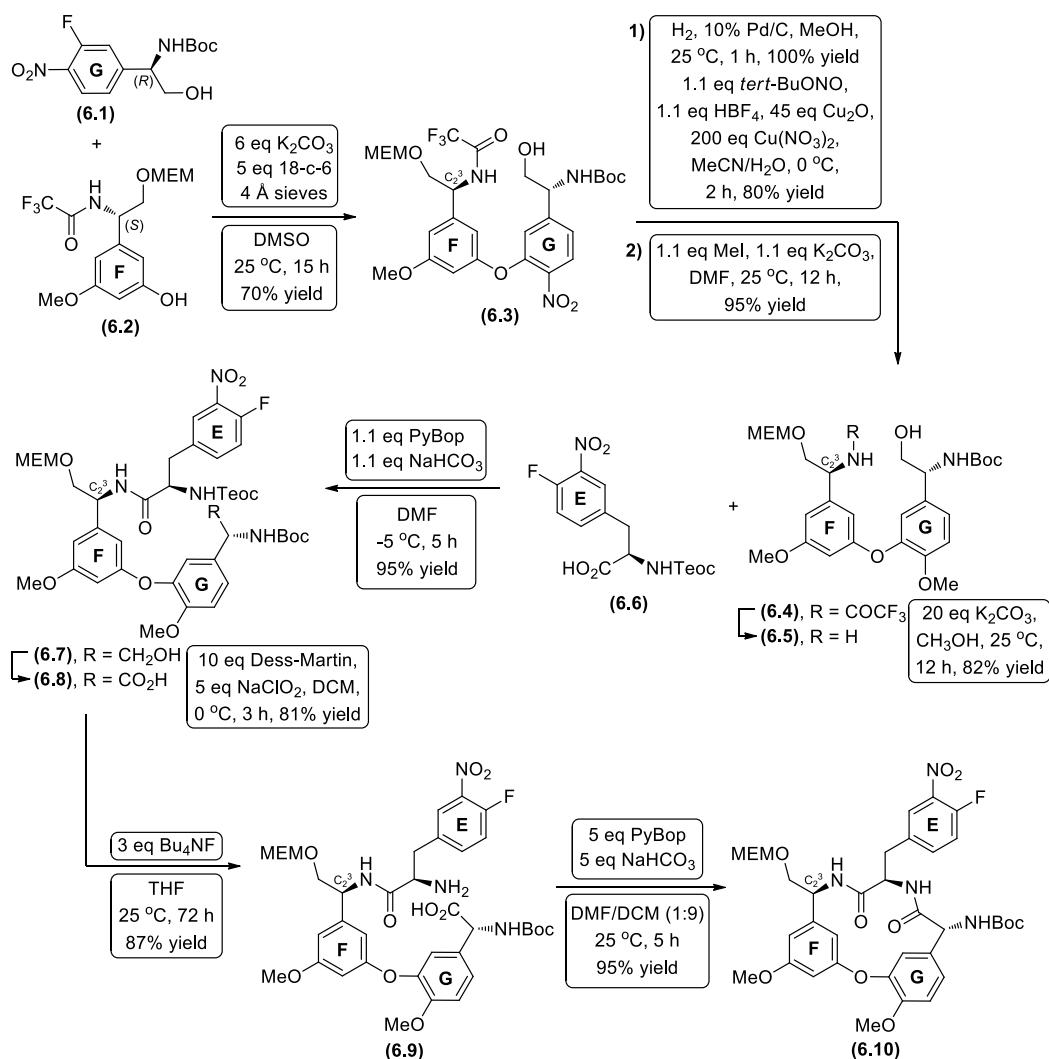
Aziridines are extensively used as ‘core’ heterocycle building blocks that can be readily transformed into a plethora of alternative entities: α - and β -amino acids, diamines, oxazolidinones, etc. Within this chapter we reported a multi-component, asymmetric Brønsted acid organocatalytic method that mediated incorporation of stable isotopes (^2H , ^{13}C , ^{15}N) into structure and function diverse optically active aziridines. The levels of isotope incorporation were recorded above 95%, with no evidence of isotope scrambling and aziridines were generated with good levels of diastereo and enantioselectivity (up to 87% e.e.). Our isotope incorporating methodology will be of significant utility in academia, medicinal, pharmaceutical, agrochemical and biological industries.

Chapter 6. Synthetic efforts towards a model fragment of teicoplanin glycopeptide antibiotic

6.1. Introduction

Glycopeptide antibiotics form a crucial part of human defence against the deadly threat of bacterial infections.²²³ The emergence of antibiotic resistant bacteria requires the discovery of new compounds or the modification of existing antibiotics, that would be more potent. For these processes to be successful it is crucial to study antibacterial drugs more rigorously and to develop new methodologies that can afford target structures more efficiently.

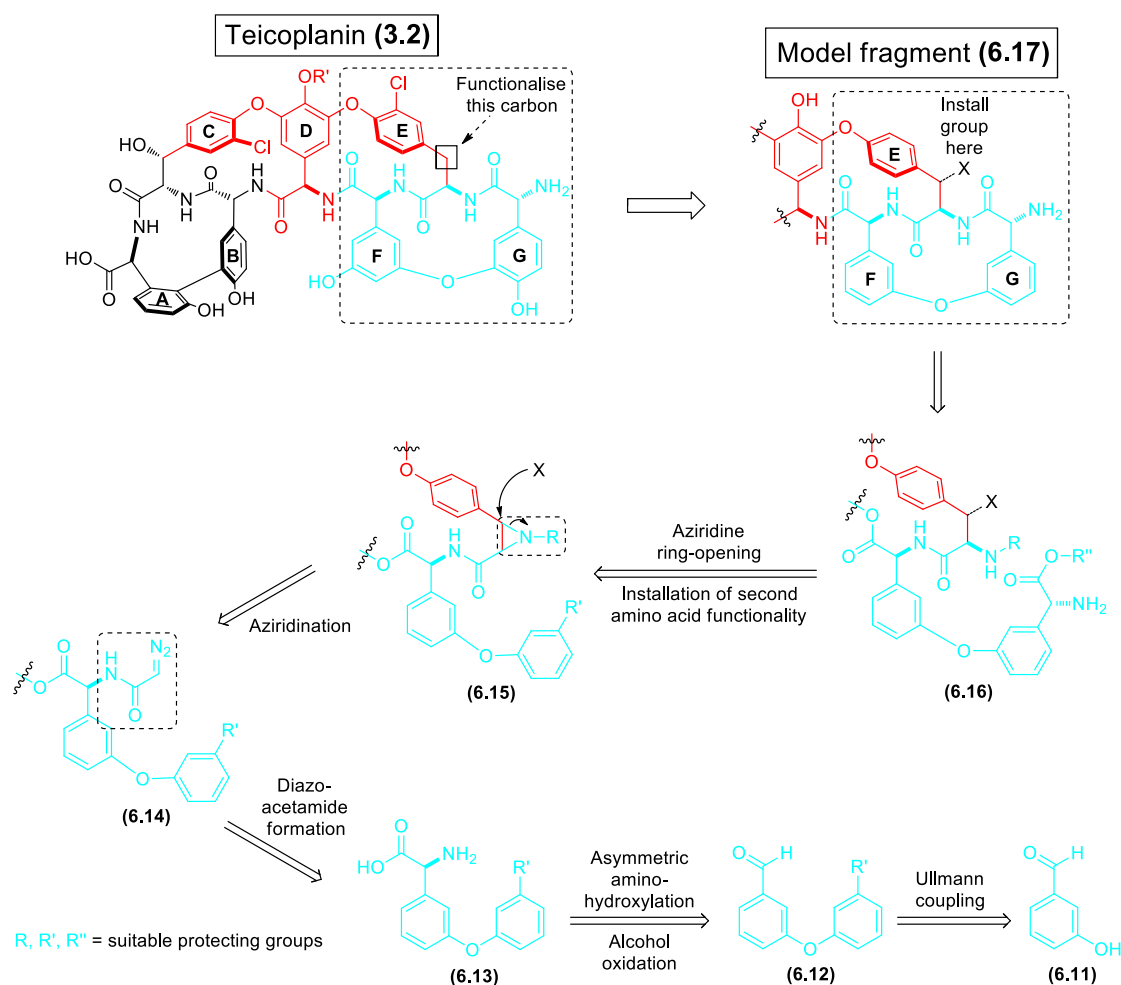
First total synthesis of teicoplanin aglycon was reported by Boger *et al*, who utilised an introduction of the **E-F-O-G** ring system onto the preformed **A-B-C-D** ring system (**Scheme 6.1**).²²⁴ A special attraction of this approach was the recognition of the common **A-B-C-D** ring system of vancomycin (**3.1**) and teicoplanin (**3.2**) and its utilisation as a key synthetic intermediate providing access to both classes of natural products. Because of concerns over the C₂³ centre epimerisation observed within the **F** ring system, Boger *et al* chosen to form the **F-O-G** biaryl ether by an intermolecular aromatic nucleophilic substitution reaction using acyclic substrates which are incapable of epimerisation.²²⁵ Thus, both the **F** ring and **G** ring amino acid precursors were utilised as the reduced α -arylglycinols (**6.1**) and (**6.2**) to avoid α -centre racemisation during the synthesis and oxidised to the corresponding carboxylic acids immediately prior to use in an amide coupling. Oxidation step proceeded exceptionally well, as the reaction conditions had been established by the group during the synthesis of vancomycin.²²⁶ After the successful coupling of the **F** and **G** ring derivatives, affording biaryl ether (**6.3**), the nitro group on the **G** ring was converted to the methoxy group in 76% total yield over two steps, affording (**6.4**).²²⁷ After removal of trifluoroacetate protecting group from the **F** ring, resulting in (**6.5**), amide coupling with the **E** ring derivative (**6.6**) was attempted. Oxidation of the primary alcohol on the **G** ring of (**6.7**) to the carboxylic acid derivative (**6.8**) and trimethylsilylethoxycarbonyl (Teoc) *N*-protecting group deprotection afforded (**6.9**). Subsequent amide coupling with amine functionality of the **E** ring furnished **E-F-O-G** fragment (**6.10**). NOE experiments confirmed the fragment had correct space orientation identical to that found in teicoplanin (**3.2**).



Scheme 6.1. Synthesis of E-F-O-G fragment (6.10) of teicoplanin (3.2) by Boger *et al*

This chapter outlines our synthetic route towards the synthesis of **E-F-O-G** model fragment (6.17) of teicoplanin (3.2) employing aziridination methodology developed within the Bew group (Scheme 6.2.). We wanted to construct the **F-O-G** fragment (blue) of teicoplanin (3.2) and append it to the **E** ring (red) *via* an aziridination reaction. The C-3 ring opening of the aziridine with various nucleophiles (**X**) would afford teicoplanin derivatives (6.17) with a modified benzylic carbon at the **E** ring. Initiating this process, we proposed a strategy to construct the **F-O-G** fragment *via* an Ullmann ether synthesis, that employed commercially available inexpensive starting materials such as 3-hydroxybenzaldehyde (6.11) and 3-bromobenzaldehyde (6.23). As this method might suffer from poor yield and harsh conditions (100 - 300 °C, stoichiometric copper catalyst), which are detrimental for compounds containing delicate functionalities and sensitive stereocenters, we opted to perform the biaryl ether coupling at the first stage of the synthesis.²²⁸ A key reaction was the installation of a chiral non-racemic centre creating optically active α -amino- β -alcohol derivative from

aldehyde (**6.12**) via the asymmetric aminohydroxylation (AA) reaction developed by Sharpless *et al.* Subsequent oxidation of an alcohol functional group was anticipated to afford the corresponding α -amino acid (**6.13**), which was hoped to be converted into the diazoacetamide derivative (**6.14**). Reaction between a suitable imine and the diazoacetamide derivative (**6.14**) was expected to afford a key fragment (**6.15**), which could be subjected to an aziridine ring-opening.



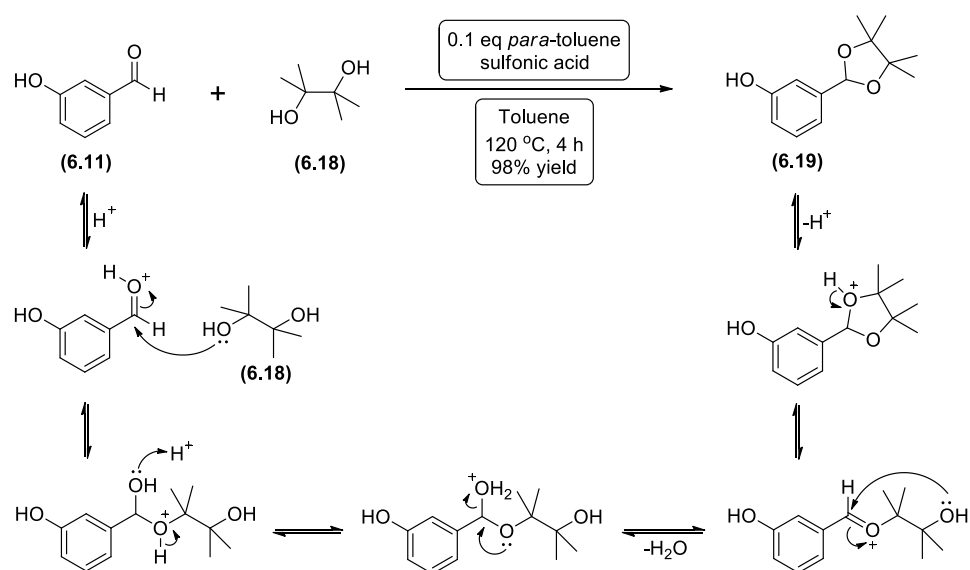
Scheme 6.2. Retrosynthetic route towards the model fragment (6.17**) of teicoplanin (**3.2**)**

Although not discussed within this thesis and will be a subject of future investigations, a nucleophilic C-3 ring-opening of (**6.15**) would afford a library of precursors (**6.16**) to teicoplanin derivatives. Removal of the protecting group (**R'**) would allow the installation of the second α -amino acid subunit on the biaryl ether and subsequently furnish the model fragment (**6.17**) via an amide coupling.

6.2. Synthesis of 3-(4,4,5,5-tetramethyl-1,3-dioxolan-2-yl)phenol (6.19)

Prior to the Ullmann biaryl ether coupling, commercially available 3-hydroxybenzaldehyde (**6.11**) was converted into the corresponding 1,3-dioxolane (**6.19**). Acetals offer robust protection of a carbonyl functional group against nucleophiles such as aqueous and non-aqueous bases, organometallic reagents or hydride reduction. However acetals can be cleaved using aqueous acid in wet solvents or when strong oxidizing agents are present.²²⁹ Cyclic acetals are generally more stable towards hydrolysis compared to acyclic acetals. Additionally, more substituted cyclic acetals possess additional resistance to nucleophilic attack due to steric hindrance. Acyclic acetals are prone to hydrolysis during aqueous reaction work-ups and can be challenging to purify using flash column chromatography due to the slightly acidic nature of silica gel.²³⁰

Following a procedure reported by Ovaa *et al*, 3-hydroxybenzaldehyde (**6.11**) was treated with pinacol (**6.18**) in refluxing toluene with 10 mol% *para*-toluenesulfonic acid as a catalyst (**Scheme 6.3**).²³¹

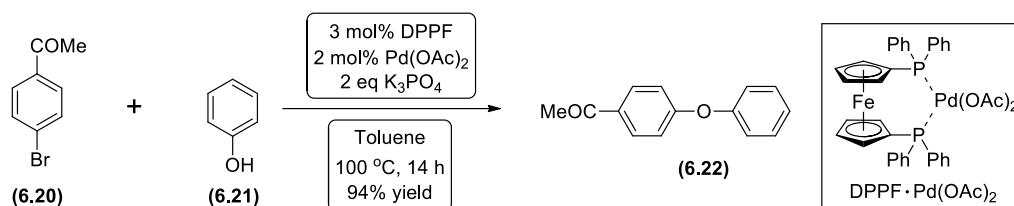


Scheme 6.3. Synthesis and the proposed mechanism of 1,3-dioxolane (**6.19**) formation

A Dean-Stark apparatus allowed the continuous removal of water from the reaction mixture, driving the equilibrium towards the protected compound. FT-IR analysis displayed the absence of the carbonyl group signal at 1672 cm⁻¹, suggesting, along with full physicochemical analysis, 3-(4,4,5,5-tetramethyl-1,3-dioxolan-2-yl)phenol (**6.19**) had been generated in an excellent 98% yield as a white powder with sufficient purity for further synthesis without any chromatographic purification.

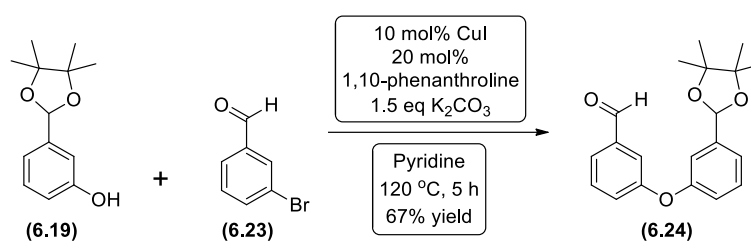
6.3. Synthesis of 3-(3-(4,4,5,5-tetramethyl-1,3-dioxolan-2-yl)phenoxy)benzaldehyde (6.24)

A search of the literature revealed a number of methods reported for biaryl ether synthesis.²³² Buchwald and Hartwig reported the palladium(II) acetate catalysed cross coupling reaction to afford biaryl ether (6.22) (Scheme 6.4).²³³ The reaction was accomplished in the presence of the mild base tripotassium phosphate and a catalytic quantity of DPPF ligand.



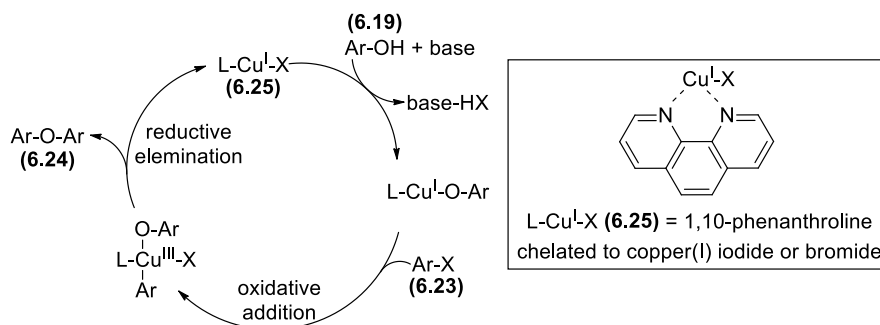
Scheme 6.4. Synthesis of biaryl ether (6.22), catalysed by palladium(II) acetate

Buchwald *et al* reported that a catalytic amount of copper(I) iodide in conjunction with 1,10-phenanthroline ligand facilitated carbon-oxygen bond formation between aryl bromides or iodides and aromatic or aliphatic alcohols.²³⁴ Thus, employing the procedure reported by Buchwald *et al*, 3-(4,4,5,5-tetramethyl-1,3-dioxolan-2-yl)phenol (6.19) was reacted with 3-bromobenzaldehyde (6.23) (Scheme 6.5). The reaction was catalysed by the copper metal chelated with 1,10-phenanthroline ligand, using the reaction conditions outlined in the scheme below. Aqueous work up and flash chromatography on silica gel afforded 3-(3-(4,4,5,5-tetramethyl-1,3-dioxolan-2-yl)phenoxy)benzaldehyde (6.24) as an orange oil in a 67% yield.



Scheme 6.5. Synthesis of biaryl ether (6.24), catalysed by copper(I) iodide (Ullmann coupling)

A proposed mechanism for biaryl ether (6.24) formation *via* a copper(I) catalysed procedure is outlined below (Scheme 6.6).²³⁵ The catalytic cycle begins with the chelation of 1,10-phenanthroline ligand (L) to the copper(I) halide. The complex (6.25) subsequently reacts with the phenol derivative (6.19) and undergoes an oxidative addition with the aryl halide (6.23), generating a copper(III) adduct. Subsequent reductive elimination affords the desired biaryl ether (6.24) and regenerates the original copper-ligand catalyst (6.25), which re-enters this catalytic cycle.²³⁶



Scheme 6.6. Proposed mechanism for the biaryl ether synthesis of (6.24) catalysed by copper(I) iodide

In the $^1\text{H-NMR}$ (500 MHz, CDCl_3) spectrum of (6.24) a singlet was observed at δ 9.95 ppm, which was assigned to the proton of the aldehyde functional group (**Figure 6.1**). Eight aromatic protons were clearly detected in the aromatic region from δ 7.60 to 6.99 ppm. The proton at the α -carbon of the dioxolane was recorded as a singlet at δ 5.95 ppm. Mass spectrometry afforded a strong ion at m/z 365.2 $[\text{M}+\text{K}]^+$, suggesting the product (6.24) had been generated. FT-IR analysis displayed a strong carbonyl peak at 1703 cm^{-1} , confirming the presence of an intact aldehyde functional group.

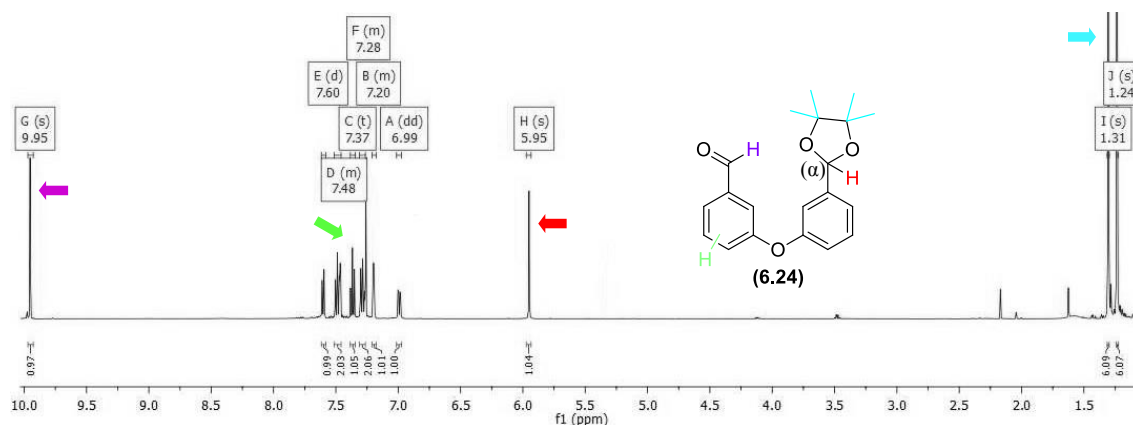


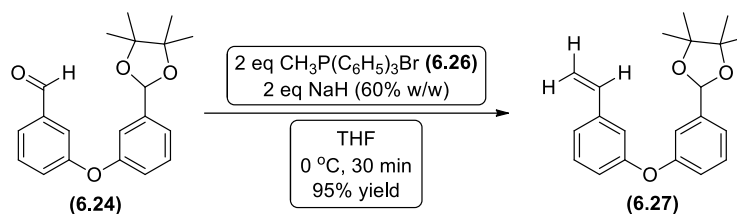
Figure 6.1. $^1\text{H-NMR}$ (500 MHz, CDCl_3) spectrum of biaryl ether (6.24)

6.4. Synthesis of 4,4,5,5-tetramethyl-2-(3-(3-vinylphenoxy)phenyl)-1,3-dioxolane (6.27)

The Wittig reaction is routinely employed in the preparation of an alkene by the reaction of an aldehyde or ketone with the phosphonium salt ylide.²³⁷

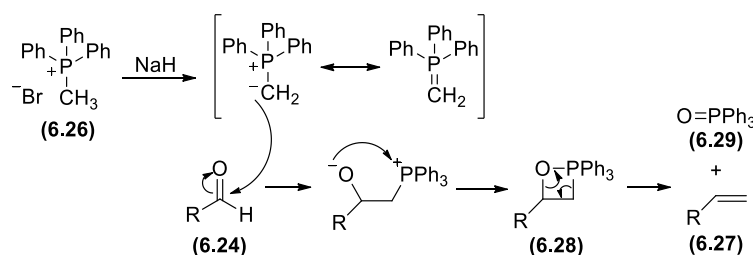
Following the procedure, originally reported by Osakada *et al*, methyltriphenylphosphonium bromide (6.26) was deprotonated irreversibly with sodium hydride and subsequently reacted with the aldehyde derivative (6.24) (**Scheme 6.7**).²³⁸ After 30 minutes, TLC analysis indicated a complete absence of the starting material. Subsequent flash chromatography on silica gel allowed the isolation of the

desired product 4,4,5,5-tetramethyl-2-(3-(3-vinylphenoxy)phenyl)-1,3-dioxolane (**6.27**) as a yellow oil in a 95% yield.



Scheme 6.7. Synthesis of styrene derivative (**6.27**) from the corresponding aromatic aldehyde (**6.24**) (Wittig reaction)

A proposed mechanism of the styrene formation, proceeds *via* a four-membered oxaphosphetane intermediate (**6.28**), which is formed after the deprotonated ylid attacks the aldehyde (**6.24**) (**Scheme 6.8**).²³⁹ The affinity of phosphorus towards oxygen, results in the collapse of oxaphosphetane (**6.28**), generating triphenylphosphine oxide (**6.29**) and styrene derivative (**6.27**). The P=O bond is one of the strongest double bonds in chemistry with its bond energy of 540 kJ mol^{-1} .²⁴⁰ Thus the Wittig reaction is irreversible and is driven forward by the formation of this P=O bond.



Scheme 6.8. Proposed mechanism of the conversion of aldehyde functionality of (**6.24**) into vinyl functionality of (**6.27**)

A complete consumption of the starting material (**6.24**) was confirmed by FT-IR analysis (no carbonyl peak at 1702 cm^{-1}) and ^{13}C -NMR analysis (no carbonyl peak at 191.7 ppm). Additionally, the ^1H -NMR (500 MHz, CDCl_3) analysis of (**6.27**) indicated an absence of a formyl proton at 9.95 ppm and a presence of a new signal at δ 6.66 ppm (dd, $J_{\text{H-H}}$ 17.6, 10.9 Hz), which was assigned to the proton H_a of the vinyl group (**Figure 6.2**). Signals associated with H_b and H_x were observed as doublets at δ 5.71 ppm and δ 5.25 ppm respectively. Proton-proton coupling constants were recorded as J_{a-b} 17.6 Hz and J_{a-x} 10.9 Hz. The data correlated well with the research published by Reynolds *et al*, who performed experiments using substituted styrenes and established relative chemical shifts and coupling constants of the vinyl protons.²⁴¹

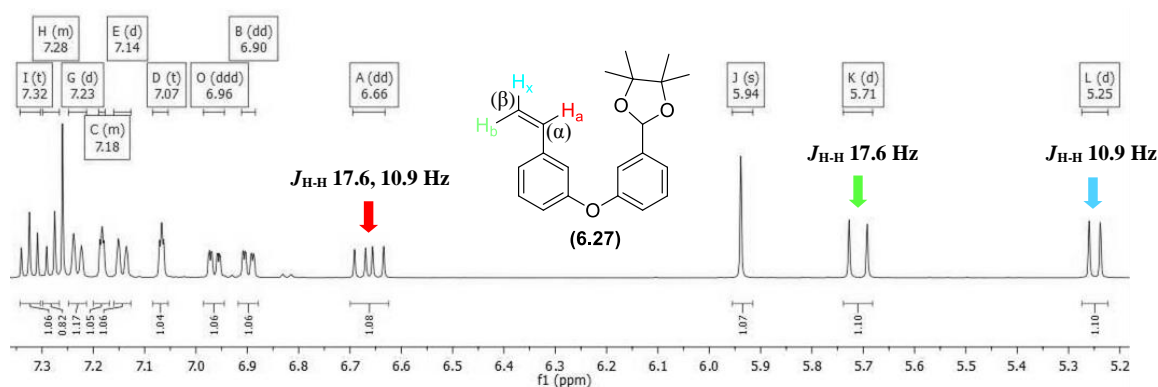


Figure 6.2. $^1\text{H-NMR}$ (500 MHz, CDCl_3) spectrum of styrene derivative (6.27)

6.5. Synthesis of chiral non-racemic benzyl (*R*)-(2-hydroxy-1-(3-(3-(4,4,5,5-tetramethyl-1,3-dioxolan-2-yl)phenoxy)phenyl)ethyl)carbamate (*R*)-(6.32)

α -Arylglycinols constitute an important class of α -amino- β -alcohols that are often found as structural motifs themselves (antitumour agents cyanocycline A and ecteinascidin 743) or serve as precursors for other valuable functionalities (α -arylglycine motif in glycopeptide antibiotics) (Figure 6.3).^{242,243}

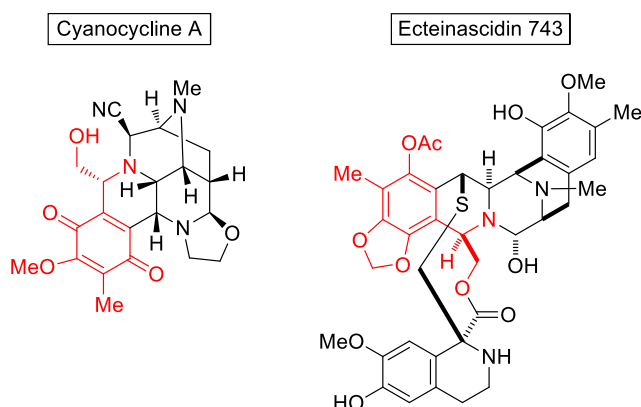


Figure 6.3. α -Arylglycinol motif (highlighted red) in the antitumor agents

Sharpless *et al* reported the conversion of styrenes to the corresponding (*R*)- or (*S*)- α -aryl-*N*-Cbz- or *N*-Boc-protected α -amino- β -alcohols *via* the catalytic asymmetric aminohydroxylation (AA) reaction on the alkene.¹⁰¹ The mechanism of the AA reaction has been closely based on mechanistic studies of its forerunner, the asymmetric dihydroxylation (AD) reaction.²⁴⁴ Ligand structure-activity studies have shed light on the origin of the enantioselectivity in the AD reaction and demonstrated the importance of an enzyme-like binding pocket present in the "dimeric" cinchona alkaloid ligands such as phthalazine ligands.²⁴⁵ Sharpless *et al* demonstrated that the cinchona alkaloid backbone is ideally suited for providing high ligand acceleration as well as enantioselectivity.²⁴⁶ The relationship between ligand structure and its activity is summarised in Figure 6.4.

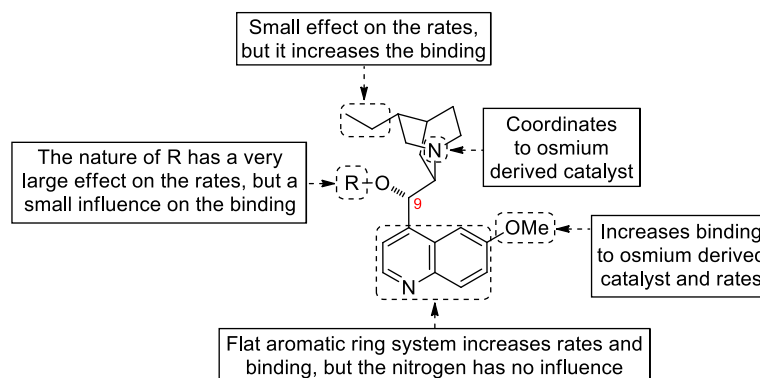


Figure 6.4. Structure-activity relations of DHQD ligand participating in AD reaction

The investigations have further shown the reaction rates were influenced chiefly by the nature of the O9 substituent of the cinchona alkaloid, with certain aromatic appendages giving especially large rate accelerations for aromatic olefins.²⁴⁷ Further evidence from binding data suggested that a stabilisation of the transition state was due to aromatic stacking interactions and a presence of a binding pocket or cleft. Thus, nearly perfect match between the phthalazine ligands and aromatic olefins with respect to rates and enantioselectivities was explained by an especially good transition-state stabilisation resulting from offset-parallel interactions between the aromatic substituent of the olefin and the phthalazine floor of the ligand, as well as favourable edge-to-face interactions with the "bystander" methoxyquinoline ring (**Figure 6.5**).

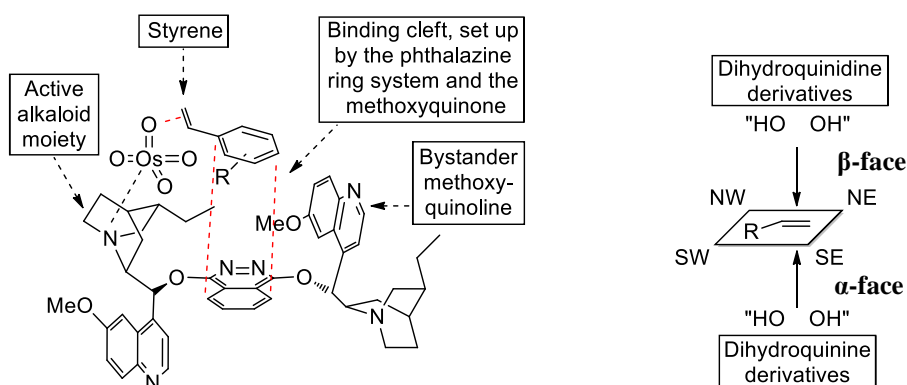
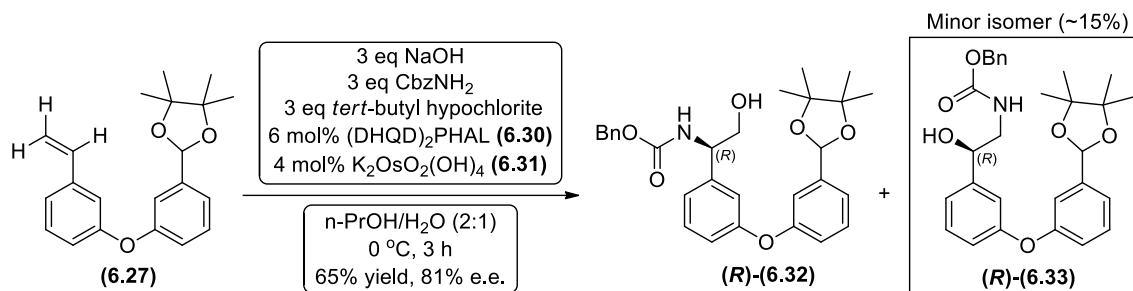


Figure 6.5. Rationalisation of enantiofacial selectivity of AD reaction

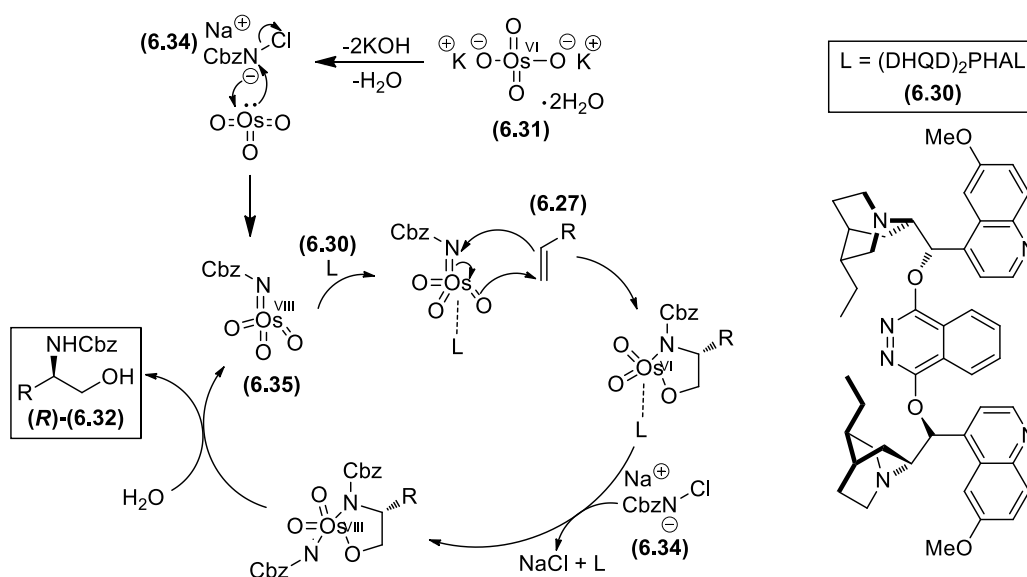
Sharpless *et al* designed a mnemonic model for predicting the enantiofacial selectivity in the AD reaction.²⁴⁸ Based on steric barriers, the "southwest quadrant" is relatively open for olefin substituents, which makes it suitable to accommodate flat, aromatic substituents or, in their absence, "large" aliphatic groups. An olefin positioned according to these constraints is attacked either from the top face (i.e., the β -face), in the case of dihydroquinidine (DHQD) derivatives, or from the bottom face (i.e., the α -face), in the case of dihydroquinine (DHQ) derived ligands.

Following the AA procedure reported by Sharpless *et al.*, a synthesis of benzyl (*R*)-(2-hydroxy-1-(3-(3-(4,4,5,5-tetramethyl-1,3-dioxolan-2-yl)phenoxy)phenyl)ethyl)-carbamate (**(R)**-(**6.32**) was attempted (**Scheme 6.9**).



Scheme 6.9. Synthesis of α -amino- β -alcohol (**(R)**-(**6.32**) via asymmetric aminohydroxylation reaction

To generate the desired α -amino- β -alcohol (**(R)**-(**6.32**), osmium catalyst was incorporated into the reaction in the form of potassium osmate dihydrate (**6.31**), a non-volatile powder, convenient for handling and storage (**Scheme 6.10**). Benzyl carbamate was reacted with sodium hydroxide and *tert*-butyl hypochlorite to afford the carbamate salt (**6.34**), which reacted with osmium(VI) to form an osmium(VIII) complex (**6.35**). Chiral alkaloid ligand hydroquinidine 1,4-phthalazinediyl diether [(DHQD)₂PHAL] (**6.30**) was used to introduce an (*R*)-chiral centre in (**(R)**-(**6.32**). Sharpless *et al.* demonstrated that switching to the hydroquinine based ligand, (DHQ)₂PHAL, reversed the enantioselectivity to (*S*). Aqueous work up and flash chromatography on silica gel afforded the desired product (**(R)**-(**6.32**) as a pale yellow oil in a 65% yield and 96% e.e.



Scheme 6.10. Proposed mechanism of the asymmetric aminohydroxylation reaction

The moderate yield (65%) of the desired product (**(R)**-(**6.32**) can be explained by the formation of the regioisomer, the secondary benzylic alcohol (**(R)**-(**6.33**), which was

also isolated and characterised. Crude $^1\text{H-NMR}$ analysis displayed $\sim 15\%$ of **(R)**-**(6.33)** present in the reaction mixture. Sharpless *et al* reported that the regioselectivity of AA reaction depended on the styrene substituents, choice of a chiral ligand, solvent, and a ligand-solvent combination. It was also reported that the regioisomers possess several characteristic peaks with NMR, therefore can be distinguished. Additionally, oxidation of regioisomers affords completely different products: a carboxylic acid or a ketone. $^1\text{H-NMR}$ spectra of α -amino- β -alcohol **(R)**-**(6.32)** and β -amino- α -alcohol **(R)**-**(6.33)** are compared in **Figure 6.6.** and **Figure 6.7.** MALDI-TOF analysis afforded a strong ion at m/z 514.4 $[\text{M}+\text{Na}]^+$, suggesting that the product **(R)**-**6.32** had been generated. The $^1\text{H-NMR}$ (500 MHz, CDCl_3) spectrum of **(R)**-**(6.32)** displayed a characteristic AB system of two distorted doublets at δ 5.12 and 5.07 ppm ($^2J_{\text{H-H}}$ 12.2 Hz), corresponding to the two aliphatic protons at the benzyl carbamate group (**Figure 6.6.**). Two protons on the β -carbon appended with the hydroxyl group were observed at δ 3.81 as a multiplet.

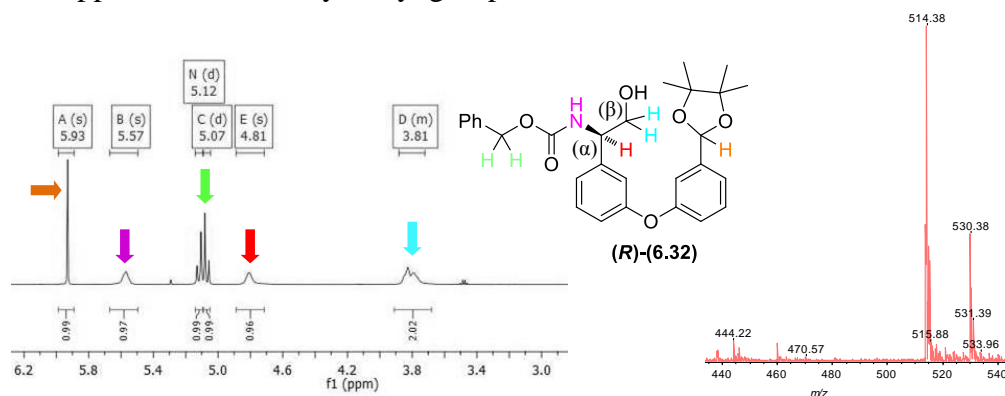


Figure 6.6. $^1\text{H-NMR}$ (500 MHz, CDCl_3) and MALDI-TOF spectra of **(R)**-**(6.32)**

In the $^1\text{H-NMR}$ (500 MHz, CDCl_3) spectrum of benzylic alcohol **(R)**-**6.33** [the *minor* regioisomer of **(R)**-**6.32**], the two aliphatic protons of benzyl carbamate group were observed as a singlet at δ 5.11 ppm [compared to two doublets of the AB system in the spectrum of **(R)**-**6.32**] (**Figure 6.7.**). Additionally, the two protons on the β -carbon were observed as separate multiplets at δ 3.55 ppm and δ 3.29 ppm.

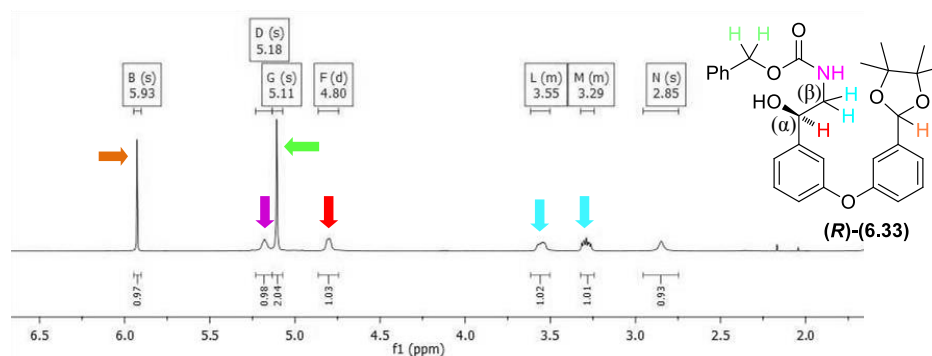


Figure 6.7. $^1\text{H-NMR}$ (500 MHz, CDCl_3) spectrum of **(R)**-**(6.33)**

To determine the enantiopurity of (*R*)-**6.32**, a chiral HPLC analysis was performed. The chiral non-racemic sample was run against the corresponding racemic α -amino- β -alcohol derivative (\pm)-(**6.32**). Enantiomeric excess was calculated to be 96% (Table 6.1.). Although the synthesis of the racemic sample (\pm)-(**6.32**) is not discussed here, it was prepared *via* the same AA procedure outlined in the synthesis of (*R*)-**6.32**, but using a mixture of [(DHQD)₂PHAL] and [(DHQ)₂PHAL] (1:1) at the 6 mol% total loading.

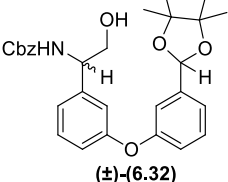
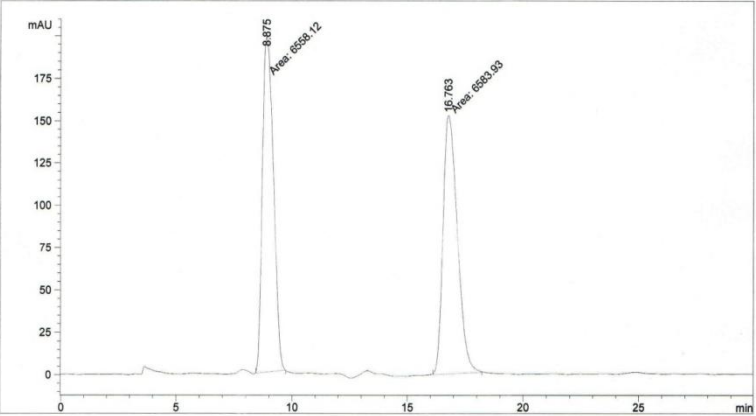
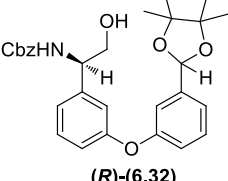
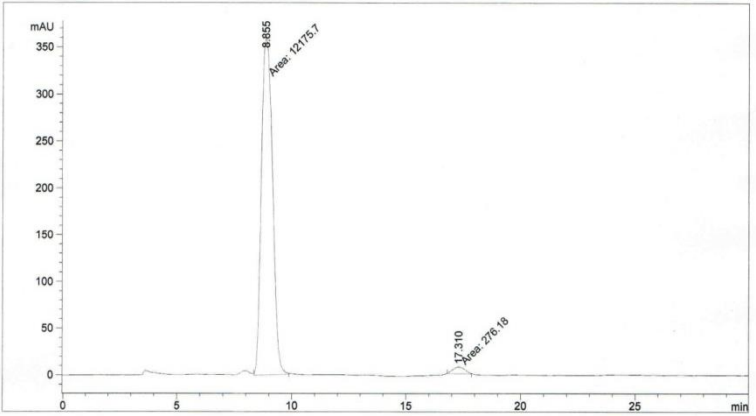
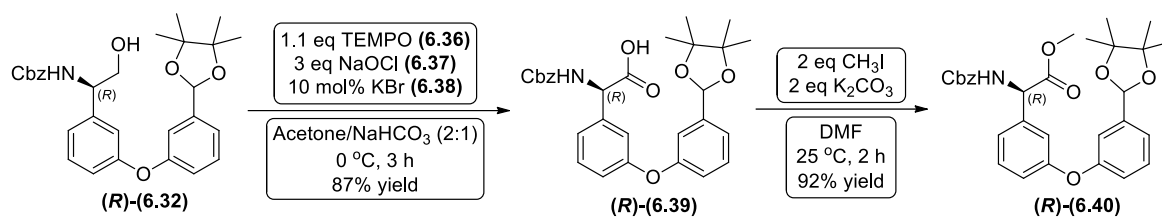
Compound	Chiral HPLC spectrum
 <p data-bbox="451 817 534 846">(\pm)-6.32</p> <p data-bbox="338 887 603 954">$R_t = 8.87, 16.76$ min racemic</p>	
 <p data-bbox="451 1254 534 1283">(<i>R</i>)-6.32</p> <p data-bbox="338 1323 603 1391">$R_t = 8.85, 17.31$ min 96% e.e.</p>	
<p data-bbox="351 1451 1380 1516">Conditions: Phenomenex Lux Cellulose-1 HPLC column, 85% <i>iso</i>-hexane : 15% <i>iso</i>-propanol, flow rate: 1 mL / min</p>	

Table 6.1. Chiral HPLC spectra of (\pm)-(**6.32**) and (*R*)-(**6.32**)

6.6. Synthesis of (*R*)-2-(((benzyloxy)carbonyl)amino)-2-(3-(3-(4,4,5,5-tetramethyl-1,3-dioxolan-2-yl)phenoxy)phenyl)acetic acid (*R*)-(**6.39**) and methyl (*R*)-2-(((benzyloxy)carbonyl)amino)-2-(3-(3-(4,4,5,5-tetramethyl-1,3-dioxolan-2-yl)phenoxy)phenyl)acetate (*R*)-(**6.40**)

The procedure reported by Boger *et al* was followed to convert the primary alcohol (*R*)-(**6.32**) directly to the desired carboxylic acid (*R*)-(**6.39**), using stoichiometric oxidants: sodium hypochlorite (**6.37**) and 2,2,6,6-tetramethyl-1-piperidine-1-oxyl (TEMPO) (**6.36**), a free radical (Scheme 6.11.).²⁴⁹ Boger *et al*

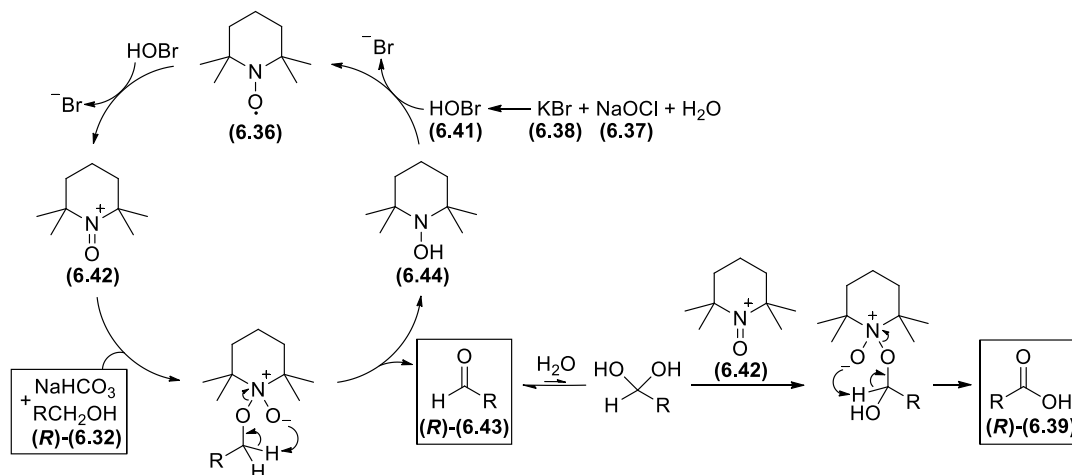
proposed that TEMPO scavenged unreacted chlorine, therefore 1.1 equivalent of TEMPO was required to prevent an unwanted chlorination of the starting material.



Scheme 6.11. Oxidation of α -amino- β -alcohol into corresponding amino acid **(R)**-**(6.39)** and subsequent esterification, affording **(R)**-**(6.40)**

During the work-up of **(R)**-**(6.39)**, the addition of saturated aqueous sodium hydrogen carbonate (5 equivalents) to the impure reaction promoted the formation of the corresponding sodium salt of the acid. The aqueous phase was washed with diethyl ether, which helped to remove organic impurities such as TEMPO (**6.36**). The washed salt was then suspended in ethyl acetate/distilled water (2:1), and the aqueous phase was acidified to pH ~ 4 with 1 M hydrochloric acid. The two phases were separated, and the aqueous phase was re-extracted with ethyl acetate twice. The combined organic phases were washed with saturated brine, dried over anhydrous magnesium sulfate and concentrated to afford the pure acid **(R)**-**(6.39)** as a colourless oil in a 87% yield.

The reaction mechanism is outlined below (**Scheme 6.12.**). Reaction between potassium bromide (**6.38**) and sodium hypochlorite (**6.37**) afforded hypobromous acid (**6.41**), which transformed TEMPO (**6.36**) into the oxoammonium salt (**6.42**) that operated as the primary oxidant, converting the primary alcohol **(R)**-**(6.32)** into the corresponding aldehyde (**6.43**). This resulted in the formation of the hydroxylamine (**6.44**) that was oxidised back to TEMPO (**6.36**), thus completing the catalytic cycle. The aqueous conditions allowed the formation of the corresponding dihydrate of the aldehyde, which was then oxidised to the corresponding carboxylic acid **(R)**-**(6.39)**.



Scheme 6.12. Proposed mechanism of the primary alcohol **(R)**-**(6.32)** oxidation into carboxylic acid **(R)**-**(6.39)**

Anelli *et al* observed a significant reaction rate acceleration when hypobromous acid (**6.41**) was used as a secondary oxidant instead of hypochlorous acid (HOCl).²⁵⁰ Similar results were observed by Petrônio *et al* and were explained by the fact that due to lower electronegativity and larger atomic radius, bromine radicals are more easily formed compared to chlorine radicals.²⁵¹

The carboxylic acid (**R**)-(**6.39**) was subsequently reacted with methyl iodide to afford the corresponding ester (**R**)-(**6.40**) as an orange oil in a 92% yield. In the ¹H-NMR (500 MHz, CDCl₃) spectrum of the ester (**R**)-(**6.40**), the methoxy group was observed as a singlet at δ 3.73 ppm (**Figure 6.8**). The HRMS analysis provided a final confirmation of the synthesis of (**R**)-(**6.40**) with [M+NH₄]⁺ ions identified at the required *m/z* (found: 537.2601, required: 537.2595).

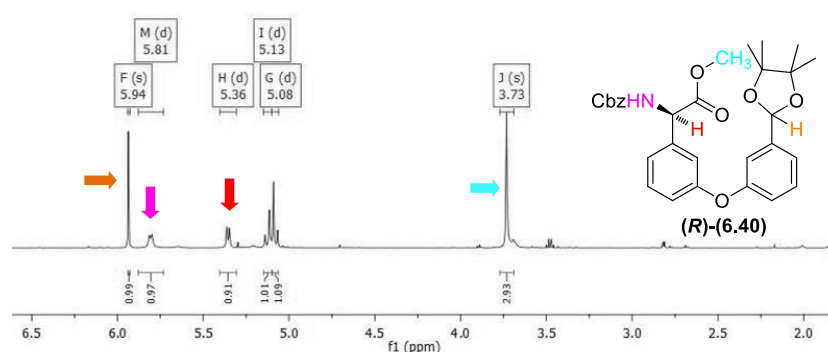
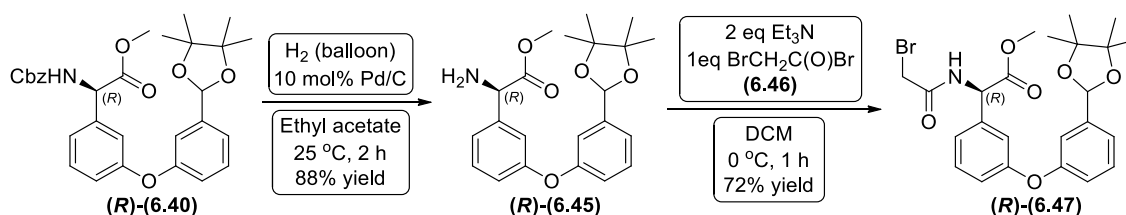


Figure 6.8. ¹H-NMR (500 MHz, CDCl₃) spectrum of (**R**)-(**6.40**)

6.7. Synthesis of methyl (**R**)-2-(2-bromoacetamido)-2-(3-(3-(4,4,5,5-tetramethyl-1,3-dioxolan-2-yl)phenoxy)phenyl)acetate (**R**)-(**6.47**)

The *N*-benzyl carbamate protecting group on (**R**)-(**6.40**) was removed *via* hydrogenation in the presence of 10 mol% palladium on carbon and a balloon filled with hydrogen gas, affording primary amine (**R**)-(**6.45**) in a 88% yield (**Scheme 6.13**). ¹H-NMR analysis confirmed the disappearance of the characteristic AB system at δ 5.13-5.08 ppm associated with the aliphatic protons of the benzyl carbamate group, as well as the absence of the corresponding aromatic protons. The FT-IR analysis of (**R**)-(**6.45**) also confirmed the benzyl carbamate group had been removed, as the carbonyl peak at 1724 cm⁻¹ was no longer observed. The ester carbonyl peak at 1741 cm⁻¹ was however still detected.



Scheme 6.13. Synthesis of (**R**)-(**6.47**)

The generated primary amine (**R**)-(**6.45**) was subsequently reacted with bromoacetyl bromide (**6.46**) and triethylamine to afford the corresponding bromoacetamide (**R**)-(**6.47**). Aqueous work up and flash chromatography on silica gel afforded the desired product (**R**)-(**6.47**) as a yellow oil in a 72% yield. The ¹H-NMR (500 MHz, CDCl₃) spectrum of the bromoacetamide (**R**)-(**6.47**) revealed two doublets of the AB system at δ 3.91 and 3.87 ppm (²J_{H-H} 13.7 Hz), which was associated with the two protons of the bromoacetamide group (**Figure 6.9**). The signal from the amide proton was observed as a doublet at δ 7.42 ppm (*J*_{H-H} 7.1 Hz), which was presumably coupled to the proton on the α-carbon at δ 5.51 ppm (d, *J*_{H-H} 7.0 Hz). In the FT-IR spectrum two carbonyl peaks were identified at 1747 cm⁻¹ and 1662 cm⁻¹ corresponding to ester and acetamide functional groups respectively.

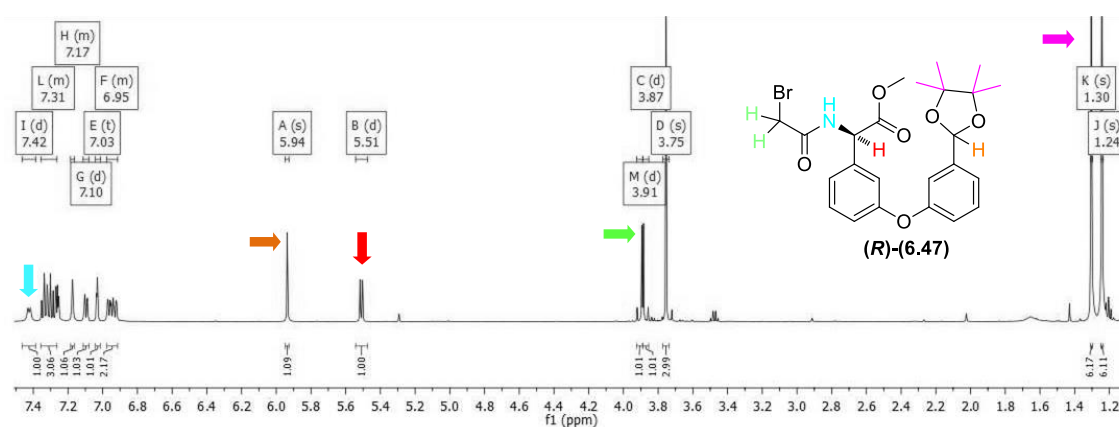
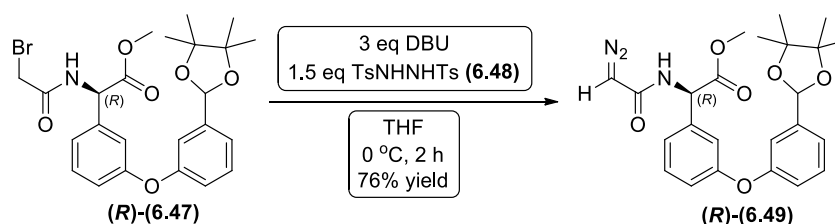


Figure 6.9. ¹H-NMR (500 MHz, CDCl₃) spectrum of bromoacetamide derivative (**R**)-(**6.47**)

6.8. Synthesis of (**R**)-methyl 2-(2-diazoacetamido)-2-(3-(3-(4,4,5,5-tetramethyl-1,3-dioxolan-2-yl)phenoxy)phenyl)acetate (**R**)-(**6.49**)

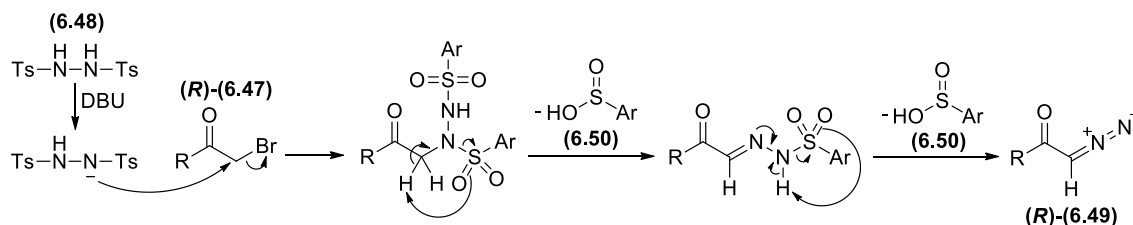
In 2007 Fukuyama *et al* published a novel synthetic method for the preparation of alkyl diazoacetates from the corresponding bromoacetates by treating the latter with *N,N'*-ditosylhydrazine (**6.48**) and 1,8-diazabicyclo[5.4.0]undec-7-ene (DBU).²⁵²

Following the procedure reported by Fukuyama *et al*, *N,N'*-ditosylhydrazine (**6.48**) was deprotonated with DBU and reacted with bromoacetamide derivative (**R**)-(**6.47**) (**Scheme 6.14**), generating (**R**)-methyl 2-(2-diazoacetamido)-2-(3-(3-(4,4,5,5-tetramethyl-1,3-dioxolan-2-yl)phenoxy)phenyl)acetate (**R**)-(**6.49**).

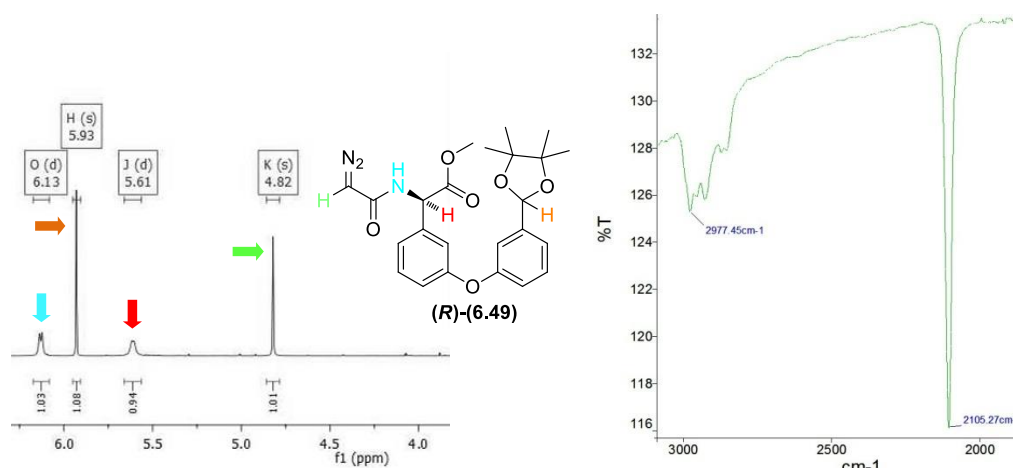


Scheme 6.14. Synthesis of diazoacetamide derivative (**R**)-(**6.49**)

A proposed mechanism involves an elimination of two equivalents of *para*-toluenesulfonic acid (**6.50**), which furnishes the desired diazoacetamide derivative (**R**)-(**6.49**) (**Scheme 6.15**). Flash chromatography on silica gel afforded the desired product (**R**)-(**6.49**) as a pale yellow oil in a 76% yield.



Within the $^1\text{H-NMR}$ (500 MHz, CDCl_3) spectrum of (**R**)-(**6.49**), a new singlet was observed at δ 4.82 ppm, which was assigned to the proton on the carbon with the diazo group (**Figure 6.10**). The FT-IR analysis supported the formation of (**R**)-(**6.49**), with a strong peak observed at 2105 cm^{-1} , corresponding to the diazo functional group.²⁵³



At this point it was very important to determine the enantiomeric excess of (**R**)-(**6.49**) in order to establish if any racemisation of α -carbon had occurred.

To determine the enantiopurity of (**R**)-(**6.49**), a chiral HPLC analysis was performed. The chiral non-racemic sample was run against the corresponding diazoacetamide derivative (\pm)-(**6.49**). Enantiomeric excess was calculated to be 94% (**Table 6.2**.)

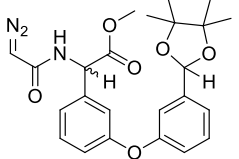
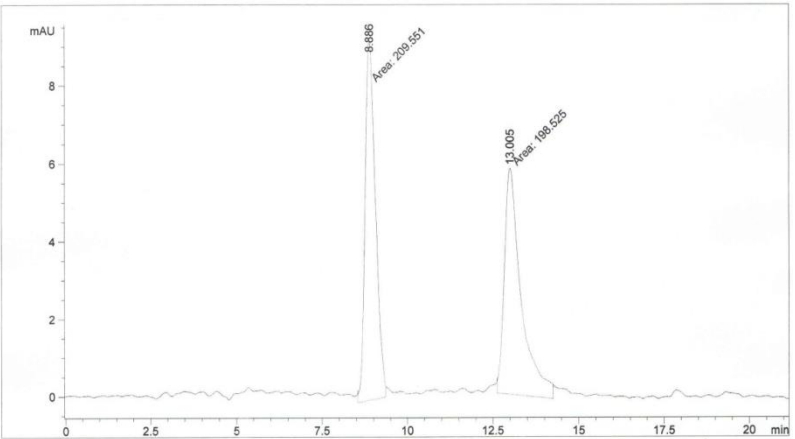
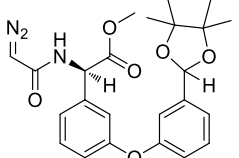
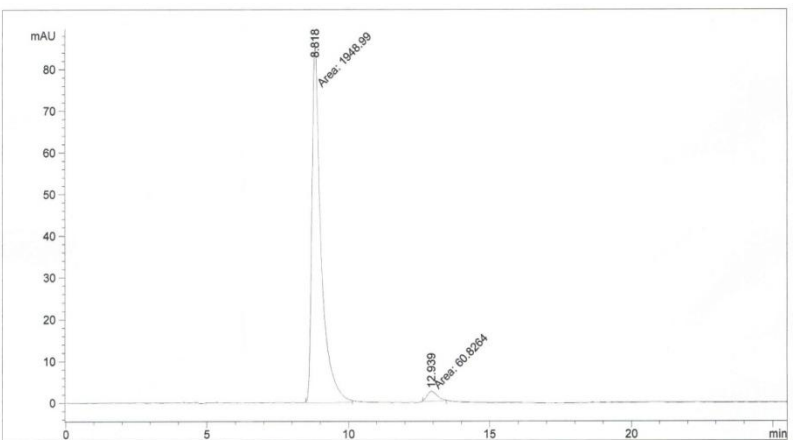
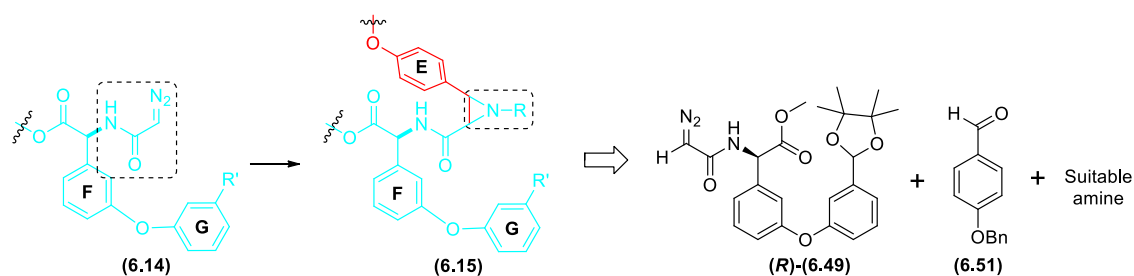
Compound	Chiral HPLC spectrum
 <p data-bbox="438 465 518 492">(±)-(6.49)</p> <p data-bbox="327 533 598 600">$R_t = 8.88, 13.00$ min racemic</p>	
 <p data-bbox="438 940 518 967">(R)-(6.49)</p> <p data-bbox="327 1008 598 1075">$R_t = 8.82, 12.94$ min 94% e.e.</p>	
<p data-bbox="343 1164 1396 1232">Conditions: Phenomenex Lux Cellulose-1 HPLC column, 80% <i>iso</i>-hexane : 20% <i>iso</i>-propanol, flow rate: 1 mL / min</p>	

Table 6.2. Chiral HPLC spectra of (±)-(6.49) and (R)-(6.49)

6.9. Synthesis of a key E-F-O-G fragment derivative *cis*-(6.55) via aziridination reaction

With the required diazoacetamide derivative (R)-(6.49) in hand we attempted a synthesis of a key E-F-O-G fragment (6.15), which subsequently could be subjected to an aziridine ring-opening, affording a library of precursors to teicoplanin derivatives (Scheme 6.16.).



Scheme 6.16. Proposed synthesis of a model E-F-O-G fragment (6.15) via aziridination reaction

We have chosen 4-benzyloxybenzaldehyde (**6.51**) to mimic the **E** ring of teicoplanin and two amines to introduce various protecting groups at the *N*-terminus of aziridine derivatives. 2,4-Dimethoxyaniline (**6.53**) was ultimately chosen due to the fact it can be cleaved under oxidative conditions affording *NH*-aziridine. Methyl 2-amino-2-methylpropanoate (**6.52**) was selected to investigate the reactivity of aliphatic amines compared to aromatic. Unfortunately, an attempt to purify a reaction that has utilised 2,4-dimethoxyaniline (**6.53**) has failed, mainly due to the small scale of the reaction. On the contrary, the synthesis and purification of aziridine derived from methyl 2-amino-2-methylpropanoate (**6.52**) was successful and is discussed below.

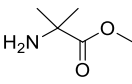
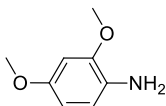
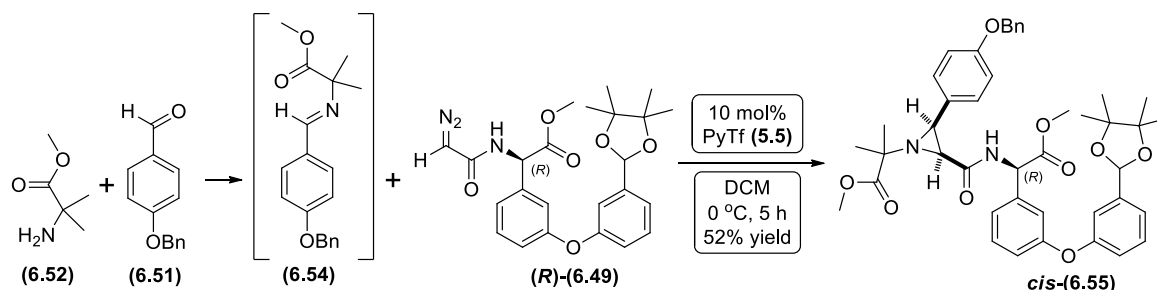
Amine selected for the aziridination reaction	 methyl 2-amino-2-methylpropanoate (6.52)	 2,4-dimethoxyaniline (6.53)
Crude aziridination product observed		
Aziridination product purified		

Table 6.3. Synthesis of a model E-F-O-G fragment (**6.15**) *via* aziridination reaction, utilising aromatic and aliphatic amines

The synthesis of *cis*-(**6.55**) was attempted utilising our standard racemic aziridination protocol outlined earlier (See **5.2. Studies towards a racemic aziridination protocol**) (Scheme 6.17.).



A slight excess (10%) of 4-benzyloxybenzaldehyde (**6.51**) ensured that all of the methyl 2-amino-2-methylpropanoate (**6.52**) was consumed and the corresponding imine

(**6.54**) was formed. Activated (flame dried) 4 Å molecular sieves were used to trap the generated water in the condensation reaction between 4-benzyloxybenzaldehyde (**6.51**) and methyl 2-amino-2-methylpropanoate (**6.52**) and shift the reaction equilibrium towards the imine (**6.54**) formation. After three hours stirring at room temperature, an aliquot was taken out and submitted to ¹H-NMR analysis; this confirmed the imine (**6.54**) formation, which was not isolated and was directly submitted to the aziridination reaction outlined in **Scheme 6.17**. Pyridinium triflate (**5.5**) was added at 10 mol% loading and the reaction flask was cooled to 0 °C. Diazoacetamide derivative (*R*)-(**6.49**) was added *via* syringe through the seal. The reaction was stirred at 0 °C and monitored by the ¹H-NMR analysis every hour. After circa 5 hours, the characteristic imine peak at δ 8.58 ppm was no longer observed. An aqueous work up and flash chromatography on silica gel afforded a colourless oil in a 52% yield.

The desired product *cis*-(**6.55**) was identified *via* ¹H-NMR (500 MHz, CDCl₃) analysis, which displayed two new doublets at δ 3.30 (*J*_{2,3} 6.8 Hz) and δ 2.84 ppm (*J*_{2,3} 6.8 Hz), that were assigned to the aziridine protons on carbons C-3 and C-2 respectively (**Figure 6.11**). The use of vicinal proton-proton coupling constants (*J*_{H-H} 6.8 Hz confirmed the *cis*-configuration of the product.

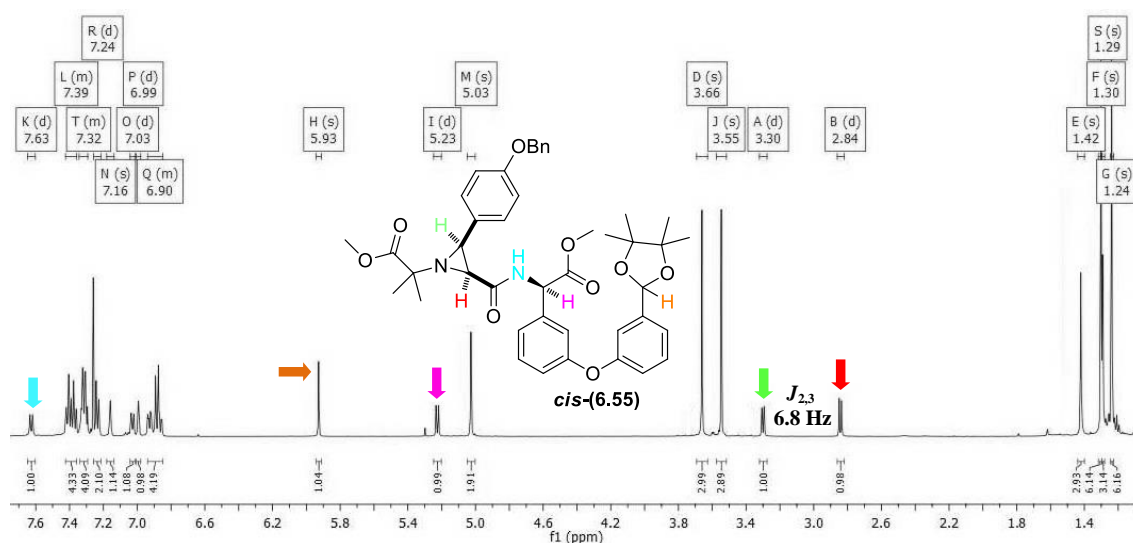


Figure 6.11. ¹H-NMR (500 MHz, CDCl₃) spectrum of *cis*-(**6.55**)

The HRMS analysis provided a final confirmation of the synthesis of *cis*-(**6.55**) with [M+H]⁺ ions found at the required *m/z* (found: 737.3435, required: 737.3433).

An interesting chromatogram was obtained when the chiral HPLC analysis of *cis*-(**6.55**) was performed. Various conditions (columns and solvent systems) were applied, but in every case one strong peak was observed (**Table 6.4**), suggesting that

non-racemic compound is obtained. Thus, we postulated the idea that the (*R*) chiral centre of the "F ring" controls the stereochemistry of the aziridine formed.

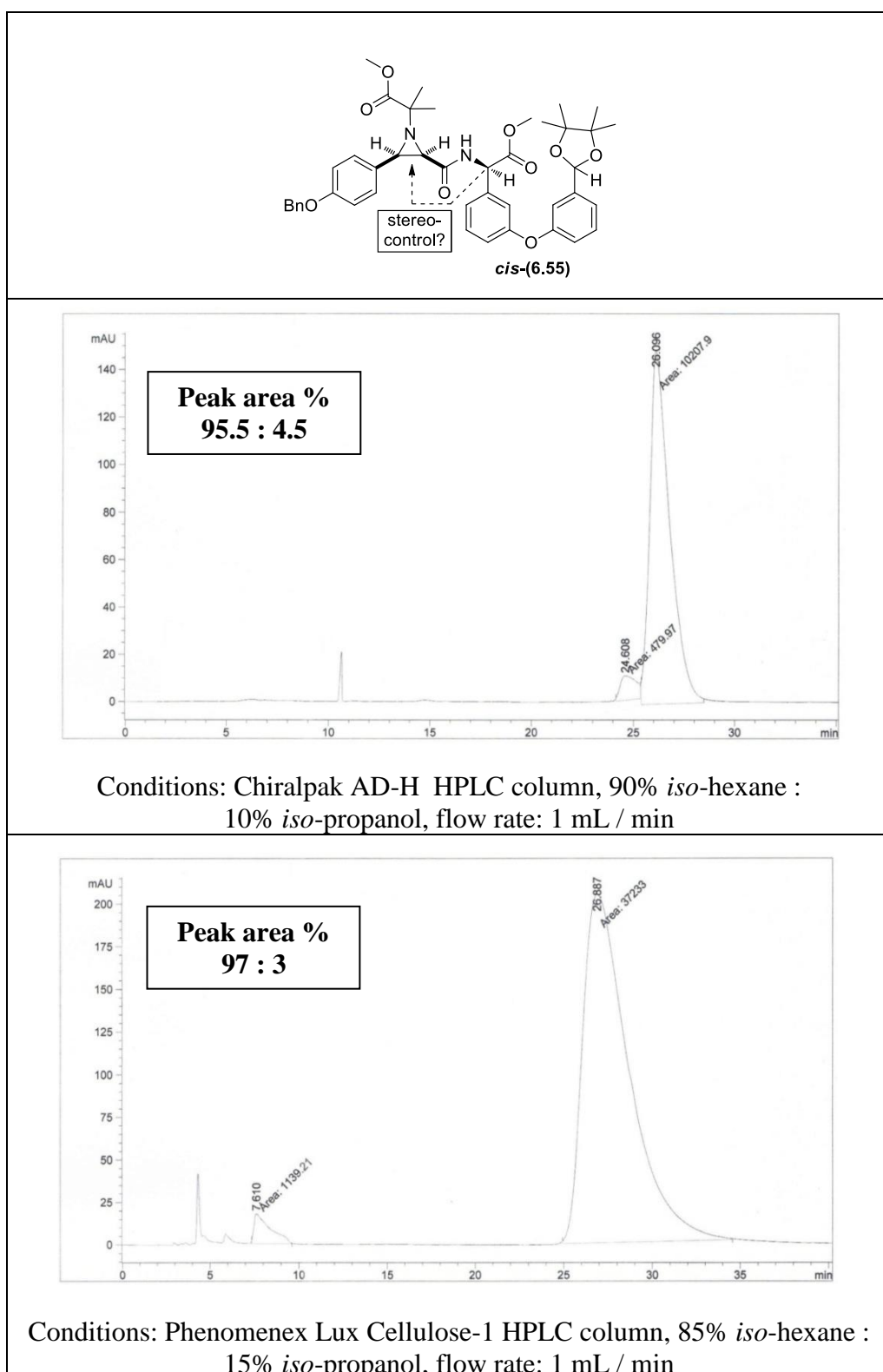
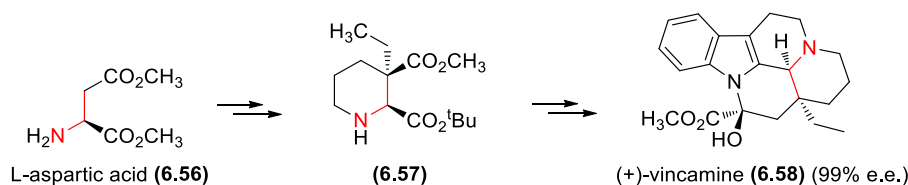


Table 6.4. Chiral HPLC spectrum of *cis*-(6.55)

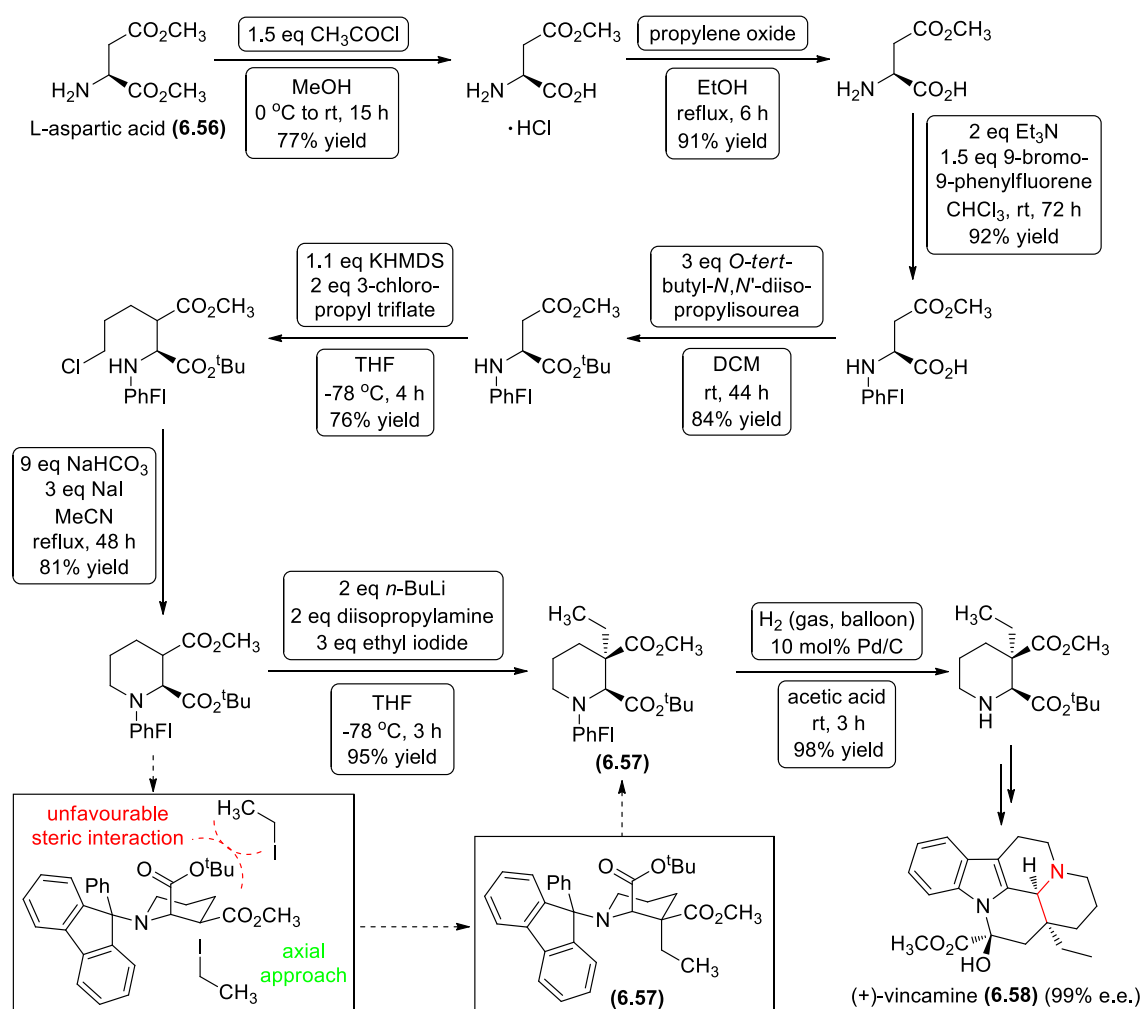
A search of the literature uncovered several reports on remote asymmetric induction. Rapoport *et al* reported the synthesis of (+)-vincamine (**6.58**) from L-aspartic acid (**6.56**) (Scheme 6.18).²⁵⁴ The chiral non-racemic α -centre of the starting amino

acid was utilised as the sole source of chiral information in the construction of the three chiral centres in the target molecule.



Scheme 6.18. Synthesis of (+)-vincamine (**(6.58)**) using L-aspartic acid (**(6.56)**) as the source of chiral induction by Rapoport *et al*

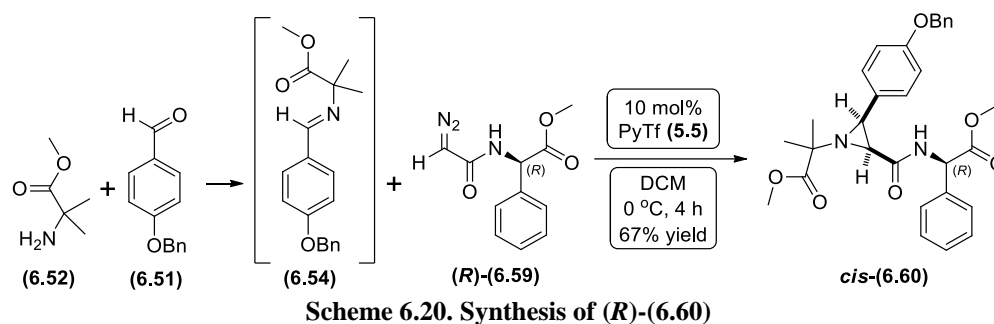
The high diastereoselectivity obtained in the alkylation of six membered ring with ethyl iodide to yield primarily (**(6.57)**) was rationalised using the fact that the electrophile, ethyl iodide, had approached the less-hindered face opposite the axial C-2 methoxycarbonyl group (**Scheme 6.19.**). The stereochemistry of (**(6.57)**) was rigorously established by COSY and NOESY experiments.



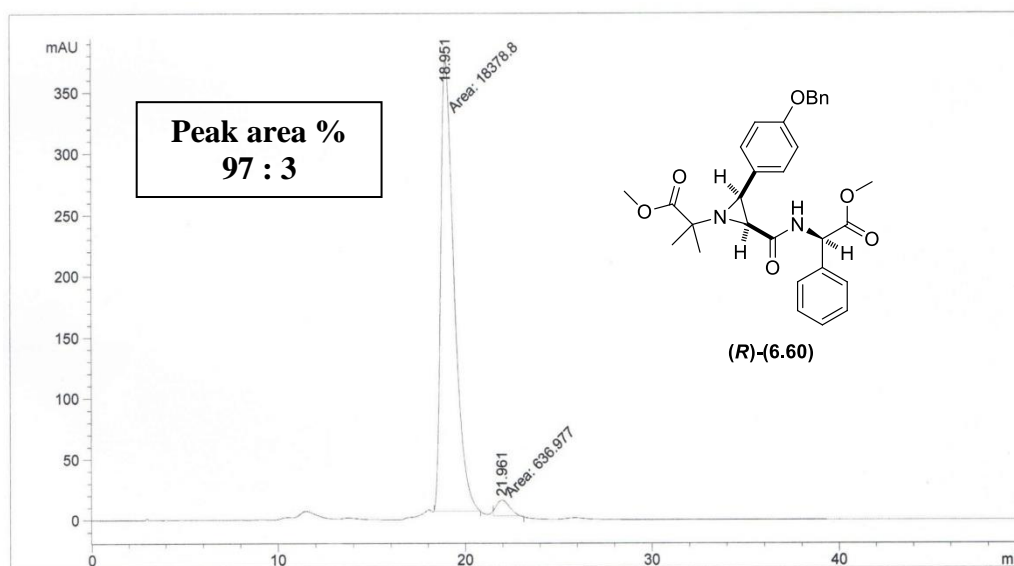
Scheme 6.19. Rationalisation of stereochemistry of the key intermediate (**(6.57)**) in the synthesis of (+)-vincamine (**(6.58)**) by Rapoport *et al*

To obtain additional evidence of the remote stereocontrol during an aziridination reaction, a model aziridine *cis*-(**(6.60)**) was synthesised utilising identical imine (**(6.54)**)

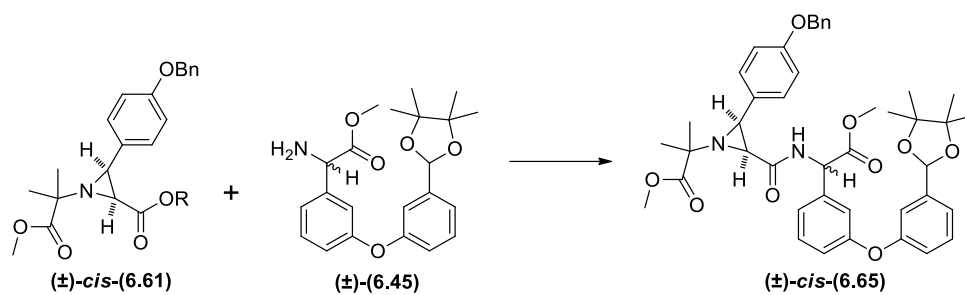
and the diazoacetamide derived from (*R*)-phenyl glycine methyl ester (**(R)**-(**6.59**), mimicking the biaryl ether diazoacetamide derivative (**(R)**-(**6.49**)



A sample of *cis*-(**6.60**) was submitted to the chiral HPLC analysis and a nearly identical chromatogram was obtained to the one observed when analysing *cis*-(**6.55**) (**Figure 6.12**). This study indicated that amino acid chiral α -centre provides a stereocontrol in the formation of aziridine.



In order to obtain a conclusive evidence, chiral chromatography spectra obtained during the analysis of *cis*-(**6.55**) and *cis*-(**6.60**) must be matched with the racemic counterparts. Aziridine (\pm)-*cis*-(**6.61**) will be synthesised as a racemic sample, separately from the **F-O-G** fragment (\pm)-(**6.45**) and joined *via* an amide coupling, affording (\pm)-*cis*-(**6.65**) as outlined in **Scheme 6.21**. However the synthesis of (\pm)-*cis*-(**6.65**) has not been attempted yet and will be the subject of future investigations.



Scheme 6.21. Synthesis of $(\pm)\text{-cis-}(6.65)$

6.10. Chapter conclusion

A successful synthesis of the key intermediate fragment of teicoplanin was performed, employing aziridination protocol developed previously. Ring-opening of the aziridine functionality would afford analogues of the antibiotic.

A further examination of the aziridine stereochemistry is required, to support a remote asymmetric induction hypothesis. Racemic and chiral systems will be investigated separately and crystallisation for a single crystal diffraction will be attempted.

By combining our studies towards teicoplanin and isotope incorporating methodologies, analogues of glycopeptide antibiotics can be generated and utilised in academia and industry.

Chapter 7. Synthesis and applications of chiral non-racemic α -aryl glycinols labelled with stable isotopes

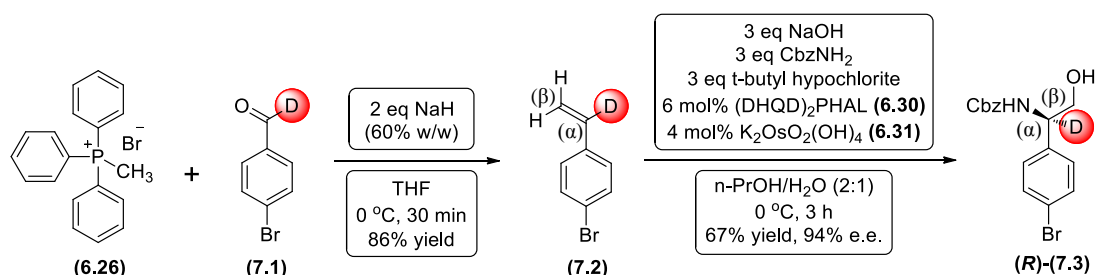
7.1. Introduction

Chiral non-racemic α -aryl glycinols can be accessed *via* the asymmetric aminohydroxylation (AA) reaction developed by Sharpless *et al*, which utilises styrenes as starting materials. We have demonstrated that the AA methodology can be used to generate a model **F-O-G** fragment of Teicoplanin [see compound (**R**)-(6.22)]. To expand the scope of the reaction, we wanted to incorporate isotope labels into optically active α -amino- β -alcohols. The applications of this chemistry can be extended to mechanistic studies and metabolic research.

With isotopically labelled aldehydes, already generated for the aziridination studies, incorporation of stable isotopes (^2H and ^{13}C) into optically active α -aryl glycinols was attempted.

7.2. Synthesis of benzyl α - ^2H -(**R**)-(1-(4-bromophenyl)-2-hydroxyethyl)carbamate (**R**)-(7.3)

α - ^2H -4-bromobenzaldehyde (**7.1**) was converted into the corresponding styrene (**7.2**) utilising the experimental procedure reported by Delmas *et al* (**Scheme 7.1**). A similar procedure was utilised previously to synthesise compound (**6.17**) (See Chapter 6). Utilising the AA protocol [used during the synthesis of compound (**R**)-(6.32)], styrene (**7.2**) was converted into the desired α -amino- β -alcohol (**R**)-(7.3) with the ^2H -label at the α -carbon. Although the synthesis is not shown here, non-labelled samples i.e. 4-bromostyrene (**7.4**) and racemic α -amino- β -alcohol (\pm)-(7.5) were generated to allow determination of deuterium incorporation and e.e. of α -amino- β -alcohol (**R**)-(7.3).



Scheme 7.1. Synthesis of α -amino- β -alcohol (**R**)-(7.3) via AA and Wittig reactions from α - ^2H -4-bromobenzaldehyde (**7.1**)

The ^1H -NMR (500 MHz, CDCl_3) spectrum of (**7.2**) displayed two singlets at δ 5.75 ppm and δ 5.29 ppm, that were assigned to H_β and H_α protons respectively (**Table 7.1**). No signal was observed in the δ 6.0 - 7.0 ppm region, which confirmed the

successful installation of deuterium at the α -carbon. Deuteration level was determined by comparing $^1\text{H-NMR}$ spectra of labelled sample (**7.2**) and non-labelled (**7.4**). Deuterium incorporation was recorded above 95%. Analysing the $^1\text{H-NMR}$ (500 MHz, CDCl_3) spectrum of non-labelled sample (**7.4**), the signal at δ 6.66 ppm (dd, $J_{\text{H-H}}$ 17.6, 10.9 Hz) was observed, which was assigned to proton H_a of styrene (**7.4**). Signals associated with H_b and H_x were observed as a doublet of doublets at δ 5.74 ppm and δ 5.28 ppm respectively. Proton-proton coupling constants were recorded as J_{a-b} 17.6 Hz and J_{b-x} 0.7 Hz for H_b and J_{a-x} 10.9 Hz and J_{b-x} 0.7 Hz for H_x .

Examining the $^{13}\text{C-NMR}$ (126 MHz, CDCl_3) spectrum of (**7.2**) the signal arising from the α -carbon was observed as a triplet at δ 135.5 ppm, resulting from splitting by the deuterium atom (**Table 7.1**). A carbon-deuterium coupling constant ($J_{\text{C-D}}$) was recorded as 23.7 Hz. The $^{13}\text{C-NMR}$ (126 MHz, CDCl_3) spectrum of (**7.4**) displayed a signal from α -carbon as a singlet at δ 135.9 ppm. The difference between δ 135.5 ppm and δ 135.9 ppm was attributed to the isotope shift effect.

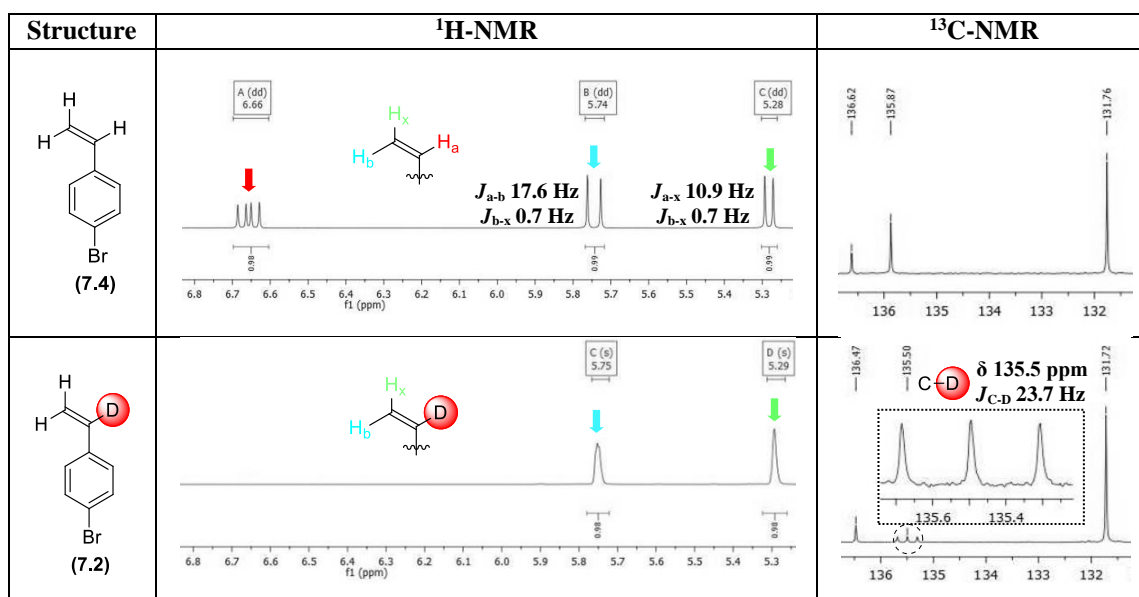


Table 7.1. $^1\text{H-NMR}$ (500 MHz, CDCl_3) and $^{13}\text{C-NMR}$ (126 MHz, CDCl_3) spectra of (**7.4**) and (**7.2**)

The $^1\text{H-NMR}$ (500 MHz, CDCl_3) spectrum of (**R**)-(**7.3**) displayed characteristic two doublets of the AB system at δ 5.12 and 5.07 ppm ($^2J_{\text{H-H}}$ 12.2 Hz), which corresponded to the two aliphatic protons associated with the benzyl carbamate group (**Table 7.2**). Furthermore the two protons on the β -carbon with the hydroxyl group were located at δ 3.80 as a multiplet. No signal was observed at the 4.5 - 5.0 ppm region. This could be explained by the fact that the proton at the α -carbon had been replaced with the deuterium atom. The $^1\text{H-NMR}$ (500 MHz, CDCl_3) spectrum of racemic non-labelled sample (\pm)-(**7.5**) displayed a singlet at 4.79 ppm, corresponding to

the proton at the α -carbon. Within the ^{13}C -NMR (126 MHz, CDCl_3) spectrum of (*R*)-(**7.3**) a signal from the α -carbon was observed as a triplet at δ 56.2 ppm as a result of splitting by deuterium. Carbon-deuterium coupling constant was recorded as $J_{\text{C-D}}$ 19.3 Hz. The signal from the α -carbon in the racemic non-labelled sample (\pm)-(**7.5**) was observed as a singlet at δ 56.6 ppm due to the isotope shift effect.

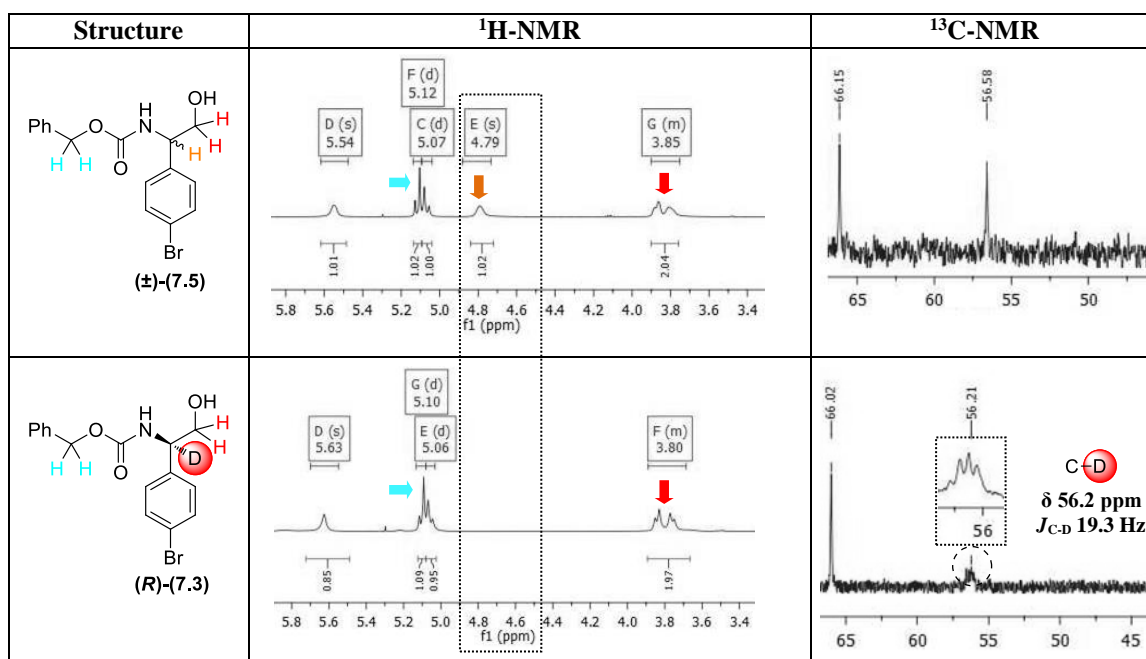
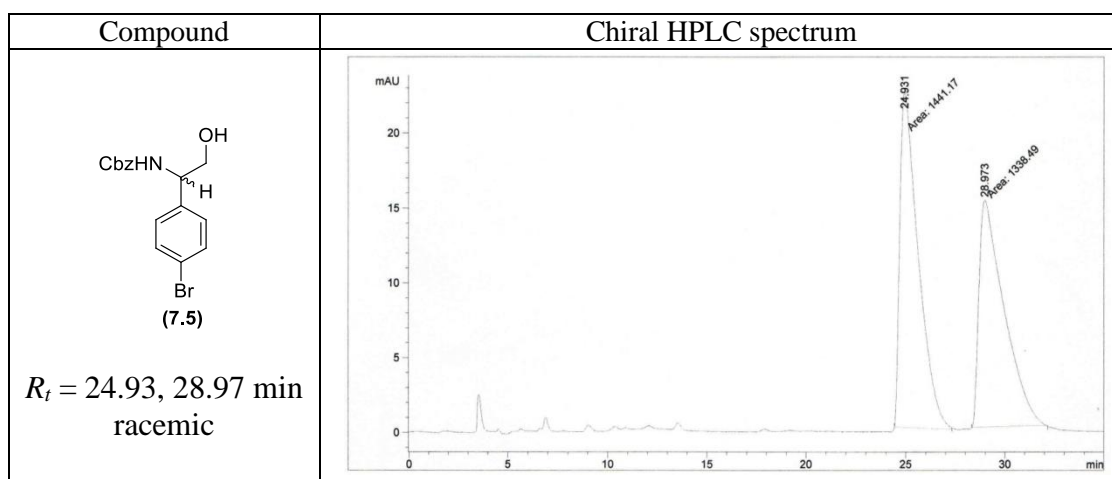


Table 7.2. ^1H -NMR (500 MHz, CDCl_3) and ^{13}C -NMR (126 MHz, CDCl_3) spectra of (*R*)-(**7.3**) and (\pm)-(**7.5**)

The HRMS analysis provided a confirmation of the synthesis of (\pm)-(**7.5**) with $[\text{M}+\text{H}]^+$ ions found at the required m/z (found: 350.0390, required: 350.0386) and (*R*)-(**7.3**) with $[\text{M}+\text{H}]^+$ ions found at the required m/z (found: 351.0452, required: 351.0449). To determine the enantiopurity of the labelled α -amino- β -alcohol (*R*)-(**7.3**) synthesised, a chiral HPLC analysis was performed. The optically active sample was run against the corresponding racemic non-labelled α -amino- β -alcohol sample (\pm)-(**7.5**). Enantiomeric excess was calculated to be 94% (Table 7.3.).



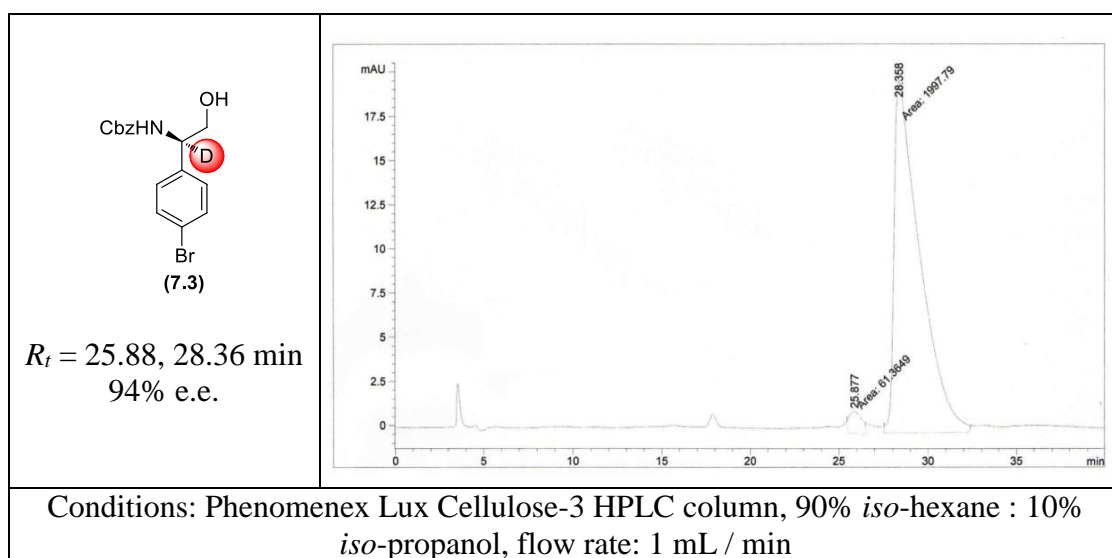
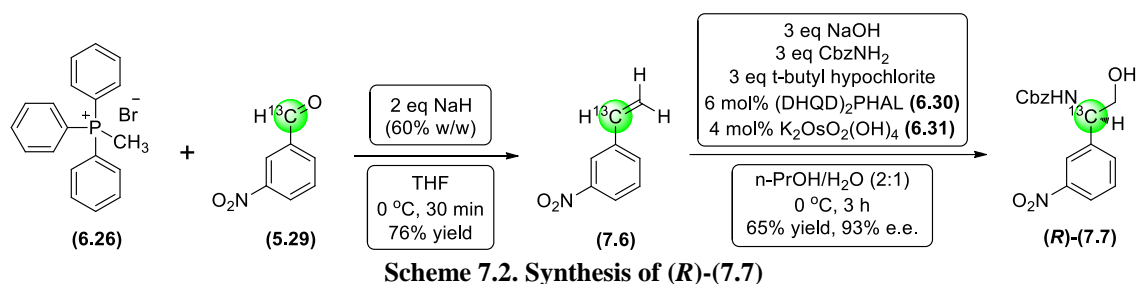


Table 7.3. Chiral HPLC spectra of (±)-(7.5) and (R)-(7.3)

7.3. Synthesis of benzyl α - ^{13}C -(R)-(2-hydroxy-1-(3-nitrophenyl)ethyl)carbamate (R)-(7.7)

α - ^{13}C -3-nitrobenzaldehyde (**5.29**) was converted to the corresponding styrene (**7.6**), that was subsequently submitted to the AA reaction to afford the desired α -amino- β -alcohol (R)-(7.7) with the ^{13}C -label on the α -carbon (Scheme 7.2).



Scheme 7.2. Synthesis of (R)-(7.7)

Examining the ^1H -NMR (500 MHz, CDCl_3) spectrum of styrene (**7.6**), the signal at δ 6.77 ppm (ddd, $J_{\text{H-H}}$ 17.5, 10.9 Hz; $J_{^{13}\text{C-H}}$ 156.8 Hz), was observed and assigned to the α -proton H_a (Figure 7.1). Typically a one-bond coupling between ^{13}C and ^1H is expected to be in the range of 150 Hz.¹³⁵ Protons H_b and H_x were observed as doublet of doublets at δ 5.90 ppm and δ 5.44 ppm respectively with proton-proton coupling constants of J_{a-b} 17.5 Hz and J_{a-x} 10.9 Hz. Two-bond ^1H - ^{13}C coupling constants were also identified at $^2J_{^{13}\text{C-H}}$ 3.2 Hz and $^2J_{^{13}\text{C-H}}$ 4.3 Hz. The long-range couplings between ^{13}C and ^1H ($^2J_{^{13}\text{C-H}}$ and $^3J_{^{13}\text{C-H}}$) have magnitude in the range of 0 - 10 Hz.

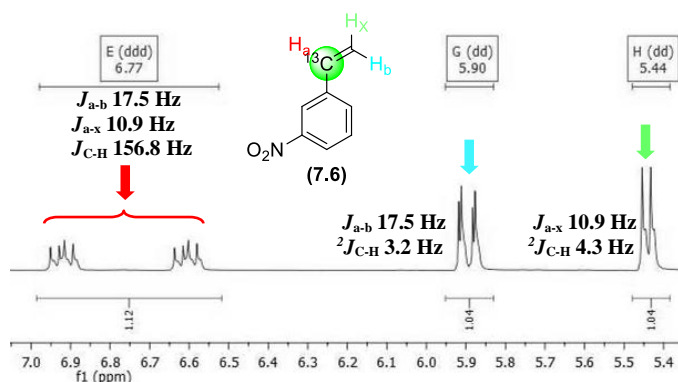


Figure 7.1. $^1\text{H-NMR}$ (500 MHz, CDCl_3) spectrum of (7.6)

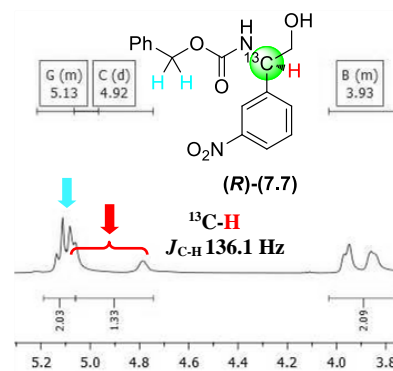


Figure 7.2. $^1\text{H-NMR}$ (500 MHz, CDCl_3) spectrum of (R)-(7.7)

The $^1\text{H-NMR}$ (500 MHz, CDCl_3) spectrum of (R)-(7.7) displayed a doublet at δ 4.92 ppm (partially obscured by the signal from Cbz- group at δ 5.13 ppm) with a large coupling constant ($J_{\text{C-H}}$ 136.1 Hz), corresponding to the proton at the α - ^{13}C (Figure 7.2.).

Within the $^{13}\text{C-NMR}$ (126 MHz, CDCl_3) spectra of (7.6) and (R)-(7.7) signals from α -carbon were observed as enhanced singlets at δ 134.9 ppm and δ 56.3 ppm respectively, as a result of ^{13}C isotope enrichment (Figure 7.3.). The signal intensity of non-labelled carbons was greatly reduced.

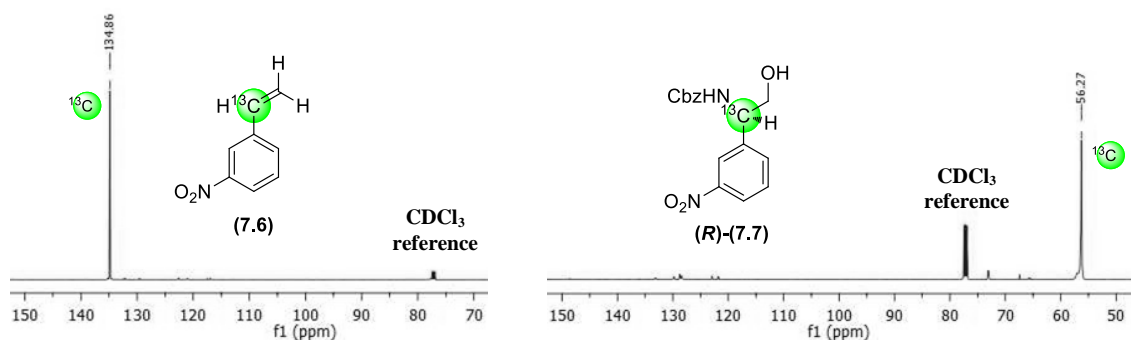


Figure 7.3. $^{13}\text{C-NMR}$ (126 MHz, CDCl_3) spectra of (7.6) and (R)-(7.7)

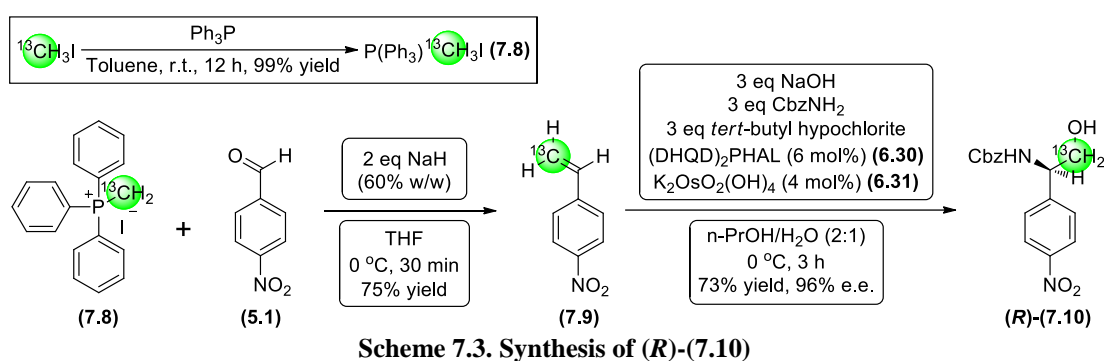
The HRMS analysis provided a confirmation of the synthesis of (7.6) with $[\text{M}+\text{H}]^+$ ions found at the required m/z (found: 151.0580, required: 151.0583) and (R)-(7.7) with $[\text{M}+\text{H}]^+$ ions found at the required m/z (found: 318.1165, required: 318.1166).

7.4. Synthesis of benzyl β - ^{13}C -(R)-(2-hydroxy-1-(4-nitrophenyl)ethyl)carbamate (R)-(7.10)

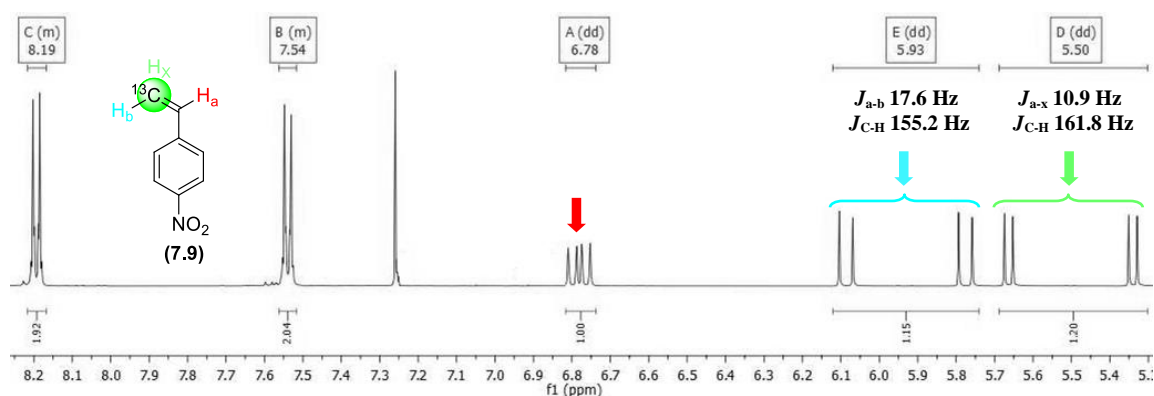
After the successful installation of ^2H and ^{13}C labels at the α -positions of compounds (R)-(7.3) and (R)-(7.7), it was considered important to investigate a

functionalisation of a β -carbon of optically active α -amino- β -alcohols. To achieve this, an isotope incorporating synthesis of the phosphonium salt was required. In order to generate ^{13}C -labelled phosphonium salt (**7.8**), the procedure reported by Takeuchi and Osakada was utilised.²⁵⁵

Equimolar amounts of triphenylphosphine and ^{13}C -labelled iodomethane were reacted as outlined below, generating $^{13}\text{CH}_3$ -methyltriphenyl phosphonium iodide (**7.8**) in a quantitative yield (**Scheme 7.3**). The resulting salt (**7.8**) was reacted with 4-nitrobenzaldehyde (**5.1**) to afford the corresponding styrene (**7.9**) with the ^{13}C label at the β -position, which was subsequently converted to (**R**)-(**7.10**).



The ^1H -NMR (500 MHz, CDCl_3) spectrum of (**7.9**) displayed a signal at δ 6.78 ppm (dd, $J_{\text{H-H}}$ 17.6, 10.9 Hz), which was assigned to the proton H_a of the styrene (**Figure 7.4**). Signals of H_b and H_x were observed as doublet of doublets at δ 5.93 ppm and δ 5.50 ppm respectively. Proton-proton coupling constants were recorded as J_{a-b} 17.6 Hz and J_{a-x} 10.9 Hz. Proton- ^{13}C coupling constants were recorded as $J_{^{13}\text{C-H}}$ 155.2 Hz and $J_{^{13}\text{C-H}}$ 161.8 Hz.



The $^1\text{H-NMR}$ (500 MHz, CDCl_3) spectrum of (*R*)-(**7.10**) displayed two doublet of doublets at δ 3.96 and 3.85 ppm ($J_{13\text{C-H}}$ 147.0 Hz; $J_{\text{H-H}}$ 12.5 Hz and $J_{13\text{C-H}}$ 143.4 Hz; $J_{\text{H-H}}$ 9.5 Hz), corresponding to the protons at the β - ^{13}C (**Figure 7.5.**).

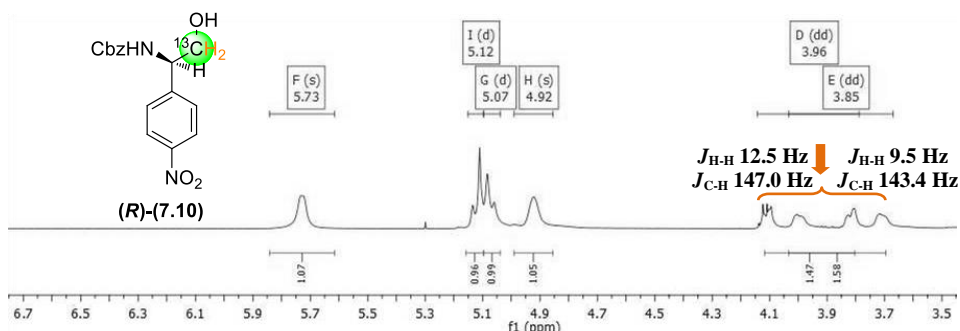
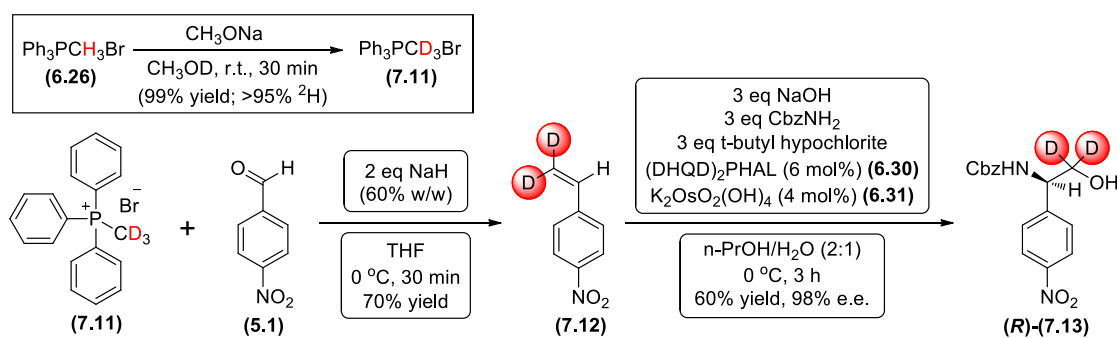


Figure 7.5. $^1\text{H-NMR}$ (500 MHz, CDCl_3) spectrum of (*R*)-(**7.10**)

7.5. Synthesis of benzyl β - ^2H , ^2H -(*R*)-(2-hydroxy-1-(4-nitrophenyl)ethyl)carbamate (*R*)-(**7.13**)

To install the ^2H -labels at the β -carbon, a suitable phosphonium salt was required. In order to synthesise ^2H -labelled phosphonium salt (**7.11**), the procedure reported by Yin *et al* was utilised.²⁵⁶ Methyltriphenylphosphonium bromide (**6.26**) was suspended in deuterated methanol and treated with catalytic amount of sodium methoxide base (**Scheme 7.4.**). After the mixture was stirred for 30 min, the solvent was removed under reduced pressure to afford ^2H -labelled methyltriphenylphosphonium bromide (**7.11**) (> 95% ^2H incorporation) in a quantitative yield. The resulting salt was reacted with 4-nitrobenzaldehyde (**5.1**) to afford the corresponding styrene (**7.12**) with two deuterium atoms installed at the β -position. Unfortunately, any attempt to purify and characterise the above styrene (**7.12**) was unsuccessful. Thus (**7.12**) was subjected to the aminohydroxylation reaction straight after simple filtration and concentration *in vacuo*. Gratifyingly, the desired amino alcohol (*R*)-(**7.13**) was afforded in a 60% yield.



Scheme 7.4. Synthesis of (*R*)-(**7.13**)

The $^1\text{H-NMR}$ (500 MHz, CDCl_3) spectrum of (*R*)-(7.13) displayed the absence of the signals in the δ 3.5 - 4.5 ppm region, which suggested successful deuteration at the β -carbon ($> 95\%$ ^2H incorporation) (**Figure 7.6.**). Further evidence was obtained from the $^2\text{H-NMR}$ (77 MHz, DCM) spectrum, where deuterium signals were observed at δ 3.87 and 3.76 ppm.

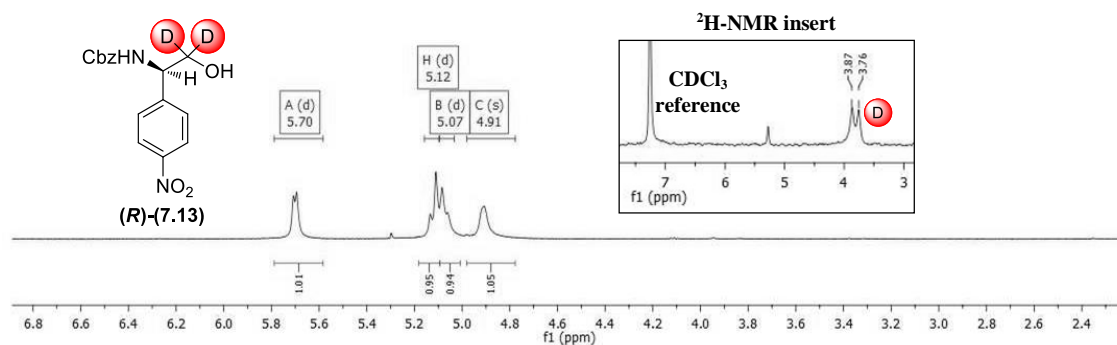


Figure 7.6. $^1\text{H-NMR}$ (500 MHz, CDCl_3) spectrum of (*R*)-(7.13) with $^2\text{H-NMR}$ (77 MHz, DCM) insert

7.6. Chapter conclusion

To summarise, during the course of this project a library of optically active α -arylglycinols has been generated. The α -amino- β -alcohols were generated in 61 - 73% yield, 93 - 98% e.e. and were ^2H or ^{13}C isotopically enriched. Isotope incorporation levels were above 95%.

It has been demonstrated, that the catalytic asymmetric aminohydroxylation reaction proves to be a powerful tool for the enantioselective one-step synthesis of N-Cbz-protected α -arylglycinols from styrenes, in good yields and excellent enantioselectivities.

α -Arylglycinols are very valuable structural units in synthetic and natural compounds. If oxidised, α -arylglycinols can be converted to the corresponding α -arylglycines, an important class of amino acids found in a wide range of bioactive compounds such as glycopeptide antibiotics.

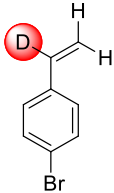
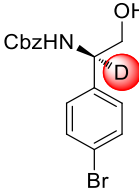
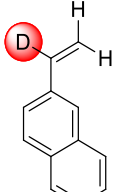
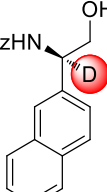
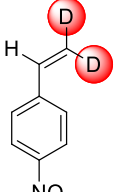
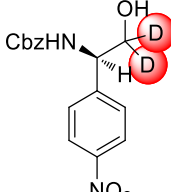
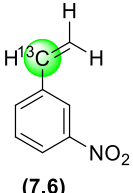
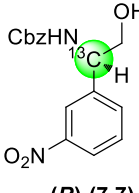
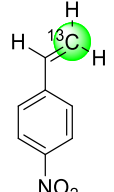
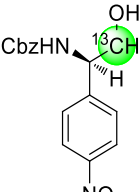
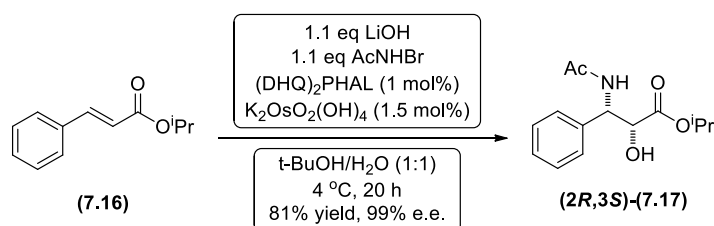
Styrene	α -amino- β -alcohol	Yield and e.e. of α -amino- β -alcohol
 <p>(7.2)</p>	 <p>(R)-(7.3)</p>	68% yield 95% e.e.
 <p>(7.14)</p>	 <p>(R)-(7.15)</p>	73% yield 93% e.e.
 <p>(7.12)</p>	 <p>(R)-(7.13)</p>	61% yield 98% e.e.
 <p>(7.6)</p>	 <p>(R)-(7.7)</p>	65% yield 93% e.e.
 <p>(7.9)</p>	 <p>(R)-(7.10)</p>	70% yield 96% e.e.

Table 7.4. Generated library of α - or β -labelled styrenes and corresponding optically active α -amino- β -alcohols

Additionally, aminohydroxylation methodology can be further extended to convert α,β -unsaturated esters to the corresponding β -hydroxyamides.²⁵⁷ Sharpless *et al* reported a synthesis of protected (2*R*,3*S*)-3-phenylisoserine (2*R*,3*S*)-(7.17), a precursor for the side chains of the anticancer drugs Taxol and Taxotere.²⁵⁸ Furthermore, isotopic labelling can be extended into the dihydroxylation reaction.



Scheme 7.5. Synthesis of (2*R*,3*S*)-(7.17)

Section 3.

Experimental

8.1. General Directions

Reactions described as under an argon or nitrogen atmosphere were conducted in flame dried apparatus. Reactions carried out at 0 °C were conducted using a water / ice bath, those at -78 °C were conducted in an acetone / solid carbon dioxide bath. Tetrahydrofuran (THF) and diethyl ether were freshly distilled from sodium wire and benzophenone under argon. Dichloromethane (DCM), propionitrile, acetonitrile and triethylamine were freshly distilled from calcium hydride under argon. Toluene was freshly distilled from sodium under argon. Petroleum ether (PET) refers to the fraction that boils between 40 and 60 °C. Chloroform and deuterated chloroform were filtered through basic aluminium oxide and stored over activated 4Å molecular sieves in darkened glass bottles. All commercially available reagents were used as supplied. However, the following reagents were treated as follows before use: phosphorus oxychloride was distilled from sodium under reduced pressure and stored under an argon atmosphere; trimethyl borate was freshly distilled from sodium and stored under an argon atmosphere.

8.2. Characterisation

Flash column chromatography was carried out on silica gel (Fluka Silica gel 60, 70-230 mesh). Analytical thin-layer chromatography (TLC) was performed on Merck plates (aluminium coated with 0.2 mm silica gel 60 F₂₅₄), with visualization by UV light and/or potassium permanganate stain followed by heating. Melting points were recorded using open capillary tubes on melting point a Stuart Scientific SMP1 apparatus and are uncorrected. ¹H and ¹³C-NMR spectra were recorded in Fourier transform mode on a Bruker Ascend 500 MHz spectrometer at the field strength indicated and unless otherwise stated deuterated chloroform was used as solvent. ¹⁵N and ²H-NMR were run, unlocked, on a Bruker Ascend 500 MHz. The ¹H-spectra were recorded in ppm and referenced to the residual CHCl₃ signal located at δ 7.26 ppm. ¹³C-NMR spectra were recorded in ppm and referenced to the residual CHCl₃ signal found at δ 77.16 ppm. Multiplicities in the NMR spectra are described as: s = singlet, d = doublet, t = triplet, q = quartet, m = multiplet, br = broad; coupling constants are reported in Hz. Ion mass/charge (*m/z*) ratios are reported as values in atomic mass units and carried out on a Shimadzu Kratos MALDI-TOF. Optical rotation values were measured on a Perkin Elmer 241 polarimeter with a 1 mL cell (path length 1 dm) and are reported as follows: $[\alpha]_D^{T(^{\circ}\text{C})}$ concentration (*c* = g / 100 mL, solvent). FT-IR spectra were recorded on a

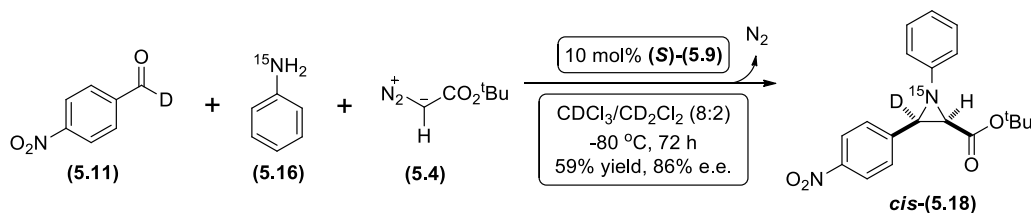
Perkin-Elmer 298 spectrometer either as a thin film or neat sample and are reported in wavenumbers (cm^{-1}). HRMS was carried out by the EPSRC at the National Mass Spectrometry Service, University of Wales, Swansea. Chiral analytical HPLC analysis was performed using Hewlett Packard Agilent 1100 HPLC system and the conditions are given as following: column, solvents, solvent ratio (%), flow rate (mL / min), retention time (min), e.e. (%).

8.3. Preparation of the Cooling Bath for Asymmetric Aziridination Reactions

As the asymmetric aziridination reactions require sustained low temperature conditions in order to induce the desired level of enantiomeric excess, the use of an immersion chiller is recommended. The bath was prepared by the addition of *iso*-propanol or acetone to a dewar flask of the appropriate size, within which the chiller arm was submerged. Care was taken to ensure the arm was settled firmly into the bottom of the flask, leaving the central space free for a large magnetic stirrer. The arm was clamped securely above the bath to ensure no movement during the reaction, and the apparatus was placed upon a magnetic stirrer plate. Efficient stirring of the bath was essential in order to achieve uniform cooling, and also in preventing build up of ice. A thermometer was suspended within the bath in order to check the correlation between the temperature of the bath and the set temperature of the chiller. Any required offset could then be implemented. At $-80\text{ }^{\circ}\text{C}$, the bath was reasonably expected to last around two weeks before requiring defrosting and change of the solvent. However, depending upon the strength of the chiller used, some heating of the bath may be observed before this point, and thus the bath may require more regular maintenance.

8.4. Synthesis of stable isotope labelled optically active aziridines

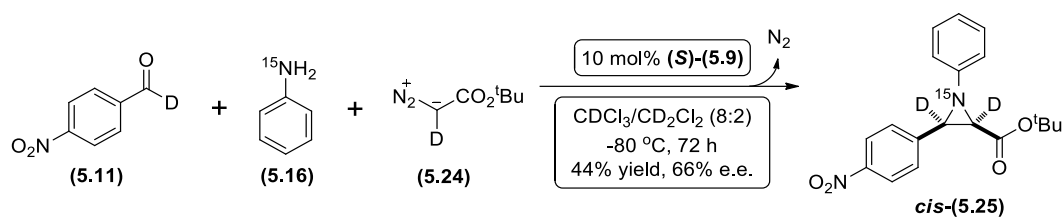
tert-butyl *cis*-1-¹⁵N-3-²H-3-(4-nitrophenyl)-1-phenylaziridine-2-carboxylate *cis*-**(5.18)**



α -²H-4-Nitrobenzaldehyde (**5.11**) (30.0 mg, 0.20 mmol) and ¹⁵N-aniline (**5.16**) (17.6 mg, 0.19 mmol) were added to a flame dried Biotage 5 mL microwave vial, containing activated 4Å molecular sieves (~ 100 mg) under nitrogen. Deuterated chloroform/deuterated dichloromethane (8:2) mixture (1 mL) was added, the vial was sealed with a PTFE crimp cap and the reaction mixture was left stirring at 25 °C for 2 hours. Catalyst (*S*)-**(5.9)** (16.4 mg, 0.02 mmol, 10 mol%) was added and the vial was cooled to -80 °C. After 30 minutes, *tert*-butyl diazoacetate (**5.4**) (30 μ L, 0.21 mmol) was added *via* syringe, and the reaction mixture was stirred at -80 °C (~ 72 hours). At this point the reaction mixture was quenched with triethylamine (0.5 mL), passed through a short plug of silica, eluted with diethyl ether and the solvent was removed under reduced pressure. The crude material was purified by flash chromatography on silica gel (3% ethyl acetate in 40-60 PET, R_f = 0.22) to afford a bright yellow solid. Subsequent physicochemical analysis confirmed this to be the title compound *cis*-**(5.18)** (39.0 mg, 0.11 mmol, 59% yield). A sample was submitted to chiral analytical HPLC analysis [Cellulose 1, *iso*-hexane / *iso*-propanol : 99 / 01, 1 mL / min, 18.5 min (1st peak), 26.2 min (2nd peak), 86% e.e.].

¹H NMR (500 MHz, CDCl₃) δ 8.22 (d, J 8.9 Hz, 2H, ArH), 7.71 (d, J 8.9 Hz, 2H, ArH), 7.29 (t, J 7.5 Hz, 2H, ArH), 7.07 (t, J 7.5 Hz, 1H, ArH), 7.04 (dd, J 7.5, 1.4 Hz, 2H, ArH), 3.19 (s, 1H, C2-H), 1.23 (s, 9H, C(CH₃)₃); ¹³C NMR (126 MHz, CDCl₃) δ 166.1 (d, J_{C-N} 4.8 Hz), 151.8 (d, J_{C-N} 2.6 Hz), 147.6, 142.5 (d, J_{C-N} 4.1 Hz), 129.4, 128.9 (d, J_{C-N} 1.8 Hz), 123.9, 123.3, 120.0 (d, J_{C-N} 3.3 Hz), 82.4, 46.6 (d, J_{C-N} 6.8 Hz), 45.74 (dt, J_{C-D} 25.5, J_{C-N} 6.8 Hz), 28.0; ²H NMR (77 MHz, CH₂Cl₂) δ 5.26 (CD₂Cl₂ ref), 3.54 (br s); ¹⁵N NMR (51 MHz, CDCl₃) δ 66.41; M.p. 124 - 126 °C (from diethyl ether / *n*-pentane); $[\alpha]_D^{23}$ -213 (c 2.0 CHCl₃); FT-IR (thin film) 2977 (C-H), 1739 (C=O), 1599/1519/1495 (C=C aromatic), 1345 (NO₂), 1227/1158 (C(O)C), 1047 (C-N), 904 (C-H bend) cm⁻¹; MS (MALDI) 343.2 [M+H]⁺; HRMS (HASP) exact mass calculated for [C₁₉H₂₀D₁¹⁵N₁N₁O₄] requires m/z 343.1529, found m/z 343.1526 [M+H]⁺.

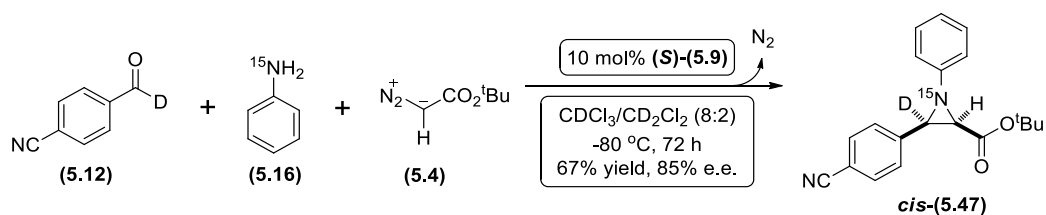
***tert*-butyl *cis*-1-¹⁵N-2,3-²H-3-(4-nitrophenyl)-1-phenylaziridine-2-carboxylate *cis*-
(5.25)**



α -²H-4-Nitrobenzaldehyde (5.11) (30.0 mg, 0.20 mmol) and ¹⁵N-aniline (5.16) (17.6 mg, 0.19 mmol) were added to a flame dried Biotage 5 mL microwave vial, containing activated 4Å molecular sieves (~ 100 mg) under nitrogen. Deuterated chloroform/deuterated dichloromethane (8:2) mixture (1 mL) was added, the vial was sealed with a PTFE crimp cap and the reaction mixture was left stirring at 25 °C for 2 hours. Catalyst (S)-(5.9) (16.4 mg, 0.02 mmol, 10 mol%) was added and the vial was cooled to -80 °C. After 30 minutes, > 95% deuterated *tert*-butyl diazoacetate (5.24) (30 μ L, 0.21 mmol) was added *via* syringe, and the reaction mixture was stirred at -80 °C (~ 72 hours). At this point the reaction mixture was quenched with triethylamine (0.5 mL), passed through a short plug of silica, eluted with diethyl ether and the solvent was removed under reduced pressure. The crude material was purified by flash chromatography on silica gel (3% ethyl acetate in 40-60 PET, R_f = 0.22) to afford a bright yellow solid. Subsequent physicochemical analysis confirmed this to be the title compound *cis*-(5.25) (30.1 mg, 0.09 mmol, 44% yield). A sample was submitted to chiral analytical HPLC analysis [Cellulose 1, *iso*-hexane / *iso*-propanol : 99 / 01, 1 mL / min, 18.3 min (1st peak), 27.6 min (2nd peak), 66% e.e.].

¹H NMR (500 MHz, CDCl₃) δ 8.22 (d, *J* 8.9 Hz, 2H, ArH), 7.71 (d, *J* 8.9 Hz, 2H, ArH), 7.29 (t, *J* 7.8 Hz, 2H, ArH), 7.14 – 6.97 (m, 3H, ArH), 1.23 (s, 9H, C(CH₃)₃); ¹³C NMR (126 MHz, CDCl₃) δ 166.1 (d, *J*_{C-N} 4.7 Hz), 151.8 (d, *J*_{C-N} 2.6 Hz), 147.7, 142.5 (d, *J*_{C-N} 4.1 Hz), 129.5, 128.9 (d, *J*_{C-N} 1.8 Hz), 123.9, 123.3, 120.0 (d, *J*_{C-N} 3.2 Hz), 82.4 (s), 46.4 (m), 45.7 (m), 28.0; ²H NMR (77 MHz, CH₂Cl₂) δ 7.26 (CDCl₃ ref), 5.26 (CD₂Cl₂ ref), 3.54 (br s), 3.14 (br s); ¹⁵N NMR (51 MHz, CDCl₃) δ 66.22; M.p. 123 - 125 °C (from diethyl ether / *n*-pentane); [α]_D²³ -161 (c 2.0 CHCl₃); FT-IR (thin film) 2979 (C-H), 1742 (C=O), 1599/1520/1491 (C=C aromatic), 1345 (NO₂), 1266/1154 (C(O)C), 1047 (C-N), 904 (C-H bend) cm⁻¹; MS (MALDI) 344.2 [M+H]⁺; HRMS (HNESP) exact mass calculated for [C₁₉H₁₉D₂¹⁵N₁N₁O₄] requires *m/z* 344.1592, found *m/z* 344.1592 [M+H]⁺.

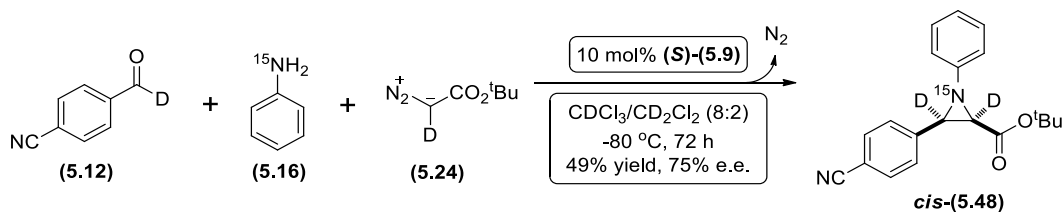
tert*-butyl *cis*-1-¹⁵N-3-²H-3-(4-cyanophenyl)-1-phenylaziridine-2-carboxylate *cis*-**(5.47)*



α -²H-4-Cyanobenzaldehyde (**5.12**) (15.0 mg, 0.12 mmol) and ¹⁵N-aniline (**5.16**) (10.1 mg, 0.11 mmol) were added to a flame dried Biotage 5 mL microwave vial, containing activated 4Å molecular sieves (~ 100 mg) under nitrogen. Deuterated chloroform/deuterated dichloromethane (8:2) mixture (1 mL) was added, the vial was sealed with a PTFE crimp cap and the reaction mixture was left stirring at 25 °C for 2 hours. Catalyst (S)-(5.9) (9.6 mg, 0.01 mmol, 10 mol%) was added and the vial was cooled to -80 °C. After 30 minutes, *tert*-butyl diazoacetate (**5.4**) (17 μ L, 0.12 mmol) was added *via* syringe, and the reaction mixture was stirred at -80 °C (~ 72 hours). At this point the reaction mixture was quenched with triethylamine (0.5 mL), passed through a short plug of silica, eluted with diethyl ether and the solvent was removed under reduced pressure. The crude material was purified by flash chromatography on silica gel (10% diethyl ether in 40-60 PET, R_f = 0.30) to afford an orange solid. Subsequent physicochemical analysis confirmed this to be the title compound *cis*-(**5.47**) (24.5 mg, 0.07 mmol, 67% yield). A sample was submitted to chiral analytical HPLC analysis [Cellulose 1, *iso*-hexane / *iso*-propanol : 99 / 01, 1 mL / min, 17.7 min (1st peak), 22.8 min (2nd peak), 85% e.e.].

¹H NMR (500 MHz, CDCl₃) δ 7.65 (s, 4H, ArH), 7.29 (t, J 7.8 Hz, 2H, ArH), 7.11 – 7.00 (m, 3H, ArH), 3.16 (s, 1H, C2-H), 1.22 (s, 9H, C(CH₃)₃); ¹³C NMR (126 MHz, CDCl₃) δ 166.2 (d, J_{C-N} 4.7 Hz), 151.9 (d, J_{C-N} 2.6 Hz), 140.5 (d, J_{C-N} 4.1 Hz), 131.9, 129.4, 128.8 (d, J_{C-N} 1.8 Hz), 123.8, 120.0 (d, J_{C-N} 3.2 Hz), 118.9, 111.6, 82.3, 46.5 (d, J_{C-N} 6.8 Hz), 45.9 (m), 27.9; ²H NMR (77 MHz, CH₂Cl₂) δ 7.26 (CDCl₃ ref), 5.26 (CD₂Cl₂ ref), 3.50 (br s); ¹⁵N NMR (51 MHz, CDCl₃) δ 65.81; M.p. 87 - 89 °C (from diethyl ether / *n*-pentane); $[\alpha]_D^{23}$ -40 (c 1.0 CHCl₃); FT-IR (thin film) 2977 (C-H), 2226 (C \equiv N), 1740 (C=O), 1593/1504 (C=C aromatic), 1205/1155 (C(O)C), 1032 (C-N), 820 (C-H bend) cm⁻¹; MS (MALDI) 361.1 [M+K]⁺; HRMS (HASP) exact mass calculated for [C₂₀H₂₀D₁¹⁵N₁N₁O₂] requires m/z 323.1631, found m/z 323.1634 [M+H]⁺.

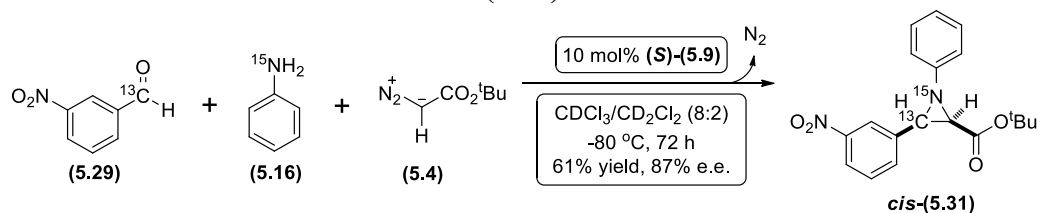
***tert*-butyl *cis*-1-¹⁵N-2,3-²H-3-(4-cyanophenyl)-1-phenylaziridine-2-carboxylate *cis*-
(5.48)**



α -²H-4-Cyanobenzaldehyde (**5.12**) (12.0 mg, 0.09 mmol) and ¹⁵N-aniline (**5.16**) (8.1 mg, 0.08 mmol) were added to a flame dried Biotage 5 mL microwave vial, containing activated 4Å molecular sieves (~ 100 mg) under nitrogen. Deuterated chloroform/deuterated dichloromethane (8:2) mixture (1 mL) was added, the vial was sealed with a PTFE crimp cap and the reaction mixture was left stirring at 25 °C for 2 hours. Catalyst (**S**)-(**5.9**) (7.5 mg, 0.01 mmol, 10 mol%) was added and the vial was cooled to -80 °C. After 30 minutes, > 95% deuterated *tert*-butyl diazoacetate (**5.24**) (14 μ L, 0.10 mmol) was added *via* syringe, and the reaction mixture was stirred at -80 °C (~ 72 hours). At this point the reaction mixture was quenched with triethylamine (0.5 mL), passed through a short plug of silica, eluted with diethyl ether and the solvent was removed under reduced pressure. The crude material was purified by flash chromatography on silica gel (10% diethyl ether in 40-60 PET, R_f = 0.30) to afford an orange solid. Subsequent physicochemical analysis confirmed this to be the title compound *cis*-(**5.48**) (15.0 mg, 0.05 mmol, 49% yield). A sample was submitted to chiral analytical HPLC analysis [Cellulose 1, *iso*-hexane / *iso*-propanol : 99 / 01, 1 mL / min, 17.9 min (1st peak), 23.4 min (2nd peak), 75% e.e.].

¹H NMR (500 MHz, CDCl₃) δ 7.65 (s, 4H, ArH), 7.29 (t, J 7.8 Hz, 2H, ArH), 7.09 – 7.01 (m, 3H, ArH), 1.22 (s, 9H, C(CH₃)₃); ¹³C NMR (126 MHz, CDCl₃) δ 166.2 (d, J_{C-N} 4.8 Hz), 151.9 (d, J_{C-N} 2.6 Hz), 140.5 (d, J_{C-N} 4.0 Hz), 131.9, 129.4 (d, J_{C-N} 1.0 Hz), 128.8 (d, J_{C-N} 1.9 Hz), 123.8, 120.0 (d, J_{C-N} 3.3 Hz), 118.9, 111.6, 82.3, 46.5 (m), 46.0 (m), 27.9; ²H NMR (77 MHz, CH₂Cl₂) δ 7.26 (CDCl₃ ref), 5.26 (CD₂Cl₂ ref), 3.50 (br s), 3.11 (br s); ¹⁵N NMR (51 MHz, CDCl₃) δ 65.60; M.p. 88 - 90 °C (from diethyl ether / *n*-pentane); $[\alpha]_D^{23}$ -30 (c 1.0 CHCl₃); FT-IR (thin film) 2977 (C-H), 2226 (C \equiv N), 1738 (C=O), 1596/1490 (C=C aromatic), 1277/1152 (C(O)C), 1052 (C-N), 817 (C-H bend) cm⁻¹; MS (MALDI) 362.1 [M+K]⁺; HRMS (HASP) exact mass calculated for [C₂₀H₁₉D₂¹⁵N₁N₁O₂] requires m/z 324.1693, found m/z 324.1697 [M+H]⁺.

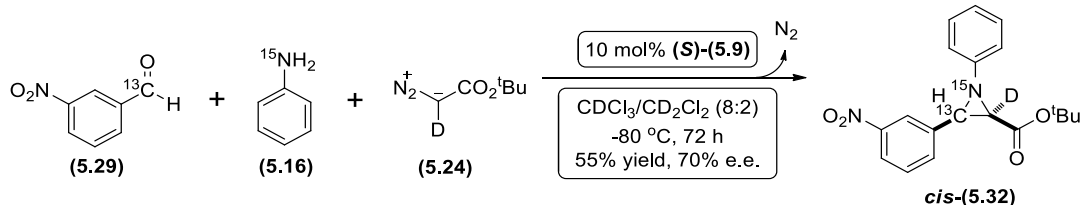
tert*-butyl *cis*-1-¹⁵N-3-¹³C-3-(3-nitrophenyl)-1-phenylaziridine-2-carboxylate *cis*-**(5.31)*



α -¹³C-3-Nitrobenzaldehyde (**5.29**) (22.0 mg, 0.14 mmol) and ¹⁵N-aniline (**5.16**) (12.2 mg, 0.13 mmol) were added to a flame dried Biotage 5 mL microwave vial, containing activated 4Å molecular sieves (~ 100 mg) under nitrogen. Deuterated chloroform/deuterated dichloromethane (8:2) mixture (1 mL) was added, the vial was sealed with a PTFE crimp cap and the reaction mixture was left stirring at 25 °C for 2 hours. Catalyst (**S**)-(**5.9**) (12.0 mg, 0.01 mmol, 10 mol%) was added and the vial was cooled to -80 °C. After 30 minutes, *tert*-butyl diazoacetate (**5.4**) (22 μ L, 0.16 mmol) was added *via* syringe, and the reaction mixture was stirred at -80 °C (~ 72 hours). At this point the reaction mixture was quenched with triethylamine (0.5 mL), passed through a short plug of silica, eluted with diethyl ether and the solvent was removed under reduced pressure. The crude material was purified by flash chromatography on silica gel (3% diethyl ether in 40-60 PET, R_f = 0.20) to afford a yellow solid. Subsequent physicochemical analysis confirmed this to be the title compound *cis*-(**5.31**) (30.0 mg, 0.09 mmol, 61% yield). A sample was submitted to chiral analytical HPLC analysis [Cellulose 1, *iso*-hexane / *iso*-propanol : 95 / 05, 1 mL / min, 9.6 min (1st peak), 13.0 min (2nd peak), 87% e.e.].

¹H NMR (500 MHz, CDCl₃) δ 8.42 – 8.36 (m, 1H, ArH), 8.17 (ddd, J 8.2, 2.3, 1.0 Hz, 1H, ArH), 7.92 – 7.85 (m, 1H, ArH), 7.54 (t, J 7.8 Hz, 1H, ArH), 7.30 (t, J 7.8 Hz, 2H, ArH), 7.11 – 7.02 (m, 3H, ArH), 3.59 (dd, J_{13C-H} 169.0, $J_{2,3}$ 6.7 Hz, 1H, C3-H), 3.17 (ddd, $J_{2,3}$ 6.7, J_{13C-H} 2.5, J_{N-H} 0.7 Hz, 1H, C2-H), 1.22 (s, 9H, C(CH₃)₃); ¹³C NMR (126 MHz, CDCl₃) δ 166.3 (dd, J_{C-N} 4.6, J_{C-13C} 1.9 Hz), 151.9 (t, J_{C-N} 2.4 Hz), 148.2 (d, J_{C-13C} 5.5 Hz), 137.4 (dd, J_{C-13C} 60.9, J_{C-N} 4.1 Hz), 134.2 (dd, J_{C-13C} 2.9, J_{C-N} 2.1 Hz), 129.4, 129.1 (d, J_{C-13C} 4.7 Hz), 123.9, 123.1 (dd, J_{C-N} 4.1, J_{C-13C} 1.9 Hz), 122.9, 120.0 (t, J_{C-N} 2.9 Hz), 82.3, 45.8 (d, J_{C-N} 7.0 Hz), 44.6 (d, J_{C-N} 6.8 Hz), 27.9; ¹⁵N NMR (51 MHz, CDCl₃) δ 66.15 (d, J_{C-N} 6.8 Hz); M.p. 118 - 120 °C (from diethyl ether / *n*-pentane); $[\alpha]_D^{23}$ -170 (c 2.0 CHCl₃); FT-IR (thin film) 2985 (C-H), 1738 (C=O), 1714, 1527/1489 (C=C aromatic), 1346 (NO₂), 1253/1150 (C(O)C), 1034 (C-N), 909/844/758 (C-H bend) cm⁻¹; MS (MALDI) 343.2 [M+H]⁺; HRMS (HNESP) Exact mass calculated for [¹³C₁C₁₈H₂₁¹⁵N₁N₁O₄]⁺ requires 343.1500, found 343.1499 [M+H]⁺.

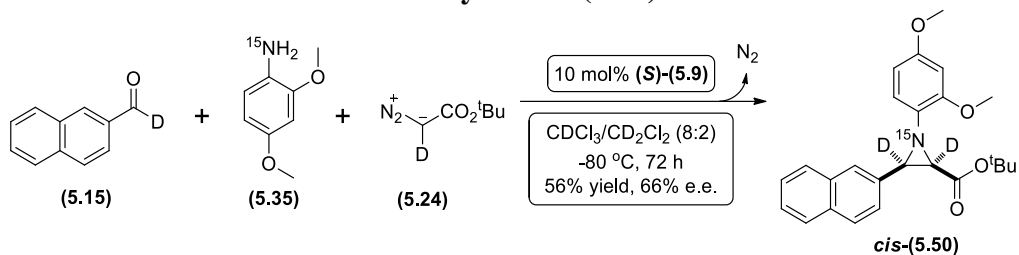
***tert*-butyl *cis*-1-¹⁵N-2-²H-3-¹³C-3-(3-nitrophenyl)-1-phenylaziridine-2-carboxylate *cis*-(**5.32**)**



α -¹³C-3-Nitrobenzaldehyde (**5.29**) (20.0 mg, 0.13 mmol) and ¹⁵N-aniline (**5.16**) (11.4 mg, 0.11 mmol) were added to a flame dried Biotage 5 mL microwave vial, containing activated 4Å molecular sieves (~ 100 mg) under nitrogen. Deuterated chloroform/deuterated dichloromethane (8:2) mixture (1 mL) was added, the vial was sealed with a PTFE crimp cap and the reaction mixture was left stirring at 25 °C for 2 hours. Catalyst **(S)**-(**5.9**) (11.0 mg, 0.01 mmol, 10 mol%) was added and the vial was cooled to -80 °C. After 30 minutes, > 95% deuterated *tert*-butyl diazoacetate (**5.24**) (20 μ L, 0.14 mmol) was added *via* syringe, and the reaction mixture was stirred at -80 °C (~ 72 hours). At this point the reaction mixture was quenched with triethylamine (0.5 mL), passed through a short plug of silica, eluted with diethyl ether and the solvent was removed under reduced pressure. The crude material was purified by flash chromatography on silica gel (3% diethyl ether in 40-60 PET, R_f = 0.20) to afford a yellow solid. Subsequent physicochemical analysis confirmed this to be the title compound *cis*-(**5.32**) (25.0 mg, 0.07 mmol, 55% yield). A sample was submitted to chiral analytical HPLC analysis [Cellulose 1, *iso*-hexane / *iso*-propanol : 95 / 05, 1 mL / min, 9.6 min (1st peak), 13.0 min (2nd peak), 70% e.e.].

¹H NMR (500 MHz, CDCl₃) δ 8.41 – 8.37 (m, 1H, ArH), 8.17 (dd, *J* 8.1, 1.6 Hz, 1H, ArH), 7.91 – 7.87 (m, 1H, ArH), 7.54 (t, *J* 7.8 Hz, 1H, ArH), 7.29 (t, *J* 7.8 Hz, 2H, ArH), 7.10 – 7.03 (m, 3H, ArH), 3.60 (d, *J*_{13C-H} 169.0 Hz, 1H, C3-H), 1.22 (s, 9H, C(CH₃)₃); ¹³C NMR (126 MHz, CDCl₃) δ 166.3 (dd, *J*_{C-N} 4.6, *J*_{C-13C} 2.0 Hz), 151.8 (t, *J*_{C-N} 2.4 Hz), 148.1 (d, *J*_{C-13C} 5.5 Hz), 137.4 (dd, *J*_{C-13C} 61.0, *J*_{C-N} 4.2 Hz), 134.2 (dd, *J*_{C-13C} 2.8, *J*_{C-N} 1.9 Hz), 129.4, 129.1 (d, *J*_{C-13C} 4.7 Hz), 123.8, 123.1 (dd, *J*_{C-N} 4.1, *J*_{C-13C} 1.9 Hz), 122.9, 120.0 (t, *J*_{C-N} 2.9 Hz), 82.3, 45.8 (d, *J*_{C-N} 7.0 Hz), 44.6 (m), 27.9; ²H NMR (77 MHz, CH₂Cl₂) δ 7.26 (CDCl₃ ref), 5.26 (CD₂Cl₂ ref), 3.12 (br s); ¹⁵N NMR (51 MHz, CDCl₃) δ 65.98 (d, *J*_{C-N} 6.8 Hz); M.p. 118 - 120 °C (from diethyl ether / *n*-pentane); [α]_D²³ -110 (c 1.0 CHCl₃); FT-IR (thin film) 2991 (C-H), 1735 (C=O), 1598/1526/1490 (C=C aromatic), 1345 (NO₂), 1251/1147 (C(O)C), 1081 (C-N), 903/815 (C-H bend) cm⁻¹; MS (MALDI) 344.2 [M+H]⁺; HRMS (HNESP) Exact mass calculated for [¹³C₁C₁₈H₂₀D₁¹⁵N₁N₁O₄]⁺ requires 344.1563, found 344.1558 [M+H]⁺.

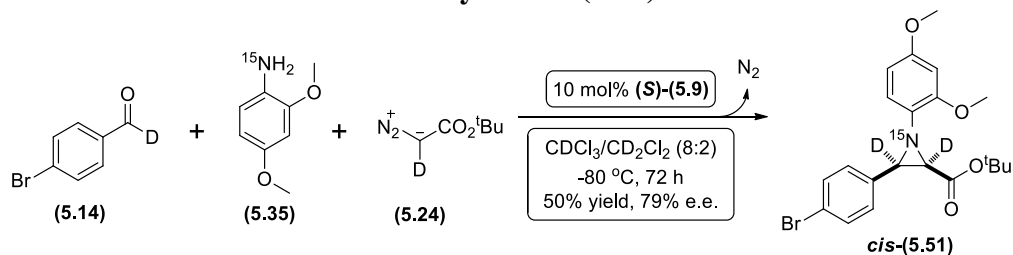
***tert*-butyl *cis*-1-¹⁵N-2,3-²H-1-(2,4-dimethoxyphenyl)-3-(naphthalen-2-yl)aziridine-2-carboxylate *cis*-(5.50)**



α -²H-2-Naphthaldehyde (5.15) (54.0 mg, 0.34 mmol) and ¹⁵N-2,4-dimethoxyaniline (5.35) (47.7 mg, 0.31 mmol) were added to a flame dried Biotage 5 mL microwave vial, containing activated 4Å molecular sieves (~ 100 mg) under nitrogen. Deuterated chloroform/deuterated dichloromethane (8:2) mixture (1 mL) was added, the vial was sealed with a PTFE crimp cap and the reaction mixture was left stirring at 25 °C for 2 hours. Catalyst (S)-(5.9) (28.6 mg, 0.03 mmol, 10 mol%) was added and the vial was cooled to -80 °C. After 30 minutes, > 95% deuterated *tert*-butyl diazoacetate (54 μ L, 0.38 mmol) was added *via* syringe, and the reaction mixture was stirred at -80 °C (~ 72 hours). At this point the reaction mixture was quenched with triethylamine (0.5 mL), passed through a short plug of silica, eluted with diethyl ether and the solvent was removed under reduced pressure. The crude material was purified by flash chromatography on silica gel (15% diethyl ether in 40-60 PET, R_f = 0.18) to afford a white solid. Subsequent physicochemical analysis confirmed this to be the title compound *cis*-(5.50) (79.0 mg, 0.19 mmol, 56% yield). A sample was submitted to chiral analytical HPLC analysis [Cellulose 1, *iso*-hexane / *iso*-propanol : 85 / 15, 1 mL / min, 7.6 min (1st peak), 9.0 min (2nd peak), 66% e.e.].

¹H NMR (500 MHz, CDCl₃) δ 8.04 (s, 1H, ArH), 7.86 – 7.77 (m, 3H, ArH), 7.65 (dd, J 8.4, 1.7 Hz, 1H, ArH), 7.50 – 7.42 (m, 2H, ArH), 6.89 (dd, J 8.4, 1.7 Hz, 1H, ArH), 6.48 (d, J 2.4 Hz, 1H, ArH), 6.40 (dd, J 8.5, 2.4 Hz, 1H, ArH), 3.79 (s, 3H, OCH₃), 3.78 (s, 3H, OCH₃), 1.12 (s, 9H, C(CH₃)₃); ¹³C NMR (126 MHz, CDCl₃) δ 167.5, 156.7, 153.2, 135.2, 133.2, 133.1, 133.0, 128.0, 127.8, 127.4, 127.2, 126.1, 126.0, 125.8, 120.0, 103.7, 99.8, 81.4, 55.8, 55.7, 47.8 (m), 46.3 (m), 27.9; ²H NMR (77 MHz, CH₂Cl₂) δ 7.26 (CDCl₃ ref), 5.27 (CD₂Cl₂ ref), 3.50 (br s), 2.91 (br s); ¹⁵N NMR (51 MHz, CDCl₃) δ 55.50; M.p. 83 - 85 °C (from diethyl ether / *n*-pentane); $[\alpha]_D^{26}$ -26 (c 1.0 CHCl₃); FT-IR (thin film) 2933 (C-H), 1743 (C=O), 1712, 1506 (C=C aromatic), 1243/1208 (C(O)C), 1037 (C-N), 840/760 (C-H bend) cm⁻¹; MS (MALDI) 409.0 [M+H]⁺; HRMS (HNESP) Exact mass calculated for [C₂₅H₂₆D₂¹⁵N₁O₄]⁺ requires 409.2109, found 409.2109 [M+H]⁺.

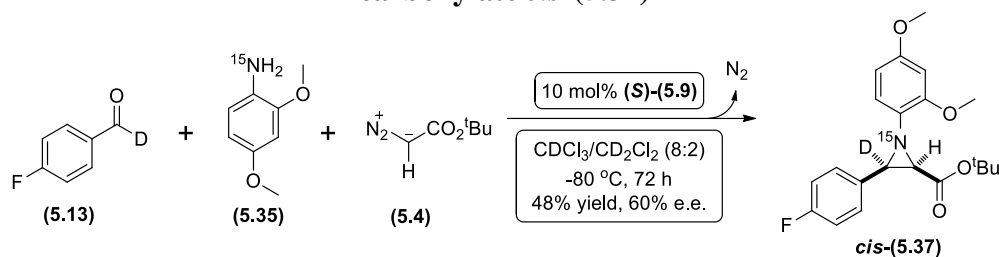
***tert*-butyl *cis*-1-¹⁵N-2,3-²H-3-(4-bromophenyl)-1-(2,4-dimethoxyphenyl)aziridine-2-carboxylate *cis*-(5.51)**



α -²H-4-Bromobenzaldehyde (**5.14**) (21.0 mg, 0.11 mmol) and ¹⁵N-2,4-dimethoxyaniline (**5.35**) (15.6 mg, 0.10 mmol) were added to a flame dried Biotage 5 mL microwave vial, containing activated 4Å molecular sieves (~ 100 mg) under nitrogen. Deuterated chloroform/deuterated dichloromethane (8:2) mixture (1 mL) was added, the vial was sealed with a PTFE crimp cap and the reaction mixture was left stirring at 25 °C for 2 hours. Catalyst (S)-(5.9) (9.4 mg, 0.01 mmol, 10 mol%) was added and the vial was cooled to -80 °C. After 30 minutes, > 95% deuterated *tert*-butyl diazoacetate (**5.24**) (18 μ L, 0.12 mmol) was added *via* syringe, and the reaction mixture was stirred at -80 °C (~ 72 hours). At this point the reaction mixture was quenched with triethylamine (0.5 mL), passed through a short plug of silica, eluted with diethyl ether and the solvent was removed under reduced pressure. The crude material was purified by flash chromatography on silica gel (20% diethyl ether in 40-60 PET, R_f = 0.27) to afford a brown solid. Subsequent physicochemical analysis confirmed this to be the title compound *cis*-(5.51) (25.0 mg, 0.06 mmol, 50% yield). A sample was submitted to chiral analytical HPLC analysis [Cellulose 1, *iso*-hexane / *iso*-propanol : 85 / 15, 1 mL / min, 6.3 min (1st peak), 6.9 min (2nd peak), 79% e.e.].

¹H NMR (500 MHz, CDCl₃) δ 7.49 – 7.38 (m, 4H, ArH), 6.81 (dd, J 8.5, 1.6 Hz, 1H, ArH), 6.45 (d, J 2.5 Hz, 1H, ArH), 6.37 (dd, J 8.5, 2.5 Hz, 1H, ArH), 3.77 (s, 3H, OCH₃), 3.77 (s, 3H, OCH₃), 1.24 (s, 9H, C(CH₃)₃); ¹³C NMR (126 MHz, CDCl₃) δ 167.2 (d, J_{C-N} 4.6 Hz), 156.7, 153.1 (d, J_{C-N} 2.6 Hz), 134.8 (d, J_{C-N} 3.1 Hz), 134.6 (d, J_{C-N} 4.1 Hz), 131.0, 129.9 (d, J_{C-N} 1.8 Hz), 121.4, 119.8 (d, J_{C-N} 1.8 Hz), 103.7, 99.8, 81.6, 55.8, 55.7, 47.0 (m), 46.7 (m), 28.0; ²H NMR (77 MHz, CH₂Cl₂) δ 7.26 (CDCl₃ ref), 5.27 (CD₂Cl₂ ref), 3.28 (br s), 2.87 (br s); ¹⁵N NMR (51 MHz, CDCl₃) δ 55.35; M.p. 115 - 118 °C (from diethyl ether / *n*-pentane); $[\alpha]_D^{26}$ -18 (c 1.0 CHCl₃); FT-IR (thin film) 2931 (C-H), 1742 (C=O), 1711, 1507 (C=C aromatic), 1229/1208/1157 (C(O)C), 1036 (C-N), 835 (C-H bend) cm⁻¹; MS (MALDI) 477.5 [M+K]⁺; HRMS (HNESP) Exact mass calculated for [C₂₁H₂₃D₂⁷⁹Br¹⁵N₁O₄]⁺ requires 437.1057, found 437.1052 [M+H]⁺.

***tert*-butyl *cis*-1-¹⁵N-3-²H-1-(2,4-dimethoxyphenyl)-3-(4-fluorophenyl)aziridine-2-carboxylate *cis*-(5.37)**

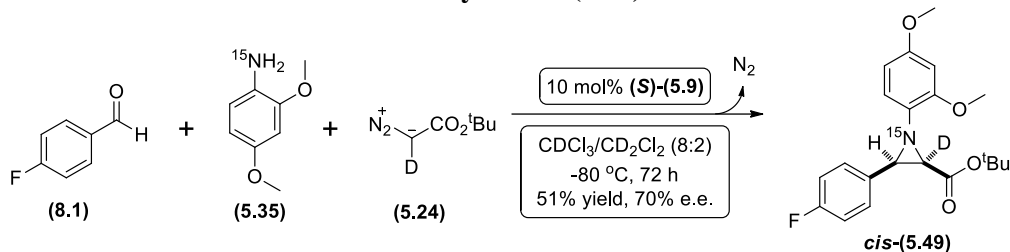


α -²H-4-Fluorobenzaldehyde (**5.13**) (20.0 mg, 0.16 mmol) and ¹⁵N-2,4-dimethoxyaniline (**5.35**) (22.2 mg, 0.14 mmol) were added to a flame dried Biotage 5 mL microwave vial, containing activated 4Å molecular sieves (~ 100 mg) under nitrogen. Deuterated chloroform/deuterated dichloromethane (8:2) mixture (1 mL) was added, the vial was sealed with a PTFE crimp cap and the reaction mixture was left stirring at 25 °C for 2 hours. Catalyst (S)-(5.9) (13.0 mg, 0.02 mmol, 10 mol%) was added and the vial was cooled to -80 °C. After 30 minutes, *tert*-butyl diazoacetate (**5.4**) (24 μ L, 0.18 mmol) was added *via* syringe, and the reaction mixture was stirred at -80 °C (~ 72 hours). At this point the reaction mixture was quenched with triethylamine (0.5 mL), passed through a short plug of silica, eluted with diethyl ether and the solvent was removed under reduced pressure. The crude material was purified by flash chromatography on silica gel (5% diethyl ether in 40-60 PET, R_f = 0.26) to afford a yellow solid. Subsequent physicochemical analysis confirmed this to be the title compound *cis*-(5.37) (29.0 mg, 0.08 mmol, 48% yield). A sample was submitted to chiral analytical HPLC analysis [Cellulose 1, *iso*-hexane / *iso*-propanol : 90 / 10, 1 mL / min, 7.7 min (1st peak), 8.9 min (2nd peak), 60% e.e.].

¹H NMR (500 MHz, CDCl₃) δ 7.56 – 7.48 (m, 2H, ArH), 7.05 – 6.98 (m, 2H, ArH), 6.82 (dd, J 8.5, 1.6 Hz, 1H, ArH), 6.46 (d, J 2.4 Hz, 1H, ArH), 6.37 (dd, J 8.5, 2.4 Hz, 1H, ArH), 3.78 (s, 3H, OCH₃), 3.77 (s, 3H, OCH₃), 2.91 (s, 1H, C₂-H), 1.23 (s, 9H, C(CH₃)₃); ¹³C NMR (126 MHz, CDCl₃) δ 167.4 (d, J_{C-N} 4.6 Hz), 162.4 (d, J_{C-F} 245.2 Hz), 156.7, 153.1 (d, J_{C-N} 2.6 Hz), 134.9 (d, J_{C-N} 3.0 Hz), 131.2 (dd, J_{C-N} 3.9, J_{C-F} 3.2 Hz), 129.8 (dd, J_{C-F} 8.1, J_{C-N} 1.7 Hz), 119.8 (d, J_{C-N} 1.8 Hz), 114.7 (d, J_{C-F} 21.5 Hz), 103.7, 99.8, 81.5, 55.8, 55.7, 47.0 (m), 46.7 (d, J_{C-N} 7.0 Hz), 28.0; ²H NMR (77 MHz, CH₂Cl₂) 7.26 (CDCl₃ ref), 5.27 (CD₂Cl₂ ref), 3.30 (br s); ¹⁵N NMR (51 MHz, CDCl₃) δ 55.60; ¹⁹F NMR (471 MHz, CDCl₃) δ -115.24; M.p. 73 - 75 °C (from diethyl ether / *n*-pentane); $[\alpha]_D^{25}$ -11.7 (c 0.5 CHCl₃); FT-IR (thin film) 2964 (C-H), 1743 (C=O), 1508/1465 (C=C aromatic), 1209/1158 (C(O)C), 1036 (C-N) cm⁻¹; MS (MALDI) 414.0

[M+K]⁺; HRMS (HASP) Exact mass calculated for [C₂₁H₂₄D₁F₁¹⁵N₁O₄]⁺ requires 376.1795, found 376.1793 [M+H]⁺.

tert-butyl *cis*-1-¹⁵N-2-²H-1-(2,4-dimethoxyphenyl)-3-(4-fluorophenyl)aziridine-2-carboxylate *cis*-(5.49)

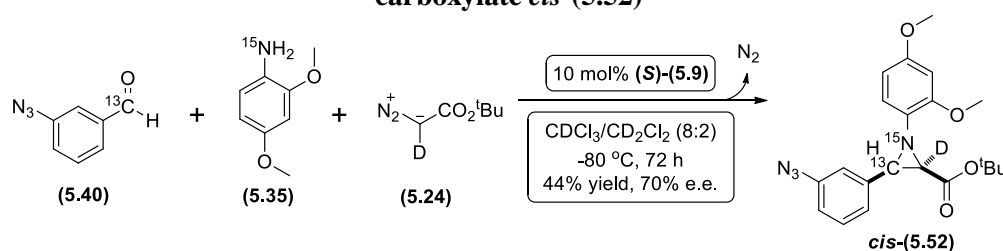


4-Fluorobenzaldehyde (**8.1**) (25.0 mg, 0.20 mmol) and ¹⁵N-2,4-dimethoxyaniline (**5.35**) (28.0 mg, 0.18 mmol) were added to a flame dried Biotage 5 mL microwave vial, containing activated 4Å molecular sieves (~ 100 mg) under nitrogen. Deuterated chloroform/deuterated dichloromethane (8:2) mixture (1 mL) was added, the vial was sealed with a PTFE crimp cap and the reaction mixture was left stirring at 25 °C for 2 hours. Catalyst (**S**)-(**5.9**) (17.0 mg, 0.02 mmol, 10 mol%) was added and the vial was cooled to -80 °C. After 30 minutes, > 95% deuterated *tert*-butyl diazoacetate (**5.24**) (31 μL, 0.22 mmol) was added *via* syringe, and the reaction mixture was stirred at -80 °C (~ 72 hours). At this point the reaction mixture was quenched with triethylamine (0.5 mL), passed through a short plug of silica, eluted with diethyl ether and the solvent was removed under reduced pressure. The crude material was purified by flash chromatography on silica gel (5% diethyl ether in 40-60 PET, R_f = 0.26) to afford a yellow solid. Subsequent physicochemical analysis confirmed this to be the title compound *cis*-(**5.49**) (39.0 mg, 0.10 mmol, 51% yield). A sample was submitted to chiral analytical HPLC analysis [Cellulose 1, *iso*-hexane / *iso*-propanol : 90 / 10, 1 mL / min, 7.8 min (1st peak), 9.0 min (2nd peak), 70% e.e.].

¹H NMR (500 MHz, CDCl₃) δ 7.55 – 7.48 (m, 2H, ArH), 7.05 – 6.98 (m, 2H, ArH), 6.82 (dd, *J* 8.5, 1.6 Hz, 1H, ArH), 6.46 (d, *J* 2.4 Hz, 1H, ArH), 6.37 (dd, *J* 8.5, 2.4 Hz, 1H, ArH), 3.78 (s, 3H, OCH₃), 3.77 (s, 3H, OCH₃), 3.38 (s, 1H, C₃-H), 1.23 (s, 9H, C(CH₃)₃); ¹³C NMR (126 MHz, CDCl₃) δ 167.4 (d, *J*_{C-N} 4.6 Hz), 162.4 (d, *J*_{C-F} 245.2 Hz), 156.7, 153.1 (d, *J*_{C-N} 2.6 Hz), 134.9 (d, *J*_{C-N} 3.1 Hz), 131.3 (dd, *J*_{C-N} 3.9, *J*_{C-F} 3.1 Hz), 129.8 (dd, *J*_{C-F} 8.1, *J*_{C-N} 1.8 Hz), 119.8 (d, *J*_{C-N} 1.8 Hz), 114.7 (d, *J*_{C-F} 21.5 Hz), 103.7, 99.8, 81.5, 55.8, 55.7, 47.0 (d, *J*_{C-N} 7.4 Hz), 46.7 (m), 28.0; ²H NMR (77 MHz, CH₂Cl₂) 7.26 (CDCl₃ ref), 5.27 (CD₂Cl₂ ref), 2.85 (br s); ¹⁵N NMR (51 MHz, CDCl₃) δ

55.62; ^{19}F NMR (471 MHz, CDCl_3) δ -115.29; M.p. 73 - 75 °C (from diethyl ether / *n*-pentane); $[\alpha]_{\text{D}}^{26}$ -21.3 (c 1.0 CHCl_3); FT-IR (thin film) 2977 (C-H), 1743 (C=O), 1506/1455 (C=C aromatic), 1209/1156 (C(O)C), 1091 (C-N), 839 (C-H bend) cm^{-1} ; MS (MALDI) 376.5 $[\text{M}+\text{H}]^+$; HRMS (HASP) Exact mass calculated for $[\text{C}_{21}\text{H}_{24}\text{D}_1\text{F}_1^{15}\text{N}_1\text{O}_4]^+$ requires 376.1795, found 376.1790 $[\text{M}+\text{H}]^+$.

***tert*-butyl *cis*-1- ^{15}N -2- ^2H -3- ^{13}C -3-(3-azidophenyl)-1-(2,4-dimethoxyphenyl)aziridine-2-carboxylate *cis*-(5.52)**

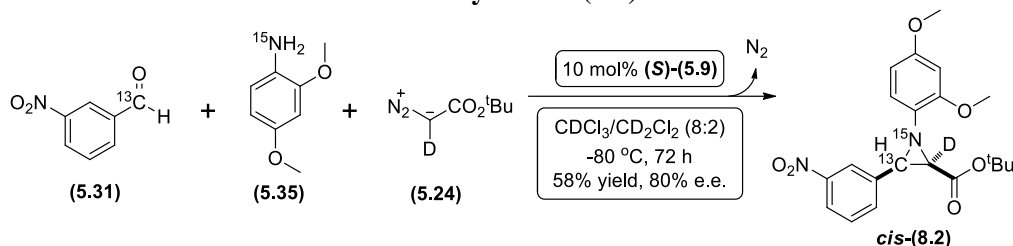


α - ^{13}C -3-Azidobenzaldehyde (5.40) (25.0 mg, 0.17 mmol) and ^{15}N -2,4-dimethoxyaniline (5.35) (23.4 mg, 0.15 mmol) were added to a flame dried Biotage 5 mL microwave vial, containing activated 4Å molecular sieves (~ 100 mg) under nitrogen. Deuterated chloroform/deuterated dichloromethane (8:2) mixture (1 mL) was added, the vial was sealed with a PTFE crimp cap and the reaction mixture was left stirring at 25 °C for 2 hours. Catalyst (S)-(5.9) (14.0 mg, 0.02 mmol, 10 mol%) was added and the vial was cooled to $-80\text{ }^\circ\text{C}$. After 30 minutes, > 95% deuterated *tert*-butyl diazoacetate (5.24) (27 μL , 0.19 mmol) was added *via* syringe, and the reaction mixture was stirred at $-80\text{ }^\circ\text{C}$ (~ 72 hours). At this point the reaction mixture was quenched with triethylamine (0.5 mL), passed through a short plug of silica, eluted with diethyl ether and the solvent was removed under reduced pressure. The crude material was purified by flash chromatography on silica gel (10% diethyl ether in 40-60 PET, $R_f = 0.21$) to afford an orange solid. Subsequent physicochemical analysis confirmed this to be the title compound *cis*-(5.52) (29.5 mg, 0.07 mmol, 44% yield). A sample was submitted to chiral analytical HPLC analysis [Cellulose 1, *iso*-hexane / *iso*-propanol : 90 / 10, 1 mL / min, 12.6 min (1st peak), 16.9 min (2nd peak), 70% *e.e.*].

^1H NMR (500 MHz, CDCl_3) δ 7.32 – 7.27 (m, 3H, ArH), 6.96 – 6.91 (m, 1H, ArH), 6.83 (dd, J 8.5, 1.6 Hz, 1H, ArH), 6.46 (d, J 2.5 Hz, 1H, ArH), 6.38 (dd, J 8.5, 2.5 Hz, 1H, ArH), 3.79 (s, 3H, OCH_3), 3.77 (s, 3H, OCH_3), 3.38 (d, $J_{^{13}\text{C}-\text{H}}$ 168.2 Hz, 1H, C3-H), 1.24 (s, 9H, $\text{C}(\text{CH}_3)_3$); ^{13}C NMR (126 MHz, CDCl_3) δ 167.3 (d, $J_{\text{C}-\text{N}}$ 2.8 Hz), 156.7, 153.1, 139.8 (d, $J_{\text{C}-^{13}\text{C}}$ 5.3 Hz), 137.8 (dd, $J_{\text{C}-^{13}\text{C}}$ 60.5, $J_{\text{C}-\text{N}}$ 3.7 Hz), 134.8, 129.3 (d, $J_{\text{C}-^{13}\text{C}}$ 4.9 Hz), 124.8, 119.9, 118.9, 118.2, 103.7, 99.8, 81.6, 55.8, 55.7, 47.3 (d, $J_{\text{C}-\text{N}}$ 7.3 Hz),

46.5 (m), 27.9; ^2H NMR (77 MHz, CH_2Cl_2) 5.26 (CD_2Cl_2 ref), 2.87 (br s); ^{15}N NMR (51 MHz, CDCl_3) δ 55.52 (d, $J_{\text{C-N}}$ 7.5 Hz); M.p. 91 - 93 °C (from diethyl ether / *n*-pentane); $[\alpha]_{\text{D}}^{25}$ -52.7 (c 2.0 CHCl_3); FT-IR (thin film) 2977 (C-H), 2115 (N_3), 1749 (C=O), 1590/1505 (C=C aromatic), 1208/1157 (C(O)C), 1035 (C-N) cm^{-1} ; MS (MALDI) 344.2 $[\text{M}+\text{H}]^+$; HRMS (HNESF) Exact mass calculated for $[\text{C}^{13}\text{C}_1\text{C}_{20}\text{H}_{24}\text{D}_1\text{N}_3\text{O}_4]^+$ requires 400.1937, found 400.1937 $[\text{M}+\text{H}]^+$.

***tert*-butyl *cis*-1- ^{15}N -2- ^2H -3- ^{13}C -1-(2,4-dimethoxyphenyl)-3-(3-nitrophenyl)aziridine-2-carboxylate *cis*-(7.2)**

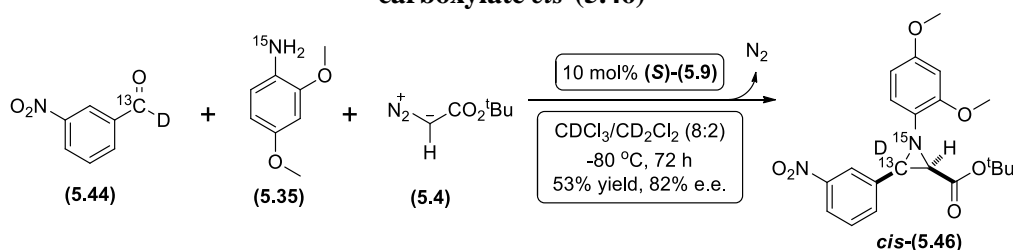


α - ^{13}C -3-Nitrobenzaldehyde (5.31) (15.0 mg, 0.10 mmol) and ^{15}N -2,4-dimethoxyaniline (5.35) (13.7 mg, 0.09 mmol) were added to a flame dried Biotage 5 mL microwave vial, containing activated 4Å molecular sieves (~ 100 mg) under nitrogen. Deuterated chloroform/deuterated dichloromethane (8:2) mixture (1 mL) was added, the vial was sealed with a PTFE crimp cap and the reaction mixture was left stirring at 25 °C for 2 hours. An aliquot was submitted to ^1H -NMR analysis, which confirmed the formation of the imine intermediate. Catalyst (S)-(5.9) (8.2 mg, 0.01 mmol, 10 mol%) was added and the vial was cooled to $-80\text{ }^\circ\text{C}$. After 30 minutes, > 95% deuterated *tert*-butyl diazoacetate (5.24) (15 μL , 0.11 mmol) was added *via* syringe, and the reaction mixture was stirred at $-80\text{ }^\circ\text{C}$, monitoring by ^1H -NMR until the reaction was deemed complete (~ 72 hours). At this point the reaction mixture was quenched with triethylamine (0.5 mL), passed through a short plug of silica, eluted with diethyl ether and the solvent was removed under reduced pressure. The crude material was purified by flash chromatography on silica gel (5% diethyl ether in 40-60 PET, $R_f = 0.15$) to afford a yellow oil. Subsequent physicochemical analysis confirmed this to be the title compound *cis*-(8.2) (23.4 mg, 0.06 mmol, 58% yield). A sample was submitted to chiral analytical HPLC analysis [Cellulose 1, *iso*-hexane / *iso*-propanol : 90 / 10, 1 mL / min, 12.1 min (1st peak), 15.0 min (2nd peak), 80% e.e.].

^1H NMR (500 MHz, CDCl_3) δ 8.47 – 8.42 (m, 1H, ArH), 8.15 (ddd, J 8.0, 2.4, 0.9 Hz, 1H, ArH), 7.95 – 7.89 (m, 1H, ArH), 7.51 (t, J 8.0 Hz, 1H, ArH), 6.84 (dd, J 8.5, 1.9 Hz, 1H, ArH), 6.47 (d, J 1.9 Hz, 1H, ArH), 6.39 (dd, J 8.5, 2.4 Hz, 1H, ArH), 3.79 (s, 3H, OCH_3), 3.78 (s, 3H, OCH_3), 3.45 (d, $J_{^{13}\text{C-H}}$ 169.3 Hz, 1H, C3-H), 1.22 (s, 9H,

$C(CH_3)_3$; ^{13}C NMR (126 MHz, $CDCl_3$) δ 166.9, 156.9, 153.1, 148.1, 137.7, 134.5, 134.2, 128.8, 123.5, 122.6, 119.8, 103.7, 99.8, 82.0, 55.8, 55.7, 46.7 (broad), 27.9; 2H NMR (77 MHz, CH_2Cl_2) 7.26 (CD_3Cl ref), 5.27 (CD_2Cl_2 ref), 2.99 (br s); ^{15}N NMR (51 MHz, $CDCl_3$) δ 56.00 (d, J_{C-N} 7.5 Hz); $[\alpha]_D^{24}$ -12.1 (c 0.5 $CHCl_3$); FT-IR (thin film) 2982 (C-H), 1746 (C=O), 1530/1505 (C=C aromatic), 1349 (NO_2), 1208/1156 (C(O)C), 1038 (C-N), 820 (C-H bend) cm^{-1} ; MS (MALDI) 404.0 $[M+H]^+$; HRMS (HNESP) Exact mass calculated for $[^{13}C_1C_{20}H_{24}D_1^{15}N_1N_1O_6]^+$ requires 404.1774, found 404.1777 $[M+H]^+$.

***tert*-butyl *cis*-1- ^{15}N -3- ^{13}C , 2H -1-(2,4-dimethoxyphenyl)-3-(3-nitrophenyl)aziridine-2-carboxylate *cis*-(5.46)**

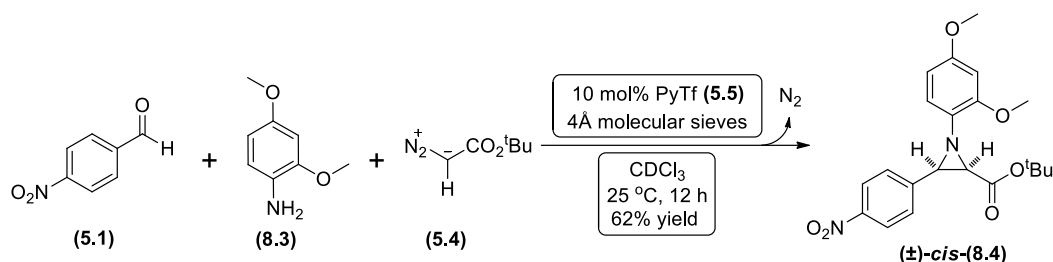


α - 2H , ^{13}C -3-Nitrobenzaldehyde (**5.44**) (15.0 mg, 0.10 mmol) and ^{15}N -2,4-dimethoxyaniline (**5.35**) (13.6 mg, 0.09 mmol) were added to a flame dried Biotage 5 mL microwave vial, containing activated 4Å molecular sieves (~ 100 mg) under nitrogen. Deuterated chloroform/deuterated dichloromethane (8:2) mixture (1 mL) was added, the vial was sealed with a PTFE crimp cap and the reaction mixture was left stirring at 25 °C for 2 hours. An aliquot was submitted to 1H -NMR analysis, which confirmed the formation of the imine intermediate. Catalyst (*S*)-(5.9) (8.0 mg, 0.01 mmol, 10 mol%) was added and the vial was cooled to -80 °C. After 30 minutes, *tert*-butyl diazoacetate (**5.4**) (16 μ L, 0.11 mmol) was added *via* syringe, and the reaction mixture was stirred at -80 °C, monitoring by 1H -NMR until the reaction was deemed complete (~ 72 hours). At this point the reaction mixture was quenched with triethylamine (0.5 mL), passed through a short plug of silica, eluted with diethyl ether and the solvent was removed under reduced pressure. The crude material was purified by flash chromatography on silica gel (5% diethyl ether in 40-60 PET, R_f = 0.15) to afford a yellow oil. Subsequent physicochemical analysis confirmed this to be the title compound *cis*-(5.46) (21.2 mg, 0.05 mmol, 53% yield). A sample was submitted to chiral analytical HPLC analysis [Cellulose 1, *iso*-hexane / *iso*-propanol : 90 / 10, 1 mL / min, 12.1 min (1st peak), 15.1 min (2nd peak), 82% e.e.].

^1H NMR (500 MHz, CDCl_3) δ 8.56 – 8.39 (m, 1H, ArH), 8.15 (d, J 8.1 Hz, 1H, ArH), 7.95 – 7.86 (m, 1H, ArH), 7.51 (t, J 7.9 Hz, 1H, ArH), 6.84 (dd, J 8.5, 1.4 Hz, 1H, ArH), 6.47 (d, J 2.3 Hz, 1H, ArH), 6.39 (dd, J 8.5, 2.5 Hz, 1H, ArH), 3.79 (s, 3H, OCH_3), 3.78 (s, 3H, OCH_3), 3.02 (d, $J_{13\text{C-H}}$ 2.1 Hz, 1H, C2-H), 1.22 (s, 9H, $\text{C}(\text{CH}_3)_3$); ^{13}C NMR (126 MHz, CDCl_3) δ 166.9, 156.9, 153.1, 148.1, 137.7, 134.5, 134.2, 128.8, 123.5, 122.6, 119.8, 103.7, 99.8, 82.0, 55.8, 55.7, 46.4 (t, $J_{\text{C-D}}$ 25.4 Hz), 27.9; ^2H NMR (77 MHz, CH_2Cl_2) 7.26 (CD_3Cl ref), 5.27 (CD_2Cl_2 ref), 3.48 (br d, $J_{\text{C-D}}$ 26.0 Hz); ^{15}N NMR (51 MHz, CDCl_3) δ 56.04 (d, $J_{\text{C-N}}$ 8.0 Hz); $[\alpha]_{\text{D}}^{24}$ -9.2 (c 0.4 CHCl_3); FT-IR (thin film) 2938 (C-H), 1740 (C=O), 1530/1507 (C=C aromatic), 1349 (NO_2), 1208/1157 (C(O)C), 1035 (C-N), 815 (C-H bend) cm^{-1} ; MS (MALDI) 404.0 $[\text{M}+\text{H}]^+$; HRMS (HNESP) Exact mass calculated for $^{13}\text{C}_1\text{C}_{20}\text{H}_{24}\text{D}_1^{15}\text{N}_1\text{N}_1\text{O}_6]^+$ requires 404.1774, found 404.1781 $[\text{M}+\text{H}]^+$.

8.5. Synthesis of racemic non-labelled aziridines

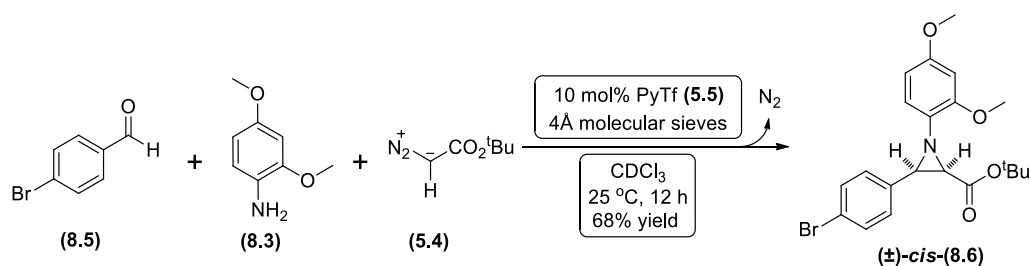
tert-butyl *cis*-1-(2,4-dimethoxyphenyl)-3-(4-nitrophenyl)aziridine-2-carboxylate (±)-*cis*-(8.4)



4-Nitrobenzaldehyde (**5.1**) (200.0 mg, 1.32 mmol), and 2,4-dimethoxyaniline (**8.3**) (193.0 mg, 1.26 mmol) were added to a flame dried Biotage 5 mL microwave vial, containing activated 4 Å molecular sieves (~ 100 mg) under nitrogen. Deuterated chloroform (2 mL) was added, the vial was sealed with a PTFE crimp cap and the reaction mixture was left stirring at 25 °C for 2 hours. An aliquot was submitted to ¹H-NMR analysis, which confirmed the formation of the imine intermediate. Pyridinium triflate (**5.5**) (30.3 mg, 0.13 mmol, 10 mol%) was added. After 5 minutes, *tert*-butyl diazoacetate (**5.4**) (183 μL, 1.32 mmol) was added *via* syringe, and the reaction mixture was stirred at 25 °C, monitoring by ¹H-NMR until the reaction was deemed complete (~ 12 hours). At this point the reaction mixture was passed through a short plug of silica, eluted with diethyl ether and the solvent was removed under reduced pressure. The crude material was purified by flash chromatography on silica gel (15% ethyl acetate in 40-60 PET, R_f = 0.35) to afford an orange solid. Subsequent physicochemical analysis confirmed this to be the title compound (±)-*cis*-(**8.4**) (327.4 mg, 0.82 mmol, 62% yield).

¹H NMR (500 MHz, CDCl₃) δ 8.20 (d, *J* 8.6 Hz, 2H, ArH), 7.73 (d, *J* 8.6 Hz, 2H, ArH), 6.83 (d, *J* 8.6 Hz, 1H, ArH), 6.47 (d, *J* 2.6 Hz, 1H, ArH), 6.39 (dd, *J* 8.6, 2.6 Hz, 1H, ArH), 3.78 (s, 3H, OCH₃), 3.77 (s, 3H, OCH₃), 3.44 (d, *J* 6.7 Hz, 1H, C3-H), 3.04 (d, *J* 6.7 Hz, 1H, C2-H), 1.22 (s, 9H, C(CH₃)₃); ¹³C NMR (126 MHz, CDCl₃) δ 166.7, 156.9, 153.1, 147.4, 143.2, 134.1, 129.2, 123.1, 119.8, 103.6, 99.7, 82.0, 55.8, 55.7, 47.02, 46.98, 28.0; M.p. 98 - 100 °C (from diethyl ether / *n*-pentane); FT-IR (KBr (neat), cm⁻¹) 2966.4 (C-H), 1735.2 (C=O), 1591.8/1505.0 (C=C aromatic), 1341.7 (NO₂), 1267.0/1206.1/1132.3 (C(O)C), 1032.7 (C-N), 819.4/743.7 (C-H bend); HRMS (HASP) exact mass calculated for [C₂₁H₂₅N₂O₆] requires *m/z*. 401.1707, found *m/z*. 401.1702 [M+H]⁺.

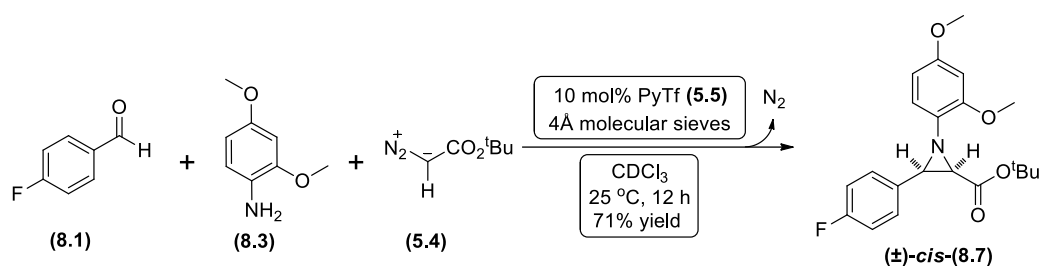
***tert*-butyl *cis*-3-(4-bromophenyl)-1-(2,4-dimethoxyphenyl)aziridine-2-carboxylate
(±)-*cis*-(**8.6**)**



4-Bromobenzaldehyde (**8.5**) (150.0 mg, 0.81 mmol), and 2,4-dimethoxyaniline (**8.3**) (118.0 mg, 0.77 mmol) were added to a flame dried Biotage 5 mL microwave vial, containing activated 4Å molecular sieves (~ 100 mg) under nitrogen. Deuterated chloroform (2 mL) was added, the vial was sealed with a PTFE crimp cap and the reaction mixture was left stirring at 25 °C for 2 hours. An aliquot was submitted to ¹H-NMR analysis, which confirmed the formation of the imine intermediate. Pyridinium triflate (**5.5**) (18.6 mg, 0.08 mmol, 10 mol%) was added. After 5 minutes, *tert*-butyl diazoacetate (**5.4**) (112 μL, 0.81 mmol) was added *via* syringe, and the reaction mixture was stirred at 25 °C, monitoring by ¹H-NMR until the reaction was deemed complete (~ 12 hours). At this point the reaction mixture was passed through a short plug of silica, eluted with diethyl ether and the solvent was removed under reduced pressure. The crude material was purified by flash chromatography on silica gel (20% ethyl acetate in 40-60 PET, R_f = 0.31) to afford a white solid. Subsequent physicochemical analysis confirmed this to be the title compound (±)-*cis*-(**8.6**) (239.3 mg, 0.55 mmol, 68% yield).

¹H NMR (500 MHz, CDCl₃) δ 7.48 – 7.41 (m, 4H, ArH), 6.82 (d, *J* 8.5 Hz, 1H, ArH), 6.45 (d, *J* 2.6 Hz, 1H, ArH), 6.37 (dd, *J* 8.5, 2.6 Hz, 1H, ArH), 3.77 (s, 3H, OCH₃), 3.77 (s, 3H, OCH₃), 3.35 (d, *J* 6.7 Hz, 1H, C3-H), 2.93 (d, *J* 6.7 Hz, 1H, C2-H), 1.23 (s, 9H, C(CH₃)₃); ¹³C NMR (126 MHz, CDCl₃) δ 167.2, 156.7, 153.1, 134.7, 134.6, 131.0, 129.9, 121.4, 119.8, 103.6, 99.7, 81.7, 55.8, 55.7, 47.2, 46.8, 28.0; M.p. 122 - 124 °C (from diethyl ether / *n*-pentane); FT-IR (KBr (neat), cm⁻¹) 2977.3 (C-H), 1739.2 (C=O), 1591.8/1505.4 (C=C aromatic), 1266.9/1205.6/1132.6(C(O)C), 1032.5 (C-N), 820.8/748.2 (C-H bend); HRMS (HNESP) exact mass calculated for [C₂₁H₂₅⁷⁹BrNO₄] requires *m/z* 434.0961, found *m/z* 434.0959 [M+H]⁺.

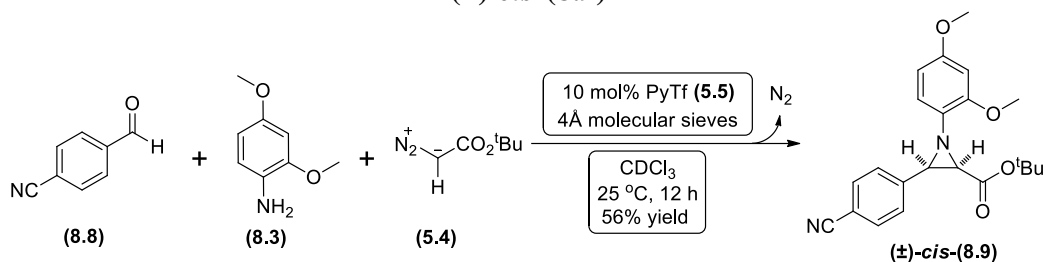
***tert*-butyl *cis*-1-(2,4-dimethoxyphenyl)-3-(4-fluorophenyl)aziridine-2-carboxylate
(±)-*cis*-(8.7)**



4-Fluorobenzaldehyde (**8.1**) (100.0 mg, 0.80 mmol), and 2,4-dimethoxyaniline (**8.3**) (117.0 mg, 0.76 mmol) were added to a flame dried Biotage 5 mL microwave vial, containing activated 4Å molecular sieves (~ 100 mg) under nitrogen. Deuterated chloroform (2 mL) was added, the vial was sealed with a PTFE crimp cap and the reaction mixture was left stirring at 25 °C for 2 hours. An aliquot was submitted to ¹H-NMR analysis, which confirmed the formation of the imine intermediate. Pyridinium triflate (**5.5**) (18.5 mg, 0.08 mmol, 10 mol%) was added. After 5 minutes, *tert*-butyl diazoacetate (**5.4**) (111 μL, 0.80 mmol) was added *via* syringe, and the reaction mixture was stirred at 25 °C, monitoring by ¹H-NMR until the reaction was deemed complete (~ 12 hours). At this point the reaction mixture was passed through a short plug of silica, eluted with diethyl ether and the solvent was removed under reduced pressure. The crude material was purified by flash chromatography on silica gel (20% ethyl acetate in 40-60 PET, R_f = 0.39) to afford a white solid. Subsequent physicochemical analysis confirmed this to be the title compound (±)-*cis*-(**8.7**) (213.8 mg, 0.57 mmol, 71% yield).

¹H NMR (500 MHz, CDCl₃) δ 7.52 (dd, *J* 8.5, 5.6 Hz, 2H, ArH), 7.01 (t, *J* 8.5 Hz, 2H, ArH), 6.83 (d, *J* 8.5 Hz, 1H, ArH), 6.45 (d, *J* 2.5 Hz, 1H, ArH), 6.37 (dd, *J* 8.5, 2.5 Hz, 1H, ArH), 3.78 (s, 3H, OCH₃), 3.77 (s, 3H, OCH₃), 3.38 (d, *J* 6.7 Hz, 1H, C3-H), 2.91 (d, *J* 6.7 Hz, 1H, C2-H), 1.22 (s, 9H, C(CH₃)₃); ¹³C NMR (126 MHz, CDCl₃) δ 167.4, 162.4 (d, *J*_{C-F} 245.2 Hz), 156.7, 153.1, 134.9, 131.2 (d, *J*_{C-F} 3.0 Hz), 129.8 (d, *J*_{C-F} 8.1 Hz), 119.8, 114.7 (d, *J*_{C-F} 21.5 Hz), 103.6, 99.7, 81.5, 55.8, 55.7, 47.1, 46.8, 27.9; ¹⁹F NMR (471 MHz, CDCl₃) δ -115.25; M.p. 71 - 73 °C (from diethyl ether / *n*-pentane); FT-IR (KBr (neat), cm⁻¹) 2971.9 (C-H), 1741.0 (C=O), 1592.4/1504.8 (C=C aromatic), 1205.4/1133.6(C(O)C), 1032.3 (C-N), 821.9 (C-H bend); HRMS (HASP) exact mass calculated for [C₂₁H₂₅FNO₄] requires *m/z* 374.1762, found *m/z* 374.1758 [M+H]⁺.

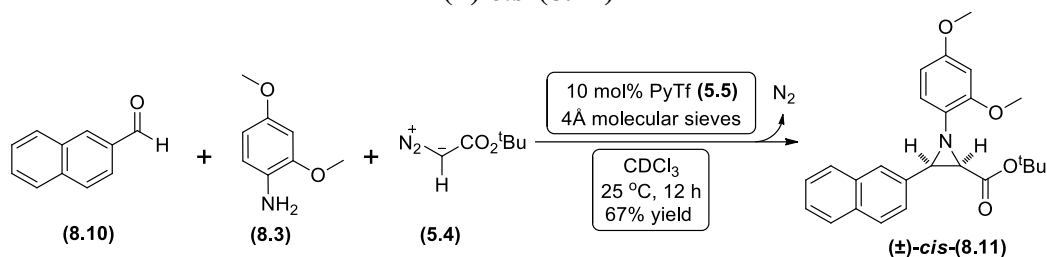
***tert*-butyl *cis*-3-(4-cyanophenyl)-1-(2,4-dimethoxyphenyl)aziridine-2-carboxylate
(±)-*cis*-(8.9)**



4-Cyanobenzaldehyde (**8.8**) (40.0 mg, 0.30 mmol), and 2,4-dimethoxyaniline (**8.3**) (44.5 mg, 0.29 mmol) were added to a flame dried Biotage 5 mL microwave vial, containing activated 4 Å molecular sieves (~ 100 mg) under nitrogen. Deuterated chloroform (2 mL) was added, the vial was sealed with a PTFE crimp cap and the reaction mixture was left stirring at 25 °C for 2 hours. An aliquot was submitted to $^1\text{H-NMR}$ analysis, which confirmed the formation of the imine intermediate. Pyridinium triflate (**5.5**) (7.0 mg, 0.03 mmol, 10 mol%) was added. After 5 minutes, *tert*-butyl diazoacetate (**5.4**) (42 μL , 0.30 mmol) was added *via* syringe, and the reaction mixture was stirred at 25 °C, monitoring by $^1\text{H-NMR}$ until the reaction was deemed complete (~ 12 hours). At this point the reaction mixture was passed through a short plug of silica, eluted with diethyl ether and the solvent was removed under reduced pressure. The crude material was purified by flash chromatography on silica gel (30% diethyl ether in 40-60 PET, R_f = 0.30) to afford a yellow solid. Subsequent physicochemical analysis confirmed this to be the title compound (**(±)-*cis*-(8.9)**) (65.2 mg, 0.17 mmol, 56% yield).

$^1\text{H NMR}$ (500 MHz, CDCl_3) δ 7.67 (d, 8.3 Hz, 2H, ArH), 7.63 (d, 8.3 Hz, 2H, ArH), 6.82 (d, J 8.5 Hz, 1H, ArH), 6.46 (d, J 2.5 Hz, 1H, ArH), 6.38 (dd, J 8.5, 2.5 Hz, 1H, ArH), 3.77 (s, 3H, OCH_3), 3.76 (s, 3H, OCH_3), 3.41 (d, J 6.7 Hz, 1H, C3-H), 3.01 (d, J 6.7 Hz, 1H, C2-H), 1.21 (s, 9H, $\text{C}(\text{CH}_3)_3$); $^{13}\text{C NMR}$ (126 MHz, CDCl_3) δ 166.8, 156.9, 153.1, 141.2, 134.2, 131.7, 129.0, 119.8, 119.1, 111.2, 103.6, 99.7, 81.9, 55.8, 55.7, 47.1, 46.9, 27.9; M.p. 91 - 93 °C (from diethyl ether / *n*-pentane); FT-IR (KBr (neat), cm^{-1}) 2978.0 (C-H), 2227.5 ($\text{C}\equiv\text{N}$), 1714.8 (C=O), 1592.5/1507.7 (C=C aromatic), 1279.4/1208.8/1159.8 (C(O)C), 1032.7 (C-N), 848.2/745.9 (C-H bend); HRMS (HNESP) exact mass calculated for $[\text{C}_{22}\text{H}_{24}\text{N}_2\text{O}_4\text{Na}]$ requires m/z 403.1628, found m/z 403.1627 $[\text{M}+\text{Na}]^+$.

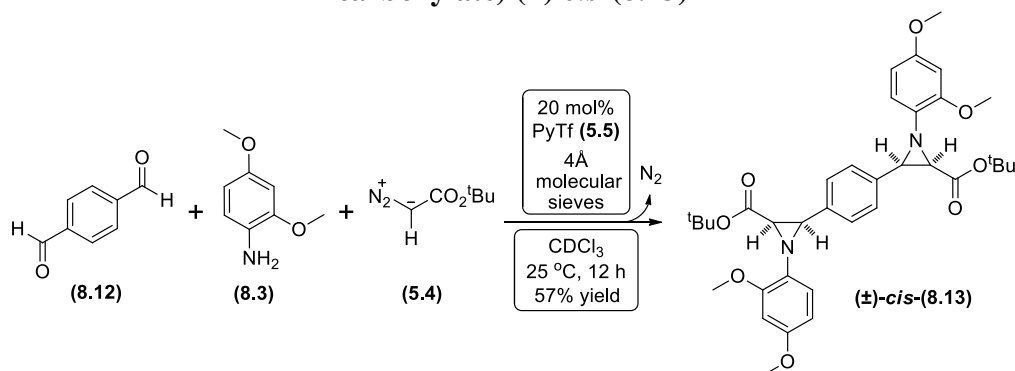
***tert*-butyl *cis*-1-(2,4-dimethoxyphenyl)-3-(naphthalen-2-yl)aziridine-2-carboxylate
(±)-*cis*-(**8.11**)**



2-Naphthalenecarbaldehyde (**8.10**) (50.0 mg, 0.32 mmol), and 2,4-dimethoxyaniline (**8.3**) (46.5 mg, 0.30 mmol) were added to a flame dried Biotage 5 mL microwave vial, containing activated 4 Å molecular sieves (~ 100 mg) under nitrogen. Deuterated chloroform (2 mL) was added, the vial was sealed with a PTFE crimp cap and the reaction mixture was left stirring at 25 °C for 2 hours. An aliquot was submitted to ¹H-NMR analysis, which confirmed the formation of the imine intermediate. Pyridinium triflate (**5.5**) (7.3 mg, 0.03 mmol, 10 mol%) was added. After 5 minutes, *tert*-butyl diazoacetate (**5.4**) (44 μL, 0.32 mmol) was added *via* syringe, and the reaction mixture was stirred at 25 °C, monitoring by ¹H-NMR until the reaction was deemed complete (~ 12 hours). At this point the reaction mixture was passed through a short plug of silica, eluted with diethyl ether and the solvent was removed under reduced pressure. The crude material was purified by flash chromatography on silica gel (20% ethyl acetate in 40-60 PET, R_f = 0.28) to afford a brown solid. Subsequent physicochemical analysis confirmed this to be the title compound (±)-*cis*-(**8.11**) (87.4 mg, 0.21 mmol, 67% yield).

¹H NMR (500 MHz, CDCl₃) δ 8.06 (s, 1H, ArH), 7.87 – 7.79 (m, 3H, ArH), 7.66 (dd, *J* 8.5, 1.3 Hz, 1H, ArH), 7.49 – 7.42 (m, 2H, ArH), 6.90 (d, *J* 8.5 Hz, 1H, ArH), 6.49 (d, *J* 2.5 Hz, 1H, ArH), 6.40 (dd, *J* 8.5, 2.5 Hz, 1H, ArH), 3.80 (s, 3H, OCH₃), 3.78 (s, 3H, OCH₃), 3.60 (d, *J* 6.8 Hz, 1H, C3-H), 3.01 (d, *J* 6.8 Hz, 1H, C2-H), 1.13 (s, 9H, C(CH₃)₃); ¹³C NMR (126 MHz, CDCl₃) δ 167.5, 156.6, 153.2, 135.1, 133.2, 133.03, 133.01, 128.0, 127.7, 127.4, 127.1, 126.1, 126.0, 125.7, 119.9, 103.6, 99.7, 81.4, 55.7, 55.6, 48.0, 47.2, 27.8; M.p. 85 - 87 °C (from diethyl ether / *n*-pentane); FT-IR (KBr (neat), cm⁻¹) 2976.3 (C-H), 1713.1 (C=O), 1592.0/1507.3 (C=C aromatic), 1278.9/1208.3/1158.4(C(O)C), 1034.0 (C-N), 824.8/750.0 (C-H bend); HRMS (HNESP) exact mass calculated for [C₂₅H₂₈NO₄] requires *m/z* 406.2013, found *m/z* 406.2009 [M+H]⁺.

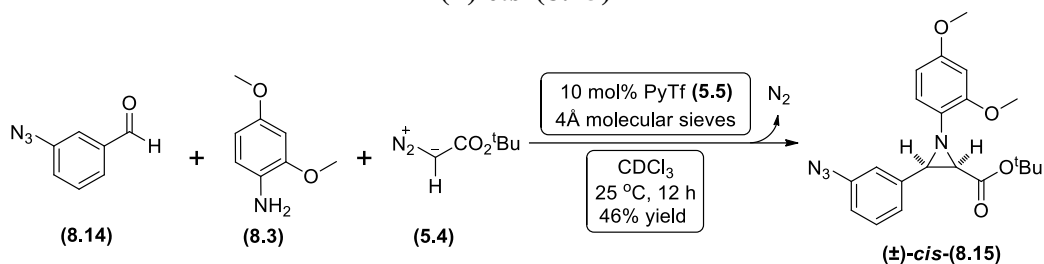
di-*tert*-butyl *cis*-3,3'-(1,4-phenylene)bis(1-(2,4-dimethoxyphenyl)aziridine-2-carboxylate) (±)-*cis*-(8.13)



1,4-Terephthalaldehyde (**8.12**) (80.0 mg, 0.60 mmol), and 2,4-dimethoxyaniline (**8.3**) (174.0 mg, 1.13 mmol) were added to a flame dried Biotage 5 mL microwave vial, containing activated 4Å molecular sieves (~ 200 mg) under nitrogen. Deuterated chloroform (4 mL) was added, the vial was sealed with a PTFE crimp cap and the reaction mixture was left stirring at 25 °C for 3 hours. An aliquot was submitted to ¹H-NMR analysis, which confirmed the formation of the imine intermediate. Pyridinium triflate (**5.5**) (27.3 mg, 0.11 mmol, 20 mol%) was added. After 5 minutes, *tert*-butyl diazoacetate (**5.4**) (165 μL, 1.20 mmol) was added *via* syringe, and the reaction mixture was stirred at 25 °C, monitoring by ¹H-NMR until the reaction was deemed complete (~ 12 hours). At this point the reaction mixture was passed through a short plug of silica, eluted with diethyl ether and the solvent was removed under reduced pressure. The crude material was purified by flash chromatography on silica gel (30% diethyl ether in 40-60 PET, R_f = 0.24) to afford a brown solid. Subsequent physicochemical analysis confirmed this to be the title compound (±)-*cis*-(**8.13**) (218.0 mg, 0.34 mmol, 57% yield).

¹H NMR (500 MHz, CDCl₃) δ 7.50 (d, *J* 1.8 Hz, 4H, ArH), 6.82 (d, *J* 8.5 Hz, 2H, ArH), 6.44 (d, *J* 1.8 Hz, 2H, ArH), 6.37 (dd, *J* 8.5, 2.6 Hz, 2H, ArH), 3.76 (d, *J* 4.5 Hz, 12H, 4xOCH₃), 3.40 (d, *J* 6.8 Hz, 2H, 2xC3-H), 2.91 (dd, *J* 6.8, 4.5 Hz, 2H, 2xC2-H), 1.26 (d, *J* 1.5 Hz, 18H, 2xC(CH₃)₃); ¹³C NMR (126 MHz, CDCl₃) δ 167.5, 167.4, 156.59, 156.58, 153.2, 135.29, 135.28, 134.6, 134.5, 127.62, 127.60, 119.9, 103.59, 103.57, 99.74, 99.70, 81.4, 55.74, 55.69, 47.89, 47.85, 47.1, 46.7, 28.0; M.p. 45 - 47 °C (from diethyl ether / *n*-pentane); FT-IR (KBr (neat), cm⁻¹) 2977.1 (C-H), 1745.9 (C=O), 1592.1/1506.4 (C=C aromatic), 1278.9/1159.2(C(O)C), 1034.1 (C-N), 847.2/736.8 (C-H bend); HRMS (HNESP) exact mass calculated for [C₃₆H₄₅N₂O₈] requires *m/z* 633.3170, found *m/z* 633.3168 [M+H]⁺.

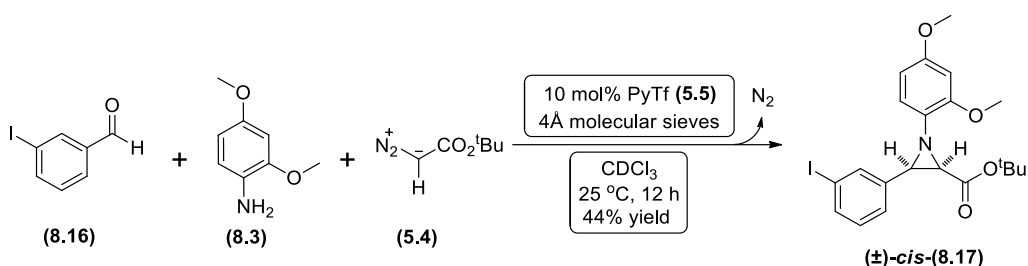
***tert*-butyl *cis*-3-(3-azidophenyl)-1-(2,4-dimethoxyphenyl)aziridine-2-carboxylate
(±)-*cis*-(8.15)**



3-Azidobenzaldehyde (**8.14**) (20.0 mg, 0.13 mmol), and 2,4-dimethoxyaniline (**8.3**) (18.7 mg, 0.12 mmol) were added to a flame dried Biotage 5 mL microwave vial, containing activated 4 Å molecular sieves (~ 100 mg) under nitrogen. Deuterated chloroform (2 mL) was added, the vial was sealed with a PTFE crimp cap and the reaction mixture was left stirring at 25 °C for 2 hours. An aliquot was submitted to ¹H-NMR analysis, which confirmed the formation of the imine intermediate. Pyridinium triflate (**5.5**) (3.1 mg, 0.01 mmol, 10 mol%) was added. After 5 minutes, *tert*-butyl diazoacetate (**5.4**) (19 μL, 0.13 mmol) was added *via* syringe, and the reaction mixture was stirred at 25 °C, monitoring by ¹H-NMR until the reaction was deemed complete (~ 12 hours). At this point the reaction mixture was passed through a short plug of silica, eluted with diethyl ether and the solvent was removed under reduced pressure. The crude material was purified by flash chromatography on silica gel (20% diethyl ether in pentane, R_f = 0.22) to afford a brown solid. Subsequent physicochemical analysis confirmed this to be the title compound (±)-*cis*-(**8.15**) (25.1 mg, 0.06 mmol, 46% yield).

¹H NMR (500 MHz, CDCl₃) δ 7.32 – 7.27 (m, 1H, ArH), 6.96 – 6.91 (m, 1H, ArH), 6.83 (d, *J* 8.5 Hz, 1H, ArH), 6.46 (d, *J* 2.6 Hz, 1H, ArH), 6.38 (dd, *J* 8.5, 2.6 Hz, 1H, ArH), 3.79 (s, 3H, OCH₃), 3.77 (s, 3H, OCH₃), 3.39 (d, *J* 6.7 Hz, 1H, C3-H), 2.95 (d, *J* 6.7 Hz, 1H, C2-H), 1.24 (s, 9H, C(CH₃)₃); ¹³C NMR (126 MHz, CDCl₃) δ 167.3, 156.7, 153.1, 139.8, 137.8, 134.8, 129.3, 124.8, 119.9, 118.9, 118.2, 103.7, 99.8, 81.6, 55.8, 55.7, 47.4, 46.7, 27.9; M.p. 87 - 89 °C (from diethyl ether / *n*-pentane); FT-IR (KBr (neat), cm⁻¹) 2934.4 (C-H), 2107.3 (N₃), 1744.0 (C=O), 1589.2/1509.1 (C=C aromatic), 1293.1/1207.9/1158.3 (C(O)C), 1032.4 (C-N), 834.4/799.9 (C-H bend); HRMS (HNESP) exact mass calculated for [C₂₁H₂₅N₄O₄] requires *m/z* 397.1870, found *m/z* 397.1871 [M+H]⁺.

***tert*-butyl *cis*-1-(2,4-dimethoxyphenyl)-3-(3-iodophenyl)aziridine-2-carboxylate (\pm)-*cis*-(**8.17**)**



3-Iodobenzaldehyde (**8.16**) (20.0 mg, 0.09 mmol), and 2,4-dimethoxyaniline (**8.3**) (11.9 mg, 0.08 mmol) were added to a flame dried Biotage 5 mL microwave vial, containing activated 4Å molecular sieves (~ 100 mg) under nitrogen. Deuterated chloroform (2 mL) was added, the vial was sealed with a PTFE crimp cap and the reaction mixture was left stirring at 25 °C for 2 hours. An aliquot was submitted to $^1\text{H-NMR}$ analysis, which confirmed the formation of the imine intermediate. Pyridinium triflate (**5.5**) (2.0 mg, 0.01 mmol, 10 mol%) was added. After 5 minutes, *tert*-butyl diazoacetate (**5.4**) (12 μL , 0.09 mmol) was added *via* syringe, and the reaction mixture was stirred at 25 °C, monitoring by $^1\text{H-NMR}$ until the reaction was deemed complete (~ 12 hours). At this point the reaction mixture was passed through a short plug of silica, eluted with diethyl ether and the solvent was removed under reduced pressure. The crude material was purified by flash chromatography on silica gel (30% diethyl ether in pentane, $R_f = 0.29$) to afford a white solid. Subsequent physicochemical analysis confirmed this to be the title compound (\pm)-*cis*-(**8.17**) (18.3 mg, 0.04 mmol, 44% yield).

$^1\text{H NMR}$ (500 MHz, CDCl_3) δ 7.93 (s, 1H, ArH), 7.64 – 7.58 (m, 1H, ArH), 7.49 (d, J 7.7 Hz, 1H, ArH), 7.06 (t, J 7.7 Hz, 1H, ArH), 6.82 (d, J 8.5 Hz, 1H, ArH), 6.46 (d, J 2.6 Hz, 1H, ArH), 6.38 (dd, J 8.5, 2.6 Hz, 1H, ArH), 3.79 (s, 3H, OCH_3), 3.77 (s, 3H, OCH_3), 3.35 (d, J 6.7 Hz, 1H, C3-H), 2.92 (d, J 6.7 Hz, 1H, C2-H), 1.24 (s, 9H, $\text{C}(\text{CH}_3)_3$); $^{13}\text{C NMR}$ (126 MHz, CDCl_3) δ 167.3, 156.8, 153.1, 138.1, 137.1, 136.6, 134.7, 129.7, 127.5, 119.8, 103.7, 99.8, 93.8, 81.8, 55.8, 55.7, 46.8, 28.0; M.p. 104 – 107 °C (from diethyl ether / *n*-pentane); FT-IR (KBr (neat), cm^{-1}) 2976.5 (C-H), 1715.6 (C=O), 1592.1/1506.1 (C=C aromatic), 1280.0/1208.7/1160.3 (C(O)C), 1049.3 (C-N), 803.4/736.1 (C-H bend); HRMS (HNESP) exact mass calculated for $[\text{C}_{21}\text{H}_{26}\text{INO}_4^{35}\text{Cl}]$ requires m/z 518.0590, found m/z 518.0583 $[\text{M}+\text{HCl}+\text{H}]^+$.

8.6. Synthesis of ring-opened aziridines

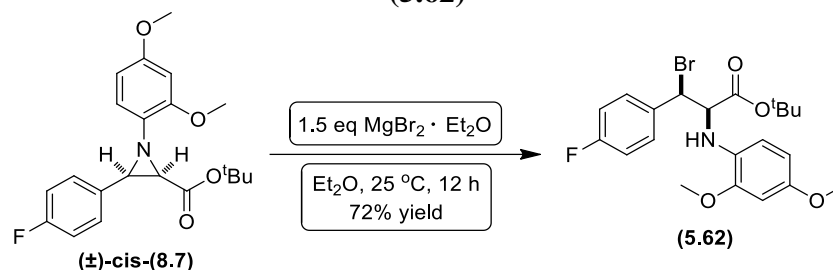
tert-butyl 3-bromo-3-(4-bromophenyl)-2-(2,4-dimethoxyphenylamino)propanoate (5.63)



tert-Butyl *cis*-3-(4-bromophenyl)-1-(2,4-dimethoxyphenyl)aziridine-2-carboxylate (\pm)-*cis*-(8.6) (20.0 mg, 0.05 mmol), and magnesium bromide diethyl etherate (17.8 mg, 0.07 mmol) were added to a flame dried 5 mL round bottom flask under nitrogen. Anhydrous diethyl ether (2 mL) was added *via* syringe, and the reaction mixture was stirred at 25 °C, monitoring by $^1\text{H-NMR}$ until the reaction was deemed complete (~ 12 hours). At this point the reaction mixture was passed through a short plug of silica, eluted with diethyl ether (10 mL), transferred into a 25 mL separating funnel and washed with saturated brine (10 mL). Organic phase was separated, dried with magnesium sulphate, filtered and the solvent removed under reduced pressure. The crude material was purified by flash chromatography on silica gel (10% diethyl ether in *n*-pentane, $R_f = 0.15$) to afford a yellow solid. Subsequent physicochemical analysis confirmed this to be the title compound (5.63) (15.0 mg, 0.03 mmol, 64% yield).

$^1\text{H NMR}$ (500 MHz, CDCl_3) δ 7.44 (s, 4H, ArH), 6.45 (d, J 2.6 Hz, 1H, ArH), 6.27 (dd, J 8.6, 2.6 Hz, 1H, ArH), 6.21 (d, J 8.6 Hz, 1H, ArH), 5.33 (d, J 5.2 Hz, 1H, CHBr), 4.85 (s, 1H, NH), 4.26 (d, J 5.2 Hz, 1H, $\text{C}\alpha\text{-H}$), 3.85 (s, 3H, OCH_3), 3.73 (s, 3H, OCH_3), 1.33 (s, 9H, $\text{C}(\text{CH}_3)_3$); $^{13}\text{C NMR}$ (126 MHz, CDCl_3) δ 169.6, 153.1, 148.8, 137.9, 131.7, 130.8, 130.5, 122.9, 111.9, 103.7, 99.5, 82.8, 64.9, 55.8, 55.8, 54.8, 27.9; M.p. 104 - 106 °C (from diethyl ether / *n*-pentane); FT-IR (KBr (neat), cm^{-1}) 3388.2 (N-H), 2925.3 (C-H), 1698.1 (C=O), 1591.6/1518.6 (C=C aromatic), 1259.1 (C(O)C), 1208.0/1153.1 (CH_2Br), 1034.5 (C-N), 797.6 (C-H bend); HRMS (HASP) exact mass calculated for $[\text{C}_{21}\text{H}_{26}^{79}\text{Br}_2\text{NO}_4]$ requires m/z 514.0214, found m/z 514.0223 $[\text{M}+\text{H}]^+$.

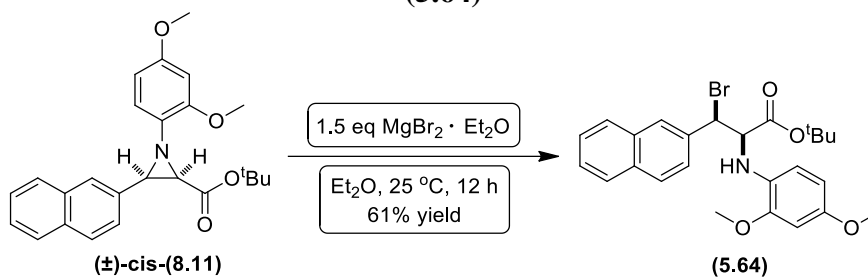
***tert*-butyl 3-bromo-2-(2,4-dimethoxyphenylamino)-3-(4-fluorophenyl)propanoate
(5.62)**



tert-Butyl *cis*-1-(2,4-dimethoxyphenyl)-3-(4-fluorophenyl)aziridine-2-carboxylate (±)-*cis*-(8.7) (40.0 mg, 0.11 mmol), and magnesium bromide diethyl etherate (41.5 mg, 0.16 mmol) were added to a flame dried 5 mL round bottom flask under nitrogen. Anhydrous diethyl ether (2 mL) was added *via* syringe, and the reaction mixture was stirred at 25 °C, monitoring by ¹H-NMR until the reaction was deemed complete (~ 12 hours). At this point the reaction mixture was passed through a short plug of silica, eluted with diethyl ether (10 mL), transferred into a 25 mL separating funnel and washed with saturated brine (10 mL). Organic phase was separated, dried with magnesium sulphate, filtered and the solvent removed under reduced pressure. The crude material was purified by flash chromatography on silica gel (25% diethyl ether in *n*-pentane, R_f = 0.35) to afford a orange solid. Subsequent physicochemical analysis confirmed this to be the title compound (5.62) (35.0 mg, 0.08 mmol, 72% yield).

¹H NMR (500 MHz, CDCl₃) δ 7.54 (dd, *J* 8.8, 5.3 Hz, 2H, ArH), 7.00 (t, *J* 8.8 Hz, 2H, ArH), 6.46 (d, *J* 2.5 Hz, 1H, ArH), 6.29 – 6.21 (m, 2H, ArH), 5.36 (d, *J* 5.5 Hz, 1H, CHBr), 4.87 (s, 1H, NH), 4.26 (d, *J* 5.5 Hz, 1H, C α -H), 3.86 (s, 3H, OCH₃), 3.73 (s, 3H, OCH₃), 1.32 (s, 9H, C(CH₃)₃); ¹³C NMR (126 MHz, CDCl₃) δ 169.7, 162.9 (d, *J*_{C-F} 248.5 Hz), 153.1, 148.8, 134.8 (d, *J*_{C-F} 3.3 Hz), 130.9, 130.6 (d, *J*_{C-F} 8.4 Hz), 115.5 (d, *J*_{C-F} 21.7 Hz), 112.0, 103.8, 99.5, 82.7, 65.3, 55.85, 55.84, 54.9, 27.9; M.p. 68 - 70 °C (from diethyl ether / *n*-pentane); FT-IR (KBr (neat), cm⁻¹) 3376.7 (N-H), 2934.1 (C-H), 1717.8 (C=O), 1604.5/1515.0 (C=C aromatic), 1259.5 (C(O)C), 1223.2/1155.8 (CH₂Br), 1035.9 (C-N), 802.6 (C-H bend); HRMS (HASP) exact mass calculated for [C₂₁H₂₆⁷⁹BrFNO₄] requires *m/z* 454.1024, found *m/z* 454.1020 [M+H]⁺.

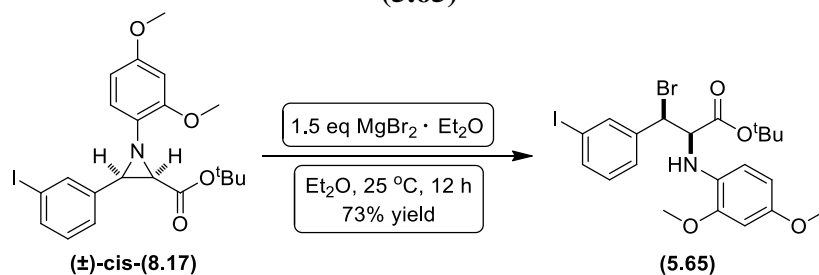
***tert*-butyl 3-bromo-2-(2,4-dimethoxyphenylamino)-3-(naphthalen-2-yl)propanoate
(5.64)**



tert-Butyl *cis*-1-(2,4-dimethoxyphenyl)-3-(naphthalen-2-yl)aziridine-2-carboxylate (\pm)-*cis*-(**8.11**) (25.0 mg, 0.06 mmol), and magnesium bromide diethyl etherate (24.0 mg, 0.09 mmol) were added to a flame dried 5 mL round bottom flask under nitrogen. Anhydrous diethyl ether (2 mL) was added *via* syringe, and the reaction mixture was stirred at 25 °C, monitoring by $^1\text{H-NMR}$ until the reaction was deemed complete (~ 12 hours). At this point the reaction mixture was passed through a short plug of silica, eluted with diethyl ether (10 mL), transferred into a 25 mL separating funnel and washed with saturated brine (10 mL). Organic phase was separated, dried with magnesium sulphate, filtered and the solvent removed under reduced pressure. The crude material was purified by flash chromatography on silica gel (25% diethyl ether in *n*-pentane, $R_f = 0.34$) to afford a brown solid. Subsequent physicochemical analysis confirmed this to be the title compound (**5.64**) (18.3 mg, 0.04 mmol, 61% yield).

$^1\text{H NMR}$ (500 MHz, CDCl_3) δ 7.91 (s, 1H, ArH), 7.83 – 7.78 (m, 3H, ArH), 7.73 (dd, J 8.6, 1.8 Hz, 1H, ArH), 7.50 – 7.46 (m, 2H, ArH), 6.46 (d, J 2.6 Hz, 1H, ArH), 6.32 (d, J 8.6 Hz, 1H, ArH), 6.25 (dd, J 8.6, 2.6 Hz, 1H, ArH), 5.52 (d, J 6.4 Hz, 1H, CHBr), 4.94 (d, J 8.6 Hz, 1H, NH), 4.42 (t, J 6.4 Hz, 1H, $\text{C}\alpha\text{-H}$), 3.86 (s, 3H, OCH_3), 3.72 (s, 3H, OCH_3), 1.23 (s, 9H, $\text{C}(\text{CH}_3)_3$); $^{13}\text{C NMR}$ (126 MHz, CDCl_3) δ 169.9, 153.0, 148.8, 136.1, 133.48, 132.9, 131.0, 128.5, 128.3, 127.8, 127.6, 126.8, 126.5, 126.5, 112.1, 103.7, 99.5, 82.6, 65.3, 56.3, 55.9, 55.8, 27.8; M.p. 79 - 82 °C (from diethyl ether / *n*-pentane); FT-IR (KBr (neat), cm^{-1}) 3395.5 (N-H), 2974.5 (C-H), 1731.0 (C=O), 1693.1/1599.1/1518.2 (C=C aromatic), 1259.8 (C(O)C), 1207.2/1154.4 (CH_2Br), 1034.6 (C-N), 820.8/751.2 (C-H bend); HRMS (HNESP) exact mass calculated for $[\text{C}_{25}\text{H}_{29}^{79}\text{BrNO}_4]$ requires: m/z 486.1274, found m/z $[\text{M}+\text{H}]^+$ 486.1271.

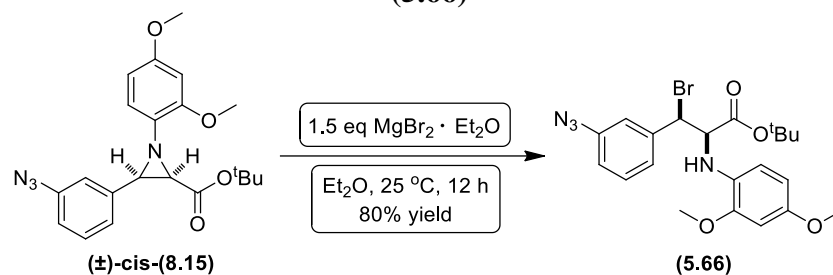
***tert*-butyl 3-bromo-2-((2,4-dimethoxyphenyl)amino)-3-(3-iodophenyl)propanoate
(5.65)**



tert-Butyl *cis*-1-(2,4-dimethoxyphenyl)-3-(3-iodophenyl)aziridine-2-carboxylate (\pm)-*cis*-(**8.17**) (15.0 mg, 0.03 mmol), and magnesium bromide diethyl etherate (12.0 mg, 0.05 mmol) were added to a flame dried 5 mL round bottom flask under nitrogen. Anhydrous diethyl ether (2 mL) was added *via* syringe, and the reaction mixture was stirred at 25 °C, monitoring by ¹H-NMR until the reaction was deemed complete (~ 12 hours). At this point the reaction mixture was passed through a short plug of silica, eluted with diethyl ether (10 mL), transferred into a 25 mL separating funnel and washed with saturated brine (10 mL). Organic phase was separated, dried with magnesium sulphate, filtered and the solvent removed under reduced pressure. The crude material was purified by flash chromatography on silica gel (30% diethyl ether in *n*-pentane, $R_f = 0.35$) to afford a white solid. Subsequent physicochemical analysis confirmed this to be the title compound (**5.65**) (13.0 mg, 0.02 mmol, 73% yield).

¹H NMR (500 MHz, CDCl₃) δ 7.84 (t, J 1.7 Hz, 1H, ArH), 7.66 – 7.60 (m, 1H, ArH), 7.53 (d, J 7.8 Hz, 1H, ArH), 7.04 (t, J 7.8 Hz, 1H, ArH), 6.45 (t, J 1.4 Hz, 1H, ArH), 6.28 (d, J 1.4 Hz, 2H, ArH), 5.23 (d, J 5.7 Hz, 1H, CHBr), 4.28 (d, J 5.7 Hz, 1H, C α -H), 3.86 (s, 3H, OCH₃), 3.73 (s, 3H, OCH₃), 1.32 (s, 9H, C(CH₃)₃); ¹³C NMR (126 MHz, CDCl₃) δ 169.5, 153.1, 148.8, 140.9, 137.9, 137.5, 130.7, 130.3, 128.3, 112.1, 103.7, 99.5, 93.9, 82.8, 65.0, 55.9, 55.8, 54.2, 27.9; M.p. 88 - 90 °C (from diethyl ether / *n*-pentane); FT-IR (KBr (neat), cm⁻¹) 3391.6 (N-H), 2963.9 (C-H), 1732.2 (C=O), 1519.8 (C=C aromatic), 1260.1 (C(O)C), 1207.6/1151.4 (CH₂Br), 1035.1 (C-N), 797.8 (C-H bend); HRMS (HNESP) exact mass calculated for [C₂₁H₂₆⁷⁹BrINO₄] requires: m/z 562.0084, found m/z [M+H]⁺ 562.0081.

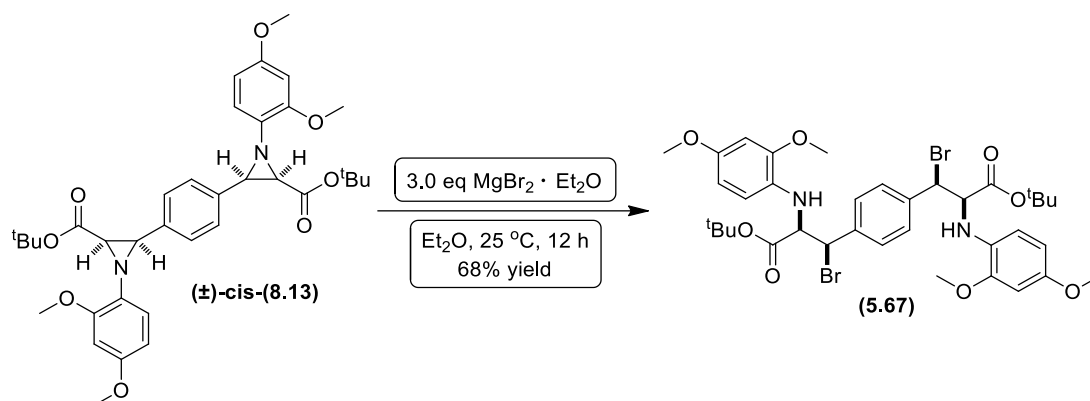
***tert*-butyl 3-(3-azidophenyl)-3-bromo-2-((2,4-dimethoxyphenyl)amino)propanoate (5.66)**



tert-Butyl 3-(3-azidophenyl)-1-(2,4-dimethoxyphenyl)aziridine-2-carboxylate (**(±)-cis-(8.15)**) (10.0 mg, 0.02 mmol), and magnesium bromide diethyl etherate (10.0 mg, 0.04 mmol) were added to a flame dried 5 mL round bottom flask under nitrogen. Anhydrous diethyl ether (2 mL) was added *via* syringe, and the reaction mixture was stirred at 25 °C, monitoring by ¹H-NMR until the reaction was deemed complete (~ 12 hours). At this point the reaction mixture was passed through a short plug of silica, eluted with diethyl ether (10 mL), transferred into a 25 mL separating funnel and washed with saturated brine (10 mL). Organic phase was separated, dried with magnesium sulphate, filtered and the solvent removed under reduced pressure. The crude material was purified by flash chromatography on silica gel (30% diethyl ether in *n*-pentane, *R_f* = 0.33) to afford a yellow solid. Subsequent physicochemical analysis confirmed this to be the title compound (**5.66**) (10.0 mg, 0.02 mmol, 80% yield).

¹H NMR (500 MHz, CDCl₃) δ 7.31 – 7.28 (m, 2H, ArH), 7.21 (s, 1H, ArH), 6.96 (dt, *J* 7.2, 1.9 Hz, 1H, ArH), 6.45 (d, *J* 2.4 Hz, 1H, ArH), 6.30 – 6.20 (m, 2H, ArH), 5.33 (d, *J* 5.4 Hz, 1H, CHBr), 4.86 (s, 1H, NH), 4.29 (d, *J* 5.4 Hz, 1H, C α -H), 3.85 (s, 3H, OCH₃), 3.73 (s, 3H, OCH₃), 1.33 (s, 9H, C(CH₃)₃); ¹³C NMR (126 MHz, CDCl₃) δ 169.5, 153.0, 148.7, 140.7, 140.3, 130.7, 129.9, 125.3, 119.5, 119.4, 111.9, 103.7, 99.5, 82.8, 64.8, 55.8, 54.8, 27.9; M.p. 61 - 63 °C (from diethyl ether / *n*-pentane); FT-IR (KBr (neat), cm⁻¹) 3397.3 (N-H), 2963.5 (C-H), 2113.8 (N₃), 1732.4 (C=O), 1519.8 (C=C aromatic), 1260.5 (C(O)C), 1208.0/1151.1 (CH₂Br), 1030.6 (C-N), 798.5 (C-H bend); HRMS (HNESP) exact mass calculated for [C₂₁H₂₅⁷⁹BrN₄O₄H] requires: *m/z* 477.1132, found *m/z* [M+H]⁺ 477.1126.

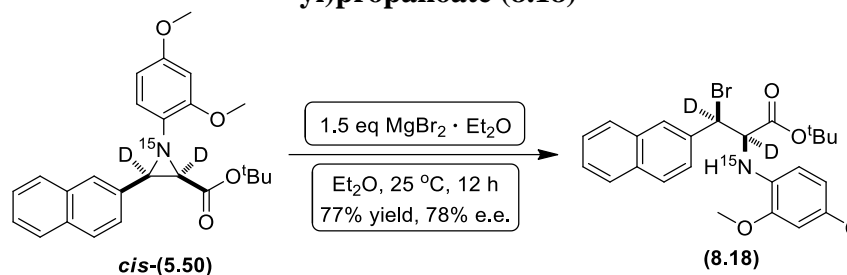
di-tert-butyl 3,3'-(1,4-phenylene)bis(3-bromo-2-((2,4-dimethoxyphenyl)amino)propanoate) (5.67)



di-tert-Butyl *cis*-3,3'-(1,4-phenylene)bis(1-(2,4-dimethoxyphenyl)aziridine-2-carboxylate) (**±**)-*cis*-**(8.13)** (10.0 mg, 0.02 mmol), and magnesium bromide diethyl etherate (12.0 mg, 0.05 mmol) were added to a flame dried 5 mL round bottom flask under nitrogen. Anhydrous diethyl ether (2 mL) was added *via* syringe, and the reaction mixture was stirred at $25\text{ }^\circ\text{C}$, monitoring by $^1\text{H-NMR}$ until the reaction was deemed complete (~ 12 hours). At this point the reaction mixture was passed through a short plug of silica, eluted with diethyl ether (10 mL), transferred into a 25 mL separating funnel and washed with saturated brine (10 mL). Organic phase was separated, dried with magnesium sulphate, filtered and the solvent removed under reduced pressure. The crude material was purified by flash chromatography on silica gel (30% diethyl ether in *n*-pentane, $R_f = 0.28$) to afford an orange oil. Subsequent physicochemical analysis confirmed this to be the title compound **(5.67)** (8.5 mg, 0.01 mmol, 68% yield).

$^1\text{H NMR}$ (500 MHz, CDCl_3) δ 7.49 (d, J 1.6 Hz, 4H, ArH), 6.44 (t, J 2.5 Hz, 2H, ArH), 6.30 – 6.18 (m, 4H, ArH), 5.34 (t, J 5.5 Hz, 2H, 2xCHBr), 4.87 (s, 2H, 2xNH), 4.26 (d, J 3.7 Hz, 2H, 2xC α -H), 3.84 (d, J 1.6 Hz, 6H, 2xOCH $_3$), 3.72 (s, 6H, 2xOCH $_3$), 1.29 (s, 18H, 2xC(CH $_3$) $_3$); $^{13}\text{C NMR}$ (126 MHz, CDCl_3) δ 168.6, 151.8, 147.6, 138.3, 129.7, 127.7, 110.8, 102.5, 98.3, 81.6, 63.7, 63.6, 54.6, 54.0, 26.7; FT-IR (KBr (neat), cm^{-1}) 3398.9 (N-H), 2976.5/2941.7 (C-H), 1730.9 (C=O), 1599.5/1518.8 (C=C aromatic), 1258.3 (C(O)C), 1207.6/1153.2 (CH $_2$ Br), 1035.0 (C-N), 835.1/732.9 (C-H bend); HRMS (HNESP) exact mass calculated for $[\text{C}_{36}\text{H}_{46}^{79}\text{Br}_2\text{N}_2\text{O}_8\text{H}]$ requires: m/z 793.1694, found m/z $[\text{M}+\text{H}]^+$ 793.1698.

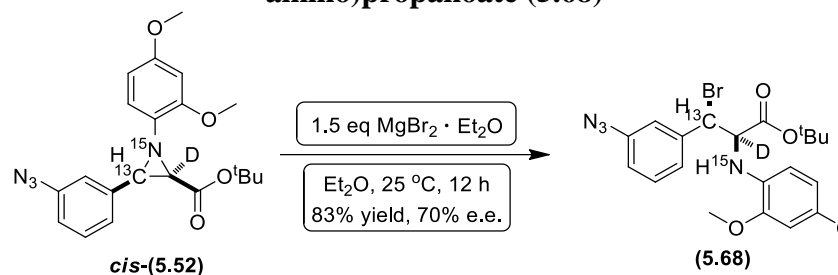
***tert*-butyl 2-¹⁵N-2,3-²H-3-bromo-2-(2,4-dimethoxyphenylamino)-3-(naphthalen-2-yl)propanoate (8.18)**



tert-Butyl *cis*-1-¹⁵N-2,3-²H-1-(2,4-dimethoxyphenyl)-3-(naphthalen-2-yl)aziridine-2-carboxylate *cis*-(**5.50**) (5.0 mg, 0.01 mmol), and magnesium bromide diethyl etherate (4.8 mg, 0.02 mmol) were added to a flame dried 10 mL round bottom flask under nitrogen. Anhydrous diethyl ether (2 mL) was added *via* syringe, and the reaction mixture was stirred at 25 °C, monitoring by ¹H-NMR until the reaction was deemed complete (~ 12 hours). At this point the reaction mixture was passed through a short plug of silica, eluted with diethyl ether (10 mL), transferred into a 25 mL separating funnel and washed with saturated brine (10 mL). Organic phase was separated, dried with magnesium sulphate, filtered and the solvent removed under reduced pressure. The crude material was purified by flash chromatography on silica gel (25% diethyl ether in *n*-pentane, R_f = 0.34) to afford a brown solid. Subsequent physicochemical analysis confirmed this to be the title compound (**8.18**) (4.5 mg, 0.01 mmol, 77% yield). A sample was submitted to chiral analytical HPLC analysis [Cellulose 3, *iso*-hexane / *iso*-propanol : 95 / 05, 1 mL / min, 24.3 min (1st peak), 42.9 min (2nd peak), 78% e.e.].

¹H NMR (500 MHz, CDCl₃) δ 7.91 (d, *J* 1.6 Hz, 1H, ArH), 7.84 – 7.77 (m, 3H, ArH), 7.72 (dd, *J* 8.5, 1.6 Hz, 1H, ArH), 7.51 – 7.46 (m, 2H, ArH), 6.46 (d, *J* 2.5 Hz, 1H, ArH), 6.37 (d, *J* 8.5 Hz, 1H, ArH), 6.26 (dd, *J* 8.5, 2.5 Hz, 1H, ArH), 3.86 (s, 3H, OCH₃), 3.72 (s, 3H, OCH₃), 1.22 (s, 9H, C(CH₃)₃); ¹³C NMR (126 MHz, CDCl₃) δ 169.7, 153.4, 148.9, 135.9, 133.5, 132.9, 131.1, 128.5, 128.3, 127.8, 127.6, 126.8, 126.6, 126.4, 112.5, 103.8, 99.5, 82.7, 55.9, 55.8, 27.8; ²H NMR (77 MHz, CH₂Cl₂) δ 7.26 (CDCl₃ ref), 5.51 (br s), 5.26 (CD₂Cl₂ ref), 4.42 (br s); M.p. 84 - 86 °C (from diethyl ether / *n*-pentane); [α]_D²³ +5.3 (c 0.3 CHCl₃); FT-IR (KBr (neat), cm⁻¹) 3389.0 (N-H), 2928.8 (C-H), 1731.9 (C=O), 1599.5/1515.0 (C=C aromatic), 1259.1 (C(O)C), 1207.5/1156.5 (CH₂Br), 1035.2 (C-N), 818.2/748.7 (C-H bend); MS (MALDI) 490.2 [M+H]⁺; HRMS (HNESP) exact mass calculated for [C₂₅H₂₇D₂⁷⁹Br₁¹⁵N₁O₄] requires *m/z* 489.1370, found *m/z* 489.1362 [M+H]⁺.

***tert*-butyl 2-¹⁵N-2-²H-3-¹³C-3-(3-azidophenyl)-3-bromo-2-((2,4-dimethoxyphenyl)amino)propanoate (5.68)**

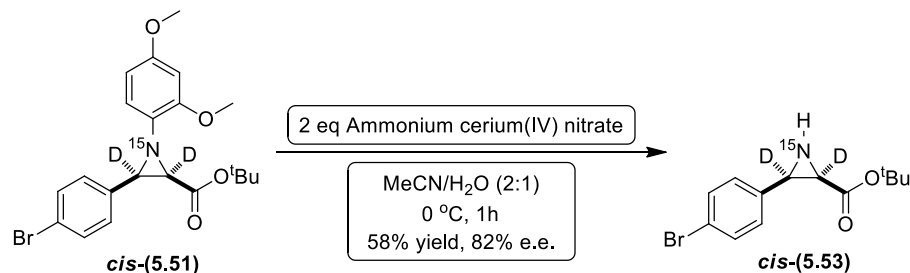


tert-Butyl *cis*-1-¹⁵N-2-²H-3-¹³C-3-(3-azidophenyl)-1-(2,4-dimethoxyphenyl)aziridine-2-carboxylate *cis*-(5.52) (20.0 mg, 0.05 mmol), and magnesium bromide diethyl etherate (19.4 mg, 0.08 mmol) were added to a flame dried 10 mL round bottom flask under nitrogen. Anhydrous diethyl ether (2 mL) was added *via* syringe, and the reaction mixture was stirred at 25 °C, monitoring by ¹H-NMR until the reaction was deemed complete (~ 12 hours). At this point the reaction mixture was passed through a short plug of silica, eluted with diethyl ether (10 mL), transferred into a 25 mL separating funnel and washed with saturated brine (10 mL). Organic phase was separated, dried with magnesium sulphate, filtered and the solvent removed under reduced pressure. The crude material was purified by flash chromatography on silica gel (30% diethyl ether in *n*-pentane, R_f = 0.33) to afford a yellow solid. Subsequent physicochemical analysis confirmed this to be the title compound (5.68) (20.0 mg, 0.04 mmol, 83% yield). A sample was submitted to chiral analytical HPLC analysis [Cellulose 3, *iso*-hexane / *iso*-propanol : 97 / 03, 1 mL / min, 12.1 min (1st peak), 15.8 min (2nd peak), 70% *e.e.*].

¹H NMR (500 MHz, CDCl₃) δ 7.34 – 7.28 (m, 2H, ArH), 7.24 – 7.18 (m, 1H, ArH), 6.99 – 6.93 (m, 1H, ArH), 6.45 (s, 1H, ArH), 6.27 (s, 2H, ArH), 5.32 (dd, J_{13C-H} 153.8, J 3.2 Hz, 1H, ¹³CHBr), 3.85 (s, 3H, OCH₃), 3.73 (s, 3H, OCH₃), 1.33 (s, 9H, C(CH₃)₃); ¹³C NMR (126 MHz, CDCl₃) δ 169.5, 153.1, 148.8, 142.9 (d, J_{C-13C} 5.9 Hz), 140.6 (d, J_{C-13C} 48.0 Hz), 140.3 (d, J_{C-13C} 4.9 Hz), 129.9 (d, J_{C-N} 4.5 Hz), 125.3 (d, J_{C-N} 3.4 Hz), 119.5 (d, J_{C-N} 3.5 Hz), 119.4, 112.1, 103.8, 99.5, 82.8, 55.85, 54.6 (d, J_{C-N} 1.7 Hz), 27.9; ²H NMR (77 MHz, CH₂Cl₂) δ 7.26 (CDCl₃ ref), 5.27 (CD₂Cl₂ ref), 4.24 (br s); ¹⁵N NMR (51 MHz, CDCl₃) δ 54.27 (d, J_{C-N} 2.0 Hz); M.p. 60 - 63 °C (from diethyl ether / *n*-pentane); [α]_D²³ +11.6 (c 1.0 CHCl₃); FT-IR (KBr (neat), cm⁻¹) 3382.3 (N-H), 2963.5 (C-H), 2113.4 (N₃), 1732.5 (C=O), 1601.7/1515.0 (C=C aromatic), 1290.9/1259.0 (C(O)C), 1208.0/1157.9 (CH₂Br), 1035.2 (C-N), 794.7 (C-H bend); MS (MALDI) 481.0 [M+H]⁺; HRMS (HNESP) exact mass calculated for [C₂₀¹³C₁H₂₅D₁⁷⁹Br₁N₃¹⁵N₁O₄] requires *m/z* 480.1199, found *m/z* 480.1187 [M+H]⁺.

8.7. Synthesis of deprotected NH-aziridines

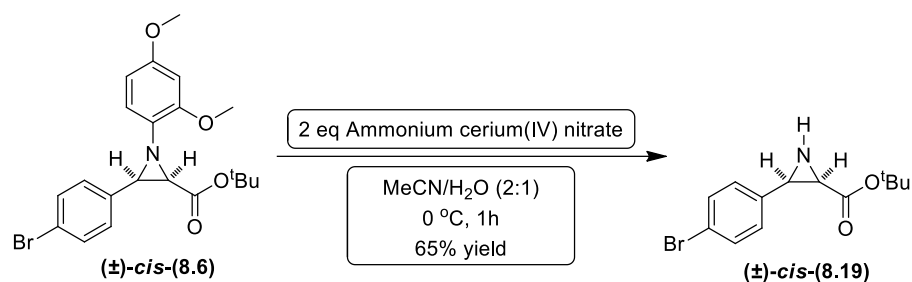
tert-butyl *cis*-1-¹⁵NH-2,3-²H-3-(4-bromophenyl)aziridine-2-carboxylate *cis*-(5.53)



A 25 mL RBF was charged with *tert*-butyl *cis*-1-¹⁵N-2,3-²H-3-(4-bromophenyl)-1-(2,4-dimethoxyphenyl)aziridine-2-carboxylate *cis*-(5.51) (20.0 mg, 0.05 mmol) in acetonitrile (1 mL) and the solution was cooled to 0 °C using an ice bath. Ammonium cerium(IV) nitrate (150 mg, 0.30 mmol) was dissolved in water (0.5 mL) and added to the flask at 0 °C. After 30 min stirring at 0 °C, no starting material was detected by TLC analysis. Saturated aqueous sodium hydrogen carbonate (10 mL) was added and the mixture was extracted with ethyl acetate (3 x 30 mL), dried with magnesium sulfate and filtered. The solvents were removed under reduced pressure, and the residue was purified by flash chromatography on basic aluminium oxide (30% diethyl ether in 40-60 PET, $R_f = 0.21$) to afford a yellow solid. Subsequent physicochemical analysis confirmed this to be the title compound *cis*-(5.53) (8.0 mg, 0.03 mmol, 58% yield). A sample was submitted to chiral analytical HPLC analysis [Cellulose 3, *iso*-hexane / *iso*-propanol : 97 / 03, 1 mL / min, 10.2 min (1st peak), 14.0 min (2nd peak), 82% *e.e.*].

¹H NMR (500 MHz, CDCl₃) δ 7.44 (d, J 7.9 Hz, 2H, ArH), 7.22 (d, J 7.9 Hz, 2H, ArH), 1.22 (s, 9H, C(CH₃)₃); ¹³C NMR (126 MHz, CDCl₃) δ 168.0, 134.3, 131.2, 129.6, 121.6, 82.2, 27.9; ²H NMR (77 MHz, DCM) δ 7.26 (CDCl₃ ref), 5.27 (CD₂Cl₂ ref), 3.29 (br s), 2.83 (br s); M.p. 132 - 134 °C (from diethyl ether / *n*-pentane); $[\alpha]_D^{25}$ -9.3 (c 0.5 CHCl₃); FT-IR (thin film) 3240 (N-H), 2970 (C-H), 1726 (C=O), 1588 (C=C aromatic), 1232//1154 (C(O)C), 1069 (C-N), 847 (C-H bend) cm⁻¹; MS (MALDI) 340.9 [M+K]⁺; HRMS (HNESP) Exact mass calculated for [C₁₃H₁₄D₂⁷⁹Br₁¹⁵N₁O₂Na₁]⁺ requires 323.0353, found 323.0354 [M+Na]⁺.

***tert*-butyl *cis*-3-(4-bromophenyl)aziridine-2-carboxylate (\pm)-*cis*-(8.19)**

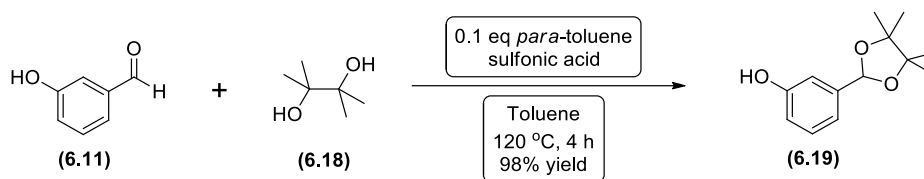


A 25 mL RBF was charged with *tert*-butyl *cis*-3-(4-bromophenyl)-1-(2,4-dimethoxyphenyl)aziridine-2-carboxylate (\pm)-*cis*-(8.6) (40.0 mg, 0.10 mmol) in acetonitrile (1 mL) and the solution was cooled to 0 °C using an ice bath. Ammonium cerium(IV) nitrate (300 mg, 0.60 mmol) was dissolved in water (0.5 mL) and added to the flask at 0 °C. After 30 min stirring at 0 °C, no starting material was detected by TLC analysis. Saturated aqueous sodium hydrogen carbonate (10 mL) was added and the mixture was extracted with ethyl acetate (3 x 30 mL), dried with magnesium sulfate and filtered. The solvents were removed under reduced pressure, and the residue was purified by flash chromatography on basic aluminium oxide (30% diethyl ether in 40-60 PET, $R_f = 0.21$) to afford a yellow solid. Subsequent physicochemical analysis confirmed this to be the title compound (\pm)-*cis*-(8.19) (17.5 mg, 0.06 mmol, 65% yield).

¹H NMR (500 MHz, CDCl₃) δ 7.43 (d, J 8.5 Hz, 2H, ArH), 7.21 (d, J 8.5 Hz, 2H, ArH), 3.37 (s, 1H, C3-H), 2.92 (s, 1H, C2-H), 1.22 (s, 9H, C(CH₃)₃); ¹³C NMR (126 MHz, CDCl₃) δ 168.0, 134.4, 131.2, 129.5, 121.6, 82.1, 37.9, 27.9; M.p. 134 - 136 °C (from diethyl ether / *n*-pentane); FT-IR (thin film) 3310 (N-H), 2978 (C-H), 1728 (C=O), 1489 (C=C aromatic), 1231/1153 (C(O)C), 1070 (C-N), 840 (C-H bend) cm⁻¹; MS (MALDI) 337.9 [M+K]⁺; HRMS (HNESP) Exact mass calculated for [C₁₃H₁₆⁷⁹BrN₁O₂Na]⁺ requires 320.0257, found 320.0259 [M+Na]⁺.

8.8. Synthesis of Teicoplanin fragment analogue

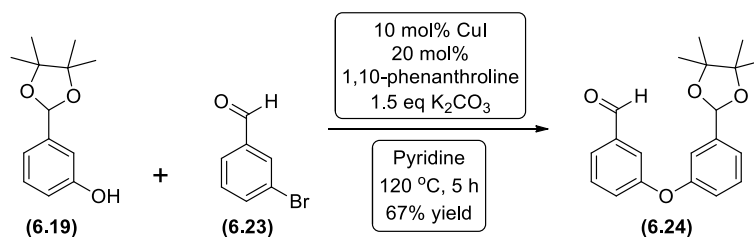
3-(4,4,5,5-tetramethyl-1,3-dioxolan-2-yl)phenol (**6.19**)



To a 50 mL flame dried round bottom flask, equipped with a Dean-Stark trap and a magnetic stirrer bar, under nitrogen was added 3-hydroxybenzaldehyde (**6.11**) (1.0 g, 8.19 mmol), pinacol (**6.18**) (1.5 g, 12.28 mmol) and *para*-toluenesulfonic acid monohydrate (156.0 mg, 0.82 mmol). Anhydrous toluene (20 mL) was added *via* syringe and the reaction was refluxed at 120 °C for 4 hours. The reaction mixture was cooled down to room temperature, diluted with toluene (30 mL), transferred into a 100 mL separating funnel, washed with saturated aqueous sodium hydrogen carbonate (40 mL), saturated brine (40 mL), dried with magnesium sulphate, filtered and the solvent removed under reduced pressure to afford a pale yellow solid. Recrystallisation from hot toluene afforded white solid, which was dried in the vacuum oven for 2 hours to afford a fine white powder. Subsequent physicochemical analysis confirmed this to be the title compound (**6.19**) (1.78 g, 8.0 mmol, 98% yield).

^1H NMR (500 MHz, CDCl_3) δ 7.17 (t, J 7.7 Hz, 1H, ArH), 7.03 (d, J 7.7 Hz, 1H, ArH), 6.96 (d, J 2.5 Hz, 1H, ArH), 6.72 (dd, J 7.7, 2.5 Hz, 1H, ArH), 6.55 (br s, 1H, OH), 5.94 (s, 1H, O-CH-O), 1.33 (s, 6H, 2 x CH_3), 1.28 (s, 6H, 2 x CH_3); ^{13}C NMR (126 MHz, CDCl_3) δ 155.9, 140.8, 129.7, 118.5, 116.1, 113.4, 99.7, 83.1, 24.3, 22.2; M.p. 137 - 139 °C (from toluene); FT-IR (thin film) 3377 (OH), 2984 (C-H), 1583/1495 (C=C aromatic), 1234/1152 (C(O)C), 865/780 (C-H bend) cm^{-1} ; MS (MALDI) 221.1 $[\text{M-H}]^+$; HRMS (HNESP) exact mass calculated for $[\text{C}_{13}\text{H}_{18}\text{O}_3\text{H}]$ requires m/z 223.1301, found m/z 223.1329 $[\text{M+H}]^+$.

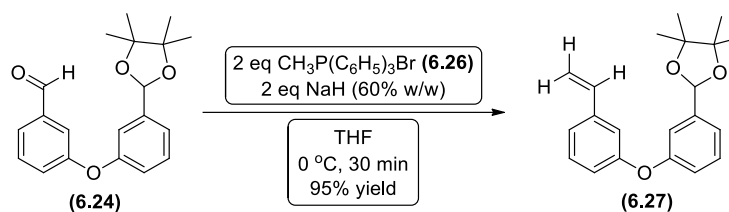
3-(3-(4,4,5,5-tetramethyl-1,3-dioxolan-2-yl)phenoxy)benzaldehyde (6.24)



3-(4,4,5,5-tetramethyl-1,3-dioxolan-2-yl)phenol (**(6.19)**) (1.0 g, 4.50 mmol), 3-bromobenzaldehyde (**(6.23)**) (0.5 mL, 4.50 mmol), potassium carbonate (0.9 g, 6.75 mmol), 1,10-phenanthroline (162.0 mg, 0.90 mmol) and copper (I) iodide (86.0 mg, 0.45 mmol) were added to a flame dried Biotage 25 mL microwave vial under nitrogen. Anhydrous pyridine (15 mL) was added *via* syringe, the vial sealed with a PTFE crimp cap and heated *via* microwave irradiation at 190 °C for 5 hours. The reaction mixture was cooled down to room temperature, diluted with dichloromethane (100 mL), transferred into a 250 mL separating funnel, washed with saturated aqueous copper (II) sulfate (100 mL), aqueous 1M hydrochloric acid (100 mL), saturated brine (40 mL), dried with magnesium sulphate, filtered and the solvent removed under reduced pressure. The crude material was purified by flash chromatography on silica gel (5% ethyl acetate in 40-60 PET, $R_f = 0.22$) to afford a yellow oil. Subsequent physicochemical analysis confirmed this to be the title compound (**(6.24)**) (0.98 g, 3.0 mmol, 67% yield).

¹H NMR (500 MHz, CDCl₃) δ 9.95 (s, 1H, CHO), 7.60 (d, *J* 7.7 Hz, 1H, ArH), 7.51 – 7.46 (m, 2H, ArH), 7.37 (t, *J* 7.7 Hz, 1H, ArH), 7.31 – 7.26 (m, 2H, ArH), 7.21 – 7.18 (m, 1H, ArH), 6.99 (dd, *J* 7.7, 2.1 Hz, 1H, ArH), 5.95 (s, 1H, O-CH-O), 1.31 (s, 6H, 2 x CH₃), 1.24 (s, 6H, 2 x CH₃); ¹³C NMR (126 MHz, CDCl₃) δ 191.7, 158.4, 156.3, 142.5, 138.2, 130.5, 130.1, 124.8, 124.6, 122.3, 119.6, 118.7, 117.4, 99.4, 83.0, 24.4, 22.3; FT-IR (thin film) 2979 (C-H), 1703 (C=O), 1584/1481 (C=C aromatic), 1253/1153 (C(O)C), 1086/789 (C-H bend) cm⁻¹; MS (MALDI) 365.2 [M+K]⁺; HRMS (HNESF) exact mass calculated for [C₂₀H₂₂O₄H] requires *m/z* 327.1598, found *m/z* 327.1595[M+H]⁺.

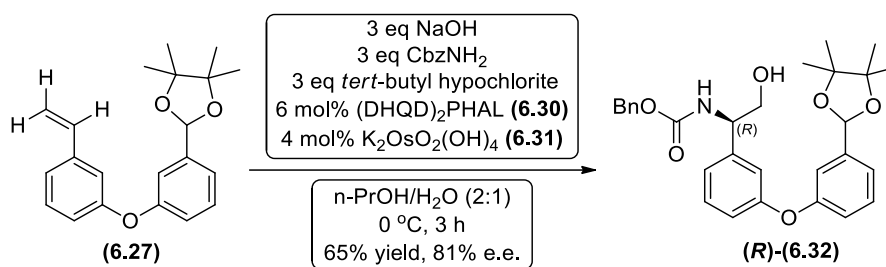
4,4,5,5-tetramethyl-2-(3-(3-vinylphenoxy)phenyl)-1,3-dioxolane (6.27)



To a 50 mL flame dried round bottom flask, equipped with a magnetic stirrer bar, under nitrogen was added methyltriphenylphosphonium bromide (**6.26**) (2.2 g, 6.13 mmol) in anhydrous tetrahydrofuran (30 mL) and the flask was cooled to 0 °C. Then sodium hydride (60% w/w in mineral oil [235.0 mg, 6.13 mmol]) was added and the mixture was stirred at 0 °C for 10 minutes. Then 3-(3-(4,4,5,5-tetramethyl-1,3-dioxolan-2-yl)phenoxy)benzaldehyde (**6.24**) (1.0 g, 3.06 mmol) was added and the mixture was stirred at 0 °C for an additional 30 minutes. The reaction mixture was diluted with ethyl acetate (100 mL), transferred into a 250 mL separating funnel, washed with saturated brine (100 mL), dried with magnesium sulphate, filtered and the solvent removed under reduced pressure. The crude material was purified by flash chromatography on silica gel (20% diethyl ether in 40-60 PET, $R_f = 0.35$) to afford a yellow oil. Subsequent physicochemical analysis confirmed this to be the title compound (**6.27**) (0.87 g, 2.7 mmol, 88% yield).

^1H NMR (500 MHz, CDCl_3) δ 7.32 (t, J 7.7 Hz, 1H, ArH), 7.30 – 7.27 (m, 1H, ArH), 7.23 (d, J 7.7 Hz, 1H, ArH), 7.19 – 7.18 (m, 1H, ArH), 7.14 (d, J 7.7 Hz, 1H, ArH), 7.07 (t, J 2.0 Hz, 1H, ArH), 6.96 (ddd, J 8.1, 2.5, 0.9 Hz, 1H, ArH), 6.90 (dd, J 8.1, 1.8 Hz, 1H, ArH), 6.66 (dd, J 17.6, 10.9 Hz, 1H, CHCH_2), 5.94 (s, 1H, O-CH-O), 5.71 (d, J 17.6 Hz, 1H, CHCH_2), 5.25 (d, J 10.9 Hz, 1H, CHCH_2), 1.31 (s, 6H, 2 x CH_3), 1.24 (s, 6H, 2 x CH_3); ^{13}C NMR (126 MHz, CDCl_3) δ 157.5, 157.3, 142.1, 139.6, 136.4, 129.9, 129.8, 121.5, 121.4, 119.1, 118.5, 116.9, 116.7, 114.7, 99.6, 82.9, 24.4, 22.3; FT-IR (thin film) 2977 (C-H), 2929 ($\text{H}_2\text{C}=\text{C}-\text{H}$), 1574/1485 (C=C aromatic), 1253/1156 (C(O)C), 1086/792 (C-H bend) cm^{-1} ; MS (MALDI) 323.2 $[\text{M}-\text{H}]^+$; HRMS (HNESP) exact mass calculated for $[\text{C}_{21}\text{H}_{24}\text{O}_3\text{H}]$ requires m/z 325.1798, found m/z 325.1801 $[\text{M}+\text{H}]^+$.

benzyl (*R*)-2-hydroxy-1-(3-(3-(4,4,5,5-tetramethyl-1,3-dioxolan-2-yl)phenoxy)phenyl)ethylcarbamate (*R*)-(6.32)

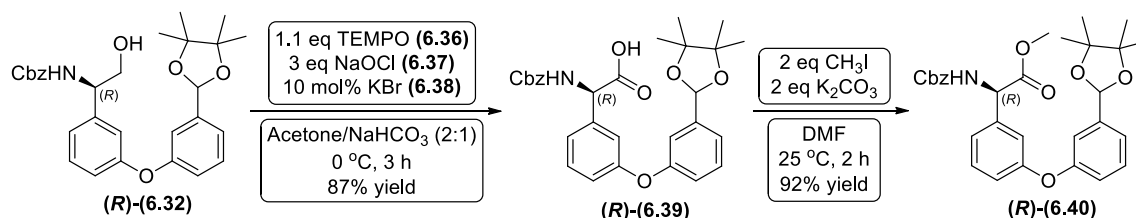


To a 25 mL round bottom flask, equipped with a magnetic stirrer bar, under nitrogen was added benzyl carbamate (489.0 mg, 3.24 mmol) and sodium hydroxide (129.0 mg, 3.24 mmol). 1-propanol (4 mL) and distilled water (5 mL) was added *via* syringe and the mixture was cooled to 0 °C. Then *tert*-butyl hypochlorite (0.37 mL, 3.24 mmol) was added and the mixture was stirred at 0 °C for 10 minutes. Then a solution of (DHQD)₂PHAL (6.30) (50.4 mg, 0.06 mmol) in 1-propanol (2 mL) was added, followed by a solution of 4,4,5,5-tetramethyl-2-(3-(3-vinylphenoxy)phenyl)-1,3-dioxolane (6.27) (350.0 mg, 1.08 mmol) in 1-propanol (4 mL). Potassium osmate dihydrate (6.31) (15.9 mg, 0.04 mmol) added at 0 °C and the reaction was stirred for 3 hours changing the colour from dark green to deep yellow. The mixture was quenched with saturated aqueous sodium sulfite solution (30 mL) at 0 °C, diluted with ethyl acetate (50 mL) and transferred into a 100 mL separating funnel. The organic layer was separated and washed with saturated brine (40 mL), dried with magnesium sulphate, filtered and the solvent removed under reduced pressure. The crude material was purified by flash chromatography on silica gel (30% ethyl acetate in 40-60 PET, $R_f = 0.26$) to afford a pale yellow oil. Subsequent physicochemical analysis confirmed this to be the title compound (*R*)-(6.32) (0.35 g, 0.7 mmol, 65% yield). A sample was submitted to chiral analytical HPLC analysis [Cellulose 1, *iso*-hexane / *iso*-propanol : 85 / 15, 1 mL / min, 8.85 min (1st peak), 17.31 min (2nd peak), 96% e.e.].

¹H NMR (500 MHz, CDCl₃) δ 7.38 – 7.22 (m, 8H, ArH), 7.18 – 7.15 (m, 1H, ArH), 7.01 (d, *J* 7.7 Hz, 1H, ArH), 7.00 – 6.91 (m, 2H, ArH), 6.89 (d, *J* 7.7 Hz, 1H, ArH), 5.93 (s, 1H, O-CH-O), 5.57 (s, 1H, NH), 5.12 (d, *J* 12.2 Hz, 1H, O-CHH-Ph), 5.07 (d, *J* 12.2 Hz, 1H, O-CHH-Ph), 4.81 (s, 1H, C α -H), 3.81 (m, 2H, CH₂OH), 2.14 (s, 1H, OH), 1.30 (s, 6H, 2 x CH₃), 1.25 (s, 6H, 2 x CH₃); ¹³C NMR (126 MHz, CDCl₃) δ 157.8, 156.9, 156.4, 142.1, 141.4, 141.4, 136.3, 130.2, 129.9, 128.7, 128.3, 121.7, 121.4, 119.3, 117.9, 117.1, 117.1, 99.5, 82.9, 67.2, 66.4, 56.9, 24.4, 22.3; $[\alpha]_D^{25}$ -15.1 (c 1.0 CHCl₃); FT-IR (thin film) 3406 (NH), 3333 (OH), 2977 (C-H), 1704 (C=O), 1584/1486 (C=C aromatic), 1255/1159 (C(O)C), 1086/736 (C-H bend) cm⁻¹; MS (MALDI) 514.4

$[M+Na]^+$; HRMS (HNESP) exact mass calculated for $[C_{29}H_{33}N_1O_6NH_4]$ requires m/z 509.2646, found m/z 509.2655 $[M+NH_4]^+$.

methyl (*R*)-2-(benzyloxycarbonylamino)-2-(3-(3-(4,4,5,5-tetramethyl-1,3-dioxolan-2-yl)phenoxy)phenyl)acetate (*R*)-(6.40)

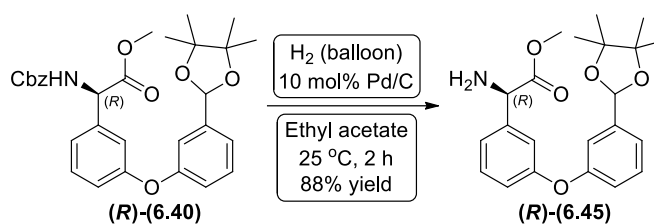


To a 25 mL round bottom flask, equipped with a magnetic stirrer bar, under nitrogen was added benzyl (*R*)-2-hydroxy-1-(3-(3-(4,4,5,5-tetramethyl-1,3-dioxolan-2-yl)phenoxy)phenyl)ethylcarbamate (*R*)-(6.32) (0.3 g, 0.61 mmol). Acetone (10 mL) and aqueous sodium hydrogen carbonate solution (5 mL) were added and the mixture was cooled to 0 °C. To this solution was added sequentially potassium bromide (**6.38**) (8.0 mg, 0.07 mmol) and TEMPO (**6.36**) (2,2,6,6-tetramethyl piperidinyloxy, free radical) (105.0 mg, 0.67 mmol). Sodium hypochlorite (**6.37**) (11% chlorine) (1.03 mL, 1.83 mmol) was added dropwise *via* syringe over a period of 10 min, while the mixture was vigorously stirred and maintained at 0 °C. After 3 hours, acetone was removed under reduced pressure, the residue was diluted with distilled water (10 mL), transferred into a 50 mL separating funnel and washed with diethyl ether (2 x 20 mL). The aqueous phase was acidified to pH 4 and extracted with ethyl acetate (2 x 20 mL). The combined organic layers were washed with saturated brine (10 mL), dried with magnesium sulphate, filtered and the solvent removed under reduced pressure to yield crude carboxylic acid derivative (*R*)-(6.39) (0.27 g, 0.53 mmol, 87% yield) as colourless oil, which was used in the next step without purification. To a 50 mL flame dried round bottom flask, equipped with a magnetic stirrer bar, under nitrogen was added crude carboxylic acid derivative (*R*)-(6.39) (200.0 mg, 0.40 mmol) and potassium carbonate (109.0 mg, 0.80 mmol). Anhydrous *N,N*-dimethylformamide (3 mL) was added *via* syringe, followed by iodomethane (0.05 mL, 0.80 mmol). After 2 hours, the reaction was diluted with ethyl acetate (50 mL) and transferred into a 100 mL separating funnel. The organic layer was washed with distilled water (5 x 25 mL), saturated brine (30 mL), dried with magnesium sulphate, filtered and the solvent removed under reduced pressure. The crude material was purified by flash chromatography on silica gel (30% diethyl ether in 40-60 PET, $R_f = 0.31$) to afford an orange oil. Subsequent

physicochemical analysis confirmed this to be the title compound (**R**)-(6.40) (190.0 mg, 0.37 mmol, 92% yield).

^1H NMR (500 MHz, CDCl_3) δ 7.38 – 7.26 (m, 8H, ArH), 7.18 – 7.16 (m, 1H, ArH), 7.09 (d, J 7.3 Hz, 1H, ArH), 7.04 (s, 1H, ArH), 6.97 – 6.90 (m, 2H, ArH), 5.94 (s, 1H, O-CH-O), 5.81 (d, J 7.3 Hz, 1H, NH), 5.36 (d, J 7.3 Hz, 1H, $\text{C}\alpha$ -H), 5.13 (d, J 12.2 Hz, 1H, O-CHH-Ph), 5.08 (d, J 12.2 Hz, 1H, O-CHH-Ph), 3.73 (s, 3H, OCH_3), 1.30 (s, 6H, 2 x CH_3), 1.24 (s, 6H, 2 x CH_3); ^{13}C NMR (126 MHz, CDCl_3) δ 171.1, 157.9, 156.7, 155.4, 142.2, 138.6, 136.2, 130.3, 129.9, 128.7, 128.4, 128.3, 121.9, 121.8, 119.3, 118.6, 117.6, 117.2, 99.5, 82.9, 67.3, 57.7, 53.0, 24.4, 22.3; $[\alpha]_{\text{D}}^{23}$ -14.8 (c 1.0 CHCl_3); FT-IR (thin film) 3326 (NH), 2977 (C-H), 1727 (C=O), 1724 (C=O), 1585/1486 (C=C aromatic), 1251/1159 (C(O)C), 1058/697 (C-H bend) cm^{-1} ; MS (MALDI) 542.4 $[\text{M}+\text{Na}]^+$; HRMS (HNESP) exact mass calculated for $[\text{C}_{30}\text{H}_{33}\text{N}_1\text{O}_7 \text{NH}_4]$ requires m/z 537.2595, found m/z 537.2601 $[\text{M}+\text{NH}_4]^+$.

methyl (*R*)-2-amino-2-(3-(3-(4,4,5,5-tetramethyl-1,3-dioxolan-2-yl)phenoxy)phenyl)acetate (*R*)-(6.45)

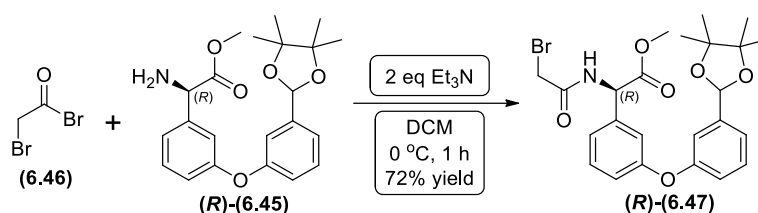


To a 25 mL round bottom flask, equipped with a magnetic stirrer bar, under nitrogen was added methyl (*R*)-2-(benzyloxycarbonylamino)-2-(3-(3-(4,4,5,5-tetramethyl-1,3-dioxolan-2-yl)phenoxy)phenyl)acetate (**R**)-(6.40) (0.2 g, 0.39 mmol) and palladium on carbon (10% w/w) (41.0 mg, 0.04 mmol). Ethyl acetate (5 mL) was added *via* syringe and the flask was sealed with suba-seal rubber septum. Then, hydrogen gas atmosphere was introduced through the septum and the reaction was stirred at 25 °C for 2 hours. At this point the reaction mixture was passed through a short plug of celite and eluted with ethyl acetate (10 mL). The solvent was removed under reduced pressure to afford a colourless oil. Subsequent physicochemical analysis confirmed this to be the title compound (**R**)-(6.45) (130.0 mg, 0.34 mmol, 88% yield).

^1H NMR (500 MHz, CDCl_3) δ 7.34 – 7.27 (m, 2H, ArH), 7.24 (d, J 7.7 Hz, 1H, ArH), 7.19 – 7.16 (m, 1H, ArH), 7.11 (d, J 7.7 Hz, 1H, ArH), 7.07 – 7.03 (m, 1H, ArH), 6.96 (ddd, J 8.1, 2.4, 0.9 Hz, 1H, ArH), 6.91 (dd, J 8.2, 1.6 Hz, 1H, ArH), 5.94 (s, 1H, O-

CH-O), 4.59 (s, 1H, C α -H), 3.71 (s, 3H, OCH₃), 1.30 (s, 6H, 2 x CH₃), 1.24 (s, 6H, 2 x CH₃); ¹³C NMR (126 MHz, CDCl₃) δ 174.2, 157.7, 156.9, 142.2, 130.2, 129.9, 121.7, 121.5, 119.3, 118.3, 117.5, 117.1, 99.6, 82.9, 58.6, 52.6, 29.8, 24.4, 22.3; [α]_D²⁵ -17.3 (c 1.0 CHCl₃); FT-IR (thin film) 3389 (NH₂), 2978 (C-H), 1740 (C=O), 1585/1484 (C=C aromatic), 1253/1157 (C(O)C), 1063/800 (C-H bend) cm⁻¹; MS (MALDI) 424.3 [M+K]⁺; HRMS (HNESP) exact mass calculated for [C₂₂H₂₇N₁O₅H] requires *m/z* 386.1962, found *m/z* 386.1964 [M+H]⁺.

methyl (*R*)-2-(2-bromoacetamido)-2-(3-(3-(4,4,5,5-tetramethyl-1,3-dioxolan-2-yl)phenoxy)phenyl)acetate (*R*)-(6.47)

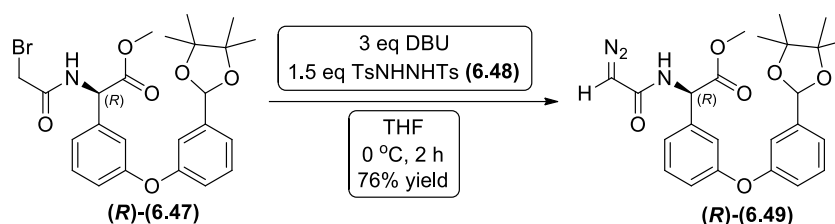


To a 25 mL flame dried round bottom flask, equipped with a magnetic stirrer bar, under nitrogen was added methyl (*R*)-2-amino-2-(3-(3-(4,4,5,5-tetramethyl-1,3-dioxolan-2-yl)phenoxy)phenyl)acetate (**(R)-(6.45)**) (0.1 g, 0.26 mmol). Anhydrous dichloromethane (5 mL) was added *via* syringe and the reaction was cooled to 0 °C. Then triethylamine (0.07 mL, 0.52 mmol) was added, followed by bromoacetyl bromide (**(6.46)**) (0.03 mL, 0.39 mmol) and the mixture was stirred at 0 °C for 1 hour. The reaction mixture was diluted with dichloromethane (5 mL), transferred into a 25 mL separating funnel, washed with aqueous 1M hydrochloric acid (10 mL), saturated aqueous sodium hydrogen carbonate (10 mL), saturated brine (10 mL), dried with magnesium sulphate, filtered and the solvent removed under reduced pressure. The crude material was purified by flash chromatography on silica gel (40% diethyl ether in pentane, R_f = 0.41) to afford a yellow oil. Subsequent physicochemical analysis confirmed this to be the title compound (**(R)-(6.47)**) (94.0 mg, 0.18 mmol, 72% yield).

¹H NMR (500 MHz, CDCl₃) δ 7.42 (d, *J* 6.9 Hz, 1H, NH), 7.36 – 7.26 (m, 3H, ArH), 7.19 – 7.16 (m, 1H, ArH), 7.10 (d, *J* 7.7 Hz, 1H, ArH), 7.03 (t, *J* 2.0 Hz, 1H, ArH), 6.98 – 6.91 (m, 2H, ArH), 5.94 (s, 1H, O-CH-O), 5.51 (d, *J* 6.9 Hz, 1H, C α -H), 3.89 (d, *J* 13.7 Hz, 1H, CHHBr), 3.89 (d, *J* 13.7 Hz, 1H, CHHBr), 3.75 (s, 3H, OCH₃), 1.30 (s, 6H, 2 x CH₃), 1.24 (s, 6H, 2 x CH₃); ¹³C NMR (126 MHz, CDCl₃) δ 170.5, 165.1, 158.0, 156.6, 142.3, 137.7, 130.4, 129.9, 121.9, 121.8, 119.4, 118.7, 117.4, 117.3, 99.5,

82.9, 56.7, 53.2, 28.6, 24.4, 22.3; $[\alpha]_D^{26}$ -24.1 (c 1.0 CHCl₃); FT-IR (thin film) 3298 (NH), 2978 (C-H), 1746 (C=O), 1662 (C=O), 1585/1485 (C=C aromatic), 1252/1157 (C(O)C), 1087 (C-H bend), 663 (C-Br) cm⁻¹; MS (MALDI) 546.4 [M+K]⁺; HRMS (HNESP) exact mass calculated for [C₂₄H₂₈⁷⁹Br₁N₁O₆Na] requires m/z 528.0992, found m/z 528.0982 [M+Na]⁺.

methyl (R)-2-(2-diazoacetamido)-2-(3-(3-(4,4,5,5-tetramethyl-1,3-dioxolan-2-yl)phenoxy)phenyl)acetate (R)-(6.49)

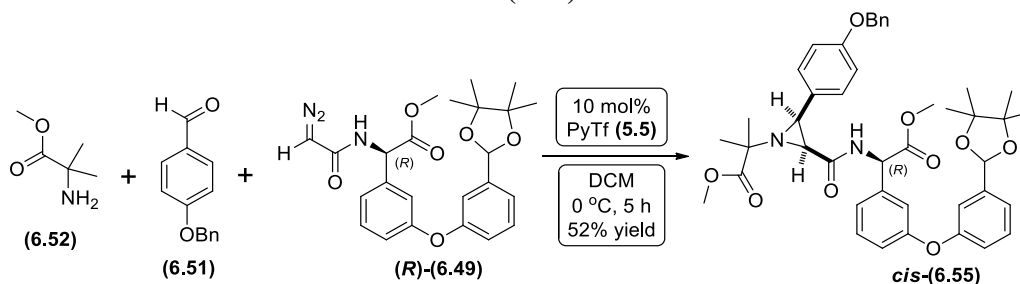


To a 25 mL flame dried round bottom flask, equipped with a magnetic stirrer bar, under nitrogen was added methyl (R)-2-(2-bromoacetamido)-2-(3-(3-(4,4,5,5-tetramethyl-1,3-dioxolan-2-yl)phenoxy)phenyl)acetate (R)-(6.47) (0.1 g, 0.20 mmol). Anhydrous tetrahydrofuran (5 mL) was added *via* syringe and the reaction was cooled to 0 °C. Then *N,N'*-ditosylhydrazine (6.48) (0.1 g, 0.30 mmol) was added, followed by 1,8-diazabicyclo[5.4.0]undec-7-ene (0.09 mL, 0.6 mmol) and the mixture was stirred at 0 °C for 2 hours. Then the solvent was removed under reduced pressure, the residue was re-dissolved in diethyl ether, passed through a short plug of silica and eluted with diethyl ether. The solvent removed under reduced pressure and the crude material was purified by flash chromatography on silica gel (40% diethyl ether in pentane, R_f = 0.33) to afford a pale yellow oil. Subsequent physicochemical analysis confirmed this to be the title compound (R)-(6.49) (68.0 mg, 0.15 mmol, 76% yield). A sample was submitted to chiral analytical HPLC analysis [Cellulose 1, *iso*-hexane / *iso*-propanol : 80 / 20, 1 mL / min, 8.82 min (1st peak), 12.94 min (2nd peak), 94% e.e.].

¹H NMR (500 MHz, CDCl₃) δ 7.35 – 7.27 (m, 2H, ArH), 7.24 (s, 1H, ArH), 7.17 – 7.15 (m, 1H, ArH), 7.09 (d, J 7.7 Hz, 1H, ArH), 7.01 (t, J 2.0 Hz, 1H, ArH), 6.95 (ddd, J 8.1, 2.5, 1.0 Hz, 1H, ArH), 6.91 (ddd, J 8.2, 2.4, 0.8 Hz, 1H, ArH), 6.13 (d, J 6.9 Hz, 1H, NH), 5.93 (s, 1H, O-CH-O), 5.61 (d, J 5.5 Hz, 1H, C α -H), 4.82 (s, 1H, CHN₂), 3.73 (s, 3H, OCH₃), 1.30 (s, 6H, 2 x CH₃), 1.24 (s, 6H, 2 x CH₃); ¹³C NMR (126 MHz, CDCl₃) δ 171.4, 165.0, 157.9, 156.7, 142.2, 138.6, 130.4, 129.9, 122.1, 121.8, 119.4, 118.6, 117.5, 117.2, 99.5, 82.9, 56.5, 53.1, 47.7, 24.4, 22.3; $[\alpha]_D^{25}$ -19.8 (c 1.0 CHCl₃); FT-IR

(thin film) 3353 (NH), 2977 (C-H), 2105 (N₂), 1746 (C=O), 1585/1485 (C=C aromatic), 1248/1156 (C(O)C), 1087/966 (C-H bend) cm⁻¹; HRMS (HNESP) exact mass calculated for [C₂₄H₂₇N₃O₆Na] requires *m/z* 476.1792, found *m/z* 476.1784 [M+Na]⁺.

methyl *cis*-2-(4-(benzyloxy)phenyl)-3-(((*R*)-2-methoxy-2-oxo-1-(3-(3-(4,4,5,5-tetramethyl-1,3-dioxolan-2-yl)phenoxy)phenyl)ethyl)carbamoyl)aziridin-1-yl)-2-methylpropanoate *cis*-(6.55)

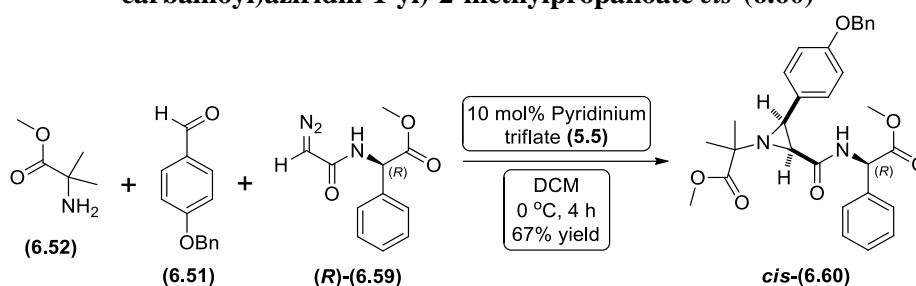


A flame dried Biotage 2 mL microwave vial was charged with, methyl 2-amino-2-methylpropanoate (**6.52**) (11.2 mg, 0.09 mmol), 4-benzyloxybenzaldehyde (**6.51**) (19.8 mg, 0.10 mmol) and activated 4Å molecular sieves (~ 100 mg) in anhydrous dichloromethane (0.5 mL) under nitrogen. After the formation of the corresponding imine was confirmed by ¹H-NMR analysis, pyridinium triflate (**5.5**) (2.2 mg, 0.01 mmol, 10 mol%) was added, the vial was sealed with a PTFE crimp cap and the reaction mixture was cooled to 0 °C. Then methyl (*R*)-2-(2-diazoacetamido)-2-(3-(3-(4,4,5,5-tetramethyl-1,3-dioxolan-2-yl)phenoxy)phenyl)acetate (**R**)-(6.49) (39.3 mg, 0.09 mmol) in dichloromethane (0.5 mL) was added *via* syringe and the reaction mixture was stirred at 0 °C, monitoring by ¹H-NMR until the reaction was deemed complete. At this point the reaction mixture was passed through a short plug of silica and eluted with dichloromethane. The solvent removed under reduced pressure and the crude material was purified by flash chromatography on silica gel (15% diethyl ether in pentane, R_f = 0.2) to afford a colourless oil. Subsequent physicochemical analysis confirmed this to be the title compound *cis*-(6.55) (37.4 mg, 0.05 mmol, 52% yield).

¹H NMR (500 MHz, CDCl₃) δ 7.63 (d, *J* 7.7 Hz, 1H, NH), 7.42 – 7.36 (m, 4H, ArH), 7.34 – 7.29 (m, 4H, ArH), 7.24 (d, *J* 8.0 Hz, 2H, ArH), 7.16 (s, 1H, ArH), 7.03 (d, *J* 7.6 Hz, 1H, ArH), 6.99 (d, *J* 1.8 Hz, 1H, ArH), 6.94 – 6.85 (m, 4H, ArH), 5.93 (s, 1H, O-CH-O), 5.23 (d, *J* 7.7 Hz, 1H, Cα-H), 5.03 (s, 2H, OCH₂Ph), 3.66 (s, 3H, OCH₃), 3.55 (s, 3H, OCH₃), 3.30 (d, *J* 6.8 Hz, 1H, C3-H), 2.84 (d, *J* 6.8 Hz, 1H, C2-H), 1.42 (s, 3H, CH₃), 1.30 (s, 6H, 2 x CH₃), 1.29 (s, 3H, CH₃), 1.24 (s, 6H, 2 x CH₃); ¹³C NMR (126 MHz, CDCl₃) δ 174.3, 170.3, 167.3, 158.4, 157.7, 156.9, 142.2, 138.9, 137.1, 130.1,

129.8, 129.0, 128.7, 128.1, 127.6, 127.5, 121.7, 121.6, 119.2, 118.3, 117.4, 117.2, 114.6, 99.5, 82.9, 70.2, 61.4, 55.3, 52.7, 52.3, 41.9, 41.1, 24.5, 24.4, 22.3, 21.5; $[\alpha]_D^{25}$ -9.8 (c 0.4 CHCl₃); FT-IR (thin film) 3380 (NH), 2979 (C-H), 1739 (C=O), 1682 (C=O), 1585/1514 (C=C aromatic), 1249/1150 (C(O)C), 1086/1010 (C-H bend) cm⁻¹; HRMS (HNESP) exact mass calculated for [C₄₃H₄₈N₂O₉H] requires m/z 737.3433, found m/z 737.3435 [M+H]⁺.

methyl *cis*-2-(4-(benzyloxy)phenyl)-3-(((*R*)-2-methoxy-2-oxo-1-phenylethyl) carbamoyl)aziridin-1-yl)-2-methylpropanoate *cis*-(6.60**)**



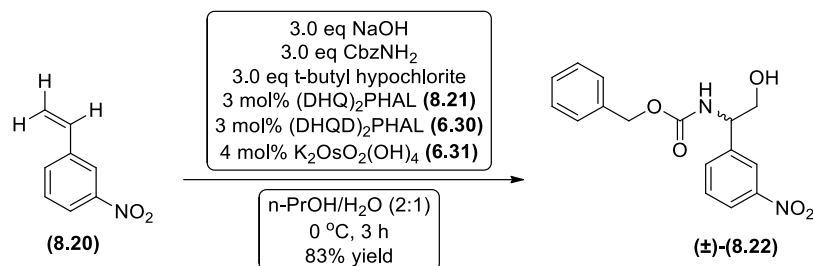
A flame dried Biotage 2 mL microwave vial was charged with, methyl 2-amino-2-methylpropanoate (**6.52**) (11.2 mg, 0.09 mmol), 4-benzyloxybenzaldehyde (**6.51**) (19.8 mg, 0.10 mmol) and activated 4Å molecular sieves (~ 100 mg) in anhydrous dichloromethane (0.5 mL) under nitrogen. After the formation of the corresponding imine was confirmed by ¹H-NMR analysis, pyridinium triflate (**5.5**) (2.2 mg, 0.01 mmol, 10 mol%) was added, the vial was sealed with a PTFE crimp cap and cooled to 0 °C. Then methyl (*R*)-2-(2-diazoacetamido)-2-phenylacetate (*R*)-(**6.59**) (22.3 mg, 0.09 mmol) in dichloromethane (0.5 mL) was added *via* syringe and the reaction mixture was stirred at 0 °C, monitoring by ¹H-NMR until the reaction was deemed complete. At this point the reaction mixture was passed through a short plug of silica and eluted with dichloromethane. The solvent removed under reduced pressure and the crude material was purified by flash chromatography on silica gel (15% diethyl ether in pentane, R_f = 0.24) to afford a colourless oil. Subsequent physicochemical analysis confirmed this to be the title compound *cis*-(**6.60**) (26.7 mg, 0.05 mmol, 55% yield).

¹H NMR (500 MHz, CDCl₃) δ 7.63 (d, *J* 7.7 Hz, 1H, NH), 7.45 – 7.36 (m, 4H, ArH), 7.35 – 7.27 (m, 8H, ArH), 6.90 (d, *J* 8.7 Hz, 2H, ArH), 5.26 (d, *J* 7.8 Hz, 1H, Cα-H), 5.04 (s, 2H, OCH₂Ph), 3.66 (s, 3H, OCH₃), 3.54 (s, 3H, OCH₃), 3.31 (d, *J* 6.8 Hz, 1H, C3-H), 2.83 (d, *J* 6.8 Hz, 1H, C2-H), 1.44 (s, 3H, CH₃), 1.30 (s, 3H, CH₃); ¹³C NMR (126 MHz, CDCl₃) δ 174.3, 170.6, 167.2, 158.4, 137.1, 137.0, 129.0, 128.9, 128.7,

128.4, 128.1, 127.6, 127.5, 127.0, 114.7, 70.2, 61.4, 55.6, 52.6, 52.3, 41.9, 41.2, 24.4, 21.5; $[\alpha]_{\text{D}}^{25}$ -32.1 (c 1.0 CHCl₃); FT-IR (thin film) 3382 (NH), 2952 (C-H), 1739 (C=O), 1678 (C=O), 1514 (C=C aromatic), 1242/1145 (C(O)C), 1018 (C-H bend) cm⁻¹; MS (MALDI) 555.0 [M+K]⁺; HRMS (HNESP) exact mass calculated for [C₃₀H₃₂N₂O₆H] requires m/z 517.2333, found m/z 517.2318 [M+H]⁺.

8.9. Synthesis of α -arylglycinols

benzyl (2-hydroxy-1-(3-nitrophenyl)ethyl)carbamate (\pm)-(8.22)

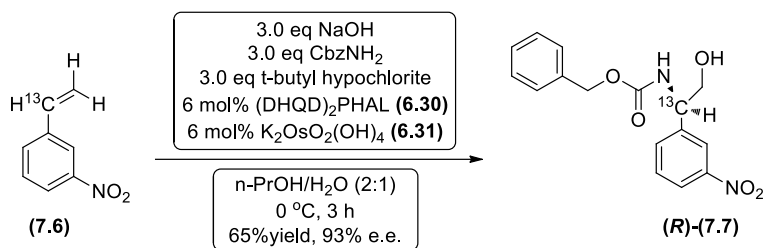


To a 25 mL round bottom flask, equipped with a magnetic stirrer bar, under nitrogen was added benzyl carbamate (365.0 mg, 2.41 mmol) and sodium hydroxide (97.0 mg, 2.41 mmol). 1-Propanol (2 mL) and distilled water (3 mL) were added *via* syringe and the mixture was cooled to 0 °C. Then *tert*-butyl hypochlorite (0.27 mL, 2.41 mmol) was added and the mixture was stirred at 0 °C for 10 minutes. Then a solution of (DHQ)₂PHAL (8.21) (18.8 mg, 0.02 mmol) and (DHQD)₂PHAL (6.30) (18.8 mg, 0.02 mmol) in 1-propanol (1 mL) was added, followed by a solution of 1-nitro-3-vinylbenzene (8.20) (120.0 mg, 0.80 mmol) in 1-propanol (3 mL). Potassium osmate dihydrate (6.31) (11.8 mg, 0.03 mmol) added at 0 °C and the reaction was stirred for 3 hours changing the colour from dark green to deep yellow. The mixture was quenched with saturated aqueous sodium sulfite solution (30 mL) at 0 °C, diluted with ethyl acetate (50 mL) and transferred into a 100 mL separating funnel. The organic layer was separated and washed with saturated brine (40 mL), dried with magnesium sulphate, filtered and the solvent removed under reduced pressure. The crude material was purified by flash chromatography on silica gel (30% ethyl acetate in 40-60 PET, $R_f = 0.29$) to afford a white solid. Subsequent physicochemical analysis confirmed this to be the title compound (\pm)-(8.22) (210.0 mg, 0.66 mmol, 83% yield).

¹H NMR (500 MHz, CDCl₃) δ 8.17 (s, 1H, ArH), 8.10 (d, *J* 7.9 Hz, 1H, ArH), 7.61 (d, *J* 6.8 Hz, 1H, ArH), 7.47 (t, *J* 7.9 Hz, 1H, ArH), 7.32 (br s, 5H, ArH), 6.00 (br s, 1H, NH), 5.11 – 5.02 (m, 2H, BnOCH₂), 4.89 (br s, 1H, C α -H), 3.86 (s, 1H, CH₂OH), 3.77 (s, 1H, CH₂OH), 2.70 (br s, 1H, OH); ¹³C NMR (126 MHz, CDCl₃) δ 156.5, 148.5, 142.1, 136.0, 133.2, 129.7, 128.6, 128.4, 128.2, 122.8, 121.7, 67.4, 65.4, 56.4; M.p. 84 – 86 °C (from diethyl ether) [lit. 85 – 86 °C]; FT-IR (thin film) 3396 (NH), 3317 (OH), 2945 (C-H), 1695 (C=O), 1531/1351 (NO₂), 1255 (C(O)C), 1056/902 (C-H bend) cm⁻¹.

The spectroscopic data is consistent with that reported in the literature.¹⁰¹

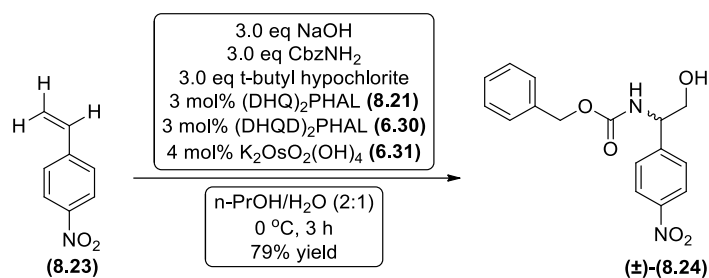
benzyl (*R*)-(α - ^{13}C -2-hydroxy-1-(3-nitrophenyl)ethyl)carbamate (*R*)-(7.7)



To a 25 mL round bottom flask, equipped with a magnetic stirrer bar, under nitrogen was added benzyl carbamate (91.0 mg, 0.60 mmol) and sodium hydroxide (24.0 mg, 0.60 mmol). 1-propanol (2 mL) and distilled water (3 mL) was added *via* syringe and the mixture was cooled to 0 °C. Then *tert*-butyl hypochlorite (0.07 mL, 0.60 mmol) was added and the mixture was stirred at 0 °C for 10 minutes. Then a solution of (DHQD)₂PHAL (**6.30**) (9.4 mg, 0.01 mmol) in 1-propanol (1 mL) was added, followed by a solution of α - ^{13}C -1-nitro-3-vinylbenzene (**7.6**) (30.0 mg, 0.20 mmol) in 1-propanol (3 mL). Potassium osmate dihydrate (**6.31**) (3.0 mg, 8.0 μmol) added at 0 °C and the reaction was stirred for 3 hours changing the colour from dark green to deep yellow. The mixture was quenched with saturated aqueous sodium sulfite solution (10 mL) at 0 °C, diluted with ethyl acetate (20 mL) and transferred into a 50 mL separating funnel. The organic layer was separated and washed with saturated brine (10 mL), dried with magnesium sulphate, filtered and the solvent removed under reduced pressure. The crude material was purified by flash chromatography on silica gel (30% ethyl acetate in 40-60 PET, $R_f = 0.29$) to afford a white solid. Subsequent physicochemical analysis confirmed this to be the title compound (*R*)-(7.7) (41.0 mg, 0.13 mmol, 65% yield). A sample was submitted to chiral analytical HPLC analysis [Cellulose 3, *iso*-hexane / *iso*-propanol : 90 / 10, 1 mL / min, 51.6 min (1st peak), 65.0 min (2nd peak), 93% e.e.].

¹H NMR (500 MHz, CDCl₃) δ 8.21 (s, 1H, ArH), 8.15 (d, J 7.9 Hz, 1H, ArH), 7.65 (s, 1H, ArH), 7.52 (t, J 7.9 Hz, 1H, ArH), 7.36 (s, 5H, ArH), 5.78 (s, 1H, NH), 5.22 – 4.97 (m, 2H, BnOCH₂), 4.92 (d, $J_{^{13}\text{C}-\text{H}}$ 136.1 Hz, 1H, $^{13}\text{C}\alpha$ -H), 4.03 – 3.70 (m, 2H, CH₂OH); ¹³C NMR (126 MHz, CDCl₃) δ 156.3, 148.6 (d, $J_{\text{C}-^{13}\text{C}}$ 4.3 Hz), 142.2, 136.1, 133.2, 129.8 (d, $J_{\text{C}-^{13}\text{C}}$ 3.9 Hz), 128.7, 128.5, 128.4, 122.9, 121.8 (d, $J_{\text{C}-^{13}\text{C}}$ 3.0 Hz), 67.4, 65.7 (d, $J_{\text{C}-^{13}\text{C}}$ 37.6 Hz), 56.3; M.p. 83 - 85 °C (from diethyl ether) [lit. 85 - 86 °C]; $[\alpha]_{\text{D}}^{24}$ -25.6 (c 0.5 CHCl₃); FT-IR (thin film) 3386 (OH), 2937 (C-H), 1698 (C=O), 1533/1350 (NO₂), 1254 (C(O)C), 1054/738 (C-H bend) cm⁻¹; MS (MALDI) 341.8 [M+Na]⁺; HRMS (HNESP) exact mass calculated for [C₁₅¹³C₁H₁₆N₂O₅H] requires m/z 318.1166, found m/z 318.1165 [M+H]⁺.

benzyl (2-hydroxy-1-(4-nitrophenyl)ethyl)carbamate (\pm)-(8.24)

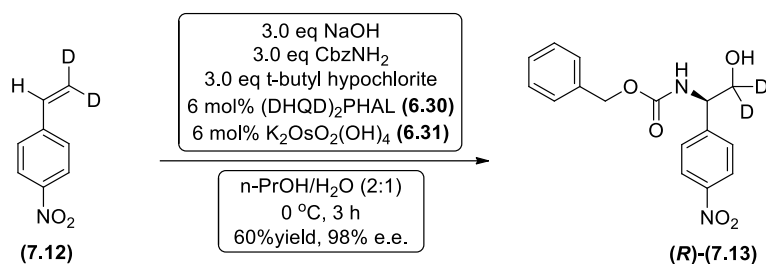


To a 25 mL round bottom flask, equipped with a magnetic stirrer bar, under nitrogen was added benzyl carbamate (304.0 mg, 2.01 mmol) and sodium hydroxide (80.0 mg, 2.01 mmol). 1-propanol (2 mL) and distilled water (3 mL) was added *via* syringe and the mixture was cooled to 0 °C. Then *tert*-butyl hypochlorite (0.23 mL, 2.01 mmol) was added and the mixture was stirred at 0 °C for 10 minutes. Then a solution of (DHQ)₂PHAL (8.21) (15.7 mg, 0.02 mmol) and (DHQD)₂PHAL (6.30) (15.7 mg, 0.02 mmol) in 1-propanol (1 mL) was added, followed by a solution of 1-nitro-3-vinylbenzene (8.23) (100.0 mg, 0.67 mmol) in 1-propanol (3 mL). Potassium osmate dihydrate (6.31) (9.9 mg, 0.03 mmol) added at 0 °C and the reaction was stirred for 3 hours changing the colour from dark green to deep yellow. The mixture was quenched with saturated aqueous sodium sulfite solution (30 mL) at 0 °C, diluted with ethyl acetate (50 mL) and transferred into a 100 mL separating funnel. The organic layer was separated and washed with saturated brine (40 mL), dried with magnesium sulphate, filtered and the solvent removed under reduced pressure. The crude material was purified by flash chromatography on silica gel (30% ethyl acetate in 40-60 PET, R_f = 0.31) to afford a white solid. Subsequent physicochemical analysis confirmed this to be the title compound (\pm)-(8.24) (167.0 mg, 0.53 mmol, 79% yield).

¹H NMR (500 MHz, CDCl₃) δ 8.16 (d, *J* 7.7 Hz, 2H, ArH), 7.46 (d, *J* 6.8 Hz, 2H, ArH), 7.34 (br s, 5H, ArH), 5.84 (s, 1H, NH), 5.10 (d, *J* 11.4 Hz, 1H, BnOCHH), 5.06 (d, *J* 11.4 Hz, 1H, BnOCHH), 4.89 (s, 1H, C α -H), 3.97 – 3.74 (m, 2H, CH₂OH), 2.30 (br s, OH); ¹³C NMR (126 MHz, CDCl₃) δ 156.4, 147.5, 147.2, 136.1, 128.7, 128.5, 128.3, 127.7, 123.9, 67.4, 65.5, 56.5; M.p. 114 - 116 °C (from diethyl ether) [lit. 110 - 111 °C]; FT-IR (thin film) 3396 (NH), 3319 (OH), 3068 (C-H), 1965 (C=O), 1520/1349 (NO₂), 1258 (C(O)C), 1056/854 (C-H bend) cm⁻¹.

The spectroscopic data is consistent with that reported in the literature.¹⁰¹

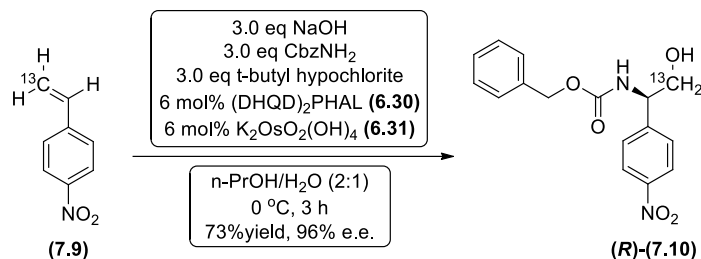
benzyl (*R*)-(2,2-di-²H-2-hydroxy-1-(4-nitrophenyl)ethyl)carbamate (*R*)-(7.13)



To a 25 mL round bottom flask, equipped with a magnetic stirrer bar, under nitrogen was added benzyl carbamate (90.0 mg, 0.60 mmol) and sodium hydroxide (23.8 mg, 0.60 mmol). 1-propanol (2 mL) and distilled water (3 mL) was added *via* syringe and the mixture was cooled to 0 °C. Then *tert*-butyl hypochlorite (0.07 mL, 0.60 mmol) was added and the mixture was stirred at 0 °C for 10 minutes. Then a solution of (DHQD)₂PHAL (**6.30**) (9.3 mg, 0.01 mmol) in 1-propanol (1 mL) was added, followed by a solution of 1-(β-di-²H-vinyl)-4-nitrobenzene (**7.12**) (30.0 mg, 0.20 mmol) in 1-propanol (3 mL). Potassium osmate dihydrate (**6.31**) (2.9 mg, 7.9 μmol) added at 0 °C and the reaction was stirred for 3 hours changing the colour from dark green to deep yellow. The mixture was quenched with saturated aqueous sodium sulfite solution (10 mL) at 0 °C, diluted with ethyl acetate (20 mL) and transferred into a 50 mL separating funnel. The organic layer was separated and washed with saturated brine (10 mL), dried with magnesium sulphate, filtered and the solvent removed under reduced pressure. The crude material was purified by flash chromatography on silica gel (30% ethyl acetate in 40-60 PET, R_f = 0.31) to afford a white solid. Subsequent physicochemical analysis confirmed this to be the title compound (**(R)**-(7.13) (38.0 mg, 0.12 mmol, 60% yield). A sample was submitted to chiral analytical HPLC analysis [Cellulose 3, *iso*-hexane / *iso*-propanol : 90 / 10, 1 mL / min, 51.2 min (1st peak), 55.0 min (2nd peak), 98% e.e.].

¹H NMR (500 MHz, CDCl₃) δ 8.20 (d, *J* 7.4 Hz, 2H, ArH), 7.49 (d, *J* 7.4 Hz, 2H, ArH), 7.35 (br s, 5H, ArH), 5.70 (d, *J* 6.4 Hz, 1H, NH), 5.12 (d, *J* 11.3 Hz, 1H, BnOCHH), 5.07 (d, *J* 11.3 Hz, 1H, BnOCHH), 4.91 (s, 1H, C α -H), 1.85 (br s, 1H, OH); ¹³C NMR (126 MHz, CDCl₃) δ 156.3, 147.5, 147.2, 136.1, 128.7, 128.5, 128.4, 127.7, 124.0, 67.4, 64.9 (t, *J*_{C-D} 22.1 Hz), 56.4; ²H NMR (77 MHz, CH₂Cl₂) δ 7.26 (CDCl₃ ref), 3.87 (br s), 3.76 (br s); M.p. 119 - 121 °C (from diethyl ether); [α]_D²⁵ -26.3 (c 0.5 CHCl₃); FT-IR (thin film) 3334 (OH), 2951 (C-H), 1695 (C=O), 1520/1349 (NO₂), 1270 (C(O)C), 1061/854 (C-H bend) cm⁻¹; MS (MALDI) 342.0 [M+Na]⁺; HRMS (HASP) exact mass calculated for [C₁₆H₁₄²H₂N₂O₅H] requires *m/z* 319.1258, found *m/z* 319.1259 [M+H]⁺.

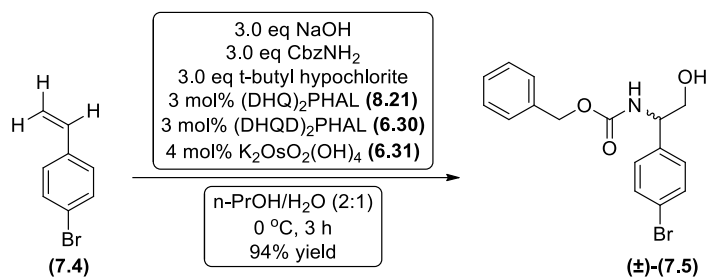
benzyl (*R*)-(2-¹³C-2-hydroxy-1-(4-nitrophenyl)ethyl)carbamate (*R*)-(7.10)



To a 25 mL round bottom flask, equipped with a magnetic stirrer bar, under nitrogen was added benzyl carbamate (151.0 mg, 1.00 mmol) and sodium hydroxide (40.0 mg, 1.00 mmol). 1-propanol (2 mL) and distilled water (3 mL) was added *via* syringe and the mixture was cooled to 0 °C. Then *tert*-butyl hypochlorite (0.11 mL, 1.00 mmol) was added and the mixture was stirred at 0 °C for 10 minutes. Then a solution of (DHQD)₂PHAL (**6.30**) (15.6 mg, 0.02 mmol) in 1-propanol (1 mL) was added, followed by a solution of 1-(β-¹³C-vinyl)-4-nitrobenzene (**7.9**) (50.0 mg, 0.33 mmol) in 1-propanol (3 mL). Potassium osmate dihydrate (**6.31**) (4.9 mg, 13.0 μmol) added at 0 °C and the reaction was stirred for 3 hours changing the colour from dark green to deep yellow. The mixture was quenched with saturated aqueous sodium sulfite solution (10 mL) at 0 °C, diluted with ethyl acetate (20 mL) and transferred into a 50 mL separating funnel. The organic layer was separated and washed with saturated brine (10 mL), dried with magnesium sulphate, filtered and the solvent removed under reduced pressure. The crude material was purified by flash chromatography on silica gel (30% ethyl acetate in 40-60 PET, R_f = 0.31) to afford a white solid. Subsequent physicochemical analysis confirmed this to be the title compound (*R*)-(7.10) (77.0 mg, 0.24 mmol, 73% yield). A sample was submitted to chiral analytical HPLC analysis [Cellulose 3, *iso*-hexane / *iso*-propanol : 90 / 10, 1 mL / min, 51.7 min (1st peak), 55.0 min (2nd peak), 96% e.e.].

¹H NMR (500 MHz, CDCl₃) δ 8.20 (d, *J* 7.8 Hz, 2H, ArH), 7.49 (d, *J* 7.8 Hz, 2H, ArH), 7.36 (s, 5H, ArH), 5.73 (s, 1H, NH), 5.12 (d, *J* 12.1 Hz, 1H, BnOCHH), 5.07 (d, *J* 12.1 Hz, 1H, BnOCHH), 4.92 (br s, 1H, Cα-H), 3.96 (dd, *J*_{13C-H} 147.0, *J* 12.5 Hz, 1H, ¹³CH₂OH), 3.85 (dd, *J*_{13C-H} 143.4, *J* 9.5 Hz, 1H, ¹³CH₂OH); ¹³C NMR (126 MHz, CDCl₃) δ 156.2, 147.6, 147.2, 136.1, 128.7, 128.5, 128.4, 127.7, 124.1, 67.4, 65.7, 48.7; M.p. 115 - 117 °C (from diethyl ether); [α]_D²⁵ -28.9 (c 0.5 CHCl₃); FT-IR (thin film) 3396 (OH), 2935 (C-H), 1695 (C=O), 1520/1348 (NO₂), 1258 (C(O)C), 1045/853 (C-H bend) cm⁻¹; MS (MALDI) 358.7 [M+K]⁺; HRMS (HASP) exact mass calculated for [C₁₅¹³C₁H₁₆N₂O₅H] requires *m/z* 318.1166, found *m/z* 318.1168 [M+H]⁺.

benzyl (1-(4-bromophenyl)-2-hydroxyethyl)carbamate (±)-(7.5)

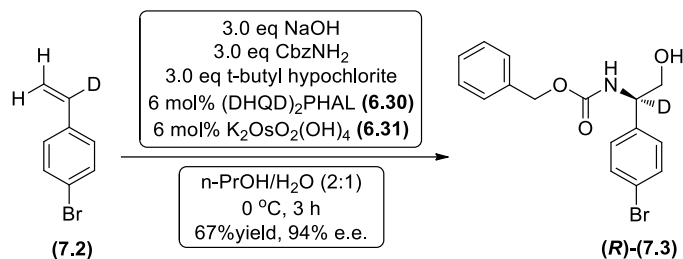


To a 25 mL round bottom flask, equipped with a magnetic stirrer bar, under nitrogen was added benzyl carbamate (248.0 mg, 1.64 mmol) and sodium hydroxide (65.6 mg, 1.64 mmol). 1-propanol (2 mL) and distilled water (3 mL) was added *via* syringe and the mixture was cooled to 0 °C. Then *tert*-butyl hypochlorite (0.19 mL, 1.64 mmol) was added and the mixture was stirred at 0 °C for 10 minutes. Then a solution of (DHQ)₂PHAL (8.21) (10.6 mg, 14 μmol) and (DHQD)₂PHAL (6.30) (10.6 mg, 14 μmol) in 1-propanol (1 mL) was added, followed by a solution of 1-bromo-4-vinylbenzene (7.4) (100.0 mg, 0.55 mmol) in 1-propanol (3 mL). Potassium osmate dihydrate (6.31) (8.0 mg, 0.02 mmol) added at 0 °C and the reaction was stirred for 3 hours changing the colour from dark green to deep yellow. The mixture was quenched with saturated aqueous sodium sulfite solution (30 mL) at 0 °C, diluted with ethyl acetate (50 mL) and transferred into a 100 mL separating funnel. The organic layer was separated and washed with saturated brine (40 mL), dried with magnesium sulphate, filtered and the solvent removed under reduced pressure. The crude material was purified by flash chromatography on silica gel (20% ethyl acetate in 40-60 PET, R_f = 0.25) to afford a white solid. Subsequent physicochemical analysis confirmed this to be the title compound (±)-(7.5) (179.0 mg, 0.51 mmol, 94% yield).

¹H NMR (500 MHz, CDCl₃) δ 7.47 (d, *J* 8.2 Hz, 2H, ArH), 7.35 (s, 5H, ArH), 7.18 (d, *J* 8.2 Hz, 2H, ArH), 5.55 (d, *J* 4.7 Hz, 1H, NH), 5.09 (m, 2H, BnOCH₂), 4.79 (s, 1H, Cα-H), 3.85 (m, 2H, CH₂OH); ¹³C NMR (126 MHz, CDCl₃) δ 156.4, 138.5, 136.2, 132.0, 128.7, 128.5, 128.4, 121.9, 67.3, 66.1, 56.6; M.p. 128 - 130 °C (from diethyl ether) [lit. 133 - 134 °C]; FT-IR (thin film) 3318 (OH), 1695 (C=O), 1541/1490 (C=C aromatic), 1270 (C(O)C), 1055/698 (C-H bend) cm⁻¹; HRMS (HNESP) exact mass calculated for [C₁₆H₁₆⁷⁹BrN₁O₃H] requires *m/z* 350.0386, found *m/z* 350.0390 [M+H]⁺.

The spectroscopic data is consistent with that reported in the literature.¹⁰¹

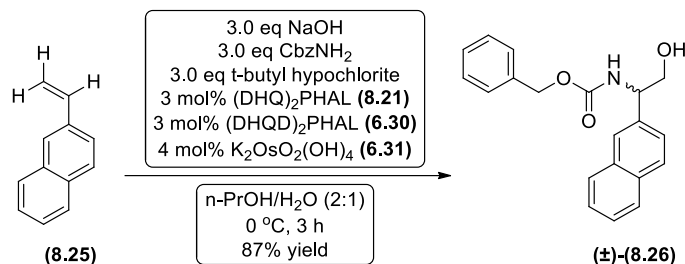
benzyl (*R*)-(1-²H-1-(4-bromophenyl)-2-hydroxyethyl)carbamate (*R*)-(7.3)



To a 25 mL round bottom flask, equipped with a magnetic stirrer bar, under nitrogen was added benzyl carbamate (246.0 mg, 1.63 mmol) and sodium hydroxide (65.0 mg, 1.63 mmol). 1-propanol (2 mL) and distilled water (3 mL) was added *via* syringe and the mixture was cooled to 0 °C. Then *tert*-butyl hypochlorite (0.18 mL, 1.63 mmol) was added and the mixture was stirred at 0 °C for 10 minutes. Then a solution of (DHQD)₂PHAL (**6.30**) (25.4 mg, 0.03 mmol) in 1-propanol (1 mL) was added, followed by a solution of α -²H-1-bromo-4-vinylbenzene (**7.2**) (100.0 mg, 0.54 mmol) in 1-propanol (3 mL). Potassium osmate dihydrate (**6.31**) (8.0 mg, 0.02 mmol) added at 0 °C and the reaction was stirred for 3 hours changing the colour from dark green to deep yellow. The mixture was quenched with saturated aqueous sodium sulfite solution (10 mL) at 0 °C, diluted with ethyl acetate (20 mL) and transferred into a 50 mL separating funnel. The organic layer was separated and washed with saturated brine (10 mL), dried with magnesium sulphate, filtered and the solvent removed under reduced pressure. The crude material was purified by flash chromatography on silica gel (20% ethyl acetate in 40-60 PET, R_f = 0.25) to afford a white solid. Subsequent physicochemical analysis confirmed this to be the title compound (*R*)-(7.3) (129.0 mg, 0.37 mmol, 67% yield). A sample was submitted to chiral analytical HPLC analysis [Cellulose 3, *iso*-hexane / *iso*-propanol : 90 / 10, 1 mL / min, 25.9 min (1st peak), 28.3 min (2nd peak), 94% e.e.].

¹H NMR (500 MHz, CDCl₃) δ 7.46 (d, *J* 7.9 Hz, 2H, ArH), 7.34 (m, 5H, ArH), 7.16 (d, *J* 7.9 Hz, 2H, ArH), 5.63 (s, 1H, NH), 5.10 (d, *J* 11.9 Hz, 1H, BnOCHH), 5.06 (d, *J* 11.9 Hz, 1H, BnOCHH), 3.80 (m, 2H, CH₂OH); ¹³C NMR (126 MHz, CDCl₃) δ 156.4, 138.4, 136.2, 132.0, 131.8, 128.7, 128.5, 127.7, 121.8, 67.2, 66.0, 56.2 (m); ²H NMR (77 MHz, CH₂Cl₂) δ 7.26 (CDCl₃ ref), 4.69 (br s); M.p. 125 - 127 °C (from diethyl ether); [α]_D²⁵ -21.1 (c 0.5 CHCl₃); FT-IR (thin film) 3318 (OH), 2942 (C-H), 1688 (C=O), 1532 (C=C aromatic), 1270 (C(O)C), 1047/824 (C-H bend) cm⁻¹; HRMS (HNESP) exact mass calculated for [C₁₆H₁₅²H₁⁷⁹Br₁N₁O₃H] requires *m/z* 351.0449, found *m/z* 351.0452 [M+H]⁺.

benzyl (2-hydroxy-1-(naphthalen-2-yl)ethyl)carbamate (±)-(8.26)

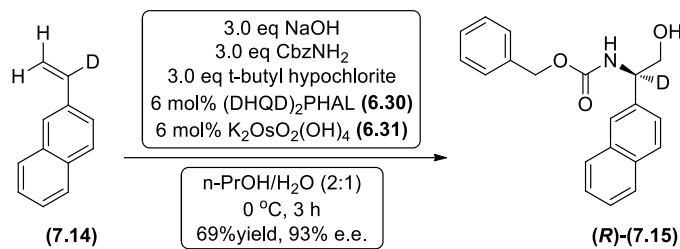


To a 25 mL round bottom flask, equipped with a magnetic stirrer bar, under nitrogen was added benzyl carbamate (294.0 mg, 1.95 mmol) and sodium hydroxide (78.0 mg, 1.95 mmol). 1-propanol (2 mL) and distilled water (3 mL) was added *via* syringe and the mixture was cooled to 0 °C. Then *tert*-butyl hypochlorite (0.22 mL, 1.95 mmol) was added and the mixture was stirred at 0 °C for 10 minutes. Then a solution of (DHQ)₂PHAL (8.21) (15.1 mg, 19 μmol) and (DHQD)₂PHAL (6.30) (15.1 mg, 19 μmol) in 1-propanol (1 mL) was added, followed by a solution of 2-vinylnaphthalene (8.25) (100.0 mg, 0.55 mmol) in 1-propanol (3 mL). Potassium osmate dihydrate (6.31) (9.6 mg, 26 μmol) added at 0 °C and the reaction was stirred for 3 hours changing the colour from dark green to deep yellow. The mixture was quenched with saturated aqueous sodium sulfite solution (30 mL) at 0 °C, diluted with ethyl acetate (50 mL) and transferred into a 100 mL separating funnel. The organic layer was separated and washed with saturated brine (40 mL), dried with magnesium sulphate, filtered and the solvent removed under reduced pressure. The crude material was purified by flash chromatography on silica gel (25% ethyl acetate in 40-60 PET, R_f = 0.24) to afford a white solid. Subsequent physicochemical analysis confirmed this to be the title compound (±)-(8.26) (181.0 mg, 0.56 mmol, 87% yield).

¹H NMR (500 MHz, CDCl₃) δ 7.84 – 7.77 (m, 3H, ArH), 7.73 (s, 1H, ArH), 7.50 – 7.46 (m, 2H, ArH), 7.46 – 7.26 (m, 6H, ArH), 5.82 (s, 1H, NH), 5.10 (m, 2H, BnOCH₂), 4.99 (s, 1H, C α -H), 3.87 (m, 2H, CH₂OH), 2.61 (s, 1H, OH); ¹³C NMR (126 MHz, CDCl₃) δ 156.6, 136.7, 136.3, 133.4, 133.0, 128.7, 128.6, 128.3, 128.0, 127.7, 126.4, 126.2, 125.5, 124.6, 67.1, 66.2, 57.3; M.p. 141 - 143 °C (from diethyl ether) [lit. 146 - 147 °C]; FT-IR (thin film) 3397 (NH), 3322 (OH), 2947 (C-H), 1695 (C=O), 1532 (C=C aromatic), 1260 (C(O)C), 1055/745 (C-H bend) cm⁻¹; HRMS (HNESP) exact mass calculated for [C₂₀H₁₉N₁O₃H] requires *m/z* 322.1438, found *m/z* 322.1441 [M+H]⁺.

The spectroscopic data is consistent with that reported in the literature.¹⁰¹

benzyl (*R*)-(1-²H-2-hydroxy-1-(naphthalen-2-yl)ethyl)carbamate (*R*)-(7.15)

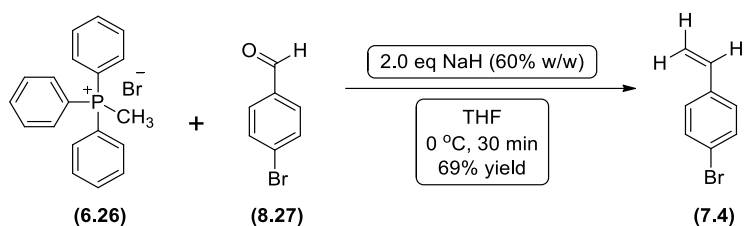


To a 25 mL round bottom flask, equipped with a magnetic stirrer bar, under nitrogen was added benzyl carbamate (467.0 mg, 3.10 mmol) and sodium hydroxide (124.0 mg, 3.10 mmol). 1-propanol (2 mL) and distilled water (3 mL) was added *via* syringe and the mixture was cooled to 0 °C. Then *tert*-butyl hypochlorite (0.35 mL, 3.10 mmol) was added and the mixture was stirred at 0 °C for 10 minutes. Then a solution of (DHQD)₂PHAL (**6.30**) (48.2 mg, 0.06 mmol) in 1-propanol (1 mL) was added, followed by a solution of α -²H-2-vinylnaphthalene (**7.14**) (160.0 mg, 1.03 mmol) in 1-propanol (3 mL). Potassium osmate dihydrate (**6.31**) (15.2 mg, 0.04 mmol) added at 0 °C and the reaction was stirred for 3 hours changing the colour from dark green to deep yellow. The mixture was quenched with saturated aqueous sodium sulfite solution (10 mL) at 0 °C, diluted with ethyl acetate (20 mL) and transferred into a 50 mL separating funnel. The organic layer was separated and washed with saturated brine (10 mL), dried with magnesium sulphate, filtered and the solvent removed under reduced pressure. The crude material was purified by flash chromatography on silica gel (20% ethyl acetate in 40-60 PET, R_f = 0.25) to afford a white solid. Subsequent physicochemical analysis confirmed this to be the title compound (*R*)-(7.15) (228.0 mg, 0.70 mmol, 69% yield). A sample was submitted to chiral analytical HPLC analysis [Cellulose 3, *iso*-hexane / *iso*-propanol : 85 / 15, 1 mL / min, 36.0 min (1st peak), 45.6 min (2nd peak), 93% e.e.].

¹H NMR (500 MHz, CDCl₃) δ 7.80 (q, *J* 7.0 Hz, 3H, ArH), 7.73 (s, 1H, ArH), 7.57 – 7.46 (m, 2H, ArH), 7.48 – 7.24 (m, 6H, ArH), 5.81 (s, 1H, NH), 5.12 (d, *J* 12.0 Hz, 1H, BnOCHH), 5.08 (d, *J* 12.0 Hz, 1H, BnOCHH), 3.87 (m, 2H, CH₂OH), 2.62 (s, 1H, OH), ¹³C NMR (126 MHz, CDCl₃) δ 156.6, 136.6, 136.3, 133.4, 133.0, 128.7, 128.6, 128.3, 128.0, 127.7, 126.5, 126.2, 125.5, 124.6, 67.2, 66.2, 56.9 (m); ²H NMR (77 MHz, CH₂Cl₂) δ 7.26 (CDCl₃ ref), 4.89 (br s); M.p. 139 - 141 °C (from diethyl ether); [α]_D²⁵ - 7.9 (c 0.5 CHCl₃); FT-IR (thin film) 3332 (OH), 3058 (C-H), 1687 (C=O), 1531 (C=C aromatic), 1264 (C(O)C), 1085/748 (C-H bend) cm⁻¹; HRMS (HNESP) exact mass calculated for [C₂₀H₁₈²H₁N₁O₃H] requires *m/z* 323.1500, found *m/z* 323.1504 [M+H]⁺.

8.10. Synthesis of styrenes

1-bromo-4-vinylbenzene (7.4)

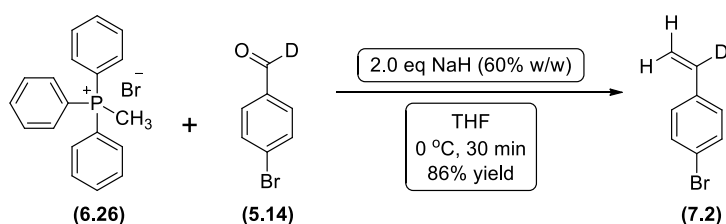


To a 25 mL flame dried round bottom flask, equipped with a magnetic stirrer bar, under nitrogen was added methyltriphenylphosphonium bromide (**6.26**) (772.0 mg, 2.16 mmol). Anhydrous tetrahydrofuran (10 mL) was added *via* syringe and the reaction was cooled to 0 °C. Then sodium hydride (60% w/w in mineral oil) (83.0 mg, 2.16 mmol) was added and the mixture was stirred at 0 °C for 10 minutes. Then 4-bromobenzaldehyde (**8.27**) (0.2 g, 1.08 mmol) was added and the mixture was stirred at 0 °C for 30 minutes. The reaction mixture was diluted with ethyl acetate (30 mL), transferred into a 50 mL separating funnel, washed with saturated brine (10 mL), dried with magnesium sulphate, filtered and the solvent removed under reduced pressure. The crude material was purified by flash chromatography on silica gel (20% diethyl ether in 40-60 PET, $R_f = 0.40$) to afford a colourless oil. Subsequent physicochemical analysis confirmed this to be the title compound (**7.4**) (137.0 mg, 0.75 mmol, 69% yield).

^1H NMR (500 MHz, CDCl_3) δ 7.48 – 7.42 (m, 2H, ArH), 7.30 – 7.26 (m, 2H, ArH), 6.66 (dd, J 17.6, 10.9 Hz, 1H, $\text{C}_\alpha\text{-H}$), 5.74 (dd, J 17.6, 0.6 Hz, 1H, $\text{C}_\beta\text{-H}$), 5.28 (dd, J 10.9, 0.6 Hz, 1H, $\text{C}_\beta\text{-H}$); ^{13}C NMR (126 MHz, CDCl_3) δ 136.6, 135.9, 131.7, 127.9, 121.7, 114.7.

The spectroscopic data is consistent with that reported in the literature.²⁵⁹

α - ^2H -1-bromo-4-vinylbenzene (7.2)

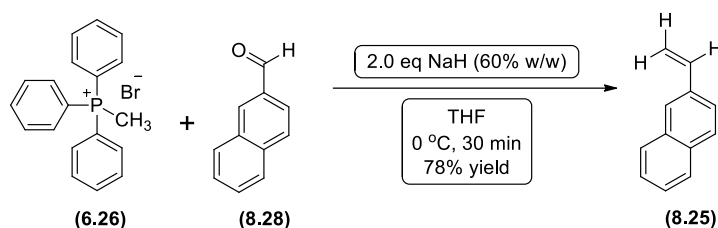


To a 25 mL flame dried round bottom flask, equipped with a magnetic stirrer bar, under nitrogen was added methyltriphenylphosphonium bromide (**6.26**) (960.0 mg, 2.70

mmol). Anhydrous tetrahydrofuran (10 mL) was added *via* syringe and the reaction was cooled to 0 °C. Then sodium hydride (60% w/w in mineral oil) (103.0 mg, 2.70 mmol) was added and the mixture was stirred at 0 °C for 10 minutes. Then α -²H-4-bromobenzaldehyde (**5.14**) (250.0 mg, 1.35 mmol) was added and the mixture was stirred at 0 °C for 30 minutes. The reaction mixture was diluted with ethyl acetate (30 mL), transferred into a 50 mL separating funnel, washed with saturated brine (10 mL), dried with magnesium sulphate, filtered and the solvent removed under reduced pressure. The crude material was purified by flash chromatography on silica gel (20% diethyl ether in 40-60 PET, $R_f = 0.40$) to afford a colourless oil. Subsequent physicochemical analysis confirmed this to be the title compound (**7.2**) (213.0 mg, 1.16 mmol, 86% yield).

¹H NMR (500 MHz, CDCl₃) δ 7.46 (d, J 8.4 Hz, 2H, ArH), 7.28 (d, J 8.4 Hz, 2H, ArH), 5.75 (s, 1H, C $_{\beta}$ -H), 5.29 (s, 1H, C $_{\beta}$ -H); ¹³C NMR (126 MHz, CDCl₃) δ 136.5, 135.5 (t, J_{C-D} 23.7 Hz), 131.7, 127.8, 121.7, 114.6; ²H NMR (77 MHz, CH₂Cl₂) δ 7.26 (CDCl₃ ref), 6.67 (br s); IR (thin film) 2954 (C-H), 2925 (H₂C=C-H), 1615/1464 (C=C aromatic), 1070/831 (C-H bend) cm⁻¹; HRMS (HNESP) exact mass calculated for [C₈H₆²H₁⁷⁹Br₁H] requires m/z 185.9846, found m/z 185.9861 [M+H]⁺.

2-vinylnaphthalene (**8.25**)

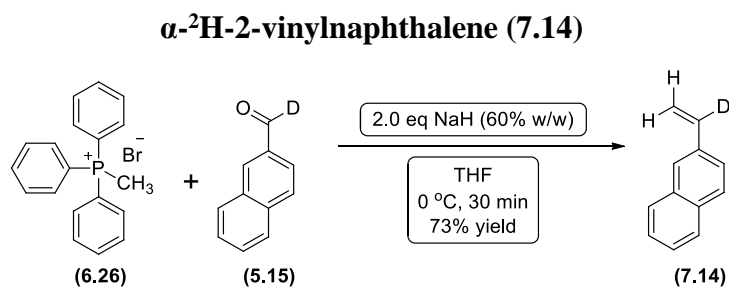


To a 25 mL flame dried round bottom flask, equipped with a magnetic stirrer bar, under nitrogen was added methyltriphenylphosphonium bromide (**6.26**) (915.0 mg, 2.56 mmol). Anhydrous tetrahydrofuran (10 mL) was added *via* syringe and the reaction was cooled to 0 °C. Then sodium hydride (60% w/w in mineral oil) (98.0 mg, 2.56 mmol) was added and the mixture was stirred at 0 °C for 10 minutes. Then 2-naphthalenecarbaldehyde (**8.28**) (0.2 g, 1.28 mmol) was added and the mixture was stirred at 0 °C for 30 minutes. The reaction mixture was diluted with ethyl acetate (30 mL), transferred into a 50 mL separating funnel, washed with saturated brine (10 mL), dried with magnesium sulphate, filtered and the solvent removed under reduced pressure. The

crude material was purified by flash chromatography on silica gel (15% diethyl ether in 40-60 PET, $R_f = 0.35$) to afford a colourless oil. Subsequent physicochemical analysis confirmed this to be the title compound (**8.25**) (154.0 mg, 1.00 mmol, 78% yield).

^1H NMR (500 MHz, CDCl_3) δ 7.83 (t, J 8.4, 3H, ArH), 7.80 (s, 1H, ArH), 7.69 (d, J 8.4 Hz, 1H, ArH), 7.50 (m, 2H, ArH), 6.94 (dd, J 18.3, 11.5 Hz, 1H, $\text{C}_\alpha\text{-H}$), 5.93 (dd, J 17.5, 3.1 Hz, 1H, $\text{C}_\beta\text{-H}$); ^{13}C NMR (126 MHz, CDCl_3) δ 137.1, 135.1, 133.7, 133.3, 128.3, 128.2, 127.8, 126.5, 126.3, 126.0, 123.3, 114.3.

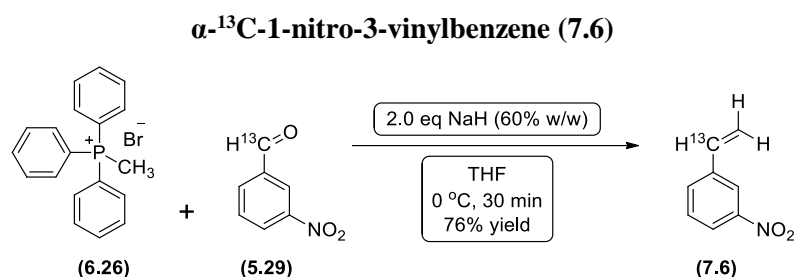
The spectroscopic data is consistent with that reported in the literature.²⁶⁰



To a 25 mL flame dried round bottom flask, equipped with a magnetic stirrer bar, under nitrogen was added methyltriphenylphosphonium bromide (**6.26**) (1.1 g, 3.18 mmol). Anhydrous tetrahydrofuran (10 mL) was added *via* syringe and the reaction was cooled to 0 °C. Then sodium hydride (60% w/w in mineral oil) (122.0 mg, 3.18 mmol) was added and the mixture was stirred at 0 °C for 10 minutes. Then α - ^2H -2-naphthaldehyde (**5.15**) (250.0 mg, 1.59 mmol) was added and the mixture was stirred at 0 °C for 30 minutes. The reaction mixture was diluted with ethyl acetate (30 mL), transferred into a 50 mL separating funnel, washed with saturated brine (10 mL), dried with magnesium sulphate, filtered and the solvent removed under reduced pressure. The crude material was purified by flash chromatography on silica gel (15% diethyl ether in 40-60 PET, $R_f = 0.35$) to afford a colourless oil. Subsequent physicochemical analysis confirmed this to be the title compound (**7.14**) (181.0 mg, 1.16 mmol, 73% yield).

^1H NMR (500 MHz, CDCl_3) δ 7.94 (t, J 8.5 Hz, 3H, ArH), 7.89 (s, 1H, ArH), 7.80 (d, J 8.5 Hz, 1H, ArH), 7.69 – 7.51 (m, 2H, ArH), 6.04 (s, 1H, $\text{C}_\beta\text{-H}$), 5.50 (s, 1H, $\text{C}_\beta\text{-H}$); ^{13}C NMR (126 MHz, CDCl_3) δ 136.7 (t, $J_{\text{C-D}}$ 23.6 Hz), 135.0, 133.6, 133.2, 128.2, 128.1, 127.7, 126.5, 126.3, 126.0, 123.2, 114.0; ^2H NMR (77 MHz, CH_2Cl_2) δ 7.26 (CDCl_3 ref), 6.98 (br s); IR (thin film) 3054 (C-H), 2951 ($\text{H}_2\text{C}=\text{C-H}$), 1615/1506 (C=C)

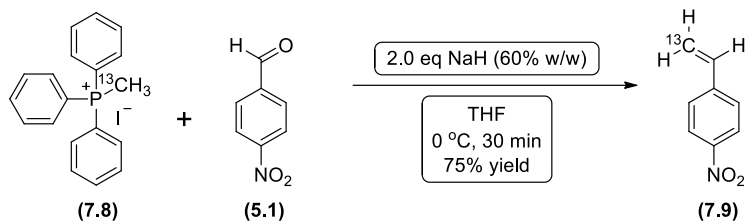
aromatic), 1264/895 (C-H bend) cm^{-1} ; HRMS (HASP) exact mass calculated for $[\text{C}_{12}\text{H}_9^2\text{H}_1\text{H}]$ requires m/z 156.0918, found m/z 156.0917 $[\text{M}+\text{H}]^+$.



To a 25 mL flame dried round bottom flask, equipped with a magnetic stirrer bar, under nitrogen was added methyltriphenylphosphonium bromide (**6.26**) (282.0 mg, 0.79 mmol). Anhydrous tetrahydrofuran (10 mL) was added *via* syringe and the reaction was cooled to 0 °C. Then sodium hydride (60 % w/w in mineral oil) (30.2 mg, 0.79 mmol) was added and the mixture was stirred at 0 °C for 10 minutes. Then α - ^{13}C -3-nitrobenzaldehyde (**5.29**) (60.0 mg, 0.39 mmol) was added and the mixture was stirred at 0 °C for 30 minutes. The reaction mixture was diluted with ethyl acetate (30 mL), transferred into a 50 mL separating funnel, washed with saturated brine (10 mL), dried with magnesium sulphate, filtered and the solvent removed under reduced pressure. The crude material was purified by flash chromatography on silica gel (20% diethyl ether in 40-60 PET, $R_f = 0.5$) to afford a pale yellow oil. Subsequent physicochemical analysis confirmed this to be the title compound (**7.6**) (45.0 mg, 0.30 mmol, 76% yield).

^1H NMR (500 MHz, CDCl_3) δ 8.30 – 8.19 (m, 1H, ArH), 8.17 – 8.04 (m, 1H, ArH), 7.76 – 7.65 (m, 1H, ArH), 7.56 – 7.44 (m, 1H, ArH), 6.77 (ddd, $J_{^{13}\text{C}-\text{H}}$ 156.8, J 17.5, 10.9 Hz, 1H, $\text{C}_\alpha\text{-H}$), 5.90 (dd, J 17.5, 3.2 Hz, 1H, $\text{C}_\beta\text{-H}$), 5.44 (dd, J 10.9, 4.3 Hz, 1H, $\text{C}_\beta\text{-H}$); ^{13}C NMR (126 MHz, CDCl_3) δ 148.7, 139.4 (d, $J_{\text{C}-^{13}\text{C}}$ 55.6 Hz), 134.8, 132.2, 129.6 (d, $J_{\text{C}-^{13}\text{C}}$ 4.5 Hz), 122.5, 121.0, 117.2 (d, $J_{\text{C}-^{13}\text{C}}$ 70.2 Hz); IR (thin film) 3091 (C-H), 2925 ($\text{H}_2\text{C}=\text{C}-\text{H}$), 1532/1350 (NO_2), 1097/920 (C-H bend) cm^{-1} ; HRMS (HASP) exact mass calculated for $[\text{C}_7^{13}\text{C}_1\text{H}_7\text{N}_1\text{O}_2\text{H}]$ requires m/z 151.0583, found m/z 151.0580 $[\text{M}+\text{H}]^+$.

β -¹³C-1-nitro-3-vinylbenzene (7.9)



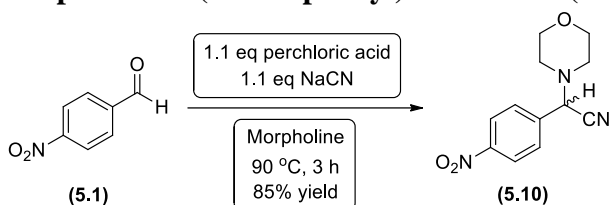
To a 25 mL flame dried round bottom flask, equipped with a magnetic stirrer bar, under nitrogen was added ¹³C-labelled methyltriphenylphosphonium iodide (**7.8**) (375.0 mg, 0.92 mmol). Anhydrous tetrahydrofuran (10 mL) was added *via* syringe and the reaction was cooled to 0 °C. Then sodium hydride (60 % w/w in mineral oil) (35.5 mg, 0.92 mmol) was added and the mixture was stirred at 0 °C for 10 minutes. Then 4-nitrobenzaldehyde (**5.1**) (70.0 mg, 0.46 mmol) was added and the mixture was stirred at 0 °C for 30 minutes. The reaction mixture was diluted with ethyl acetate (30 mL), transferred into a 50 mL separating funnel, washed with saturated brine (10 mL), dried with magnesium sulphate, filtered and the solvent removed under reduced pressure. The crude material was purified by flash chromatography on silica gel (20% diethyl ether in 40-60 PET, $R_f = 0.45$) to afford a yellow oil. Subsequent physicochemical analysis confirmed this to be the title compound (**7.9**) (52.0 mg, 0.35 mmol, 75% yield).

¹H NMR (500 MHz, CDCl₃) δ 8.22 – 8.17 (m, 2H, ArH), 7.56 – 7.52 (m, 2H, ArH), 6.78 (dd, J 17.6, 10.9 Hz, 1H, C $_{\alpha}$ -H), 5.93 (dd, $J_{13\text{C-H}}$ 155.2, 17.6 Hz, 1H, C $_{\beta}$ -H), 5.50 (dd, $J_{13\text{C-H}}$ 161.8, 10.9 Hz, 1H, C $_{\beta}$ -H); ¹³C NMR (126 MHz, CDCl₃) δ 143.9, 135.1 (d, $J_{\text{C-}^{13}\text{C}}$ 69.5 Hz), 132.7, 126.9 (d, $J_{\text{C-}^{13}\text{C}}$ 4.3 Hz), 124.1, 118.7; IR (thin film) 3079 (C-H), 2931 (H₂C=C-H), 1515/1345 (NO₂), 1110/858 (C-H bend) cm⁻¹; HRMS (HASP) exact mass calculated for [C₇¹³C₁H₇N₁O₂H] requires m/z 151.0583, found m/z 151.0581 [M+H]⁺.

8.11. Synthesis of isotopically labelled aldehydes

The procedures reported below for the synthesis of (5.10) and (5.11) are representative and were used to create a library of deuterated aldehydes (5.12), (5.13), (5.14) and (5.15).

2-morpholino-2-(4-nitrophenyl)acetonitrile (5.10)

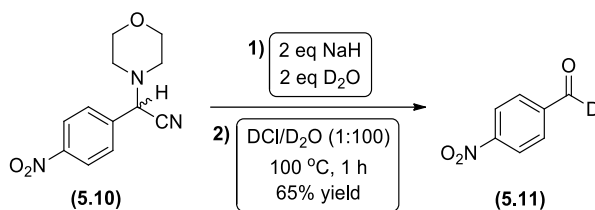


To a 150 mL flame dried round bottom flask, equipped with a magnetic stirrer bar, under nitrogen was added morpholine (5 mL), followed by a dropwise addition of perchloric acid (1.3 mL, 21.84 mmol) over 5 minutes. 4-nitrobenzaldehyde (5.1) (3.0 g, 19.85 mmol) in morpholine (25 mL) was added dropwise with care and the resulting solution was stirred at 70 °C for 2 hours. Sodium cyanide (1.07 g, 21.84 mmol) in water (10 mL) was added dropwise and the reaction was heated at 90 °C for 1 hour. Then, the reaction was allowed to cool slightly before pouring onto crushed ice. The resulting precipitate was collected by vacuum filtration and recrystallised from hot ethanol to afford orange crystals. Subsequent physicochemical analysis confirmed this to be the title compound (5.10) (4.16 g, 16.83 mmol, 85% yield).

¹H NMR (500 MHz, CDCl₃) δ 8.29 (d, *J* 8.6 Hz, 2H, ArH), 7.78 (d, *J* 8.6 Hz, 2H, ArH), 4.90 (s, 1H, CH), 3.82 – 3.67 (m, 4H, CH₂OCH₂), 2.68 – 2.52 (m, 4H, CH₂NCH₂); ¹³C NMR (126 MHz, CDCl₃) δ 148.6, 139.7, 129.1, 124.2, 114.2, 66.7, 62.0, 50.2.

The spectroscopic data is consistent with that reported in the literature.¹⁸³

α -²H-4-nitrobenzaldehyde (**5.11**)

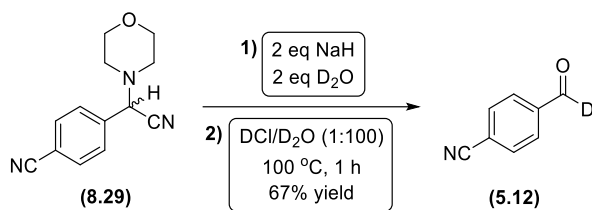


To a 50 mL flame dried round bottom flask, equipped with a magnetic stirrer bar, under nitrogen was added 2-morpholino-2-(4-nitrophenyl)acetonitrile (**5.10**) (4.0 g, 16.18 mmol) and anhydrous *N,N*-dimethylformamide (20 mL). The reaction was cooled to 0 °C with an ice bath and sodium hydride (60% w/w in mineral oil [1.94 g, 48.54 mmol]) was added to the reaction. The resulting slurry was stirred vigorously at 0 °C for 1 hour. At this point, deuterium oxide (1.8 mL, 97.08 mmol) was added *via* syringe and the reaction was allowed to warm to room temperature over 1 hour. Then the reaction was cooled to 0 °C and thionyl chloride was added slowly *via* syringe until pH ~ 3. After 10 minutes stirring, the reaction was allowed to warm to room temperature, at which point it was diluted with diethyl ether (100 mL), transferred into a 250 mL separating funnel, washed with saturated brine (100 mL), dried with magnesium sulphate, filtered and the solvent removed under reduced pressure to afford a solid. At this point, deuterium oxide (10 mL) was added *via* syringe, followed by deuterium chloride (0.1 mL) and the solution was refluxed at 100 °C for 2 hours. The reaction was allowed to cool to room temperature, at which point it was diluted with diethyl ether (100 mL), transferred into a 250 mL separating funnel, washed with saturated aqueous sodium hydrogen carbonate (50 mL), saturated brine (100 mL), dried with magnesium sulfate, filtered and the solvent removed under reduced pressure. The crude material was purified by flash chromatography on silica gel (10% diethyl ether in 40-60 PET, $R_f = 0.31$) to afford a yellow solid. Subsequent physicochemical analysis confirmed this to be the title compound (**5.11**) (1.6 g, 10.45 mmol, 65% yield).

¹H NMR (500 MHz, CDCl₃) δ 8.38 (d, *J* 8.8 Hz, 2H), 8.07 (d, *J* 8.8 Hz, 2H); ¹³C NMR (126 MHz, CDCl₃) δ 190.2 (t, J_{C-D} 27.4 Hz), 151.2, 140.1 (t, J_{C-D} 3.5 Hz), 130.6, 124.4; ²H NMR (77 MHz, CH₂Cl₂) δ 10.11 (br s), 7.26 (CDCl₃ ref).

The spectroscopic data is consistent with that reported in the literature.²⁶¹

α -²H-4-cyanobenzaldehyde (**5.12**)

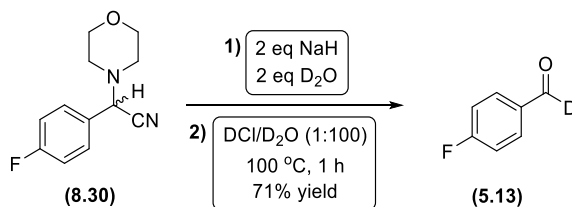


The procedure used for the synthesis of **(5.11)** was utilised to obtain **(5.12)** as a white solid after flash chromatography on silica gel (10% diethyl ether in 40-60 PET, $R_f = 0.35$). Subsequent physicochemical analysis confirmed this to be the title compound **(5.12)** (1.0 g, 7.58 mmol, 67% yield).

¹H NMR (500 MHz, CDCl₃) δ 7.95 (d, J 8.3 Hz, 2H), 7.88 (d, J 8.3 Hz, 2H); ¹³C NMR (126 MHz, CDCl₃) δ 190.8 (t, J_{C-D} 28.1 Hz), 141.7, 133.8 (t, J_{C-D} 3.3 Hz), 129.4, 118.3, 117.1; ²H NMR (77 MHz, CH₂Cl₂) δ 10.03 (br s), 7.26 (CDCl₃ ref).

The spectroscopic data is consistent with that reported in the literature.²⁶²

α -²H-4-fluorobenzaldehyde (**5.13**)

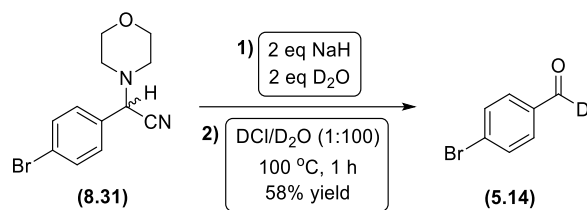


The procedure used for the synthesis of **(5.11)** was utilised to obtain **(5.13)** as a white solid after flash chromatography on silica gel (5% diethyl ether in 40-60 PET, $R_f = 0.26$). Subsequent physicochemical analysis confirmed this to be the title compound **(5.13)** (1.9 g, 15.18 mmol, 71% yield).

¹H NMR (500 MHz, CDCl₃) δ 7.90 (m, 2H), 7.32 (m, 2H); ¹³C NMR (126 MHz, CDCl₃) δ 190.0 (t, J_{C-D} 26.2 Hz), 169.2 (d, J_{C-F} 245.9 Hz), 133.1 (dt, J_{C-D} 3.3, J_{C-F} 3.1 Hz Hz), 132.4 (d, J_{C-F} 7.9 Hz), 116.9 (d, J_{C-F} 21.4 Hz); ²H NMR (77 MHz, CH₂Cl₂) δ 9.91 (br s), 7.26 (CDCl₃ ref).

The spectroscopic data is consistent with that reported in the literature.²⁶³

α -²H-4-bromobenzaldehyde (5.14)

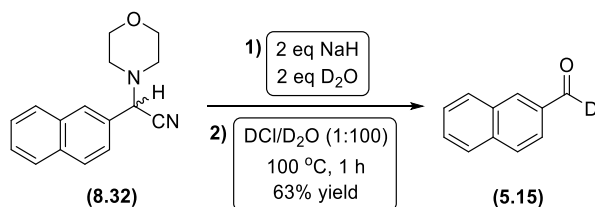


The procedure used for the synthesis of **(5.11)** was utilised to obtain **(5.14)** as a white solid after flash chromatography on silica gel (10% diethyl ether in 40-60 PET, $R_f = 0.32$). Subsequent physicochemical analysis confirmed this to be the title compound **(5.14)** (2.1 g, 11.29 mmol, 58% yield).

¹H NMR (500 MHz, CDCl₃) δ 7.74 (d, J 8.6 Hz, 2H), 7.66 (d, J 8.6 Hz, 2H); ¹³C NMR (126 MHz, CDCl₃) δ 188.3 (t, J_{C-D} 25.8 Hz), 136.1, 133.7 (t, J_{C-D} 3.2 Hz), 131.4, 128.6; ²H NMR (77 MHz, CH₂Cl₂) δ 9.96 (br s), 7.26 (CDCl₃ ref).

The spectroscopic data is consistent with that reported in the literature.²⁶²

α -²H-4-naphthaldehyde (5.15)

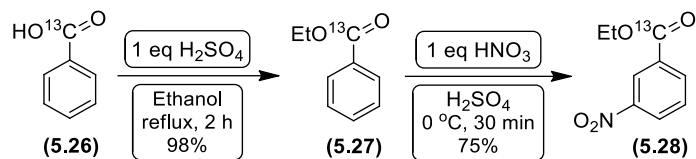


The procedure used for the synthesis of **(5.11)** was utilised to obtain **(5.15)** as a white solid after flash chromatography on silica gel (15% diethyl ether in 40-60 PET, $R_f = 0.39$). Subsequent physicochemical analysis confirmed this to be the title compound **(5.15)** (1.7 g, 10.81 mmol, 63% yield).

¹H NMR (500 MHz, CDCl₃) δ 7.85 (t, J 8.1 Hz, 3H, ArH), 7.71 (s, 1H, ArH), 7.63 (d, J 8.1 Hz, 1H, ArH), 7.51 (m, 2H, ArH); ¹³C NMR (126 MHz, CDCl₃) δ 192.4 (t, J_{C-D} 26.6 Hz), 137.2, 134.9, 134.1 (t, J_{C-D} 2.4 Hz), 132.6, 130.6, 129.3, 128.7, 127.9, 127.2, 124.4; ²H NMR (77 MHz, CH₂Cl₂) δ 10.15 (br s), 7.26 (CDCl₃ ref).

The spectroscopic data is consistent with that reported in the literature.²⁶³

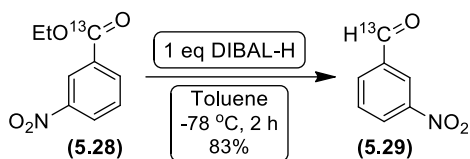
ethyl α - ^{13}C -3-nitrobenzoate (5.28)



To a 25 mL round bottom flask, equipped with a magnetic stirrer bar, under nitrogen was added α - ^{13}C -benzoic acid (**5.26**) (0.5 g, 4.06 mmol) and concentrated sulfuric acid (0.2 mL, 4.06 mmol) in ethanol (5 mL). The reaction was refluxed for 2 hours, cooled to room temperature and the solvent was removed under reduced pressure to afford ethyl α - ^{13}C -3-nitrobenzoate (**5.27**) (0.6 g, 3.97 mmol, 98% yield), as an orange oil, which was used in the subsequent step without any further purification. To a 25 mL round bottom flask, equipped with a magnetic stirrer bar, under nitrogen was added ethyl α - ^{13}C -3-nitrobenzoate (**5.27**) (120.0 mg, 0.79 mmol) and concentrated sulfuric acid (4 mL). The reaction was cooled to $0\text{ }^\circ\text{C}$ and concentrated nitric acid (0.03 mL, 0.79 mmol) was syringed slowly with vigorous stirring. After 30 minutes stirring at $0\text{ }^\circ\text{C}$, the reaction was poured carefully onto cold saturated aqueous sodium hydrogen carbonate (20 mL) and extracted with diethyl ether (3 x 20 mL). The combined organic layers were dried over magnesium sulfate and evaporated. The crude material was purified by flash chromatography on silica gel (10% diethyl ether in 40-60 PET, $R_f = 0.26$) to afford a white solid. Subsequent physicochemical analysis confirmed this to be the title compound (**5.28**) (116.0 g, 0.59 mmol, 75% yield).

^1H NMR (500 MHz, CDCl_3) δ 8.84 – 8.79 (m, 1H), 8.40 – 8.32 (m, 2H), 7.63 (t, J 8.0 Hz, 1H), 4.45 – 4.39 (m, 2H), 1.41 (td, J 7.1, 2.2 Hz, 3H); ^{13}C NMR (126 MHz, CDCl_3) δ 164.5, 148.3 (d, $J_{\text{C}-^{13}\text{C}}$ 5.5 Hz), 135.3 (d, $J_{\text{C}-^{13}\text{C}}$ 2.5 Hz), 132.3 (d, $J_{\text{C}-^{13}\text{C}}$ 75.8 Hz), 129.7 (d, $J_{\text{C}-^{13}\text{C}}$ 4.8 Hz), 127.3, 124.6 (d, $J_{\text{C}-^{13}\text{C}}$ 2.9 Hz), 62.0 (d, $J_{\text{C}-^{13}\text{C}}$ 2.3 Hz), 14.3 (d, $J_{\text{C}-^{13}\text{C}}$ 2.0 Hz); M.p. $43 - 45\text{ }^\circ\text{C}$ (from diethyl ether / 40-60 PET); IR (thin film) 2981 (C-H), 1695 (C=O), 1534/1351 (NO_2), 1288/1244 (C(O)C), 1082 (C-H bend) cm^{-1} ; HRMS (HASP) exact mass calculated for $[\text{C}_8^{13}\text{C}_1\text{H}_9\text{N}_1\text{O}_4\text{H}]$ requires m/z 196.0682, found m/z 196.0676 $[\text{M}+\text{H}]^+$.

α -¹³C-3-nitrobenzaldehyde (**5.29**)

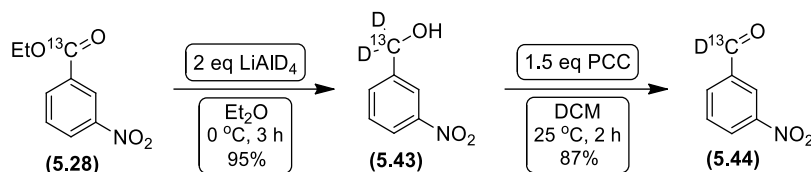


To a 50 mL flame dried round bottom flask, equipped with a magnetic stirrer bar, under nitrogen was added ethyl α -¹³C-3-nitrobenzoate (**5.28**) (200.0 mg, 1.02 mmol) and anhydrous toluene (10 mL). The flask was cooled to -78 °C and DIBAL-H (0.8 mL of a 1.2 M solution in toluene) was added dropwise over 20 minutes. The reaction was stirred for a further 2 hours at -78 °C, before being quenched by the dropwise addition of dry methanol (2 mL). The reaction was allowed to warm to about -20 °C internal temperature, and then poured into a vigorously stirred solution of Rochelle's salt (1.2 M aqueous potassium sodium tartrate, 20 mL). The viscous solution was stirred vigorously for 1 hour, after which time it settled to two clear phases. The organic layer was separated, and the aqueous layer extracted with diethyl ether (3 x 20 mL). The combined organic layers were dried over magnesium sulfate and evaporated. The crude material was purified by flash chromatography on silica gel (3% diethyl ether in 40-60 PET, $R_f = 0.28$) to afford a pale yellow solid. Subsequent physicochemical analysis confirmed this to be the title compound (**5.29**) (0.13 g, 0.85 mmol, 83% yield).

¹H NMR (500 MHz, CDCl₃) δ 10.13 (d, J_{13C-H} 179.1 Hz, 1H), 8.75 – 8.70 (m, 1H), 8.50 (ddd, J 8.2, 2.2, 0.9 Hz, 1H), 8.26 – 8.22 (m, 1H), 7.77 (t, J 8.0 Hz, 1H); ¹³C NMR (126 MHz, CDCl₃) δ 189.8, 134.7 (d, J_{C-13C} 3.7 Hz), 130.5 (d, J_{C-13C} 4.9 Hz), 128.7, 124.7 (d, J_{C-13C} 4.8 Hz); M.p. 59 - 61 °C (from diethyl ether / 40-60 PET); IR (thin film) 2972 (C-H), 1706 (C=O), 1535/1351 (NO₂), 1084/785 (C-H bend) cm⁻¹; HRMS (HASP) exact mass calculated for [C₆¹³C₁H₅N₁O₃H] requires m/z 153.0373, found m/z 153.0376 [M+H]⁺.

Due to ¹³C enrichment, the reduced intensity of some signals was observed in the ¹³C-NMR spectrum.

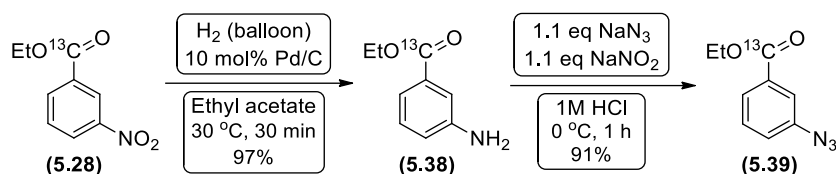
α - ^{13}C , ^2H -3-nitrobenzaldehyde (5.44)



To a 25 mL flame dried round bottom flask, equipped with a magnetic stirrer bar, under nitrogen was added a suspension of lithium aluminium deuteride (77.0 mg, 2.04 mmol) in anhydrous diethyl ether (10 mL). The flask was cooled to $0\text{ }^\circ\text{C}$ and a solution of ethyl α - ^{13}C -3-nitrobenzoate (**5.28**) (200.0 mg, 1.02 mmol) in anhydrous diethyl ether (1 mL) was added. After addition, the reaction mixture was warmed to $35\text{ }^\circ\text{C}$ and stirred for 5 h. The reaction mixture was cooled $0\text{ }^\circ\text{C}$ again, and distilled water (2 mL) was added. The precipitated inorganic salt was filtered off and washed with diethyl ether. Organic phase was washed with dried over magnesium sulfate, and evaporated to afford α -di- ^2H , ^{13}C -3-nitrobenzyl alcohol (**5.43**) (152.0 mg, 0.97 mmol, 95% yield) as a white solid. The crude product was used in the subsequent step without any further purification. To a 25 mL flame dried round bottom flask, equipped with a magnetic stirrer bar, under nitrogen was added a solution of benzyl alcohol derivative (**5.43**) (150.0 mg, 0.96 mmol) in anhydrous dichloromethane (5 mL). The flask was cooled to $0\text{ }^\circ\text{C}$ and PCC (207.0 mg, 0.96 mmol) in dichloromethane (15 mL) was added. The dark solution obtained was stirred for 1 hour at room temperature. The dark solids were filtered from the reaction mixture and washed with dichloromethane. The filtrate obtained was washed with saturated aqueous sodium hydrogen carbonate (50 mL), 1 M aqueous hydrochloric acid (50 mL), saturated brine (100 mL), dried with magnesium sulphate, filtered and the solvent removed under reduced pressure. The crude material was purified by flash chromatography on silica gel (3% diethyl ether in 40-60 PET, $R_f = 0.28$) to afford a pale yellow solid. Subsequent physicochemical analysis confirmed this to be the title compound (**5.44**) (128.0 mg, 0.84 mmol, 87% yield).

^1H NMR (500 MHz, CDCl_3) δ 8.75 – 8.71 (m, 1H), 8.49 (ddd, J 8.2, 2.0, 1.0 Hz, 1H), 8.24 (ddt, J 7.4, 4.6, 1.3 Hz, 1H), 7.77 (t, J 7.9 Hz, 1H); ^{13}C NMR (126 MHz, CDCl_3) δ 189.5 (t, $J_{\text{C-D}}$ 27.4 Hz), 148.9 (d, $J_{\text{C-}^{13}\text{C}}$ 3.8 Hz), 137.4 (dt, $J_{\text{C-}^{13}\text{C}}$ 53.3, $J_{\text{C-D}}$ 3.8 Hz), 134.7 (d, $J_{\text{C-}^{13}\text{C}}$ 3.7 Hz), 130.5 (d, $J_{\text{C-}^{13}\text{C}}$ 4.7 Hz), 128.7, 124.7 (d, $J_{\text{C-}^{13}\text{C}}$ 4.8 Hz); ^2H NMR (77 MHz, CH_2Cl_2) δ 10.09 (d, $J_{\text{C-D}}$ 27.5 Hz), 7.26 (CDCl_3 ref); M.p. $60 - 62\text{ }^\circ\text{C}$ (from diethyl ether / 40-60 PET); IR (thin film) 2969 (C-H), 1698 (C=O), 1531/1348 (NO_2), 1081/783 (C-H bend) cm^{-1} ; HRMS (HASP) exact mass calculated for $[\text{C}_6^{13}\text{C}_1\text{H}_4^2\text{H}_1\text{N}_1\text{O}_3\text{H}]$ requires m/z 154.0439, found m/z 154.0436 $[\text{M}+\text{H}]^+$.

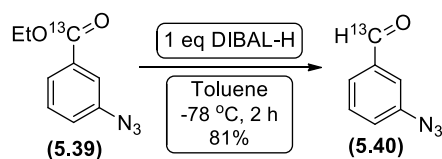
α -¹³C-3-azidobenzaldehyde (**5.40**)



To a 25 mL round bottom flask, equipped with a magnetic stirrer bar, under nitrogen was added ethyl α -¹³C-3-nitrobenzoate (**5.28**) (110.0 mg, 0.56 mmol) and palladium on carbon (10% w/w) (59.7 mg, 0.056 mmol). Ethyl acetate (5 mL) was added *via* syringe and the flask was sealed with sub-a-seal rubber septum. Then, hydrogen gas atmosphere was introduced through the septum and the reaction was stirred at 25 °C for 2 hours. At this point the reaction mixture was passed through a short plug of celite and eluted with ethyl acetate (10 mL). The solvent was removed under reduced pressure to afford an orange oil. Subsequent physicochemical analysis confirmed this to be ethyl α -¹³C-3-aminobenzoate (**5.38**) (91.0 mg, 0.55 mmol, 97% yield). To a 25 mL round bottom flask, equipped with a magnetic stirrer bar, under nitrogen was added ethyl α -¹³C-3-aminobenzoate (**5.38**) (90.0 mg, 0.54 mmol) and 1 M hydrochloric acid (5 mL). The flask was cooled to 0 °C and sodium nitrite (41.1 mg, 0.60 mmol) in distilled water (5 mL) was added. The reaction mixture was stirred for 10 min at 0 °C, sodium azide (42.2 mg, 0.65 mmol) was added and the mixture was allowed to warm to room temperature over 1 hour. The reaction was diluted with ethyl acetate (50 mL) and was washed with saturated brine (20 mL), dried with magnesium sulfate, filtered and the solvent removed under reduced pressure. The crude material was purified by flash chromatography on silica gel (5% diethyl ether in 40-60 PET, R_f = 0.22) to afford an orange oil. Subsequent physicochemical analysis confirmed this to be the title compound (**5.39**) (95.0 mg, 0.49 mmol, 91% yield).

¹H NMR (500 MHz, CDCl₃) δ 7.84 – 7.80 (m, 1H), 7.72 – 7.70 (m, 1H), 7.42 (td, J 7.9, 1.1 Hz, 1H), 7.19 (ddd, J 8.0, 2.4, 1.0 Hz, 1H), 4.39 (qd, J 7.1, 3.0 Hz, 2H), 1.40 (t, J 7.1 Hz, 3H); ¹³C NMR (126 MHz, CDCl₃) δ 165.7, 140.5 (d, J_{C-13C} 5.6 Hz), 132.3 (d, J_{C-13C} 74.7 Hz), 129.8 (d, J_{C-13C} 5.0 Hz), 126.0 (d, J_{C-13C} 2.3 Hz), 123.3, 119.9 (d, J_{C-13C} 2.7 Hz), 61.3 (d, J_{C-13C} 2.3 Hz), 14.3 (d, J_{C-13C} 2.1 Hz). IR (thin film) 2984 (C-H), 2121 (N₃), 1682 (C=O), 1289/1241 (C(O)C), 1099 (C-H bend) cm⁻¹; HRMS (HASP) exact mass calculated for [C₈¹³C₁H₉N₃O₂H] requires m/z 192.0712, found m/z 192.0719 [M+H]⁺.

α -¹³C-3-azidobenzaldehyde (**5.40**)

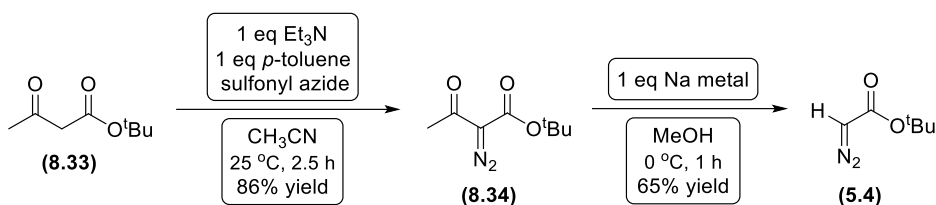


To a 50 mL flame dried round bottom flask, equipped with a magnetic stirrer bar, under nitrogen was added ethyl α -¹³C-3-azidobenzoate (**5.39**) (90.0 mg, 0.47 mmol) and anhydrous toluene (10 mL). The flask was cooled to -78 °C and DIBAL-H (0.5 mL of a 1.2 M solution in toluene) was added dropwise over 20 minutes. The reaction was stirred for a further 2 hours at -78 °C, before being quenched by the dropwise addition of dry methanol (2 mL). The reaction was allowed to warm to circa -20 °C internal temperature, and then poured into a vigorously stirred solution of Rochelle's salt (1.2 M aqueous potassium sodium tartrate, 20 mL). The viscous solution was stirred vigorously for 1 hour, after which time it settled to two clear phases. The organic layer was separated, and the aqueous layer extracted with diethyl ether (3 x 20 mL). The combined organic layers were dried over magnesium sulfate and evaporated. The crude material was purified by flash chromatography on silica gel (5% diethyl ether in 40-60 PET, $R_f = 0.25$) to afford a yellow oil. Subsequent physicochemical analysis confirmed this to be the title compound (**5.40**) (0.57 g, 0.38 mmol, 81% yield).

¹H NMR (500 MHz, CDCl₃) δ 9.99 (d, J_{13C-H} 176.2 Hz, 1H), 7.67 – 7.62 (m, 1H), 7.57 – 7.50 (m, 2H), 7.30 – 7.24 (m, 1H); ¹³C NMR (126 MHz, CDCl₃) δ 191.3, 141.6 (d, J_{C-13C} 5.4 Hz), 137.9 (d, J_{C-13C} 53.2 Hz), 130.6 (d, J_{C-13C} 5.2 Hz), 126.8 (d, J_{C-13C} 4.3 Hz), 125.0, 119.1 (d, J_{C-13C} 3.9 Hz); IR (thin film) 2994 (C-H), 2114 (N₃), 1696 (C=O), 1479 (C=C aromatic), 1103 (C-H bend) cm⁻¹; HRMS (HASP) exact mass calculated for [C₆¹³C₁H₅N₃O₁H] requires m/z 149.0539, found m/z 149.0535 [M+H]⁺.

8.12. Synthesis of diazoacetates

tert-butyl diazoacetate (**5.4**)

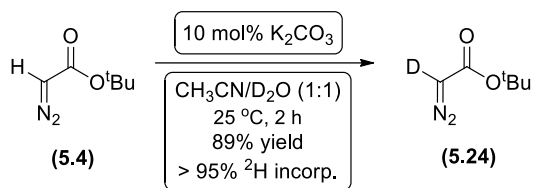


To a 500 mL flame dried round bottom flask, equipped with a magnetic stirrer bar, under nitrogen was added *tert*-butyl acetoacetate (**8.33**) (25.2 mL, 0.15 mol), triethylamine (21.3 mL, 0.15 mol) and anhydrous acetonitrile (100 mL). The mixture was stirred for 5 minutes at room temperature and then *para*-toluenesulfonyl azide (23.0 mL, 0.15 mol) was injected dropwise *via* syringe over a period of 15 minutes. The mixture was left stirring for 2.5 hours and then the solvent was removed under reduced pressure. The resulting yellow semi-solid material was triturated with diethyl ether (100 mL), transferred into a 250 mL separating funnel and washed with potassium hydroxide (4.5 g) in distilled water (50 mL), potassium hydroxide (750 mg) in distilled water (25 mL) and finally just distilled water (25 mL). Organic phase was dried over magnesium sulfate and evaporated to obtain orange semisolid (**8.34**) (24.0 g, 0.13 mol, 86% yield), which was used in the subsequent step without any further purification. To a 250 mL flame dried three-necked round bottom flask, equipped with a magnetic stirrer bar, dropping funnel, internal thermometer, under nitrogen was added *tert*-butyl diazoacetoacetate (20.0 g, 0.11 mol) and anhydrous methanol (50 mL). The reaction was cooled down to 0 °C and sodium metal pieces (2.5 g, 0.11 mol), that were dissolved in the ice cold anhydrous methanol (50 mL) where added *via* a dropping funnel slowly so the temperature of the reaction does not exceed 5 °C. After the addition was completed, the mixture was left stirring at 0 °C for 30 minutes. Then dark red mixture was poured into a conical flask with ice cold distilled water (100 mL) and saturated brine was added (100 mL). The mixture was transferred into a 1 L separating funnel and extracted with diethyl ether (3 x 200 mL). The combined organic layers were washed with distilled water (200 mL), dried over magnesium sulfate and evaporated. The crude material was purified by flash chromatography on silica gel (5% diethyl ether in 40-60 PET, R_f = 0.3) to afford a yellow oil. Subsequent physicochemical analysis confirmed this to be the title compound (**5.4**) (10.3 g, 0.07 mol, 65% yield).

¹H NMR (500 MHz, CDCl₃) δ 4.59 (s, 1H), 1.44 (s, 9H); ¹³C NMR (126 MHz, CDCl₃) δ 166.3, 81.4, 46.7, 28.3.

The spectroscopic data is consistent with that reported in the literature.¹⁹³

²H-labelled *tert*-butyl diazoacetate (**5.24**)



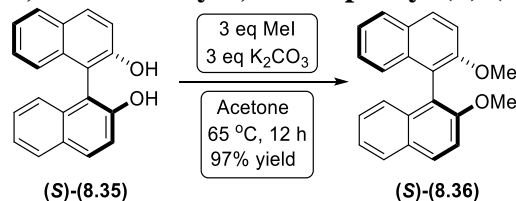
To a 250 mL flame dried three-necked round bottom flask, equipped with a magnetic stirrer bar, under nitrogen was added *tert*-butyl diazoacetate (**5.4**) (1.0 g, 7.03 mmol), potassium carbonate (0.1 g, 0.70 mmol) and anhydrous acetonitrile/D₂O 1:1 mixture (10 mL). The resulting mixture was stirred vigorously for 2 hours at room temperature and then extracted with dichloromethane (3 x 30 mL). The combined organic layers were washed with distilled water (200 mL), dried over magnesium sulfate and evaporated to afford a yellow oil. Subsequent physicochemical analysis confirmed this to be the title compound (**5.24**) (0.9 g, 6.29 mol, 89% yield).

¹H NMR (500 MHz, CDCl₃) δ 1.48 (s, 9H); ¹³C NMR (126 MHz, CDCl₃) δ 166.3, 81.5, 46.5 (d, *J*_{C-D} 29.9 Hz), 28.4; ²H NMR (77 MHz, CH₂Cl₂) δ 7.26 (CDCl₃ ref), 4.59 (br s).

The spectroscopic data is consistent with that reported in the literature.¹⁹³

8.13. Synthesis of the aziridination catalyst (*S*)-3,3'-bis(anthracen-9-yl)-[1,1']-binaphthalen-2,2'-yl *N*-triflyl phosphoramidate (*S*)-(5.9)

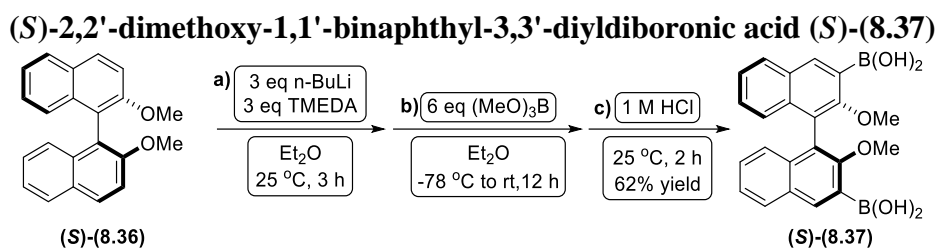
(*S*)-2,2'-dimethoxy-1,1'-dinaphthyl (*S*)-(8.36)



A flame dried 500 mL two-necked round bottom flask, fitted with a reflux condenser and a magnetic stirrer bar, under nitrogen was charged with (*S*)-1,1'-bi-2-naphthol (**(S)-(8.35)**) (10.0 g, 0.35 mol) in acetone (250 mL) affording a white suspension. Iodomethane (6.5 mL, 1.05 mol) and potassium carbonate (14.5 g, 1.05 mol) were added and the yellow mixture was refluxed for 12 hours under nitrogen atmosphere. The solvent was removed under reduced pressure. The resulting white solid was washed with distilled water (150 mL) and dried in a vacuum oven overnight at 80 °C to afford a fine white powder. Subsequent physicochemical analysis confirmed this to be the title compound (*S*)-2,2'-dimethoxy-1,1'-dinaphthyl (**(S)-(8.36)**) (10.7 g, 0.34 mol, 97% yield).

¹H NMR (400 MHz, CDCl₃) δ 7.98 (d, *J* 9.0 Hz, ArH), 7.87 (d, *J* 9.0 Hz, ArH), 7.48 (d, *J* 9.0 Hz, ArH), 7.31 (t, *J* 8.1 Hz, ArH), 7.21 (t, *J* 8.1 Hz, ArH), 7.10 (d, *J* 8.5 Hz, ArH), 3.77 (s, 6H, 2xOCH₃). ¹³C NMR (126 MHz, CDCl₃) δ 155.1, 134.1, 129.5, 129.3, 128.0, 126.4, 125.4, 123.6, 119.7, 114.4, 57.0; [α]_D²¹ = -52.0 (c 1.0 CHCl₃); IR (thin film) 3047/2957 (C-H), 1590/1505/1460 (C=C aromatic), 1262/1248 (C(O)C) cm⁻¹; MS (MALDI) 314.0 [M+H]⁺.

The spectroscopic data is consistent with that reported in the literature.¹⁷³

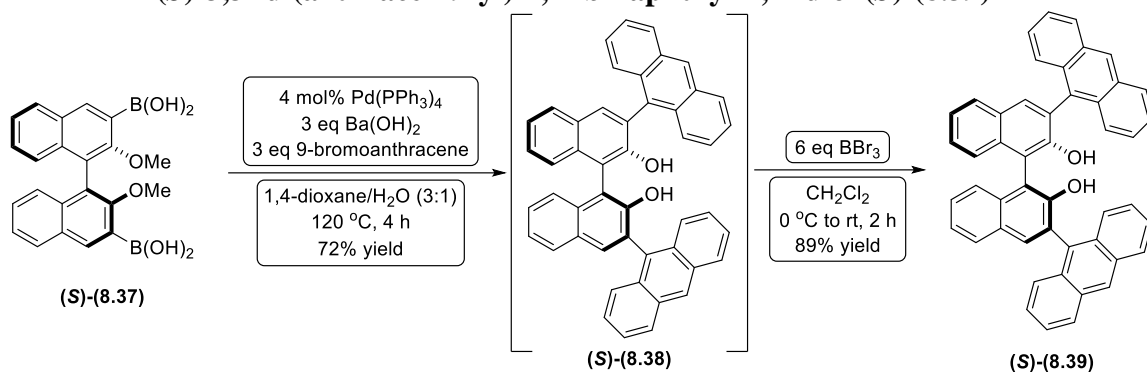


A flame dried 500 mL three-necked round bottom flask, fitted with a dropping funnel, a magnetic stirrer bar, under nitrogen was charged with *N,N,N',N'*-tetramethylethylenediamine (7.1 mL, 0.48 mol) and anhydrous diethyl ether (200 mL). A 2.5 M solution of *n*-butyllithium (22.7 mL, 0.48 mol) in hexanes was added *via* syringe at room temperature. The cloudy yellow solution was stirred for 30 minutes, (S)-2,2'-dimethoxy-1,1'-dinaphthyl (S)-(8.36) (5.0 g, 0.16 mol) was added in one portion and the reaction mixture was stirred for 3 hours at room temperature. The resulting light brown suspension was cooled to -78 °C using a dry ice/acetone bath. Trimethyl borate (12.4 mL, 1.11 mol) was added *via* a dropping funnel over a period of 10 minutes. The mixture was allowed to warm slowly to room temperature for 12 hours with continuous stirring. A yellow colloid was observed in the solution. The flask was cooled to 0 °C and 1 M hydrochloric acid (100 mL) was added slowly. The observed colloid turned into a light brown suspension, which was left stirring for 2 hours at room temperature. The organic layer was separated and washed with 1 M hydrochloric acid (2 x 50 mL), saturated brine (2 x 50 mL), dried with magnesium sulfate and concentrated under reduced pressure. Recrystallisation from toluene afforded the desired product as a fine white powder. Subsequent physicochemical analysis confirmed this to be the title compound (S)-2,2'-dimethoxy-1,1'-binaphthyl-3,3'-diyldiboronic acid (S)-(8.37) (3.9 g, 0.10 mol, 62% yield).

¹H NMR (500 MHz, CDCl₃) δ 8.55 (s, 2H, ArH), 7.92 (d, *J* 8.0 Hz, 2H, ArH), 7.36 (t, *J* 7.5 Hz, 2H, ArH), 7.25 (t, *J* 7.5 Hz, 2H, ArH), 7.09 (d, *J* 8.0 Hz, 2H, ArH), 5.98 (s, 4H, 2xB(OH)₂), 3.23 (s, 6H, 2xOCH₃); ¹³C NMR (126 MHz, DMSO) δ 159.1, 135.8, 134.7, 130.1, 129.4, 128.7, 127.0, 125.5, 124.7, 123.2, 61.0; IR (thin film) 3392 (OH) 2941 (C-H), 1588/1493 (C=C aromatic), 1335 (B-O), 1263/1217 (C(O)C), 1008 (C-B) cm⁻¹; MS (MALDI) 401.9 [M+H]⁺.

The spectroscopic data is consistent with that reported in the literature.¹⁷³

(S)-3,3'-di(anthracen-9-yl)-1,1'-binaphthyl-2,2'-diol (S)-(8.39)



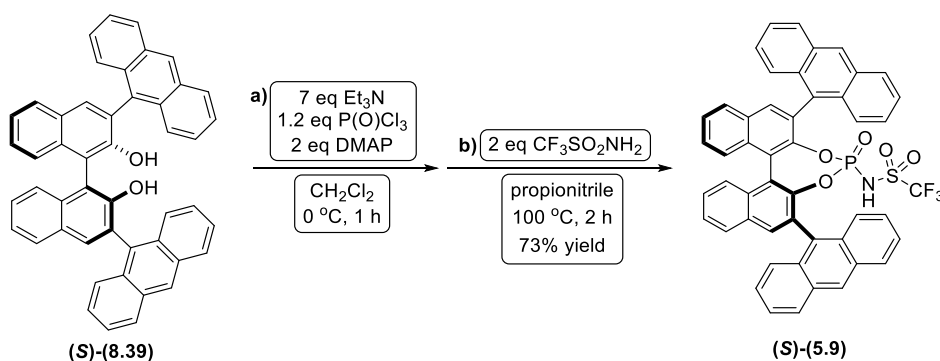
A 25 mL two-necked round bottom flask, fitted with a reflux condenser and a magnetic stirrer bar, under nitrogen was charged with (S)-2,2'-dimethoxy-1,1'-binaphthyl-3,3'-diyl diboronate (S)-(8.37) (0.5 g, 1.24 mmol), tetrakis(triphenylphosphine)palladium (57.0 mg, 0.05 mmol), barium hydroxide octahydrate (1.2 g, 3.73 mmol) and 9-bromoanthracene (1.0 g, 3.73 mmol) in 1,4-dioxane (9 mL) / distilled water (3 mL) mixture. The solvent was degassed by nitrogen gas and the mixture was refluxed at 125 °C for 4 hours. The flask was allowed to cool to room temperature and solvent was removed under reduced pressure. The resulting residue was redissolved in dichloromethane (50 mL) and washed with 1 M hydrochloric acid (2 x 50 mL), saturated brine (2 x 50 mL), dried with anhydrous magnesium sulfate and concentrated under reduced pressure to afford a brown solid (S)-(8.38) (0.6 g, 0.9 mmol, 72% yield), which was used in the subsequent step without any further purification.

A flame dried 25 mL round bottom flask, fitted with a magnetic stirrer bar, under nitrogen was charged with (S)-(8.38) (0.6 g, 0.9 mmol) and anhydrous dichloromethane (50 mL). Boron tribromide (0.5 mL, 5.4 mmol) was added dropwise at 0 °C and the mixture was left stirring at room temperature for 4 hours. Then it was cooled to 0 °C and quenched with distilled water (10 mL). The organic layer was separated and washed with 1 M hydrochloric acid (2 x 30 mL), saturated brine (2 x 30 mL), dried with anhydrous magnesium sulfate and concentrated under reduced pressure. The crude material was purified by flash chromatography on silica gel (20% ethyl acetate in 40-60 PET, R_f = 0.28) to afford an orange solid. Subsequent physicochemical analysis confirmed this to be the title compound (S)-3,3'-di(anthracen-9-yl)-1,1'-binaphthyl-2,2'-diol (S)-(8.39) (0.5 g, 0.80 mmol, 89% yield).

^1H NMR (400 MHz, CDCl_3) δ 8.58 (s, 2H, ArH), 8.10 (d, J 8.3 Hz, 2H, ArH), 8.06 (d, J 8.3 Hz, 2H, ArH), 8.02 (s, 2H, ArH), 7.86 (d, J 8.6 Hz, 2H, ArH), 7.85 (d, J 6.9 Hz, 2H, ArH), 7.67 (d, J 8.8 Hz, 2H, ArH), 7.58 (d, J 8.8 Hz, 2H, ArH), 7.52 – 7.37 (m, 10H, ArH), 7.20 – 7.16 (m, 2H, ArH), 5.07 (s, 2H, 2xOH); ^{13}C NMR (101 MHz, CDCl_3) δ 150.1, 133.1, 132.2, 130.7, 130.6, 130.0, 129.9, 129.9, 128.5, 127.8, 127.7, 127.6, 126.9, 126.6, 126.3, 125.4, 125.3, 125.2, 124.5, 124.50, 124.4, 124.0, 123.4, 112.7; $[\alpha]_{\text{D}}^{25} = -131.3$ (c 1.0 CHCl_3); IR (thin film) 3530 (OH), 3050 (C-H), 1498 (C=C aromatic), 1263/1217 (C-O) cm^{-1} ; MS (MALDI) 637.9 $[\text{M}+\text{H}]^+$.

The spectroscopic data is consistent with that reported in the literature.¹⁷³

(*S*)-3,3'-bis(anthracen-9-yl)-[1,1']-binaphthalen-2,2'-yl *N*-triflyl phosphoramidate (*S*)-(5.9)



A 25 mL two-necked round bottom flask, fitted with a reflux condenser and a magnetic stirrer bar, under nitrogen was charged with (*S*)-3,3'-di(anthracen-9-yl)-1,1'-binaphthyl-2,2'-diol (*S*)-(8.39) (0.2 g, 0.31 mmol) and anhydrous dichloromethane (3 mL). To the solution were added in sequence anhydrous triethylamine (0.3 mL, 2.17 mmol), phosphorus oxychloride (35.0 μL , 0.37 mmol) and 4-dimethylaminopyridine (77.0 mg, 0.63 mmol) at 0 °C and the reaction mixture was stirred for 1 hour. Anhydrous propionitrile (2 mL) was added followed by trifluoromethanesulfonamide (93.0 mg, 0.63 mmol). The mixture was refluxed at 100 °C for 2 hours. The mixture was allowed to cool to room temperature, quenched with distilled water (1 mL), stirred for 20 minutes and extracted with diethyl ether (3 x 20 mL). The combined organic layers were washed with saturated aqueous sodium hydrogen carbonate solution (2 x 30 mL) and 4 M hydrochloric acid (2 x 30 mL). The organic phase was dried over anhydrous

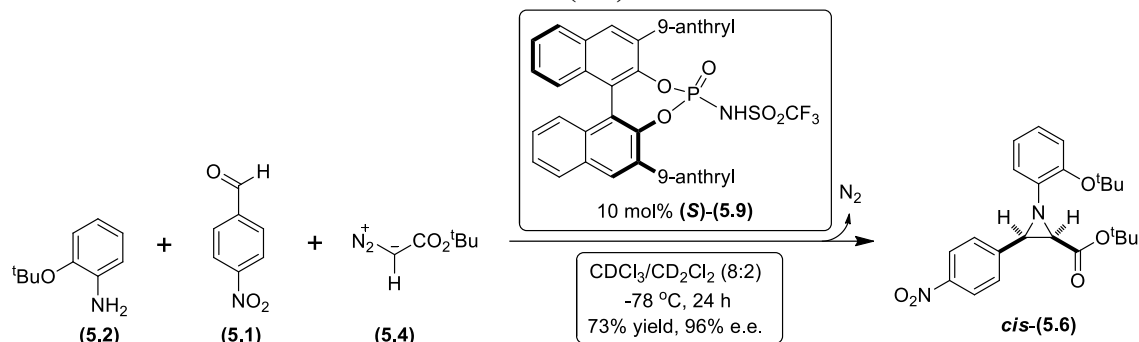
magnesium sulfate and concentrated under reduced pressure. The crude material was purified by flash chromatography on silica gel (30% ethyl acetate in 40-60 PET, $R_f = 0.25$) to afford an orange solid, which could be a salt (pH ~ 7). The solid was dissolved in dichloromethane (20 mL) and washed with 6 M hydrochloric acid (2 x 20 mL). The organic layer was dried over anhydrous magnesium sulfate and concentrated under reduced pressure to afford a cream solid (pH ~ 2). Subsequent physicochemical analysis confirmed this to be the title compound (*S*)-3,3'-bis(anthracen-9-yl)-[1,1']-binaphthalen-2,2'-yl *N*-triflyl phosphoramidate (**S**)-(5.9) (190.0 mg, 0.23 mmol, 73% yield).

^1H NMR (500 MHz, CDCl_3) δ 8.53 (s, 1H, ArH), 8.48 (s, 1H, ArH), 8.18 (m, 2H, ArH), 8.09 – 7.98 (m, 5H, ArH), 7.90 (d, J 8.3 Hz, 1H, ArH), 7.78 – 7.65 (m, 6H, ArH), 7.65 – 7.59 (m, 2H, ArH), 7.59 – 7.53 (m, 2H, ArH), 7.46 – 7.39 (m, 3H, ArH), 7.38 – 7.31 (m, 3H, ArH), 7.24 – 7.11 (m, 2H, ArH); ^{13}C NMR (126 MHz, CDCl_3) δ 146.9, 146.8, 146.4, 146.30, 134.3, 134.1, 132.8, 131.8, 131.6, 131.5, 131.4, 131.3, 131.2, 131.1, 130.9, 130.8, 130.7, 130.6, 130.5, 130.1, 128.7, 128.5, 128.4, 128.2, 128.1, 127.8, 127.6, 127.5, 127.4, 127.3, 126.9, 126.8, 126.7, 126.6, 126.5, 126.14, 126.13, 126.0, 125.7, 125.2, 125.1, 124.7, 124.5, 122.9, 122.8, 122.25, 122.24, 120.2, 117.6; ^{19}F NMR (471 MHz, CDCl_3) δ -79.73; ^{31}P NMR (202 MHz, CDCl_3) δ 0.35; IR (thin film) 3530 (NH), 3055 (C-H), 1445 (C=C aromatic), 1303 (CF_3), 1296 (P=O), 1261/1199 (C-O), 1101 (S=O), 956 (P-O), 733 (C-S) cm^{-1} ; MS (MALDI) 830.9 $[\text{M}+\text{H}]^+$.

The spectroscopic data is consistent with that reported in the literature.¹⁷³

8.14. Asymmetric synthesis of the model aziridines using catalyst (S)-(5.9)

tert-butyl *cis*-1-(2-*tert*-butoxyphenyl)-3-(4-nitrophenyl)aziridine-2-carboxylate *cis*-(5.6)

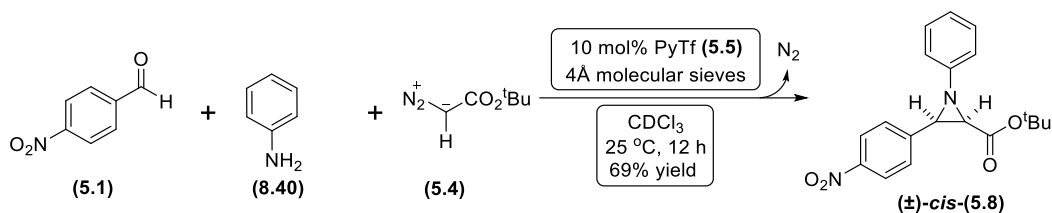


4-Nitrobenzaldehyde (**5.1**) (70.0 mg, 0.46 mmol) and *tert*-butoxyaniline (**5.2**) (72.7 mg, 0.44 mmol) were added to a flame dried Biotage 5 mL microwave vial, containing activated 4Å molecular sieves (~ 100 mg) under nitrogen. Deuterated chloroform/deuterated dichloromethane (8:2) mixture (1 mL) was added, the vial was sealed with a PTFE crimp cap and the reaction mixture was left stirring at 25 °C for 2 hours. Catalyst (S)-(5.9) (38.5 mg, 0.05 mmol, 10 mol%) was added and the vial was cooled to -78 °C. After 30 minutes, *tert*-butyl diazoacetate (**5.4**) (71 µL, 0.51 mmol) was added *via* syringe, and the reaction mixture was stirred at -80 °C (~ 24 hours). At this point the reaction mixture was quenched with triethylamine (0.5 mL), passed through a short plug of silica, eluted with diethyl ether and the solvent was removed under reduced pressure. The crude material was purified by flash chromatography on silica gel (5% diethyl ether in 40-60 PET, $R_f = 0.22$) to afford a yellow solid. Subsequent physicochemical analysis confirmed this to be the title compound *cis*-(5.6) (141.0 mg, 0.34 mmol, 73% yield). A sample was submitted to chiral analytical HPLC analysis [Chiralpak AD-H column, *iso*-hexane / *iso*-propanol : 95 / 05, 1 mL / min, 6.3 min (1st peak), 10.4 min (2nd peak), 96% e.e.].

¹H NMR (500 MHz, CDCl₃) δ 8.20 (d, *J* 8.8 Hz, 2H, ArH), 7.72 (d, *J* 8.8 Hz, 2H, ArH), 7.07 – 6.90 (m, 4H, ArH), 3.53 (d, *J* 6.8 Hz, 1H, C3-H), 3.14 (d, *J* 6.8 Hz, 1H, C2-H), 1.35 (s, 9H, C(CH₃)₃), 1.22 (s, 9H, C(CH₃)₃); ¹³C NMR (126 MHz, CDCl₃) δ 166.4, 148.1, 147.5, 145.6, 143.1, 129.1, 123.6, 123.2, 123.1, 123.0, 120.9, 82.0, 80.5, 47.8, 46.8, 28.8, 27.9; FT-IR (thin film) 2980 (C-H), 1742 (C=O), 1603/1520/1489 (C=C aromatic), 1345 (NO₂), 1225/1162 (C(O)C), 1049 (C-N), 912 (C-H bend) cm⁻¹.

The spectroscopic data is consistent with that reported in the literature.¹⁶⁴

***tert*-butyl *cis*-1-phenyl-3-(4-nitrophenyl)aziridine-2-carboxylate (\pm)-*cis*-(**5.8**)**



4-nitrobenzaldehyde (**5.1**) (20.0 mg, 0.13 mmol), and aniline (**8.40**) (22.0 mg, 0.12 mmol) were added to a flame dried Biotage 5 mL microwave vial, containing activated 4Å molecular sieves (~ 100 mg) under nitrogen. Deuterated chloroform (2 mL) was added, the vial was sealed with a PTFE crimp cap and the reaction mixture was left stirring at 25 °C for 2 hours. An aliquot was submitted to ¹H-NMR analysis, which confirmed the formation of the imine intermediate. Pyridinium triflate (**5.5**) (3.3 mg, 0.01 mmol, 10 mol%) was added. After 5 minutes, *tert*-butyl diazoacetate (**5.4**) (18 μL, 0.13 mmol) was added *via* syringe, and the reaction mixture was stirred at 25 °C, monitoring by ¹H-NMR until the reaction was deemed complete (~ 12 hours). At this point the reaction mixture was passed through a short plug of silica, eluted with diethyl ether and the solvent was removed under reduced pressure. The crude material was purified by flash chromatography on silica gel (5% diethyl ether in 40-60 PET, R_f = 0.35) to afford an orange solid. Subsequent physicochemical analysis confirmed this to be the title compound (\pm)-*cis*-(**5.8**) (32.4 mg, 0.08 mmol, 69% yield).

¹H NMR (500 MHz, CDCl₃) δ 8.22 (d, *J* 8.8 Hz, 2H, ArH), 7.71 (d, *J* 8.8 Hz, 2H, ArH), 7.29 (t, *J* 7.9 Hz, 2H, ArH), 7.10 – 7.02 (m, 3H, ArH), 3.59 (d, *J* 6.8 Hz, 1H, C3-H), 3.19 (d, *J* 6.8 Hz, 1H, C2-H), 1.23 (s, 9H, C(CH₃)₃); ¹³C NMR (126 MHz, CDCl₃) δ 166.1, 151.8, 147.6, 142.6, 129.4, 128.9, 123.9, 123.34, 120.0, 82.4, 46.6, 46.1, 27.9; FT-IR (thin film) 2972 (C-H), 1741 (C=O), 1605/1512/1494 (C=C aromatic), 1343 (NO₂), 1219/1159 (C(O)C), 1051 (C-N) cm⁻¹.

The spectroscopic data is consistent with that reported in the literature.¹⁷³

References

- ¹ Alberts, B.; Johnson, A.; Lewis, J.; Raff, M.; Roberts, K.; Walter, P. *Molecular Biology of the Cell*; 4th edition; New York: Garland Science; **2002**
- ² Xu, R.; Ye, Y.; Zhao, W.; *Introduction to Natural Products Chemistry*; CRC Press, **2011**
- ³ Rosenberg, D.; Kartvelishvily, E.; Shleper, M.; Klinker, C. M. C.; Bowser, M. T.; Wolosker, H.; *FASEB J.* **2010**, *24*, 2951–2961
- ⁴ Crow, J. P.; Marecki, J. C.; Thompson, M.; *Neurology Research International* **2012**, 1–8
- ⁵ D’Aniello, S.; Somorjai, I.; Garcia-Fernández, J.; Topo, E.; D’Aniello, A.; *FASEB J.* **2011**, *25*, 1014–1027
- ⁶ Richter, K.; Egger, R.; Kreil, G.; *Science* **1987**, *238*, 200–202
- ⁷ Nagata, Y.; Masui, R.; Akino, T.; *Experientia* **1992**, *48*, 986–988.
- ⁸ Raman, S. B.; Rathinasabapathi, B.; *Plant Physiol.* **2003**, *132*, 1642–1651
- ⁹ Kinnersley, A. M.; Turano, F. J.; *Critical Reviews in Plant Sciences* **2000**, *19*, 479–509
- ¹⁰ Williams, R. M.; Hendrix, J. A.; *Chem. Rev.* **1992**, *92*, 889–917
- ¹¹ Williams, R. M. *Synthesis of Optically Active Alpha-Amino Acids*; Baldwin, J. E., Ed.; Pergamon Press: Oxford, **1989**
- ¹² Dougherty, D. A.; *Curr. Opin. Chem. Biol.* **2000**, *4*, 645–652
- ¹³ Williams, R. M.; *Synthesis of Optically Active Alpha-Amino Acids*; Elsevier, **2013**
- ¹⁴ Strecker, A.; *Justus Liebigs Ann. Chem.* **1850**, *75*, 27–45
- ¹⁵ Wang, Z.; Strecker Synthesis, *Comprehensive Organic Name Reactions and Reagents*; John Wiley & Sons, **2010**
- ¹⁶ Iyer, M. S.; Gigstad, K. M.; Namdev, N. D.; Lipton, M.; *Amino Acids* **1996**, *11*, 259–268
- ¹⁷ Vineyard, B. D.; Knowles, W. S.; Sabacky, M. J.; Bachman, G. L.; Weinkauff, D. J.; *J. Am. Chem. Soc.* **1977**, *99*, 5946–5952
- ¹⁸ Knowles, W. S.; *Acc. Chem. Res.* **1983**, *16*, 106–112
- ¹⁹ Beresford, K. J. M.; Church, N. J.; Young, D. W.; *Org. Biomol. Chem.* **2006**, *4*, 2888–2897
- ²⁰ Stamm, H. *J. Prakt. Chem.* **1999**, *341* (4), 319–331
- ²¹ Kainosho, M.; Torizawa, T.; Iwashita, Y.; Terauchi, T.; Mei Ono, A.; Güntert, P.; *Nature* **2006**, *440*, 52–57
- ²² Harding, J. R.; Hughes, R. A.; Kelly, N. M.; Sutherland, A.; Willis, C. L.; *J. Chem. Soc., Perkin Trans. 1* **2000**, 3406–3416
- ²³ Buděšínský, M.; Ragnarsson, U.; Lankiewicz, L.; Grehn, L.; Slaninová, J.; Hlaváček, J.; *Amino Acids* **2005**, *29*, 151–160
- ²⁴ Jones, D. H.; Cellitti, S. E.; Hao, X.; Zhang, Q.; Jahnz, M.; Summerer, D.; Schultz, P. G.; Uno, T.; Geierstanger, B. H.; *J. Biomol. NMR* **2010**, *46*, 89–100
- ²⁵ Tanner, D.; *Angew. Chem. Int. Ed. Engl.* **1994**, *33*, 599–619
- ²⁶ Bach, R. D.; Dmitrenko, O.; *J. Org. Chem.* **2002**, *67*, 3884–3896
- ²⁷ Lawrence, S. A.; *Amines: Synthesis, Properties and Applications*; Cambridge University Press, **2004**
- ²⁸ Gembitskii, P. A.; Loim, N. M.; Zhuk, D. S.; *Russian Chemical Reviews* **1966**, *35*, 105–122
- ²⁹ Clayden, J.; Greeves, N.; Warren, S.; *Organic Chemistry*; Oxford University Press, **2012**
- ³⁰ Pearson, W. H.; Lian, B. W.; Bergmeier, S. C.; *Comprehensive Heterocyclic Chemistry II*; Pergamon: Oxford, **1996**, 1–60
- ³¹ Pellissier, H.; *Adv. Synth. Catal.* **2014**, *356*, 1899–1935
- ³² Atkinson, R. S.; *Tetrahedron* **1999**, *55*, 1519–1559
- ³³ Sweeney, J. B.; *Chem. Soc. Rev.* **2002**, *31*, 247–258
- ³⁴ Li, Z.; Conser, K. R.; Jacobsen, E. N.; *J. Am. Chem. Soc.* **1993**, *115*, 5326–5327
- ³⁵ Evans, D. A.; Faul, M. M.; Bilodeau, M. T.; Anderson, B. A.; Barnes, D. M.; *J. Am. Chem. Soc.* **1993**, *115*, 5328–5329
- ³⁶ Li, Z.; Quan, R. W.; Jacobsen, E. N.; *J. Am. Chem. Soc.* **1995**, *117*, 5889–5890
- ³⁷ Antilla, J. C.; Wulff, W. D.; *J. Am. Chem. Soc.* **1999**, *121*, 5099–5100
- ³⁸ Bao, J.; Wulff, W. D.; Rheingold, A. L.; *J. Am. Chem. Soc.* **1993**, *115*, 3814–3815
- ³⁹ Hu, G.; Huang, L.; Huang, R. H.; Wulff, W. D.; *J. Am. Chem. Soc.*, **2009**, *131*, 15615–15617

- ⁴⁰ Antilla, J. C.; Wulff, W. D.; *J. Am. Chem. Soc.* **1999**, *121*, 5099–5100
- ⁴¹ O'Connor, M. J.; Ernst, R. E.; Schoenborn, J. E.; Holm, R. H.; *J. Am. Chem. Soc.* **1968**, *90*, 1744–1752
- ⁴² Loncaric, C.; Wulff, W. D.; *Org. Lett.* **2001**, *3*, 3675–3678
- ⁴³ Rao, A. V. R.; Rao, S. P.; Bhanu, M. N.; *J. Chem. Soc., Chem. Commun.* **1992**, *11*, 859–860
- ⁴⁴ Kawamoto, A. M.; Wills, M.; *J. Chem. Soc., Perkin Trans. 1* **2001**, 1916–1928
- ⁴⁵ Bull, J. A.; Boultonwood, T.; Taylor, T. A.; *Chem. Commun.* **2012**, *48*, 12246–12248
- ⁴⁶ Botuha, C.; Chemla, F.; Ferreira, F.; Pérez-Luna, A.; *Heterocycles in Natural Product Synthesis*; John Wiley & Sons, **2011**, 1–39
- ⁴⁷ Hata, T.; Hoshi, T.; Kanamori, K.; Matsumae, A.; Sano, Y.; Shima, T.; Sugawara, R.; *J. Antibiot.* **1956**, *9*, 141–146
- ⁴⁸ Wakaki, S.; Marumo, H.; Tomioka, K.; Shimizu, G.; Kato, E.; Kamada, H.; Kudo, S.; Fujimoto, Y.; *Antibiot. Chemother.* **1958**, *8*, 228–240
- ⁴⁹ Kinoshita, S.; Uzu, K.; Nakano, K.; Shimizu, M.; Takahashi, T.; Matsui, M.; *J. Med. Chem.* **1971**, *14*, 103–109
- ⁵⁰ Beijnen, J. H.; Lingeman, H.; Van Munster, H. A.; Underberg, W. J. M.; *Journal of Pharmaceutical and Biomedical Analysis* **1986**, *4*, 275–295
- ⁵¹ Kinoshita, S.; Uzu, K.; Nakano, K.; Takahashi, T. *J. Med. Chem.* **1971**, *14*, 109–112
- ⁵² Tomasz, M.; Lipman, R.; Chowdary, D.; Pawlak, J.; Verdine, G. L.; Nakanishi, K.; *Science* **1987**, *235*, 1204–1208
- ⁵³ Rink, S. M.; Lipman, R.; Alley, S. C.; Hopkins, P. B.; Tomasz, M.; *Chem. Res. Toxicol.* **1996**, *9*, 382–389
- ⁵⁴ Iyer, V. N.; Szybalski, W.; *Science* **1964**, *145*, 55–58
- ⁵⁵ Gustafson, D. L.; Pritsos, C. A.; *Cancer Res.* **1993**, *53*, 5470–5474
- ⁵⁶ Paz, M. M.; *Chem. Res. Toxicol.* **2009**, *22*, 1663–1668
- ⁵⁷ Vaupel, P.; Harrison, L.; *The Oncologist* **2004**, *9*, 4–9
- ⁵⁸ Naganawa, H.; Usui, N.; Takita, T.; Hamada, M.; Umezawa, H.; *J. Antibiot.* **1975**, *28*, 828–829
- ⁵⁹ Schirmeister, T.; *Arch. Pharm. Pharm. Med. Chem.* **1996**, *329*, 239–244
- ⁶⁰ Schirmeister, T.; *Biopolymers* **1999**, *51*, 87–97
- ⁶¹ Breuning, A.; Vicik, R.; Schirmeister, T.; *Tetrahedron: Asymm.* **2003**, *14*, 3301–3312
- ⁶² Legters, J.; Thijs, L.; Zwanenburg, B.; *Tetrahedron* **1991**, *47*, 5287–5294
- ⁶³ McCoull, W.; Davis, F. A.; *Synthesis* **2000**, *10*, 1347–1365
- ⁶⁴ Mall, T.; Stamm, H.; *Chem. Ber.* **1988**, *121*, 1353–1355
- ⁶⁵ Kumar, M.; Gandhi, S.; Kalra, S. S.; Singh, V. K.; *Synth. Commun.* **2008**, *38*, 1527–1532
- ⁶⁶ Takeuchi, H.; Koyama, K.; *J. Chem. Soc., Perkin Trans. 2* **1981**, *1*, 121–126
- ⁶⁷ Kim, Y.; Ha, H.-J.; Yun, S. Y.; Lee, W. K.; *Chem. Commun.* **2008**, *36*, 4363–4365
- ⁶⁸ Bodenan, J.; Chanet-Ray, J.; Vessiere, R.; *Synthesis* **1992**, *3*, 288–292
- ⁶⁹ Morán-Ramallal, R.; Liz, R.; Gotor, V.; *Org. Lett.* **2007**, *9*, 521–524
- ⁷⁰ Kim, Y.; Ha, H.-J.; Han, K.; Ko, S. W.; Yun, H.; Yoon, H. J.; Kim, M. S.; Lee, W. K.; *Tetrahedron Lett.* **2005**, *46*, 4407–4409
- ⁷¹ Righi, G.; D'Achille, R.; Bonini, C.; *Tetrahedron Lett.* **1996**, *37*, 6893–6896
- ⁷² Tanner, D.; He, H. M.; Somfai, P.; *Tetrahedron* **1992**, *48*, 6069–6078
- ⁷³ Nagaoka, H.; Kishi, Y.; *Tetrahedron* **1981**, *37*, 3873–3888
- ⁷⁴ Shambayati, S.; Schreiber, S. L.; Blake, J. F.; Wierschke, S. G.; Jorgensen, W. L.; *J. Am. Chem. Soc.* **1990**, *112*, 697–703
- ⁷⁵ Davis, F. A.; Liang, C.-H.; Liu, H.; *J. Org. Chem.* **1997**, *62*, 3796–3797
- ⁷⁶ Xiong, C.; Wang, W.; Cai, C.; Hruby, V. J.; *J. Org. Chem.* **2002**, *67*, 1399–1402
- ⁷⁷ Davis, F. A.; Deng, J.; Zhang, Y.; Haltiwanger, R. C.; *Tetrahedron* **2002**, *58*, 7135–7143
- ⁷⁸ Ismail, F. M. D.; Levitsky, D. O.; Dembitsky, V. M.; *Eur. J. Med. Chem.* **2009**, *44*, 3373–3387
- ⁷⁹ Dembitsky, D. V. M.; Terent'ev, A. O.; Levitsky, D. O.; *Natural Products*; Springer Berlin Heidelberg, **2013**
- ⁸⁰ Bansal, R. K.; *Heterocyclic Chemistry*; New Age International, **1999**

- ⁸¹ Korzybski, T.; Kowszyk-Gindifer, Z.; Kurylowicz, W.; *Antibiotics: Origin, Nature and Properties*; Elsevier, **2013**
- ⁸² Davies, J.; Davies, D.; *Microbiol. Mol. Biol. Rev.* **2010**, *74*, 417–433
- ⁸³ Waksman, S. A.; *Journal of the History of Medicine and Allied Sciences* **1973**, *XXVIII*, 284–286
- ⁸⁴ Morar, M.; Wright, G. D.; *Annual Review of Genetics* **2010**, *44*, 25–51
- ⁸⁵ Williams, D. H.; *Nat. Prod. Rep.* **1996**, *13*, 469–477
- ⁸⁶ Tipper, D. J.; Strominger, J. L.; *Proc. Natl. Acad. Sci. USA* **1965**, *54*, 1133–1141
- ⁸⁷ Abraham, E. P.; Chain, E.; *Nature* **1940**, *46*, 837
- ⁸⁸ McCormick, M. H.; McGuire, J. M.; Pittenger, G. E.; Pittenger, R. C.; Stark, W. M.; *Antibiot. Annu.* **1955-1956**, *3*, 606–611
- ⁸⁹ Wold, J. S.; Turnipseed, S. A.; *Reviews of Infectious Diseases* **1981**, *3*, 224–229
- ⁹⁰ Evans, D. A.; Katz, J. L.; Peterson, G. S.; Hintermann, T.; *J. Am. Chem. Soc.* **2001**, *123*, 12411–12413
- ⁹¹ Rybak, M. J.; *Clin. Infect. Dis.* **2006**, *42*, 35–39
- ⁹² Perkins, H. R.; *Biochem. J.* **1969**, *111*, 195–205
- ⁹³ Williams, D. H.; Williamson, M. P.; Butcher, D. W.; Hammond, S. J.; *J. Am. Chem. Soc.* **1983**, *105*, 1332–1339
- ⁹⁴ Evans, D. A.; Katz, J. L.; Peterson, G. S.; Hintermann, T.; *J. Am. Chem. Soc.* **2001**, *123*, 12411–12413
- ⁹⁵ Zhang, F.; Sun, H.; Song, Z.; Zhou, S.; Wen, X.; Xu, Q.-L.; Sun, H.; *J. Org. Chem.* **2015**, *80*, 4459–4464
- ⁹⁶ Gunsior, M.; Breazeale, S. D.; Lind, A. J.; Ravel, J.; Janc, J. W.; Townsend, C. A.; *Chemistry & Biology* **2004**, *11*, 927–938
- ⁹⁷ Watkins, J.; Collingridge, G.; *Trends Pharmacol. Sci.* **1994**, *15*, 333–342
- ⁹⁸ Siengalewicz, P.; Rinner, U.; Mulzer, J.; *Chem. Soc. Rev.* **2008**, *37*, 2676–2690
- ⁹⁹ Evans, D. A.; Evrad, D. A.; Rychnovsky, S. D.; Früh, T.; Whittingham, W. G.; deVries, K. M.; *Tetrahedron Lett.* **1992**, *33*, 1189–1192
- ¹⁰⁰ Lloyd-Williams, P.; Albericio, F.; Giralt, E. *Chemical Approaches to the Synthesis of Peptides and Proteins*; CRC Press, 1997
- ¹⁰¹ Reddy, K. L.; Sharpless, K. B.; *J. Am. Chem. Soc.* **1998**, *120*, 1207–1217
- ¹⁰² Arthur, M.; Molinas, C.; Bugg, T. D.; Wright, G. D.; Walsh, C. T.; Courvalin, P.; *Antimicrob. Agents Chemother.* **1992**, *36*, 867–869
- ¹⁰³ Walsh, C. T.; *Science* **1993**, *261*, 308–309
- ¹⁰⁴ Walsh, C. T.; Fisher, S. L.; Park, I.-S.; Prahalad, M.; Wu, Z.; *Chemistry & Biology* **1996**, *3*, 21–28
- ¹⁰⁵ Evans, D. A.; Wood, M. R.; Trotter, B. W.; Richardson, T. I.; Barrow, J. C.; Katz, J. L.; *Angew. Chem. Int. Ed.* **1998**, *37*, 2700–2704
- ¹⁰⁶ Crowley, B. M.; Boger, D. L.; *J. Am. Chem. Soc.* **2006**, *128*, 2885–2892
- ¹⁰⁷ Nicas, T. I.; Mullen, D. L.; Flokowitsch, J. E.; Preston, D. A.; Snyder, N. J.; Stratford, R. E.; Cooper, R. D.; *Antimicrob. Agents Chemother.* **1995**, *39*, 2585–2587
- ¹⁰⁸ Nicas, T. I.; Zeckel, M. L.; Braun, D. K.; *Trends in Microbiology* **1997**, *5*, 240–249
- ¹⁰⁹ Nagarajan, R.; *J. Antibiot.* **1993**, *46*, 1181–1195
- ¹¹⁰ Beauregard, D. A.; Williams, D. H.; Gwynn, M. N.; Knowles, D. J.; *Antimicrob. Agents Chemother.* **1995**, *39*, 781–785
- ¹¹¹ Beauregard, D. A.; Maguire, A. J.; Williams, D. H.; Reynolds, P. E.; *Antimicrob. Agents Chemother.* **1997**, *41*, 2418–2423
- ¹¹² Bauer, A.; Brönstrup, M.; *Nat. Prod. Rep.* **2013**, *31*, 35–60
- ¹¹³ Soddy, F.; *J. Chem. Soc., Trans.* **1911**, *99*, 72–83
- ¹¹⁴ Thomson, J. J.; *Rays of Positive Electricity and Their Application to Chemical Analyses*; London, New York, Longmans, Green and Co., **1913**
- ¹¹⁵ Aston, F. W.; *Isotopes*; London, Edward Arnold and Co., **1922**
- ¹¹⁶ Birge, R. T.; Menzel, D. H.; *Phys. Rev.* **1931**, *37*, 1669–1671
- ¹¹⁷ Urey, H. C.; Brickwedde, F. G.; Murphy, G. M.; *Phys. Rev.* **1932**, *40*, 1–15
- ¹¹⁸ Urey, H. C.; *Science* **1933**, *78*, 566–571

- ¹¹⁹ Harbeson, S. L.; Tung, R. D.; In *Annual Reports in Medicinal Chemistry*; John E. Macor, Ed.; Academic Press, **2011**; *46*, 403–417
- ¹²⁰ Lewis, G. N.; Macdonald, R. T.; *J. Am. Chem. Soc.* **1933**, *55*, 4730–4731
- ¹²¹ Meier-Augenstein, W.; Kemp, H. F.; Stable Isotope Analysis: General Principles and Limitations. In *Wiley Encyclopedia of Forensic Science*; John Wiley & Sons, **2009**
- ¹²² Nič, M.; Jirát, J.; Košata, B.; Jenkins, A.; McNaught, A.; Kinetic Isotope Effect. In *IUPAC Compendium of Chemical Terminology*; **2009**
- ¹²³ Leskovac, V.; Kinetic Isotope Effects. In *Comprehensive Enzyme Kinetics*; Springer US, **2004**
- ¹²⁴ Upadhyay, S. K.; *Chemical Kinetics and Reaction Dynamics*; Springer Science & Business Media, **2007**
- ¹²⁵ Foster, A. B.; *Trends in Pharmacological Sciences* **1984**, *5*, 524–527
- ¹²⁶ Selwood, P. W.; Frost, A. A.; *J. Am. Chem. Soc.* **1933**, *55*, 4335–4336
- ¹²⁷ Jones, J. R.; *J. Labelled Cpd. Radiopharm.* **1969**, *5*, 305–311
- ¹²⁸ Godin, J.-P.; Ross, A. B.; Rezzi, S.; Poussin, C.; Martin, F.-P.; Fuerholz, A.; Cléroux, M.; Mermoud, A.-F.; Tornier, L.; Arce Vera, F.; Pouteau, E.; Ramadan, Z.; Kochhar, S.; Fay, L.-B.; *Anal. Chem.* **2010**, *82*, 646–653
- ¹²⁹ Kushner, D. J.; Baker, A.; Dunstall, T. G.; *Can. J. Physiol. Pharmacol.* **1999**, *77*, 79–88
- ¹³⁰ Iglesias, J.; Sleno, L.; Volmer, D. A.; *Curr. Drug Metab.* **2012**, *13*, 1213–1225
- ¹³¹ Harbeson, S. L.; Tung, R. D.; *Drug Discovery & Development magazine* **2010**, *13*, 22
- ¹³² Harbeson, S. L.; Tung, R. D.; In *Annual Reports in Medicinal Chemistry*; John E. Macor, Ed.; Academic Press, **2011**; *46*, 403–417
- ¹³³ Fischer, J.; Ganellin, C. R.; Rotella, D. P.; *Analogue-Based Drug Discovery III*; John Wiley & Sons, **2013**, 56–58
- ¹³⁴ Sanderson, K.; Big Interest in Heavy Drugs. *Nature News* **2009**
- ¹³⁵ Jacobsen, N. E.; *NMR Spectroscopy Explained*; John Wiley & Sons, **2007**, 131
- ¹³⁶ Levitt, M. H.; *Spin Dynamics: Basics of Nuclear Magnetic Resonance*; John Wiley & Sons, **2008**, 12
- ¹³⁷ Atzrodt, J.; Derdau, V.; Fey, T.; Zimmermann, J.; *Angew. Chem. Int. Ed. Engl.* **2007**, *46*, 7744–7765
- ¹³⁸ Heller, M.; Mattou, H.; Menzel, C.; Yao, X.; *J. Am. Soc. Mass Spec.* **2003**, *14*, 704–718
- ¹³⁹ Junk, T.; Catallo, W. J.; *Tetrahedron Lett.* **1996**, *37*, 3445–3448
- ¹⁴⁰ Perrotin, P.; Sinnema, P.-J.; Shapiro, P. J.; *Organometallics* **2006**, *25*, 2104–2107
- ¹⁴¹ Ingold, C. K.; Raisin, C. G.; Wilson, C. L.; Bailey, C. R.; Topley, B.; *J. Chem. Soc.* **1936**, 915–925
- ¹⁴² Larsen, J. W.; Chang, L. W.; *J. Org. Chem.* **1978**, *43*, 3602–3602
- ¹⁴³ Leis, H. J.; Windischhofer, W.; Wintersteiger, R.; *Biol. Mass Spectrom.* **1994**, *23*, 637–641
- ¹⁴⁴ Falardeau, P.; Oates, J. A.; Brash, A. R.; *Analytical Biochemistry* **1981**, *115*, 359–367
- ¹⁴⁵ Scheiget, J.; Berthelette, C.; Li, C.; Zamboni, R. J.; *J. Label. Compd. Radiopharm.* **2004**, *47*, 881–889
- ¹⁴⁶ Berthelette, C.; Scheiget, J.; *J. Label. Compd. Radiopharm.* **2004**, *47*, 891–894
- ¹⁴⁷ Lygo, B.; Humphreys, L. D.; *Tetrahedron Lett.* **2002**, *43*, 6677–6679
- ¹⁴⁸ Krüger, J.; Manmontri, B.; Fels, G.; *Eur. J. Org. Chem.* **2005**, 1402–1408
- ¹⁴⁹ Maegawa, T.; Fujiwara, Y.; Inagaki, Y.; Monguchi, Y.; Sajiki, H.; *Adv. Synth. Catal.* **2008**, *350*, 2215–2218
- ¹⁵⁰ Garnett, J. L.; Sollich-Baumgartner, W. A.; *J. Phys. Chem.* **1964**, *68*, 3177–3183
- ¹⁵¹ Sajiki, H.; Ito, N.; Esaki, H.; Maesawa, T.; Maegawa, T.; Hirota, K.; *Tetrahedron Lett.* **2005**, *46*, 6995–69
- ¹⁵² Ito, N.; Watahiki, T.; Maesawa, T.; Maegawa, T.; Sajiki, H.; *Adv. Synth. Catal.* **2006**, *348*, 1025–1028
- ¹⁵³ Maegawa, T.; Akashi, A.; Esaki, H.; Aoki, F.; Sajiki, H.; Hirota, K.; *Synlett* **2005**, 845–847
- ¹⁵⁴ Cioffi, E. A.; Prestegard, J. H.; *Tetrahedron Lett.* **1986**, *27*, 415–418
- ¹⁵⁵ Bokatzian-Johnson, S. S.; Maier, M. L.; Bell, R. H.; Alston, K. E.; Le, B. Y.; Cioffi, E. A.; *J. Label. Compd. Radiopharm.* **2007**, *50*, 380–383
- ¹⁵⁶ Foster, A. B.; *Trends in Pharmacological Sciences* **1984**, *5*, 524–527

- ¹⁵⁷ Najjar, S. E.; Blake, M. I.; Benoit, P. A.; Lu, M. C.; *J. Med. Chem.* **1978**, *21*, 555–558
- ¹⁵⁸ Sharma, R.; Strelevitz, T. J.; Gao, H.; Clark, A. J.; Schildknecht, K.; Obach, R. S.; Ripp, S. L.; Spracklin, D. K.; Tremaine, L. M.; Vaz, A. D. N.; *Drug Metab Dispos* **2012**, *40*, 625–634
- ¹⁵⁹ Cleland, W. W.; *Archives of Biochemistry and Biophysics* **2005**, *433*, 2–12.
- ¹⁶⁰ Kelly, N. M.; Sutherland, A.; Willis, C. L.; *Nat. Prod. Rep.* **1997**, *14*, 205–219
- ¹⁶¹ Cellitti, S. E.; Jones, D. H.; Lagpacan, L.; Hao, X.; Zhang, Q.; Hu, H.; Brittain, S. M.; Brinker, A.; Caldwell, J.; Bursulaya, B.; Spraggon, G.; Brock, A.; Ryu, Y.; Uno, T.; Schultz, P. G.; Geierstanger, B. H.; *J. Am. Chem. Soc.* **2008**, *130*, 9268–9281
- ¹⁶² Verardi, R.; Traaseth, N. J.; Masterson, L. R.; Vostrikov, V. V.; Veglia, G.; *Adv Exp Med Biol* **2012**, *992*, 35–62
- ¹⁶³ Hill, R. K.; Abächerli, C.; Hagishita, S.; *Can. J. Chem.* **1994**, *72*, 110–113
- ¹⁶⁴ Bew, S. P.; Carrington, R.; Hughes, D. L.; Liddle, J.; Pesce, P.; *Adv. Synth. Catal.* **2009**, *351*, 2579–2588
- ¹⁶⁵ Williams, A. L.; Johnston, J. N.; *J. Am. Chem. Soc.*, **2004**, *126*, 1612–1613
- ¹⁶⁶ Dewick, P. M.; *Essentials of Organic Chemistry: For Students of Pharmacy, Medicinal Chemistry and Biological Chemistry*; John Wiley & Sons, **2006**
- ¹⁶⁷ Yadav, J. S.; Reddy, B. V. S.; Reddy, P. N.; Shesha Rao M.; *Synthesis*, **2003**, *9*, 1387–1390
- ¹⁶⁸ Bansal, R. K.; *Heterocyclic Chemistry*; 3rd ed.; New Age International Publishers, **1999**, 11
- ¹⁶⁹ Casarrubios, L.; Pérez, J. A.; Brookhart, M.; Templeton, J. L.; *J. Org. Chem.*, **1996**, *61*, 8358–8359
- ¹⁷⁰ Karplus, M.; *J. Am. Chem. Soc.* **1963**, *85*, 2870–2871
- ¹⁷¹ Vetticatt, M. J.; Desai, A. A.; Wulff, W. D.; *J. Org. Chem.*, **2013**, *78*, 5142–5152
- ¹⁷² Zhang, Y.; Lu, Z.; Wulff, W.; *Synlett*, **2009**, *17*, 2715–2739
- ¹⁷³ Pesce, P.; ‘*Organocatalytic methods towards the synthesis of chiral racemic and chiral non-racemic C_{2,3}-difunctionalised N-alkyl and N-arylaziridines*’, Doctoral Thesis, University of East Anglia, **2010**
- ¹⁷⁴ Nakashima, D.; Yamamoto, H.; *J. Am. Chem. Soc.*, **2006**, *128*, 9626–9627
- ¹⁷⁵ Gridnev, I. D.; Kouchi, M.; Sorimachi, K.; Terada, M.; *Tetrahedron. Lett.*, **2007**, *48*, 497–500
- ¹⁷⁶ Wyatt, W. F.; *Trans. Faraday Soc.* **1929**, *25*, 43–48
- ¹⁷⁷ Freedman, T. B.; Cao, X.; Dukor, R. K.; Nafie, L. A.; *Chirality* **2003**, *15*, 743–758
- ¹⁷⁸ Felipe, L. G.; Jr, J. M. B.; Baldoqui, D. C.; Nascimento, I. R.; Kato, M. J.; He, Y.; Nafie, L. A.; Furlan, M.; *Org. Biomol. Chem.* **2012**, *10*, 4208–4214
- ¹⁷⁹ Beresford, K. J. M.; Young, D. W.; *Tetrahedron* **1996**, *52*, 9891–9900
- ¹⁸⁰ Davies, P. W.; Martin, N.; Spencer, N.; *Beilstein J Org Chem* **2011**, *7*, 839–846
- ¹⁸¹ Crimaldi, K.; Lichter, R. L.; *J. Org. Chem.* **1980**, *45*, 1277–1281
- ¹⁸² Tarburton, P.; Edasery, J. P.; Kingsbury, C. A.; Sopchik, A. E.; Cromwell, N. H.; *J. Org. Chem.* **1979**, *44*, 2041–2042
- ¹⁸³ Bennett, D. J.; Kirby, G.W.; Moss, V. A.; *Chem. Comm.*, **1967**, 218
- ¹⁸⁴ Hanson, J. R.; *The Organic Chemistry of Isotopic Labelling*; RSC Publishing, **2011**, 51
- ¹⁸⁵ Wang, M.; Funabiki, K.; Matsui, M.; *Dyes and Pigments* **2003**, *57*, 77–86
- ¹⁸⁶ Gakh, Y. G.; Gakh, A. A.; Gronenborn, A. M.; *Magn. Reson. Chem.* **2000**, *38*, 551–558
- ¹⁸⁷ Anslyn, E. V.; Dougherty, D. A.; *Modern Physical Organic Chemistry*; University Science Books, **2006**
- ¹⁸⁸ Shestakova, T. S.; Deev, S. L.; Ulomskii, E. N.; Rusinov, V. L.; Kodess, M. I.; Chupakhin, O. N.; *Arkivoc* **2009**, *4*, 69–78
- ¹⁸⁹ Ladurée, D.; Florentin, D.; Robba, M.; *Journal of Heterocyclic Chemistry* **1980**, *17*, 1189–1193
- ¹⁹⁰ Ulomskii, E. N.; Deev, S. L.; Shestakova, T. S.; Rusinov, V. L.; Chupakhin, O. N.; *Russian Chemical Bulletin* **2002**, *51*, 1737–1743
- ¹⁹¹ Hollmann, D.; Bähn, S.; Tillack, A.; Beller, M.; *Chem. Commun.* **2008**, 3199–3201
- ¹⁹² Maas, G.; *Angew. Chem. Int. Ed.* **2009**, *48*, 8186–8195
- ¹⁹³ Bew, S. P.; Ashford, P.-A.; Bachera, D. U.; *Synthesis*, **2013**, *7*, 903–912
- ¹⁹⁴ Hutton, W. C.; Likos, J. J.; Gard, J. K.; Garbow, J. R.; *J. Label. Compd. Radiopharm.* **1998**, *41*, 87–95

- ¹⁹⁵ Qiu, F.; Rivera, M.; Stark, R. E.; *J.M.R.* **1998**, *130*, 76–81
- ¹⁹⁶ Baker, J. W.; Hey, L.; *J. Chem. Soc.* **1932**, 1226–1231
- ¹⁹⁷ Kalvin, D. M.; Woodard, R. W.; *Tetrahedron*, 1984, *40*, 3387–3392
- ¹⁹⁸ Bruckner, R.; Harmata, M.; *Organic mechanisms*; Spektrum Akademischer, **2007**, 796
- ¹⁹⁹ Blake, M. E.; Bartlett, K. L.; Jones, M.; *J. Am. Chem. Soc.* **2003**, *125*, 6485–6490
- ²⁰⁰ Mazumdar, A.; Xue, Z.; Mayer, M. A.; *Synlett* **2007**, *13*, 2025–2028
- ²⁰¹ Iskra, J.; Stavber, S.; Zupan, M.; *Tetrahedron Lett.* **2008**, *49*, 893–895
- ²⁰² Kim, J.; Chang, S.; *Chem. Commun.* **2008**, 3052–3054
- ²⁰³ Marsh, E. N. G.; Suzuki, Y.; *ACS Chem. Biol.* **2014**, *9*, 1242–1250
- ²⁰⁴ Lichter, R. L.; Wasylshen, R. E.; *J. Am. Chem. Soc.* **1975**, *97*, 1808–1813
- ²⁰⁵ Chiba, S.; *Synlett*, **2012**, *01*, 21–44
- ²⁰⁶ Wilson, G. O.; Porter, K. A.; Weissman, H.; White, S. R.; Sottos, N. R.; Moore, J. S.; *Adv. Synth. Catal.* **2009**, *351*, 1817–1825
- ²⁰⁷ Bhuiyan, M. D. H.; Zhu, K.-X.; Jensen, P.; Try, A. C.; *Eur. J. Org. Chem.* **2010**, 4662–4670
- ²⁰⁸ Hu, M.; Li, J.; Yao, S. Q.; *Org. Lett.* **2008**, *10*, 5529–5531
- ²⁰⁹ Brase, S.; Banert, K.; *Organic Azides*; John Wiley & Sons, **2010**, 80
- ²¹⁰ Nagata, S.; Sato, H.; Sugikawa, K.; Kokado, K.; Sada, K.; *Cryst. Eng. Comm.* **2012**, *14*, 4137–4141
- ²¹¹ O'Hagan, D.; Goss, R. J. M.; Meddour, A.; Courtieu, J.; *J. Am. Chem. Soc.* **2002**, *125*, 379–387
- ²¹² Baciocchi, E.; Mandolini, L.; Rol, C.; *J. Am. Chem. Soc.* **1980**, *102*, 7597–7598
- ²¹³ Jarrahpour, A.; Zarei, M.; *Molecules* **2007**, *12*, 2364–2379
- ²¹⁴ Tanoue, Y.; Terada, A.; *Bulletin of the Chemical Society of Japan* **1988**, *61*, 2039–2045
- ²¹⁵ Molinaro, C.; Scott, J. P.; Shevlin, M.; Wise, C.; Ménard, A.; Gibb, A.; Junker, E. M.; Lieberman, D.; *J. Am. Chem. Soc.* **2015**, *137*, 999–1006
- ²¹⁶ Nilsson, M.; Hämäläinen, M.; Ivarsson, M.; Gottfries, J.; Xue, Y.; Hansson, S.; Isaksson, R.; Fex, T.; *J. Med. Chem.* **2009**, *52*, 2708–2715
- ²¹⁷ Takahashi, M.; Suzuki, N.; Ishikawa, T.; *J. Org. Chem.* **2013**, *78*, 3250–3261
- ²¹⁸ Righi, G.; Chionne, A.; Bonini, C.; *Eur. J. Org. Chem.* **2000**, *2000*, 3127–3131
- ²¹⁹ Righi, G.; Catullo, S.; *Synthetic Communications* **2004**, *34*, 85–97
- ²²⁰ Righi, G.; Ciabrone, S.; Esuperanzi, E.; Montini, F.; Pelagalli, R.; *J. Heterocyclic Chem.* **2010**, *47*, 564–568
- ²²¹ Yamaguchi, K.; Ueki, R.; Yamada, H.; Aoyama, Y.; Nonaka, H.; Sando, S.; *Anal. Methods* **2011**, *3*, 1664–1666
- ²²² Barnes, P. J.; *Am. J. Respir. Crit. Care Med.* **2003**, *167*, 813–818
- ²²³ Butler, M. S.; Hansford, K. A.; Blaskovich, M. A. T.; Halai, R.; Cooper, M. A.; *J. Antibiot.* **2014**, *67*, 631–644
- ²²⁴ Boger, D. L.; Kim, S. H.; Miyazaki, S.; Strittmatter, H.; Weng, J.-H.; Mori, Y.; Rogel, O.; Castle, S. L.; McAtee, J. J.; *J. Am. Chem. Soc.* **2000**, *122*, 7416–7417
- ²²⁵ Barna, J. C.; Williams, D. H.; Strazzolini, P.; Malabarba, A.; Leung, T. W.; *J. Antibiot.* **1984**, *37*, 1204–1208
- ²²⁶ Boger, D. L.; Miyazaki, S.; Kim, S. H.; Wu, J. H.; Castle, S. L.; Loiseleur, O.; Jin, Q.; *J. Am. Chem. Soc.* **1999**, *121*, 10004–10011
- ²²⁷ Boger, D. L.; Kim, S. H.; Mori, Y.; Weng, J.-H.; Rogel, O.; Castle, S. L.; McAtee, J. J.; *J. Am. Chem. Soc.* **2001**, *123*, 1862–1871
- ²²⁸ Moroz, A. A.; Shvartsberg, M. S.; *Russian Chemical Reviews* **1974**, *43*, 679–689
- ²²⁹ Wuts, P. G. M.; Greene, T. W.; *Protective Groups in Organic Synthesis*; John Wiley & Sons, 4th ed. **2007**
- ²³⁰ Huet, F.; Lechevallier, A.; Pellet, M.; Conia, J. M.; *Synthesis* **1978**, 63–65
- ²³¹ Albers, H. M. H. G.; Hendrickx, L. J. D.; van Tol, R. J. P.; Hausmann, J.; Perrakis, A.; Ova, H.; *J. Med. Chem.* **2011**, *54*, 4619–4626
- ²³² Frlan, R.; Kikelj, D.; *Synthesis* **2006**, *14*, 2271–2285
- ²³³ Miyaura, N.; Buchwald, S. L.; *Cross-Coupling Reactions: A Practical Guide*; Springer Science & Business Media, **2002**

- ²³⁴ Altman, R. A.; Shafir, A.; Choi, A.; Lichtor, P. A.; Buchwald, S. L.; *J. Org. Chem.* **2007**, *73*, 284–286
- ²³⁵ Evano, G.; Blanchard, N.; *Copper-Mediated Cross-Coupling Reactions*; John Wiley & Sons, **2013**
- ²³⁶ Sambigiagio, C.; Marsden, S. P.; Blacker, A. J.; McGowan, P. C. *Chem. Soc. Rev.* **2014**, *43*, 3525–3550
- ²³⁷ Delmas, M.; Bigot, Y. L.; Gaset, A.; Gorrichon, J. P.; *Synthetic Communications* **1981**, *11*, 125–132
- ²³⁸ Takeuchi, D.; Osakada, K.; *Chem. Commun.* **2002**, 646–647
- ²³⁹ Byrne, P. A.; Gilheany, D. G.; *Chemical Society Reviews* **2013**, *42*, 6670
- ²⁴⁰ Goldwhite, H.; *Introduction to Phosphorous Chemistry*; Cambridge University Press, **1981**
- ²⁴¹ Reynolds, W. F.; Peat, I. R.; Hamer, G. K.; *Can. J. Chem.* **1974**, *52*, 3415–3423
- ²⁴² Kaniskan, H. Ü.; Garner, P.; *J. Am. Chem. Soc.* **2007**, *129*, 15460–15461
- ²⁴³ Endo, A.; Yanagisawa, A.; Abe, M.; Tohma, S.; Kan, T.; Fukuyama, T.; *J. Am. Chem. Soc.* **2002**, *124*, 6552–6554
- ²⁴⁴ Bodkin, J. A.; McLeod, M. D.; *J. Chem. Soc., Perkin Trans. 1* **2002**, *24*, 2733–2746
- ²⁴⁵ Kolb, H. C.; VanNieuwenhze, M. S.; Sharpless, K. B.; *Chem. Rev.* **1994**, *94*, 2483–2547
- ²⁴⁶ Sharpless, K. B.; Amberg, W.; Beller, M.; Chen, H.; Hartung, J.; Kawanami, Y.; Lubben, D.; Manoury, E.; Ogino, Y.; *J. Org. Chem.* **1991**, *56*, 4585–4588
- ²⁴⁷ Jacobsen, E. N.; Marko, I.; Mungall, W. S.; Schroeder, G.; Sharpless, K. B.; *J. Am. Chem. Soc.* **1988**, *110*, 1968–1970
- ²⁴⁸ Sharpless, K. B.; Amberg, W.; Bennani, Y. L.; Crispino, G. A.; Hartung, J.; Jeong, K. S.; Kwong, H. L.; Morikawa, K.; Wang, Z. M.; *J. Org. Chem.* **1992**, *57*, 2768–2771
- ²⁴⁹ Boger, D. L.; Borzilleri, R. M.; Nukui, S.; *J. Org. Chem.* **1996**, *61*, 3561–3565
- ²⁵⁰ Anelli, P. L.; Biffi, C.; Montanari, F.; Quici, S.; *J. Org. Chem.* **1987**, *52*, 2559–2562
- ²⁵¹ Petrônio, M. S.; Ximenes, V. F.; *Luminescence* **2013**, *28*, 853–859
- ²⁵² Toma, T.; Shimokawa, J.; Fukuyama, T.; *Org. Lett.* **2007**, *9*, 3195–3197
- ²⁵³ Regitz, M.; *Diazo Compounds: Properties and Synthesis*; Academic Press, Inc., **1986**
- ²⁵⁴ Gmeiner, P.; Feldman, P. L.; Chu-Moyer, M. Y.; Rapoport, H.; *J. Org. Chem.* **1990**, *55*, 3068–3074
- ²⁵⁵ Takeuchi, D.; Osakada, K.; *Chem. Commun.* **2002**, 646–647
- ²⁵⁶ Yin, G.; Wu, Y.; Liu, G.; *J. Am. Chem. Soc.* **2010**, *132*, 11978–11987
- ²⁵⁷ Demko, Z. P.; Bartsch, M.; Sharpless, K. B.; *Org. Lett.* **2000**, *2*, 2221–2223
- ²⁵⁸ Bruncko, M.; Schlingloff, G.; Sharpless, K. B.; *Angew. Chem. Int. Ed. Engl.* **1997**, *36*, 1483–1486
- ²⁵⁹ Davi, M.; Lebel, H.; *Org. Lett.* **2009**, *11*, 41–44
- ²⁶⁰ Huang, J.-M.; Lin, Z.-Q.; Chen, D.-S.; *Org. Lett.* **2012**, *14*, 22–25
- ²⁶¹ Price, K. E.; Broadwater, S. J.; Walker, B. J.; McQuade, D. T.; *J. Org. Chem.* **2005**, *70*, 3980–3987
- ²⁶² Brookhart, M.; Cheng, C.; *Angew. Chem. Int. Ed. Engl.* **2012**, *51*, 9422–9424
- ²⁶³ Wang, A.; Jiang, H.; *J. Org. Chem.* **2010**, *75*, 2321–2326

Appendix

All x-ray crystallographic data collection and structure analysis carried out by Dr Mateusz B. Pitak, UK National Crystallography Service, Southampton. (M.Pitak@soton.ac.uk)

Appendix 1: X-ray crystal structure and crystallographic data for (±)-*cis*-(5.8).

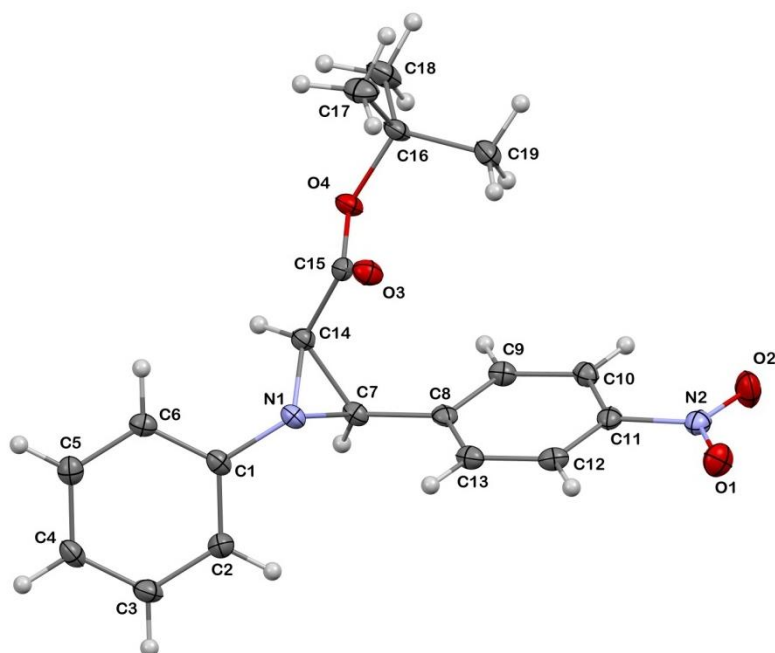


Figure 1. Molecular structure of **2014ncs0678 (VZ087)**. Displacement ellipsoids – 50% probability.

Table 1. Crystal data and structure refinement details.

Identification code	2014ncs0678 (VZ087)	
Empirical formula	C ₁₉ H ₂₀ N ₂ O ₄	
Formula weight	340.37	
Temperature	100(2) K	
Wavelength	0.71075 Å	
Crystal system	Orthorhombic	
Space group	P2 ₁ 2 ₁ 2 ₁	
Unit cell dimensions	<i>a</i> = 6.02830(10) Å	<i>α</i> = 90°
	<i>b</i> = 15.5813(5) Å	<i>β</i> = 90°
	<i>c</i> = 18.3695(12) Å	<i>γ</i> = 90°
Volume	1725.42(13) Å ³	
Z	4	
Density (calculated)	1.310 Mg / m ³	
Absorption coefficient	0.093 mm ⁻¹	
<i>F</i> (000)	720	
Crystal	Shard; colourless	
Crystal size	0.180 × 0.070 × 0.020 mm ³	
<i>θ</i> range for data collection	3.429 – 27.481°	
Index ranges	–7 ≤ <i>h</i> ≤ 6, –20 ≤ <i>k</i> ≤ 11, –23 ≤ <i>l</i> ≤ 23	
Reflections collected	12619	
Independent reflections	3923 [<i>R</i> _{int} = 0.0262]	

Completeness to $\theta = 25.242^\circ$	99.6 %
Absorption correction	Semi-empirical from equivalents
Max. and min. transmission	1.000 and 0.820
Refinement method	Full-matrix least-squares on F^2
Data / restraints / parameters	3923 / 0 / 229
Goodness-of-fit on F^2	1.029
Final R indices [$F^2 > 2\sigma(F^2)$]	$R1 = 0.0328$, $wR2 = 0.0708$
R indices (all data)	$R1 = 0.0394$, $wR2 = 0.0757$
Absolute structure parameter	-0.5(4)
Extinction coefficient	n/a
Largest diff. peak and hole	0.167 and $-0.161 \text{ e } \text{\AA}^{-3}$

Diffractometer: Rigaku AFC12 goniometer equipped with an enhanced sensitivity (HG) Saturn724+ detector mounted at the window of an FR-E+ SuperBright molybdenum rotating anode generator with HF Varimax optics (100m focus). **Cell determination and data collection:** CrystalClear-SM Expert 2.0 r11 (Rigaku, 2011). **Data reduction, cell refinement and absorption correction:** CrystalClear-SM Expert 2.1 r29 (Rigaku, 2011). **Structure solution:** SUPERFLIP (Palatinus, L. & Chapuis, G. (2007). *J. Appl. Cryst.* 40, 786-790). **Structure refinement:** SHELXL-2013 (Sheldrick, G.M. (2008). *Acta Cryst.* A64, 112-122).

Special details:

Absolute configuration cannot be reliably determined based on anomalous dispersion effect due to lack of heavier element in the crystal structure (>Si), however the relative configuration can be assigned as R, R or S,S on C7 and C14.

Table 2. Atomic coordinates [$\times 10^4$], equivalent isotropic displacement parameters [$\text{\AA}^2 \times 10^3$] and site occupancy factors. U_{eq} is defined as one third of the trace of the orthogonalized U^{ij} tensor.

Atom	x	y	z	U_{eq}	<i>S.o.f.</i>
C1	546(3)	-3072(1)	-8601(1)	15(1)	1
C2	343(3)	-2221(1)	-8385(1)	19(1)	1
C3	1647(3)	-1594(1)	-8712(1)	22(1)	1
C4	3140(4)	-1812(1)	-9258(1)	21(1)	1
C5	3326(3)	-2661(1)	-9475(1)	19(1)	1
C6	2051(3)	-3293(1)	-9147(1)	16(1)	1
C7	-2990(3)	-3688(1)	-8127(1)	16(1)	1
C8	-3914(3)	-4002(1)	-7419(1)	16(1)	1
C9	-6020(3)	-4366(1)	-7415(1)	17(1)	1
C10	-6957(3)	-4657(1)	-6771(1)	17(1)	1
C11	-5745(3)	-4567(1)	-6137(1)	17(1)	1
C12	-3627(3)	-4225(1)	-6123(1)	18(1)	1
C13	-2714(3)	-3940(1)	-6775(1)	18(1)	1
C14	-1979(3)	-4320(1)	-8652(1)	15(1)	1
C15	-1927(3)	-5247(1)	-8440(1)	16(1)	1
C16	-3912(3)	-6581(1)	-8727(1)	19(1)	1
C17	-1853(4)	-7143(1)	-8748(1)	27(1)	1
C18	-5447(4)	-6790(2)	-9358(1)	29(1)	1
C19	-5146(4)	-6633(2)	-8006(1)	24(1)	1
N1	-597(3)	-3739(1)	-8227(1)	15(1)	1
N2	-6754(3)	-4837(1)	-5446(1)	19(1)	1
O1	-5638(3)	-4772(1)	-4889(1)	26(1)	1
O2	-8663(3)	-5107(1)	-5453(1)	31(1)	1
O3	-863(2)	-5540(1)	-7942(1)	21(1)	1
O4	-3334(2)	-5673(1)	-8870(1)	19(1)	1

Table 3. Bond lengths [\AA] and angles [$^\circ$].

C1-C2	1.390(3)
-------	----------

C1-C6	1.396(3)
C1-N1	1.424(2)
C2-C3	1.390(3)
C2-H2	0.9500
C3-C4	1.390(3)
C3-H3	0.9500
C4-C5	1.386(3)
C4-H4	0.9500
C5-C6	1.386(3)
C5-H5	0.9500
C6-H6	0.9500
C7-N1	1.456(2)
C7-C8	1.498(2)
C7-C14	1.506(3)
C7-H7	1.0000
C8-C13	1.390(3)
C8-C9	1.390(3)
C9-C10	1.387(3)
C9-H9	0.9500
C10-C11	1.382(3)
C10-H10	0.9500
C11-C12	1.384(3)
C11-N2	1.469(2)
C12-C13	1.391(3)
C12-H12	0.9500
C13-H13	0.9500
C14-N1	1.456(2)
C14-C15	1.496(3)
C14-H14	1.0000
C15-O3	1.208(2)
C15-O4	1.336(2)
C16-O4	1.480(2)
C16-C18	1.518(3)
C16-C17	1.520(3)
C16-C19	1.521(3)
C17-H17A	0.9800
C17-H17B	0.9800
C17-H17C	0.9800
C18-H18A	0.9800
C18-H18B	0.9800
C18-H18C	0.9800
C19-H19A	0.9800
C19-H19B	0.9800
C19-H19C	0.9800
N2-O2	1.225(2)
N2-O1	1.230(2)
C2-C1-C6	119.89(18)
C2-C1-N1	121.10(17)
C6-C1-N1	118.73(18)
C1-C2-C3	119.82(19)
C1-C2-H2	120.1
C3-C2-H2	120.1
C4-C3-C2	120.38(19)
C4-C3-H3	119.8
C2-C3-H3	119.8
C5-C4-C3	119.57(19)
C5-C4-H4	120.2
C3-C4-H4	120.2
C6-C5-C4	120.53(18)

C6-C5-H5	119.7
C4-C5-H5	119.7
C5-C6-C1	119.81(19)
C5-C6-H6	120.1
C1-C6-H6	120.1
N1-C7-C8	117.41(16)
N1-C7-C14	58.85(12)
C8-C7-C14	119.59(17)
N1-C7-H7	116.2
C8-C7-H7	116.2
C14-C7-H7	116.2
C13-C8-C9	119.99(17)
C13-C8-C7	121.53(17)
C9-C8-C7	118.49(17)
C10-C9-C8	120.60(17)
C10-C9-H9	119.7
C8-C9-H9	119.7
C11-C10-C9	118.08(18)
C11-C10-H10	121.0
C9-C10-H10	121.0
C10-C11-C12	122.86(17)
C10-C11-N2	118.71(17)
C12-C11-N2	118.43(17)
C11-C12-C13	118.14(17)
C11-C12-H12	120.9
C13-C12-H12	120.9
C8-C13-C12	120.29(17)
C8-C13-H13	119.9
C12-C13-H13	119.9
N1-C14-C15	116.61(15)
N1-C14-C7	58.88(11)
C15-C14-C7	118.18(15)
N1-C14-H14	116.9
C15-C14-H14	116.9
C7-C14-H14	116.9
O3-C15-O4	126.61(19)
O3-C15-C14	125.05(17)
O4-C15-C14	108.26(16)
O4-C16-C18	102.29(15)
O4-C16-C17	110.74(16)
C18-C16-C17	110.76(18)
O4-C16-C19	108.68(16)
C18-C16-C19	110.79(17)
C17-C16-C19	113.04(17)
C16-C17-H17A	109.5
C16-C17-H17B	109.5
H17A-C17-H17B	109.5
C16-C17-H17C	109.5
H17A-C17-H17C	109.5
H17B-C17-H17C	109.5
C16-C18-H18A	109.5
C16-C18-H18B	109.5
H18A-C18-H18B	109.5
C16-C18-H18C	109.5
H18A-C18-H18C	109.5
H18B-C18-H18C	109.5
C16-C19-H19A	109.5
C16-C19-H19B	109.5
H19A-C19-H19B	109.5
C16-C19-H19C	109.5

H19A–C19–H19C	109.5
H19B–C19–H19C	109.5
C1–N1–C14	118.19(15)
C1–N1–C7	120.04(16)
C14–N1–C7	62.27(12)
O2–N2–O1	123.46(17)
O2–N2–C11	118.53(16)
O1–N2–C11	118.01(16)
C15–O4–C16	121.36(15)

Symmetry transformations used to generate equivalent atoms:

Table 4. Anisotropic displacement parameters [$\text{\AA}^2 \times 10^3$]. The anisotropic displacement factor exponent takes the form: $-2\pi^2[h^2a^{*2}U^{11} + \dots + 2hk a^* b^* U^{12}]$.

Atom	U^{11}	U^{22}	U^{33}	U^{23}	U^{13}	U^{12}
C1	16(1)	15(1)	16(1)	3(1)	-4(1)	-2(1)
C2	22(1)	18(1)	18(1)	-2(1)	1(1)	-2(1)
C3	28(1)	14(1)	24(1)	0(1)	-2(1)	-3(1)
C4	22(1)	20(1)	21(1)	5(1)	-2(1)	-8(1)
C5	17(1)	23(1)	18(1)	2(1)	-1(1)	-1(1)
C6	16(1)	15(1)	18(1)	0(1)	-3(1)	0(1)
C7	14(1)	14(1)	19(1)	2(1)	-2(1)	-1(1)
C8	17(1)	10(1)	19(1)	1(1)	1(1)	2(1)
C9	17(1)	16(1)	18(1)	0(1)	-3(1)	1(1)
C10	14(1)	16(1)	22(1)	0(1)	1(1)	0(1)
C11	20(1)	12(1)	18(1)	1(1)	3(1)	3(1)
C12	19(1)	15(1)	19(1)	-3(1)	-4(1)	2(1)
C13	16(1)	15(1)	23(1)	-2(1)	-2(1)	0(1)
C14	17(1)	14(1)	16(1)	1(1)	-1(1)	-1(1)
C15	15(1)	15(1)	17(1)	-1(1)	3(1)	-1(1)
C16	23(1)	13(1)	22(1)	1(1)	-2(1)	-6(1)
C17	29(1)	17(1)	36(1)	-3(1)	-1(1)	2(1)
C18	36(1)	20(1)	30(1)	3(1)	-8(1)	-11(1)
C19	25(1)	17(1)	28(1)	3(1)	5(1)	-5(1)
N1	15(1)	14(1)	18(1)	2(1)	-1(1)	-2(1)
N2	24(1)	16(1)	18(1)	0(1)	2(1)	2(1)
O1	30(1)	30(1)	18(1)	3(1)	-3(1)	1(1)
O2	24(1)	42(1)	26(1)	1(1)	5(1)	-11(1)
O3	23(1)	17(1)	22(1)	2(1)	-5(1)	-1(1)
O4	23(1)	13(1)	21(1)	1(1)	-3(1)	-5(1)

Table 5. Hydrogen coordinates [$\times 10^4$] and isotropic displacement parameters [$\text{\AA}^2 \times 10^3$].

Atom	<i>x</i>	<i>y</i>	<i>z</i>	U_{eq}	<i>S.o.f.</i>
H2	-685	-2068	-8015	23	1
H3	1516	-1013	-8561	26	1
H4	4027	-1383	-9481	25	1
H5	4335	-2812	-9851	23	1
H6	2201	-3875	-9294	20	1
H7	-3744	-3180	-8348	19	1
H9	-6825	-4416	-7858	20	1
H10	-8389	-4911	-6766	21	1
H12	-2818	-4186	-5680	21	1
H13	-1263	-3701	-6780	21	1
H14	-2140	-4189	-9183	18	1

H17A	-2293	-7749	-8743	41	1
H17B	-926	-7021	-8322	41	1
H17C	-1011	-7022	-9193	41	1
H18A	-4653	-6708	-9818	43	1
H18B	-6739	-6408	-9343	43	1
H18C	-5940	-7387	-9319	43	1
H19A	-5659	-7222	-7927	35	1
H19B	-6425	-6245	-8017	35	1
H19C	-4149	-6465	-7609	35	1

Appendix 2: X-ray crystal structure and crystallographic data for (5.63).

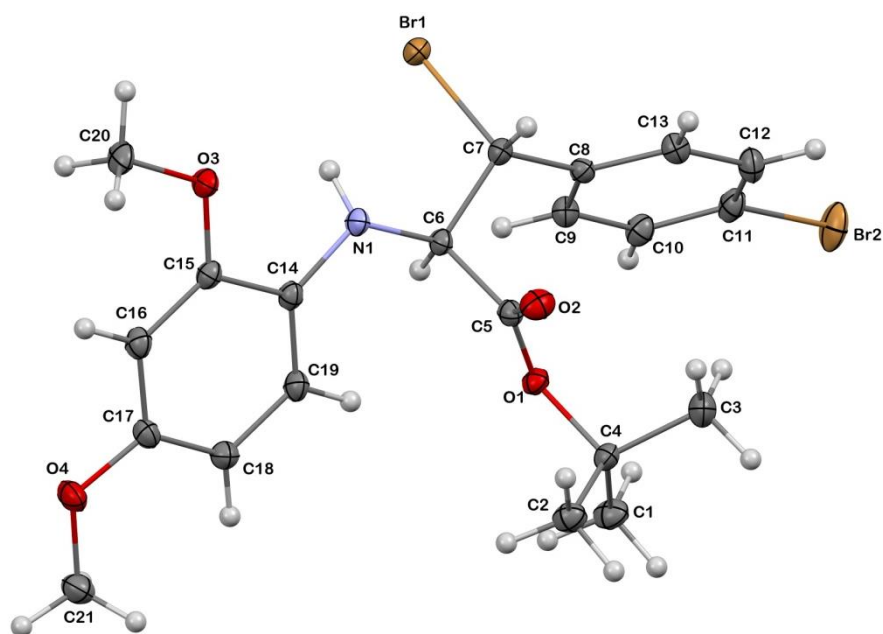


Figure 1. Molecular structure 2014ncs0738 (VZ 106). Displacement ellipsoids - 50% probability.

Table 1. Crystal data and structure refinement details.

Identification code	2014ncs0738 (VZ 106)	
Empirical formula	C ₂₁ H ₂₅ Br ₂ NO ₄	
Formula weight	515.24	
Temperature	100(2) K	
Wavelength	0.71075 Å	
Crystal system	Triclinic	
Space group	<i>P</i> -1	
Unit cell dimensions	<i>a</i> = 8.6732(3) Å	<i>α</i> = 94.425(7)°
	<i>b</i> = 9.6569(3) Å	<i>β</i> = 106.088(8)°
	<i>c</i> = 13.4178(9) Å	<i>γ</i> = 93.023(7)°
Volume	1073.37(10) Å ³	
<i>Z</i>	2	
Density (calculated)	1.594 Mg / m ³	
Absorption coefficient	3.802 mm ⁻¹	

$F(000)$	520
Crystal	Block; Colorless
Crystal size	0.150 × 0.060 × 0.030 mm ³
θ range for data collection	3.116 – 27.464°
Index ranges	–11 ≤ h ≤ 11, –11 ≤ k ≤ 12, –17 ≤ l ≤ 17
Reflections collected	14442
Independent reflections	4905 [$R_{int} = 0.0276$]
Completeness to $\theta = 25.242^\circ$	99.6 %
Absorption correction	Semi-empirical from equivalents
Max. and min. transmission	1.000 and 0.804
Refinement method	Full-matrix least-squares on F^2
Data / restraints / parameters	4905 / 0 / 258
Goodness-of-fit on F^2	1.105
Final R indices [$F^2 > 2\sigma(F^2)$]	$R1 = 0.0242$, $wR2 = 0.0678$
R indices (all data)	$R1 = 0.0265$, $wR2 = 0.0691$
Extinction coefficient	n/a
Largest diff. peak and hole	0.915 and –0.814 e Å ^{–3}

Diffraction: Rigaku AFC12 goniometer equipped with an enhanced sensitivity (HG) Saturn724+ detector mounted at the window of an FR-E+ SuperBright molybdenum rotating anode generator with HF Varimax optics (100m focus). **Cell determination and data collection:** CrystalClear-SM Expert 2.0 r11 (Rigaku, 2011). **Data reduction, cell refinement and absorption correction:** CrystalClear-SM Expert 2.1 r29 (Rigaku, 2011). **Structure solution:** SUPERFLIP (Palatinus, L. & Chapuis, G. (2007). *J. Appl. Cryst.* 40, 786-790). **Structure refinement:** SHELXL-2013 (Sheldrick, G.M. (2008). *Acta Cryst.* A64, 112-122).

Special details:

This compound crystallises in centrosymmetric spacegroup. Unit cell contains two opposite enantiomers (racemic mixture).

Table 2. Atomic coordinates [$\times 10^4$], equivalent isotropic displacement parameters [$\text{\AA}^2 \times 10^3$] and site occupancy factors. U_{eq} is defined as one third of the trace of the orthogonalized U^{ij} tensor.

Atom	x	y	z	U_{eq}	S.o.f.
C1	8674(2)	1696(2)	2692(2)	23(1)	1
C2	9481(2)	4078(2)	3659(2)	21(1)	1
C3	6883(2)	3644(2)	2200(2)	25(1)	1
C4	8086(2)	3035(2)	3081(1)	17(1)	1
C5	6497(2)	3363(2)	4337(1)	15(1)	1
C6	5637(2)	2507(2)	4980(1)	14(1)	1
C7	3842(2)	2434(2)	4389(1)	15(1)	1
C8	3477(2)	1692(2)	3306(1)	14(1)	1
C9	3944(2)	344(2)	3165(1)	17(1)	1
C10	3627(2)	–349(2)	2179(1)	18(1)	1
C11	2811(2)	313(2)	1331(1)	19(1)	1
C12	2341(2)	1648(2)	1440(1)	21(1)	1
C13	2689(2)	2340(2)	2438(1)	18(1)	1
C14	7523(2)	3091(2)	6714(1)	15(1)	1
C15	7824(2)	3669(2)	7757(1)	15(1)	1
C16	9319(2)	3641(2)	8469(1)	18(1)	1
C17	10554(2)	3003(2)	8162(1)	17(1)	1
C18	10284(2)	2411(2)	7155(1)	18(1)	1
C19	8771(2)	2469(2)	6439(1)	17(1)	1
C20	6763(2)	4733(2)	9060(1)	21(1)	1
C21	13275(2)	2399(2)	8650(2)	24(1)	1
Br1	2580(1)	1433(1)	5179(1)	18(1)	1
Br2	2315(1)	–660(1)	–20(1)	30(1)	1
N1	5964(2)	3095(2)	6044(1)	16(1)	1
O1	7237(2)	2521(1)	3818(1)	15(1)	1
O2	6460(2)	4610(1)	4317(1)	21(1)	1
O3	6523(2)	4214(1)	7997(1)	18(1)	1

Table 3. Bond lengths [Å] and angles [°].

C1–C4	1.522(3)
C1–H1A	0.9800
C1–H1B	0.9800
C1–H1C	0.9800
C2–C4	1.520(2)
C2–H2A	0.9800
C2–H2B	0.9800
C2–H2C	0.9800
C3–C4	1.523(2)
C3–H3A	0.9800
C3–H3B	0.9800
C3–H3C	0.9800
C4–O1	1.486(2)
C5–O2	1.209(2)
C5–O1	1.332(2)
C5–C6	1.544(2)
C6–N1	1.440(2)
C6–C7	1.534(2)
C6–H6	1.0000
C7–C8	1.512(2)
C7–Br1	1.9863(17)
C7–H7	1.0000
C8–C13	1.390(2)
C8–C9	1.397(2)
C9–C10	1.385(2)
C9–H9	0.9500
C10–C11	1.384(3)
C10–H10	0.9500
C11–C12	1.383(3)
C11–Br2	1.9013(18)
C12–C13	1.395(3)
C12–H12	0.9500
C13–H13	0.9500
C14–C19	1.387(2)
C14–N1	1.401(2)
C14–C15	1.414(2)
C15–O3	1.375(2)
C15–C16	1.384(2)
C16–C17	1.404(3)
C16–H16	0.9500
C17–C18	1.378(2)
C17–O4	1.381(2)
C18–C19	1.402(2)
C18–H18	0.9500
C19–H19	0.9500
C20–O3	1.429(2)
C20–H20A	0.9800
C20–H20B	0.9800
C20–H20C	0.9800
C21–O4	1.429(2)
C21–H21A	0.9800
C21–H21B	0.9800
C21–H21C	0.9800
N1–H1	0.8601

C4-C1-H1A	109.5
C4-C1-H1B	109.5
H1A-C1-H1B	109.5
C4-C1-H1C	109.5
H1A-C1-H1C	109.5
H1B-C1-H1C	109.5
C4-C2-H2A	109.5
C4-C2-H2B	109.5
H2A-C2-H2B	109.5
C4-C2-H2C	109.5
H2A-C2-H2C	109.5
H2B-C2-H2C	109.5
C4-C3-H3A	109.5
C4-C3-H3B	109.5
H3A-C3-H3B	109.5
C4-C3-H3C	109.5
H3A-C3-H3C	109.5
H3B-C3-H3C	109.5
O1-C4-C2	110.01(14)
O1-C4-C1	101.57(14)
C2-C4-C1	111.58(15)
O1-C4-C3	109.17(14)
C2-C4-C3	112.64(16)
C1-C4-C3	111.30(16)
O2-C5-O1	126.68(17)
O2-C5-C6	123.40(16)
O1-C5-C6	109.92(14)
N1-C6-C7	112.51(14)
N1-C6-C5	112.94(14)
C7-C6-C5	105.35(13)
N1-C6-H6	108.6
C7-C6-H6	108.6
C5-C6-H6	108.6
C8-C7-C6	112.53(14)
C8-C7-Br1	108.58(11)
C6-C7-Br1	109.40(11)
C8-C7-H7	108.8
C6-C7-H7	108.8
Br1-C7-H7	108.8
C13-C8-C9	119.11(16)
C13-C8-C7	120.71(15)
C9-C8-C7	120.18(15)
C10-C9-C8	120.99(16)
C10-C9-H9	119.5
C8-C9-H9	119.5
C11-C10-C9	118.61(17)
C11-C10-H10	120.7
C9-C10-H10	120.7
C12-C11-C10	121.95(17)
C12-C11-Br2	119.38(14)
C10-C11-Br2	118.66(14)
C11-C12-C13	118.76(17)
C11-C12-H12	120.6
C13-C12-H12	120.6
C8-C13-C12	120.56(17)
C8-C13-H13	119.7
C12-C13-H13	119.7
C19-C14-N1	124.00(16)
C19-C14-C15	117.48(16)
N1-C14-C15	118.37(15)

O3–C15–C16	123.94(16)
O3–C15–C14	114.92(15)
C16–C15–C14	121.12(16)
C15–C16–C17	119.78(16)
C15–C16–H16	120.1
C17–C16–H16	120.1
C18–C17–O4	125.12(16)
C18–C17–C16	120.25(16)
O4–C17–C16	114.63(16)
C17–C18–C19	119.25(16)
C17–C18–H18	120.4
C19–C18–H18	120.4
C14–C19–C18	122.10(16)
C14–C19–H19	118.9
C18–C19–H19	118.9
O3–C20–H20A	109.5
O3–C20–H20B	109.5
H20A–C20–H20B	109.5
O3–C20–H20C	109.5
H20A–C20–H20C	109.5
H20B–C20–H20C	109.5
O4–C21–H21A	109.5
O4–C21–H21B	109.5
H21A–C21–H21B	109.5
O4–C21–H21C	109.5
H21A–C21–H21C	109.5
H21B–C21–H21C	109.5
C14–N1–C6	119.03(14)
C14–N1–H1	110.8
C6–N1–H1	111.0
C5–O1–C4	122.25(14)
C15–O3–C20	116.24(14)
C17–O4–C21	116.08(15)

Symmetry transformations used to generate equivalent atoms:

Table 4. Anisotropic displacement parameters [$\text{\AA}^2 \times 10^3$]. The anisotropic displacement factor exponent takes the form: $-2\pi^2[h^2a^*2U^{11} + \dots + 2hk a^* b^* U^{12}]$.

Atom	U^{11}	U^{22}	U^{33}	U^{23}	U^{13}	U^{12}
C1	21(1)	27(1)	20(1)	-6(1)	9(1)	0(1)
C2	19(1)	22(1)	22(1)	-1(1)	7(1)	-2(1)
C3	24(1)	37(1)	16(1)	6(1)	4(1)	4(1)
C4	16(1)	22(1)	13(1)	2(1)	6(1)	1(1)
C5	13(1)	19(1)	12(1)	-1(1)	2(1)	2(1)
C6	14(1)	17(1)	11(1)	-1(1)	3(1)	2(1)
C7	15(1)	18(1)	12(1)	2(1)	5(1)	1(1)
C8	12(1)	16(1)	13(1)	0(1)	3(1)	-1(1)
C9	18(1)	18(1)	15(1)	2(1)	4(1)	2(1)
C10	21(1)	17(1)	16(1)	-1(1)	6(1)	-1(1)
C11	22(1)	22(1)	12(1)	-3(1)	5(1)	-5(1)
C12	23(1)	23(1)	14(1)	3(1)	1(1)	0(1)
C13	17(1)	18(1)	16(1)	2(1)	3(1)	2(1)
C14	16(1)	16(1)	12(1)	0(1)	3(1)	-1(1)
C15	18(1)	15(1)	13(1)	0(1)	5(1)	1(1)
C16	19(1)	19(1)	13(1)	-2(1)	3(1)	0(1)
C17	15(1)	20(1)	15(1)	1(1)	1(1)	0(1)
C18	16(1)	22(1)	17(1)	1(1)	5(1)	2(1)
C19	19(1)	20(1)	11(1)	-1(1)	3(1)	0(1)

C20	24(1)	26(1)	12(1)	-3(1)	4(1)	4(1)
C21	17(1)	29(1)	24(1)	2(1)	3(1)	4(1)
Br1	16(1)	25(1)	15(1)	3(1)	6(1)	2(1)
Br2	48(1)	27(1)	13(1)	-5(1)	6(1)	-5(1)
N1	15(1)	21(1)	10(1)	-2(1)	3(1)	1(1)
O1	16(1)	17(1)	13(1)	-1(1)	6(1)	1(1)
O2	23(1)	16(1)	24(1)	1(1)	10(1)	4(1)
O3	18(1)	24(1)	12(1)	-3(1)	4(1)	4(1)
O4	17(1)	32(1)	16(1)	-2(1)	-1(1)	5(1)

Table 5. Hydrogen coordinates [$\times 10^4$] and isotropic displacement parameters [$\text{\AA}^2 \times 10^3$].

Atom	x	y	z	U_{eq}	<i>S.o.f.</i>
H1A	9262	1900	2187	34	1
H1B	7750	1029	2358	34	1
H1C	9389	1296	3282	34	1
H2A	10179	3657	4244	31	1
H2B	9063	4910	3922	31	1
H2C	10100	4338	3183	31	1
H3A	7418	3916	1682	38	1
H3B	6466	4464	2481	38	1
H3C	5991	2944	1869	38	1
H6	6004	1543	4979	17	1
H7	3498	3403	4331	18	1
H9	4487	-103	3755	20	1
H10	3962	-1259	2086	22	1
H12	1792	2087	847	25	1
H13	2384	3262	2525	21	1
H16	9509	4051	9163	21	1
H18	11113	1967	6948	22	1
H19	8594	2069	5743	20	1
H20A	5762	5081	9147	31	1
H20B	7616	5493	9254	31	1
H20C	7077	3982	9509	31	1
H21A	13533	2873	8089	36	1
H21B	12945	1416	8409	36	1
H21C	14227	2468	9255	36	1
H1	5261	2772	6327	19	1

Table 6. Hydrogen bonds [\AA and $^\circ$].

$D-H\cdots A$	$d(D-H)$	$d(H\cdots A)$	$d(D\cdots A)$	$\angle(DHA)$
C1-H1A \cdots Br2 ⁱ	0.98	2.97	3.4990(19)	114.7
C2-H2B \cdots O2	0.98	2.47	3.044(2)	117.4
C3-H3B \cdots O2	0.98	2.46	3.046(2)	118.2
C7-H7 \cdots O2 ⁱⁱ	1.00	2.53	3.286(2)	132.4
C18-H18 \cdots Br1 ⁱⁱⁱ	0.95	3.01	3.8236(19)	144.3
C19-H19 \cdots O1	0.95	2.61	3.403(2)	141.7
C20-H20B \cdots O4 ^{iv}	0.98	2.64	3.204(2)	116.7
N1-H1 \cdots Br1	0.86	2.62	3.1410(15)	120.5

Symmetry transformations used to generate equivalent atoms:

(i) $-x+1, -y, -z$ (ii) $-x+1, -y+1, -z+1$ (iii) $x+1, y, z$

(iv) $-x+2, -y+1, -z+2$

